ROLE OF HSPA8 IN PATHOLOGICAL OUTCOMES IN THE HOST DURING MALARIA

A Thesis

Submitted in Partial

Fulfillment of the Requirements for the Degree of

Doctor of Philosophy

by

ALOK KUMAR PANDEY

176106024

Department of Biosciences and Bioengineering

Indian Institute of Technology Guwahati

Guwahati, Assam, 781039, India

May 2024

Indian Institute of Technology Guwahati

Department of Biosciences and Bioengineering

Declaration

I, **Alok Kumar Pandey**, am privileged to present this thesis entitled **"Role of HSPA8 in Pathological Outcomes in the Host during Malaria",** culminating my research efforts in the field of malaria and hemolytic diseases. This work represents an original contribution to understanding the role of HSPA8 in a hemin-like environment. Throughout this research endeavor, I have adhered to the highest standards of academic integrity and ethics. All sources of information, including data, ideas, and concepts, have been duly acknowledged and referenced, following the guidelines provided by my institution. I have not plagiarized or misrepresented the work of others in any form. I affirm that this thesis is the result of my original research work conducted under the guidance of my mentor, Prof. Vishal Trivedi, and in compliance with the regulations of my academic institution, the **Department of Biosciences and Bioengineering, Indian Institute of Technology Guwahati.** I declare that this work has not been submitted for any other degree or examination at any other university or institution.

November 28, 2024

Alok Kumar Pandey

(176106024)

Indian Institute of Technology Guwahati

Department of Biosciences and Bioengineering

Certificate

This is to certify that the thesis entitled **"Role of HSPA8 in Pathological Outcomes in the Host during Malaria"**, submitted by Alok Kumar Pandey, bearing registration number **176106024**, has been prepared under my supervision and is a record of the candidate's original research work. This thesis fulfills the requirements for the Doctor of Philosophy degree in malaria and hemolytic diseases at the **Indian Institute of Technology Guwahati.** The findings presented in this thesis are original and contribute to the existing knowledge in the explored area of research. To the best of my knowledge, I certify that this thesis represents original work and has not been submitted for any degree or examination at any other institute or university. The research follows the ethical standards outlined by the Indian Institute of Technology and relevant regulatory bodies. Additionally, we emphasize that the thesis has meticulously acknowledged all research materials obtained from external sources. Moreover, we have diligently cited and attributed any textual content, illustrations, tables, figures, and other elements borrowed from external sources to the best of our knowledge and following scholarly conventions.

November 28, 2024,

Prof. Vishal Trivedi

(Supervisor)

Acknowledgements

It was all dark at the beginning of this long arduous, obscure journey, in the pursuit of reaching my goal, but the dawn was brought into my life by the grace, benediction, and blessing of "Almighty God". On the path to achieving this venture, I was shaped, guided, and rejuvenated by valuable ideas, criticisms, and suggestions from many people who assisted me in reaching this destination. Although words are not enough to express my sincere gratitude but still, I shall still try to comprehend as far as I can.

Foremost, I would like to express my heartfelt gratitude to my thesis supervisor, Prof. Vishal Trivedi for his continuous guidance, freedom towards research, and academic support throughout my graduate studies. I thank him for the best training I got in his lab which will certainly help me to grow as a researcher.

I also owe my gratitude to the present head of my department, Prof. Rakhi Chaturvedi, and ex-HODs, Prof. Kannan Pakshirajan and Prof. Latha Rangan.

I would also like to thank my esteemed Doctoral committee members, Prof. Vibin Ramakrishnan, Prof. Sachin kumar, and Prof. Kaustubha Mohanty, whose guidance and inspiration helped me immensely.

I am specially thankful to each past and current member of Prof. Trivedi's Lab specially Dr. Sooram Banesh, Dr. Anil Kumar, Dr. Rafi Uz Zama Khan, Mr. Siddhart Neog, Mr. Rajendra Prasad, Mr. Shirish Bhagwan Kathane, Ms. Eena Dodwani, Mr. Rakesh, Late Ms. Sikha, Mr. Umesh, Mr. Sai, Mr. Shyamji, Ms. Neha, Mr. Sandeep, Mr. Divyanshu, and Ms. Arunima for extending their helping hands and motivation throughout this Ph.D. tenure. Their companionship made my stay in the laboratory comfortable, and memorable. It would have not been possible to tackle the ups and downs of my Ph.D. journey without their constant stand by my side. It is very difficult to say goodbye to them but I will always carry with me the emotional bond that we shared during this journey and will miss them in my future labs.

I give my special thanks to my friends Arman, Alok, and Suraj for sharing this unbreakable bond of friendship which keeps me sometimes sane and mostly insane. Distances never separated us as they made sure that we remained connected under all the circumstances.

I sincerely thank my lifeline of IITG whom I call a family away from family that included. Arman Mohanty, Alok Senapati, Suraj Kumar Panda, Rafi, Siddharth Ajit Kumar, Ankush Sontakke, Seema Lokhanwala, Sonia, Sahil Dhull, Prateek Dasgupta, Arupam Patra, Mahesh, Noor Mohammed, and Manoj. I want to thank them for giving me such wonderful memories during our meals, tea time, parties, night walks, trips, and endless talks. I am obliged by the special place they have for me in their heart.

I am grateful to my parents Smt. Sharda Devi Shri Surendra Chandra Pandey and my in-laws Smt. Hemlata Singh and Shri. Ravindra Pratap Singh, my sisters Dr. Pratibha Pandey and Mrs Vandana Pandey, my brother Praveen Kumar pandey, Bhabhi Namita Verma Pandey, and my beloveds Pihu, Misha, Advik, and Krisha for their unlimited faith, patience and confidence that has made me whatever, I am today.

I express my sincere respect and love for my wife, Dr. Priya Singh, who has always been there to hold my hands and say, " I believe you; you can do it". Thanks to her for believing in my abilities, encouraging me throughout this journey, and giving me hope whenever I felt low. I am also grateful to my enthusiastic, loving, and understanding in-laws; without whose support, this journey would not have been possible.

I would also like to thank the Department of Biosciences and Bioengineering and Central Instrument Facility (CIF) for providing analytical instruments that were extremely helpful during my research work. I am thankful to my institute (Indian Institute of Technology, Guwahati) for giving me ample scope to conduct my research work and granting me a fellowship during my PhD tenancy.

I have made a small effort to express my feelings from the bottom of my heart to one and all who were directly or indirectly part of this journey.

Thank you all for being with me.

Alok Kumar Pandey

Table of Contents

Chapter I: Introduction and Literature Review

Chapter II: Experimental Procedures

Chapter III: Role Transformation of HSPA8 after Binding Hemin to Catalyze Heme Polymerization

Chapter IV: Hemin Competitively Inhibits HSPA8 ATPase Activity Mitigating its Foldase Function

Chapter V: HSPA8 Impedes Hemin-induced Cellular Toxicity in Liver Cells

List of Figures

List of Tables

Abbreviations

ADP	Adenosine Diphosphate	**DMEM**	Dulbecco's Modified Eagle Medium
AIHA	Autoimmune Hemolytic Anemia	**DNAJ**	DNA J-domain
ALT	Alanine Transaminase	**EDTA**	Ethylene Diamine Tetra Acetic acid
AST	Aspartate Aminotransferase	**EHT**	Electron High Tension
ATG 5	Autophagy Related 5	**Elf2α**	Eukaryotic translation initiator factor 2 alpha subunit
ATP	Adenosine Triphosphate	**EPO**	Eosinophil Peroxidase
Bach1	BTB domain And CNC Homolog 1	**ERK**	Extracellular signal-Regulated Kinase
BAG1	Bag family molecular chaperone regulator 1	**FTIR**	Fourier Transform Infrared Spectroscopy
BBB	Blood-Brain Barrier	**GCN2**	General Control non-depressible 2
BSA	Bovine Serum Albumin	**GDP**	Guanosine Diphosphate
CCL1	C-C motif Chemokine Ligand 1	**GSH**	Glutathione
CCl5	Chemokine (C-C motif) Ligand 5	**GST**	Glutathione S-Transferase
CD	Circular Dichroism	**GTP**	Guanosine Triphosphate
CD163	Cluster of Differentiation 163	**H_2O_2**	Hydrogen peroxide
CD36	Cluster of Differentiation 36	**Hb**	Hemoglobin
CD91	Cluster of Differentiation 91	**HBB**	Hemoglobin subunit Beta

CXCL8	C-X-C motif Chemokine Ligand 8	**HBP23**	Heme Binding Protein 23
DAMP	Damage-Associated Molecular Pattern	**HCP1**	Heme Carrier Protein 1
HO	Heme Oxygenase	**mRNA**	Messenger RNA
HRI	Heme Regulated Inhibitor	**MTT**	3-(4,5-dimethylthiazol-2-yl0-2,5 diphenyl tetrazolium bromide
HRP	Horseradish Peroxidase	**MMP-3**	Matrix Mettaloproteinase-3
HSC70	Heat Shock Cognate 70	**MMP-9**	Matrix Mettaloproteinase-9
HSP	Heat Shock Protein	**MPO**	Myeloperoxidase
HSPA8	Heat Shock Protein Family A member 8	**MDH**	Malate Dehydrogenase
HSPA8_CT	HSPA8 C-terminal Domain	**MetHb**	Methemoglobin
HSPA8_NBD	HSPA8 Nucleotide Binding Domain	**NADH**	Nicotinamide Adenine Dinucleotide (NAD) + Hydrogen (H)
Hz	Hemozoin	**NALP3**	NACHT, Leucine-rich region, and PYD^2 domains containing protein 3
IL-1β	InterLeukin-1 beta	**NF-ƙB**	Nuclear Factor kappa B
IL-6	Interleukin-6	**Ni-NTA**	Nickel-Nitrilotriacetic acid
IL-8	Interleukin-8	**NP-40**	Nonidet P-40
ISR	Integrated Stress Response	**NPT**	Isothermal-isobaric (NPT) ensemble
ITC	Isothermal Calorimetry	**OD**	Optical Density
IVH	Intraventricular Hemorrhage	**PBS**	Phosphate Buffered Saline
JNK	c-Jun N-terminal Kinase	**PC12**	Pheochromocytoma 12
LC3	Light Chain 3	**PCR**	Polymerase Chain Reaction
LDH	Lactate Dehydrogenase	**PDB**	Protein Data Bank

LPO	Lactoperoxidase	**PERK**	PKR-like Endoplasmic Reticulum Kinase
MCP-1	Monocyte Chemoattractant Protein-1	**PKR**	Protein Kinase R
pO_2	Partial pressure of oxygen	**SGOT**	Serum Glutamic-Oxaloacetic Transaminase
PS	Phosphatidylserine	**SGPT**	Serum Glutamic Pyruvic Transaminase
RANTES	Regulated upon Activation, Normal T cell Expressed and Secreted	**TLR2**	Toll-Like Receptor 2
RBC	Red Blood Cell	**TLR9**	Toll Like Receptor 9
Rh factor	Rhesus factor	**TNF-α**	Tumor Necrosis Factor-alpha
ROS	Reactive Oxygen Species	**TPO**	Thyroid Peroxidase
SDS-PAGE	Sodium Dodecyl Sulphate-Polyacrylamide Gel Electrophoresis	**TSPO**	Translocator Protein

Units

Å	Angstrom	**nm**	Nanometer
°C	Degree Celsius	**kcal/mole**	Kilocalorie per mole
%	percent	**kJ/mole**	Kilojoule per mole
µM	Micromolar	**mg**	Milligram
µW	Microwatt	**kV**	Kilovolt
µg/ml	Microgram per milliliter	**mm**	Millimeter
µmole/min	Micromoles per minute	**U/L**	Units per Liter
µl	Microliter	**g**	Gram
µg	Microgram	**mdeg**	Millidegrees
mM	illimolar	**ml**	Milliliter
mg/ml	milligram per milliliter	**ps**	Picosecond
		nM	Nanomolar
ns	Nanosecond	**cm^{-1}**	Centimeter inverse

Chapter I

Introduction and Literature Review

1.1 Malaria: a life-threatening disease

Malaria is a life-threatening disease caused by the parasites of the *Plasmodium* genus and transmitted to humans by an infected female *Anopheles* mosquito bite. In humans, five *Plasmodium* species, including *P. falciparum*, *P. vivax*, *P. malaria*e, *P. ovale*, and *P. knowlesi*, can cause malaria, with *P.falciparum* and *P. vivax* being the most widely distributed. *P. falciparum* is the most dangerous and lethal being responsible for most malaria-related deaths globally[1]. According to the World Malaria Report 2023, the malaria burden is rapidly increasing worldwide. Statistically, an estimated 249 million cases, including 608,000 deaths, were reported in 85 malaria-endemic countries in 2022. About 36 % of the total pregnancies reported in 2022 in 33 transmission countries were exposed to malaria infection. Total malaria deaths among children below five years of age remained at 76% since 2015. India lies among countries with high malaria burden, with approximately 34 lakh cases and 5.511 deaths reported in 2022. Major challenges in combating malaria include the emergence of drug-resistant strains, particularly in Southeast Asia, access to effective diagnosis and treatment, especially in remote rural areas, and sub-effective mosquito control measures[2].

1.2 The life cycle of the malaria parasite

Malaria parasites exhibit a complex life cycle, exploiting humans and female *Anopheles* mosquitoes as hosts[3]. The cycle begins with a bite of an infected female *Anopheles*, injecting the infective sporozoites into the human bloodstream (**Figure 1.1**). These sporozoites reach the liver, traveling through the blood and infecting the liver cells. In the hepatocytes, they multiply asexually, forming numerous merozoites, which are released back into the bloodstream following maturation. The liver stage of malaria is asymptomatic and lasts from 5 to 126 days. These merozoites invade through specific receptors and infect the red blood cells (RBCs). Inside the RBCs, these sequentially develop into ring forms, trophozoites, and schizonts. The schizonts contain numerous merozoites, and they rupture the RBCs, causing merozoite release into the bloodstream. These merozoites are capable of infecting new RBCs, continuing the infection-replication cycle. The characteristic malaria symptoms like fever, chills, and anemia arise due to this schizont-induced RBC rupture. A population of the merozoites differentiates and develops into sexual forms, the gametocytes, which are again ingested by a mosquito during a blood meal.

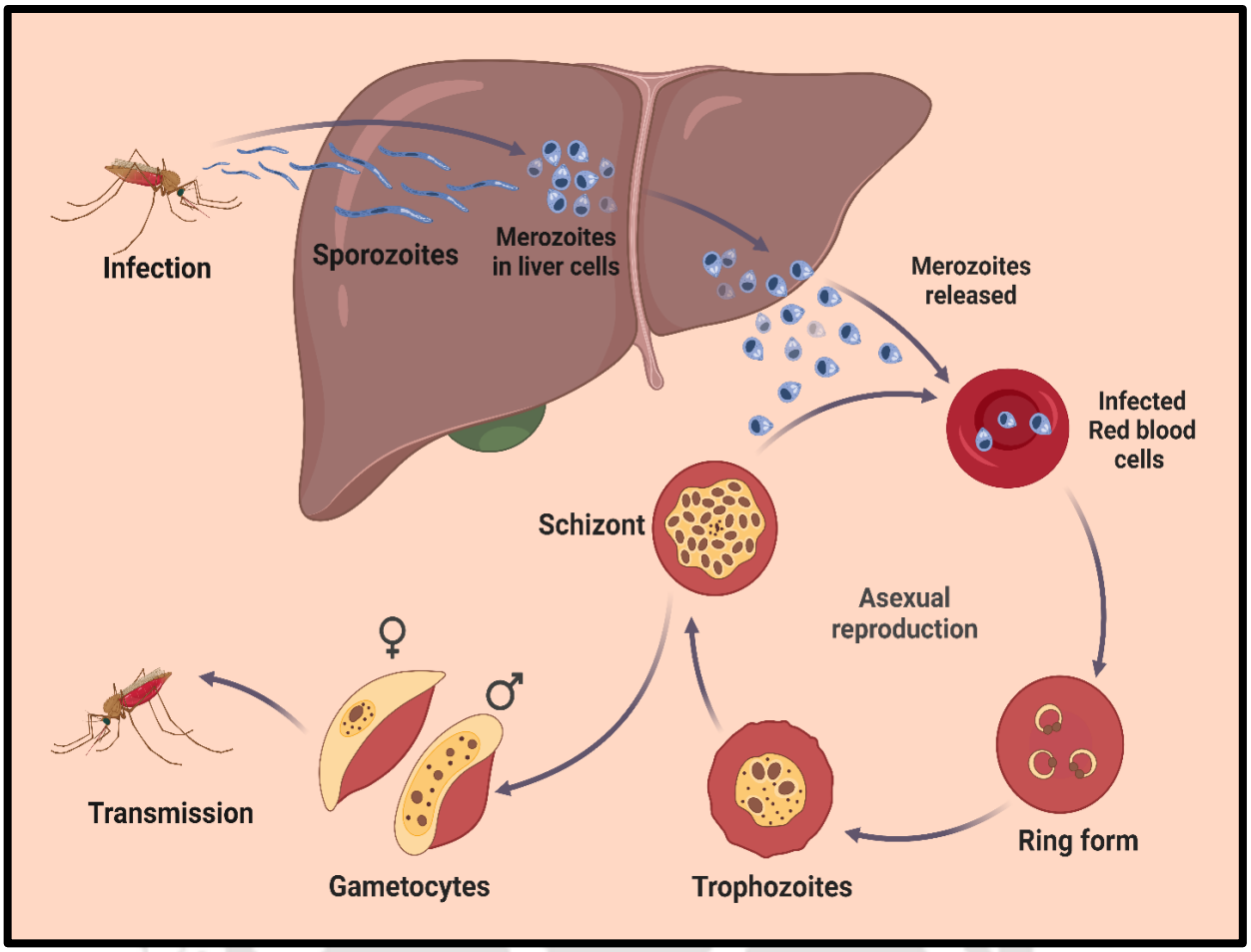

Figure 1.1: The life cycle of the malaria parasite.

In the mosquito mid-gut, these develop into male and female gametocytes, followed by fertilization and zygote formation. The zygote develops into a mobile ookinete, which penetrates the mid-gut wall and forms an oocyst. Thousands of sporozoites are formed into the oocysts, leading to its rupture and the release of the sporozoites into the mosquito body cavity. These sporozoites migrate to the salivary glands of the mosquito, where they can infect another human through a mosquito bite, completing the cycle.

1.3 Hemolysis

The term “Hemolysis” finds its origin in the Greek words “hemo”, meaning blood, and “lysis”, meaning breakdown. It refers to the rupture or destruction of the RBCs, causing hemoglobin to be released into its surrounding fluid, like plasma. Based on the site of occurrence, hemolysis can be of two main types: intravascular hemolysis and extravascular hemolysis. RBC lysis occurring

within the bloodstream leading to the hemoglobin (Hb) release into the plasma is categorized as intravascular. In contrast, extravascular hemolysis is characterized by RBC lysis outside the bloodstream, primarily in the liver and spleen, where they are phagocytosed and broken down by macrophages[4]. Major causes of hemolysis include the presence of RBC-targeting antibodies like in autoimmune hemolytic anemia, certain medications, toxins, and infections like malaria and *Clostridium*. Complications arising due to hemolysis depend upon its cause and extent of severity. While the body can quickly compensate for mild lysis through increased erythropoiesis, severe or chronic hemolysis can lead to anemia characterized by a persistent reduction in the number of RBCs and Hb levels. Anemia leads to pathological symptoms like fatigue, weakness, pale skin, and shortness of breath[5].

1.4 Hemolytic diseases

Hemolytic diseases encompass a group of disorders characterized by hemolysis or accelerated destruction of RBCs. Hemolysis leads to the release of hemoglobin and its derived products like methemoglobin, free heme, hematin, and hemin in the plasma[4, 6]. A variety of factors are responsible for the occurrence of hemolytic diseases, including genetic factors, immune responses, certain infections, and medications[5]. Understanding these diseases' underlying mechanisms and consequences is crucial for effective disease management.

The most prominent category of hemolytic diseases is hemolytic anemia, where erythropoiesis is outpaced by premature RBC destruction. Inherent defects within the RBCs result in intrinsic types of hemolytic anemia, for example, sickle cell anemia where the RBCs assume a sickle shape due to mutations in the hemoglobin subunit beta (HBB) gene. Hemolysis due to external factors, like an immune attack on native RBCs causing Autoimmune Hemolytic Anemia (AIHA), Rhesus (Rh) factor incompatibility between a mother and fetus causing erythroblastosis fetalis and bacterial or parasitic infection causing various diseases like malaria, leads to the extrinsic type of hemolytic anemia[7].

Hemolytic diseases are symptomatically characterized by diverse symptoms, but a few common symptoms include enlarged spleen, dark urine, jaundice, and fatigue[8]. These are diagnosed through blood tests to assess the levels of hemoglobin, bilirubin, and a few other markers. Coombs test is another diagnostic approach for such diseases, which identifies the antibodies present on the surface of RBCs. The strategy to treat such diseases varies based on the underlying cause. Common

strategies employed for the treatment of hemolytic diseases include immune suppressive medication, target-specific medications in case of infections, and blood transfusion. Surgical removal of the spleen is also considered in extreme cases to minimize RBC destruction[5, 8].

1.5 Hemoglobin degradation

Hb is a key component of red blood cells that plays a central role in the transport of oxygen and carbon dioxide between the lungs and various other tissues. Its synthesis, function, and eventual degradation occur through a well-defined cycle. Hemolysis leads to the release of large amounts of hemoglobin into the bloodstream. Degradation of Hb occurs through a finely orchestrated biological process[9]. A controlled degradation is essential for homeostasis management, renewal of the RBCs, and the recycling of molecular components. In humans, the process of hemoglobin degradation starts with phagocytosis of aged or diseased RBCs, majorly by the macrophages of the liver and spleen (**Figure 1.2**).

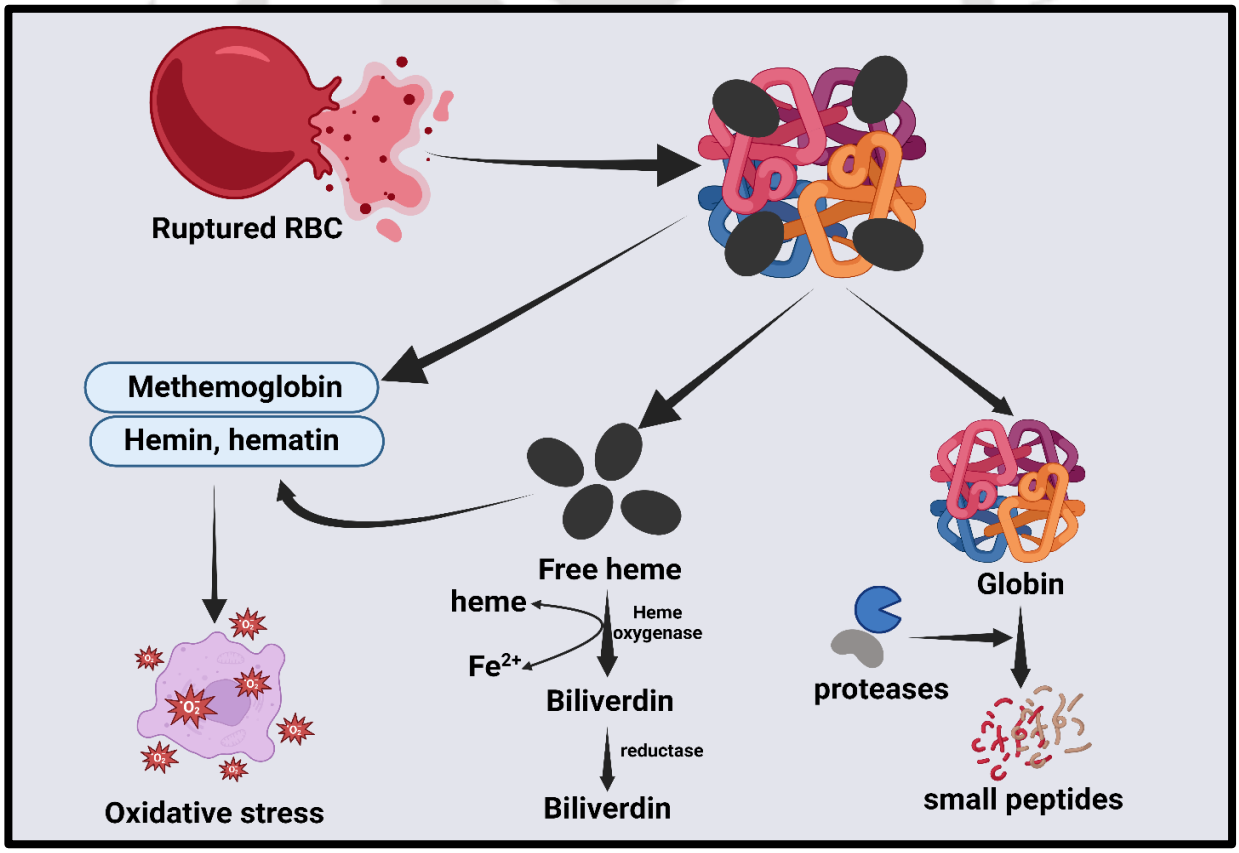

Figure 1.2: Hemoglobin degradation in humans.

The engulfed RBCs eventually release free hemoglobin into the intracellular microenvironment[10]. After Hb internalization, its degradation commences with the removal of heme, the iron-containing prosthetic group, from the globin chains. Enzymatic cleavage of heme by heme oxygenase yields biliverdin, carbon monoxide, and free iron. Biliverdin is subsequently converted to bilirubin, and the free iron is recycled within the body for storage and future use[11, 12]. The globin chains, on the other hand, are broken down into individual amino acids by a set of proteolytic enzymes, including cathepsins and other lysosomal enzymes[13]. The free heme in the bloodstream is spontaneously converted to various heme-derived pro-oxidant molecules, including hemin and methemoglobin.

The malaria parasite feeds on hemoglobin during its intraerythrocytic cycle, leading to its degradation (**Figure 1.3**).

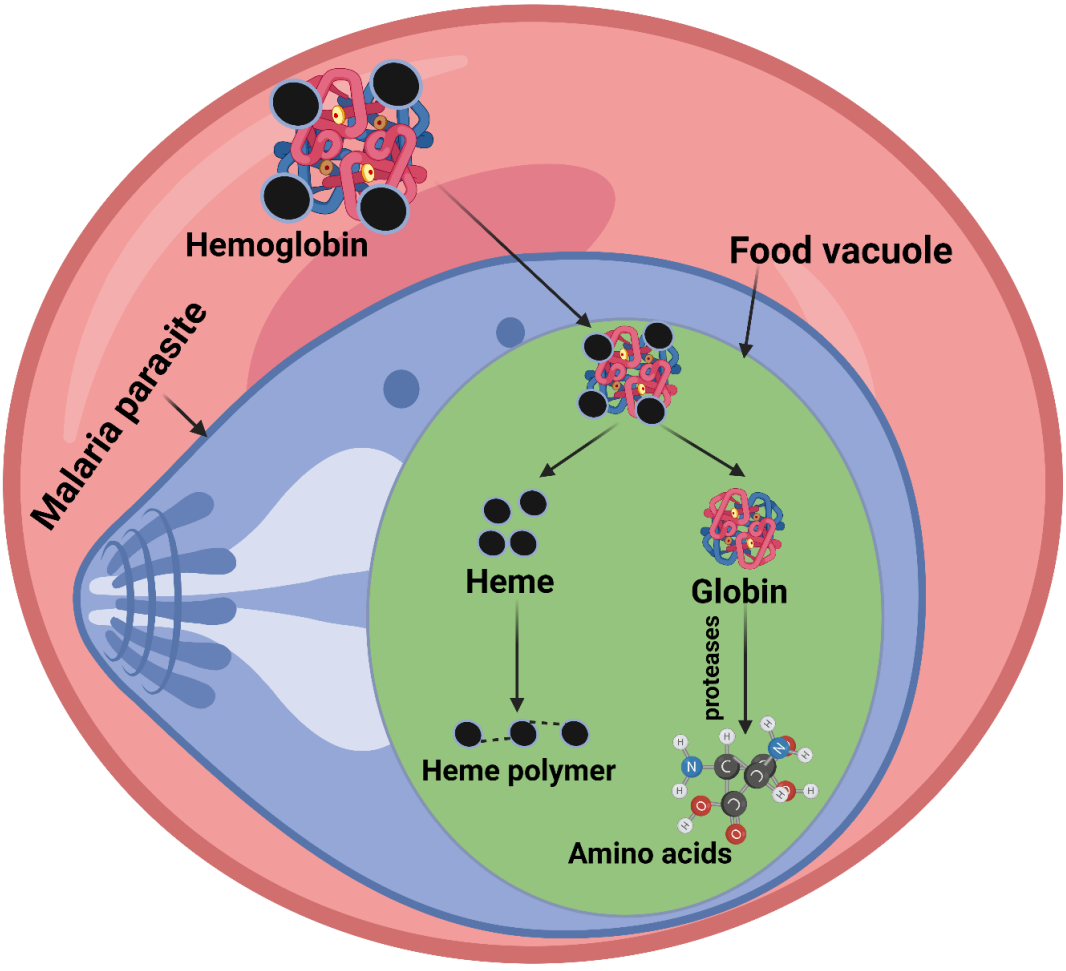

Figure 1.3: Hemoglobin degradation in the malaria parasite.

The parasite ingests about 80% of the host Hb through its cytosome, which transports it to an acidic digestive vacuole. In the food vacuole, hemoglobin eventually breaks down into free heme and globin. The parasites lack the canonical heme oxygenase system for the degradation of heme, and thus, they must take a unique pathway to combat the toxicity caused by accumulated heme. They crystallize the heme into a nontoxic heme polymer, Hemozoin[9]. The formation of hemozoin is believed to be through enzymes catalyzing the polymerization, protein-mediated polymerization by histidine-rich proteins and heme detoxification proteins, and lipid mediation[14].

1.6 Pro-oxidant molecules and cellular homeostasis

Red blood cell rupture and the degradation of hemoglobin lead to the formation of various pro-oxidant molecules inside the intracellular environment. These molecules are highly toxic to various cells, tissues, and organs and lead to homeostatic imbalance, leaving them under oxidative stress. These pro-oxidant molecules include hemoglobin, methemoglobin, free heme/hemin, hematin, and hemozoin. The presence of iron in these molecules is responsible for their toxicity, and these molecules individually contribute to the overall pathologies associated with hemolytic disorders[15].

1.6.1 Methemoglobin (MetHb)

Excessive hemolysis during malaria results in elevated levels of free hemoglobin in the circulation. Being highly unstable, free Hb (Fe^{2+}) having ferrous iron reacts with oxygen to form oxy-hemoglobin/oxygenated ferrous Hb ($Hb(Fe(II)O_2)$), which is readily oxidized to its ferric state, resulting in the formation of methemoglobin (Fe^{3+}) (**Reaction 1**). Hb oxidation by reactive oxygen species (**Reaction 3**) can also convert Hb into a highly unstable intermediate, ferryl hemoglobin (Fe [IV]=O), which eventually converts into methemoglobin (**Reaction 4**) through an electron transfer[16]. The reactions leading to the formation of methemoglobin are as under[17]:

$$\mathbf{Hb(Fe(II)O_2) \longrightarrow Hb(Fe(III)) + O_2^{\bullet}} \qquad \textbf{Reaction 1}$$

$$\mathbf{2O_2^{\bullet} + 2H^{1} \longrightarrow O_2 + H_2O_2} \qquad \textbf{Reaction 2}$$

$$\mathbf{H_2O_2 + Hb(Fe(II)O_2) \longrightarrow Hb(Fe\text{-}IV)\!=\!O} \qquad \textbf{Reaction 3}$$

$$\mathbf{Hb(Fe\text{-}IV)\!=\!O \longrightarrow Fe(III) + porphyrin\ breakdown} \qquad \textbf{Reaction 4}$$

MetHb can also be produced by the reaction of nitric oxide with oxyhemoglobin, resulting in the formation of methemoglobin and nitrate (NO_3^-)[18], mutations in the cytochrome b5 reductase enzyme, which is responsible for the reduction of methemoglobin[19], and conditions that give rise to an imbalance in the redox states.

During normal states, the level of MetHb remains below 2%, but during conditions of stress, the level can reach its toxic levels (≈10%). Methemoglobin levels are increased during infections and diseases like malaria[20], exposure to oxidizing agents, nitrite exposure[21], certain toxins and medications[22], and hereditary enzyme deficiencies[23]. The condition of elevated methemoglobin levels is termed 'methemoglobinemia', and it can be acquired or hereditary depending upon its cause. Other extrinsic factors like metabolic by-products and inflammatory mediators also disturb the cellular redox balance, leading to Hb oxidation and methemoglobin formation. Prolonged methemoglobinemia can be very toxic to various cells, tissues, and organs. MetHb, independent of heme or free iron release from it, can activate endothelial cells through nuclear factor kappa-light-chain-enhancer of activated B cells (NF-κB) mediated Interleukin-6 (IL-6), Interleukin-8 (IL-8), and E-selectin stimulation[24]. This stimulation intensifies the cellular inflammatory response. MetHb accumulation can have clinical consequences. Even a non-anemic person having high levels (20-30%) of methemoglobin can show symptoms of anemia like fatigue, weakness, dizziness, etc. Levels of 50% or more can even lead to dysrhythmias, seizures, coma, and death[25].

1.6.1.1 Impact of Methemoglobin on RBC homeostasis

Excessive RBC lysis results in the release of high amounts of hemoglobin, which eventually causes higher levels of methemoglobin in the circulation. The redox reactions inside RBCs leading to the production of methemoglobin are the major source of RBC oxidative stress and aging [26]. This oxidative stress may lead to lipid peroxidation, carbonylation of proteins[27], and reduced glutathione (GSH) levels inside the RBCs. It may also cause cytoskeletal changes and a reduction in membrane fragility. Oxidative stress inside the RBCs causes phosphatidylserine (PS) externalization, generating sticky patches that lead to the aggregation of RBCs[28] and the blockage of blood vessels. Extracellular methemoglobin destroys more RBCs by triggering the production of reactive oxygen species and making RBCs susceptible to osmotic stress[28]. H_2O_2-activated MetHb causes lipid peroxidation in the red blood cell membrane[29]. MetHb also

possesses an intrinsic pseudo-peroxidase[30] and catalase[31] activity, which also contributes significantly to the generation of oxidative stress and lysis of red blood cells.

1.6.1.2 Methemoglobin-associated Cellular Toxicity

Besides causing cytoskeletal changes, PS externalization, and opsonization of red blood cells, MetHb accumulation inflicts toxicity to several different cells. Macrophages are responsible for the opsonization of parasitized and aged RBCs. Inside the macrophages, the red blood cells are ruptured by macrophages, resulting in the release of MetHb. MetHb exposure has been shown to reduce macrophage viability in a dose-dependent manner, induce damage to its membrane, and accumulate particulate matter in the cytosol. MetHb induces apoptosis in the macrophages through the generation of multiple reactive oxygen species (ROS) spikes[32]. The heme released from MetHb provides a potentially damaging iron and amplifies oxidant-mediated injury of the endothelial cells[33]. MetHb can potentially activate inflammatory response in endothelial cells by the stimulation of cytokines and the expression of cell adhesion molecule E-selectin[24]. It induces chemokine response and the release of interleukins through the activation of NF-κB, extracellular signal-regulated kinase (ERK), and c-Jun N-terminal kinase (JNK) pathways in human alveolar epithelial cells[34]. Depending upon its concentration, MetHb can also contribute to the proliferation of human tumor cells through the release of its ferric ion[35]. MetHb, as a damage-associated molecular pattern (DAMP), can lead to the production of neutrophil-reacting oxygen moieties and enhance proinflammatory cytokines expression, inducing apoptosis in the neutrophils through the toll like-receptor 2 (TLR2)/ NF-κB pathway[36]. MetHb accommodates hemin as a substrate and converts it into a heme polymer and synergistically amplifies the toxic effects of heme or heme polymer[37].

1.6.1.3 Methemoglobin-associated tissue and organ toxicity

Prolonged production of high MetHb amounts during various pathological states can lead to adverse effects on various vital organs. Gastro-intestinal hemorrhage and oesophageal bleeding can lead to the accumulation of MetHb in the liver causing liver cirrhosis[38]. Prolonged methemoglobinemia can also cause tissue hypoxia and induce cardiac and respiratory failure[39]. During cerebral malaria, intraventricular hemorrhage (IVH) in the cerebrum leads to hemoglobin release and MetHb formation, which causes inflammation and severe neurodevelopmental

impairments in preterm infants[40]. Maternal methemoglobinemia is shown to be a possible cause of iron deposits in the fetal and infant brain, leading to their death[41]. Acute nitrite methemoglobinemia has been shown to create circulatory disturbance in rat brains, leading to a modulation in the oxygen regime and the degree of pO2 differentiated distribution, causing functional disturbances in the brain[42]. A case study shows that toxin-induced methemoglobinemia can lead to hypoxic brain and kidney injury in adults[43]. Methemoglobinemia is a major contributor to the headaches attributed to hypoxia and/or hypercapnia[44]. One another case study shows a drastic reduction in the total lipid contents of the myelin, grey, and white matter of the brain during congenital methemoglobinemia[45]. MetHb can have deleterious effects on renal function and cause acute renal injury[46]. MetHb-induced renal failure is associated with increased preglomerular resistance and decreased glomerular filtration rates, leading to anuria[47]. MetHb also has a role in hemoglobinuric nephrosis[48].

1.6.2 Hemin

Hemin or protoporphyrin IX is an iron-containing porphyrin formed from a heme group. Hemin crystals, also known as "Teichmann crystals," were first crystallized by Ludwik Karol Teichmann in 1853 from blood. Later, in 1930, it was chemically synthesized by Hans Fischer. It is released through ferric hemoglobin (Hb-Fe^{3+}) degradation during conditions of abnormal extracellular or extravascular Hb accumulation e.g. malaria[6]. It can be assembled endogenously from heme group containing entities, for example, during the turnover of aged RBCs, and can be accumulated in the body during hemolysis and vascular injuries. The formation of hemin (Fe III) is a spontaneous process and occurs through the autoxidation of free heme (Fe II). The coordinating ion in hemin is a chloride (Cl^-) ion which makes it different from other related products like hematin where the coordinating ion is a hydroxyl (OH^-) ion. The iron of hemin is in a ferric (Fe^{3+}) state and being able to produce reactive oxygen species, is majorly responsible for the toxic effects of hemin[49].

Hemin is a biologically active molecule that has crucial roles in various physiological processes. It acts as a cofactor for the catalytic activity of certain enzymes especially those involved in cellular detoxification and antioxidant defense[50, 51]. Hemin can also interact with transcription factors like Bach1 and Nrf2 systems and influence the cellular signaling pathways[52, 53]. Unlike many other substances, hemin can easily penetrate through the Blood-Brain Barrier and thus can

modulate neurological functions[54]. Hemin has a few medical applications, for example, hemin administration can alleviate symptoms and prevent the attacks of acute porphyrias[55]. Hemin can also suppress inflammatory and autoimmune cell responses[56].

Although normal hemin levels are crucial for governing many physiological processes, hemin accumulation to abnormal levels is highly toxic to the corresponding cells, tissue, or organ (**Figure 1.4**).

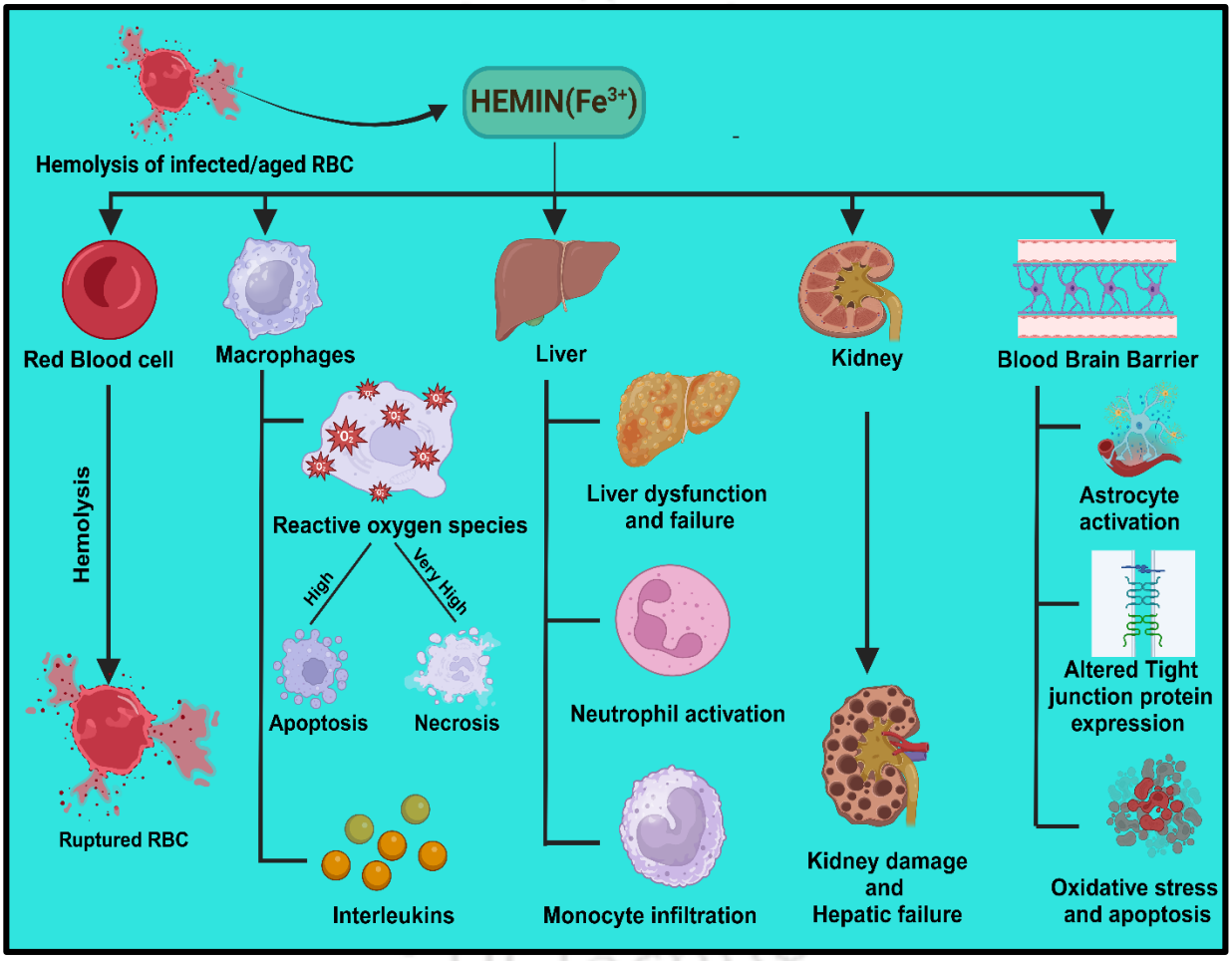

Figure 1.4: Toxic effects of hemin on various cells, tissues, and organs.

Higher hemin levels (up to 20 μM) can be achieved during conditions like porphyrias, hemorrhage, and malaria[57]. Hemin majorly exerts its toxic effects through the production of reactive oxygen species and causing oxidative damage to various macromolecules[58-60]. Hemin toxicity majorly

gives rise to complications in the normal functioning of the liver, kidneys, and Blood-Brain Barrier[61].

1.6.2.1 Impact of hemin on RBC homeostasis

The auto-oxidation of the ferrous heme coming from hemoglobin leads to the formation of ferric heme or hemin. Hemin binds to the normal RBC membrane causing the development of grain-like topological deformations[62] and induces substantial lysis[63]. Hemin also reduces the deformability of normal RBCs compromising the microcirculatory blood flow in vessels[64]. It destabilizes the RBC membrane skeleton by weakening the interaction between spectrin, protein4.1, and actin[65]. The hemolysis leads to hemin internalization in more RBCs causing more lytic burden in the systemic circulation. Hemin can transport easily through membranes and thus fosters the aggregation of RBC membrane proteins through their peroxidation[66]. It also promotes lipid peroxidation[67], oxidation of sulfhydryl groups[68], loss of potassium, and swelling causing hemolysis by a colloid-osmotic process. These eryptotic cells may adhere to the vascular walls and compromise the microcirculation. Like MetHb, exposure to hemin also causes PS externalization in RBCs leading to their phagocytosis by macrophages and elimination from systemic circulation proceeding to anemia[69]. Hemin has been shown to induce the expression of critical autophagy-related genes like Beclin-1, LC3, and Atg5 in an erythroleukemia cell type[70].

1.6.2.2 Hemin-associated cellular toxicity

Besides severely affecting the RBCs, extracellular hemin can reach various other cells via systemic circulation and cause deleterious effects. Hemin is shown to disturb macrophage immune response and increase the secretions of cytokines like TNFα, RANTES, CCL1, and MCP-1 through its interaction with CD36 receptor protein and activation of downstream signalling[71]. Phagocytosis of robust red blood cells by macrophages can promote hemin-induced apoptosis in macrophages[72]. Hemin also induces ferroptosis in the macrophages through the expression of metalloproteinases[73]. Hemin can be accumulated by the brain cells through the expression of heme carrier protein 1 (HCP1) and produce toxic effects leading to lactate dehydrogenase (LDH) release[74]. Hemin is shown to produce iron-dependent oxidative damage to neurons and iron-independent toxicity and cell death in astrocytes through the activation of ERKs[75-77]. Hemin has also been shown to cause apoptosis in pheochromocytoma (PC12) and neuroblastoma cells

during intracerebral hemorrhage[78]. The colonic epithelium is susceptible to hemin toxicity through the involvement of a translocator protein (TSPO)[79]. Hemin causes H_2O_2-mediated injury, lipid peroxidation, mitochondrial dysfunction, and autophagy in endothelial cells[80, 81].

1.6.2.3 Hemin-associated organ toxicity

Hemin accumulation for a longer period can also confer severe organ toxicity. Hemin is a major source of secondary brain damage occurring after an intracerebral hemorrhagic stroke[82, 83]. Hemin is supposed to be involved in neurodegeneration by inhibiting the large conduction potassium channel[84]. The role of hemin is implicated in the chest syndrome pathogenesis and it has been shown to cause impairment in the lung microvascular endothelial barrier through necroptosis[85]. Hemin exposure leads to the disruption in the blood brain barrier (BBB) by modulating the expressions of tight junction proteins, Ig extravasation, and causing oxidative stress[86]. Intravascular hemolysis increases the hemin burden in the liver and leads to liver dysfunction through NF-κB activation and infiltration of the neutrophils[87]. Even a strong induction of heme oxygenase (a heme detoxifying protein) cannnot prevent renal damage caused by hemin after ischemic reperfusion injury[88]. Hemin indirectly mediates renal damage majorly by causing dysfunction in the peritubular endothelium[89].

1.6.3 Hemozoin

Hemozoin is the byproduct of the malaria parasite's metabolism playing a crucial role in the pathogenesis of malaria. The degradation of hemoglobin in the food vacuole while the parasite feeds on it leads to the accumulation of heme imposing a serious threat to the parasite. The parasite protects itself by converting heme into an insoluble crystalline molecule, hemozoin, within its digestive vacuole. Hemozoin serves as a malaria diagnostic marker and the pathway of hemozoin formation is a known target for some antimalarial drugs. Although the conversion of heme to hemozoin is a protective strategy employed by the parasite, its accumulation can be deleterious to various cells and tissues in the host[90].

1.6.3.1 Impact of hemozoin on RBC homeostasis

RBCs are the first to be exposed to hemozoin toxicity coming from the malaria parasite. Hemozoin interacts with the lipids of the red blood cells generating toxic products responsible for modulating macrophage immune reactivity[91]. A high level of hemozoin alone increases the number of

spleen macrophages leading to anemia via hypersplenism[92]. It can induce apoptosis in erythroid precursors[93] hindering the development of new RBCs through the generating of 4-hydroxynonenal, a highly reactive aldehyde[94].

1.6.3.2 Hemozoin-associated cellular toxicity

During severe malaria, the overproduction of hemozoin leads to its deposition in various other cells affecting various cellular phenomena. Hemozoin can activate toll like-receptor 9 (TLR9)-mediated immune response[95] and the hyperactive nucleotide-binding domain, leucine-rich-containing family, pyrin domain-containing-3 (NALP3) inflammasome complex causing IL-1β release in the macrophages[96]. Its exposure can cause monocyte malfunction through the production of a large amount of hydroxyl fatty acids and 4-hydroxynonenal[97, 98]. Hemozoin can directly activate endothelial cells leading to morphological changes similar to angiogenesis. It upregulates proteins like chemokine (C-X_C motif) ligand 8 (CXCL8), C-C motif chemokine ligand 5 (CCL5), matrix metalloprotenase -3 (MMP-3), and matrix metalloprotenase-9 (MMP-9) indicating endothelial breakdown[99]. Malaria-related lung inflammation and acute respiratory distress syndrome are correlated with the amounts of hemozoin present in the circulation[100]. Hemozoin contributes to the pathogenesis of cerebral malaria by inducing apoptosis in human nerve cells and astrocytes[101].

1.6.3.3 Hemozoin-associated tissue and organ toxicity

Sequestration of hemozoin during malaria has been reported at many physiological sites, especially the liver, spleen, lungs, brain, placenta, and bone marrow[102]. Hemozoin accumulation correlates with the expression of immunomodulatory genes and leakage of tissue injury indicating enzymes in the liver causing hepatomegaly[103]. In mouse spleen, a high level of hemozoin was reported even after 180 and 270 days post clearance of the parasites suggesting a long-term impact of hemozoin[104]. The kidneys and eyes are also reported to accumulate and be affected by hemozoin[105]. In the fetal placenta, natural hemozoin elicits a differential immune response in the outermost monolayer syncytiotrophoblast by activating the extracellular signal-regulated kinases 1/2 (ERK1/2 pathway)[106].

1.7 Cellular responses to stress

The pathophysiological changes due to hemolysis-related stress leading to the homeostatic imbalance in various cell types is a big challenge for cellular health and survival. Various cells employ several stress management strategies to counter the homeostatic imbalance and induced toxicity due to the accumulation of hemin and other Hb-derived pro-oxidant products.

1.7.1 Heme detoxification systems in humans

The accumulation of heme/hemin during various pathological states like malaria induces the activation of a myriad of heme-detoxification systems in humans which either chelate the hemin molecule or sequester the free iron of hemin to neutralize its toxic effects.

1.7.1.1 Heme oxygenase (HO) system

The heme oxygenase system is a critical pathway involved in the breakdown of heme/hemin. This system has a crucial role in maintaining cellular homeostasis, oxidative stress regulation, and cytoprotective and anti-inflammatory effects. Two main isoforms of HO are present in humans with HO-1 being the inducible form of the enzyme and HO-2 being the constitutively expressed form. HO-1 is upregulated during oxidative stress and inflammation. Both proteins are membrane-bound and located in the endoplasmic reticulum. Primarily heme oxygenase is involved in the catalytic breakdown of hemin into biliverdin, carbon monoxide, and iron. The heme ring is cleaved at the alpha-meso carbon leading to biliverdin release. Biliverdin is subsequently reduced to bilirubin by a reductase and the free iron is sequestered by ferritin for storage or utility in cellular processes like heme synthesis, etc.

1.7.1.2 Extra-HO systems

Several other mechanisms than the HO system are also involved in the detoxification of hemin. The extra-HO system includes the chelation of hemin by heme-binding proteins, heme transporters, and scavenging by various other molecules.

Hemopexin

It is a plasma protein that binds hemin strongly forming a heme-hemopexin complex which is cleared out from the circulation by macrophages via the CD91 receptor.

Haptoglobin

It is also a heme-binding plasma protein that forms a Haptaglobin-hemin complex which is cleared out by macrophages via its internalization involving the CD163 receptor.

Albumin

It is also an abundantly available heme-binding protein found in the plasma. It forms a heme-albumin complex with hemin and prevents the progression of its toxic effects.

Ferritin

Ferritin is a protein that sequesters the free iron released from heme breakdown and stores it in a non-toxic form for utilization in various iron-dependent cellular processes.

Various other minor non-heme oxygenase systems like glutathione (GSH), Heme binding protein 23 (HBP23), xanthin oxidase, and NADPH P-450 reductase are also involved in the detoxification of hemin.

1.7.2 Heme detoxification in parasite

The malaria parasite does not possess any heme oxygenase system making it incapable of breaking the hemin molecule. Instead, the parasite has evolved sophisticated systems to combat the induced heme toxicity arising due to Hb degradation by the parasite[107].

Heme polymerization

The parasite polymerizes the hemin accumulated into its cytosol into a stable, insoluble, inert, and non-toxic crystalline pigment known as the malaria pigment or Hemozoin[108]. This pigment is stored in the digestive vacuole of the parasite and excreted with other waste products.

Heme transporters

The malaria parasite has specific transporter proteins for heme transport. These facilitate heme-uptake by the parasite and subsequently its detoxification and utilization in metabolic processes[109].

Heme-resistance

Other than detoxification, the parasite has developed alternate ways to fight hemin toxicity. For example, the parasite upregulates antioxidant enzymes and pathways to combat oxidative stress.

1.7.3 Heme Polymerization by Peroxidases

Peroxidases are a class of enzymes involved in the H_2O_2-dependent cataytic oxidation of several substrates. These have roles in a wide range of biological processes like immune response, cell signaling, and combating reactive oxygen species (ROS). Several peroxidases are found in humans including Thyroid peroxidase (TPO) involved in the synthesis of thyroid hormones, Myeloperoxidase (MPO), having a role in immune responses, Lactoperoxidase (LPO) involved in innate immune defense against pathogens, Eosinophil peroxidase (EPO) involved in the innate defense against parasite and allergy, and Catalase which is not a strict peroxidase but catalyze the decomposition of hydrogen peroxide into water and oxygen thus protecting cells from H_2O_2-mediated oxidative damage[110]. Peroxidases are known to polymerize aromatic substrates like guaiacol through a single-electron transfer mechanism.

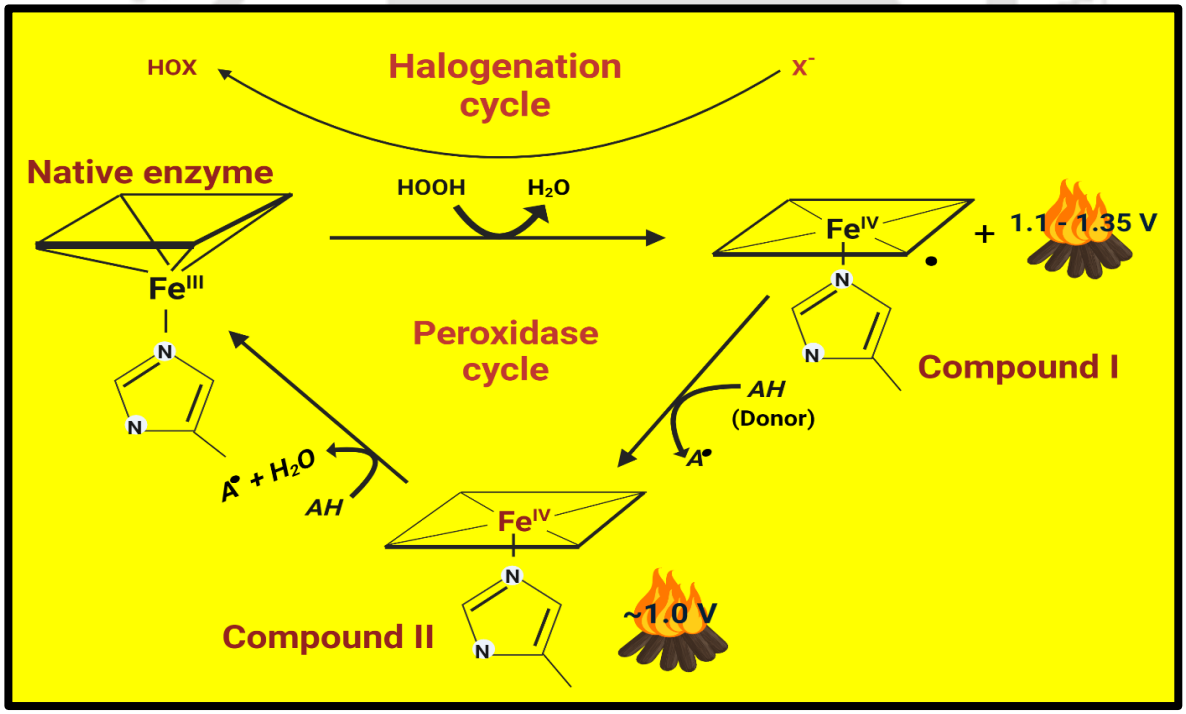

Figure 1.5: The classical peroxidase cycle to catalyze substrate oxidation.

Horseradish peroxidase (HRP), a model peroxidase enzyme, has been shown to catalyze the polymerization of heme into a heme polymer[111] thus reducing its toxic effects. This process

involves the transfer of a single electron from the enzyme leading to the formation of highly reactive intermediates. These intermediates accept electrons from hemin (an aromatic donor) resulting in free radicals generation. These heme radicals subsequently interact to form the heme polymer. The mechanism of a classical peroxidase cycle is shown in Figure 1.5.

1.7.4 Integrated stress response (ISR)

The integrated stress response refers to a conserved eukaryotic mechanism crucial for maintaining cellular homeostasis during stress.

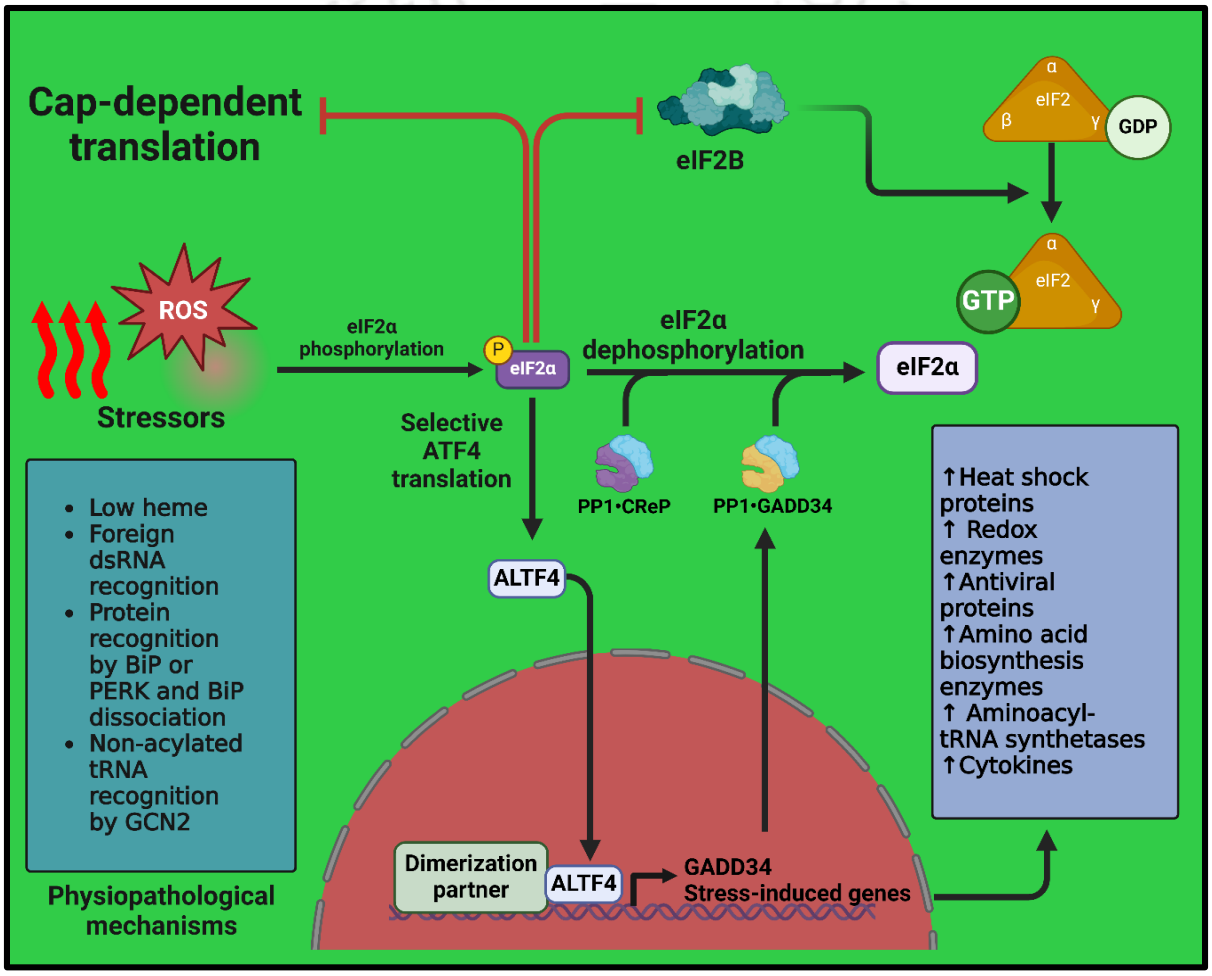

Figure 1.6: Integrated cell response during heat and oxidative stress in mammalian cells.

It is a multiplex signaling cascade triggered by diverse cellular stressors like nutrient deprivation, intracellular oxidation, bacterial and viral infections, chemicals, medicaments, and toxins[112].

The cellular stimulus initiates the cascade (**Figure 1.6**) followed by the phosphorylation of the α-subunit of one of the four elF2α kinases, PERK (PKR-like endoplasmic reticulum kinase), GCN2 (general control non-depressible 2), PKR (Protein kinase R), and HRI (Heme regulated inhibitor).

These kinases are phosphorylated depending on the type of stimulus. The activation of elF2α through Ser51 phosphorylation leads to a global inhibition in the synthesis of proteins. The elF2α activation inhibits the guanine nucleotide exchange factor essential for GDP to GTP exchange by elF2. This prevents the formation of the ternary complex elF2-GTP-tRNAiMet, necessary to initiate translation. The global inhibition of protein synthesis allows for the conservation of energy and resources, and selective translation throughout the stress period. The selective translation ensures the translation of specific mRNAs encoding stress-responsive genes against a particular type of stress, for example, heat and oxidative stress induce the selective translation of mRNAs encoding Heat shock proteins[113], etc. Based on the load and duration of the stress ISR either promotes cell survival or initiates apoptosis or autophagy to remove destroyed cells. Malfunctioning of ISR is implicated in neurodegenerative and metabolic diseases, cancer, etc. The ISR pathway is a promising target to modulate the cellular responses during miscellaneous stress states.

1.8 Heat Shock Proteins (HSPs) – Role in heat and oxidative stress

Malaria brings with it both heat stress due to fever and oxidative stress due to the accumulation of pro-oxidant Hb degradation products. Heat and oxidative stress lead to the degradation and damage of many physiologically relevant proteins. These can lead to unfolding of functional proteins and are also responsible for the misfolding of nascent proteins. The selective synthesis of heat shock proteins through the integrated stress response signaling (**Figure 1.7**) is a major cellular response associated with heat and oxidative stress.

In the world of cellular biology, the orchestration of life-sustaining physiological processes relies on the proper folding and assembly of proteins. Cells have an indigenous protective mechanism to guide the proper folding of proteins and thus maintain cellular proteostasis. Heat shock proteins are a diverse class of proteins majorly involved in the correct folding, stability, and functionality of other proteins within the cell. These are essential components of the cellular machinery, tirelessly working to prevent protein misfolding, and aggregation during cellular stress[114].

Besides their major role in protein folding, HSPs are also involved in other cellular phenomena. They have a critical role in protein trafficking and targeting. They help in shuttling proteins to their designated compartments ensuring their availability at the right location and at the right time for the intended function[115]. HSPs are among the most effective arsenal of cells that monitor protein health and also respond to stressors like heat shock and oxidative stress, that adversely affect cellular proteostasis[116, 117].

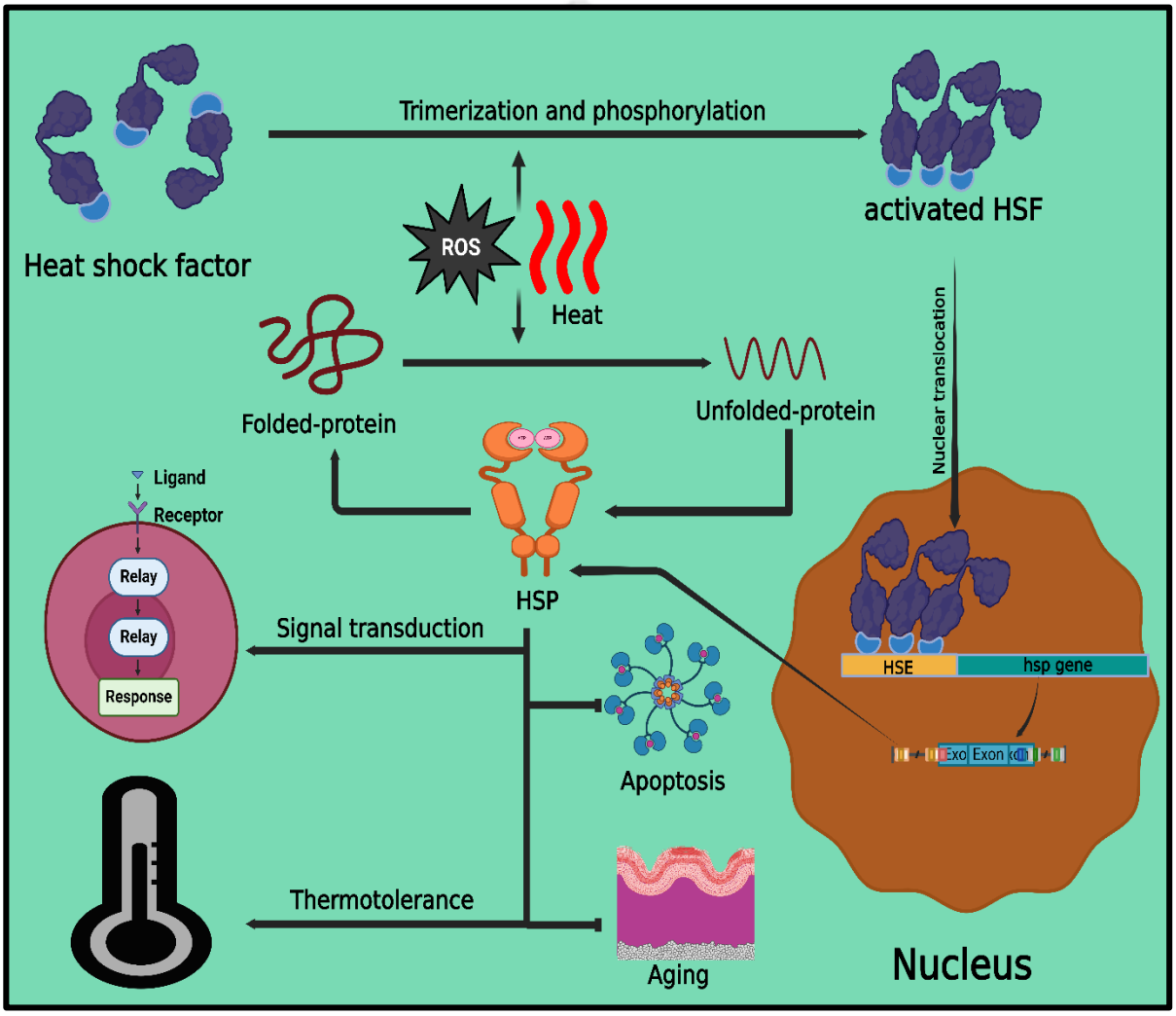

Figure 1.7: Oxidative stress-induced selective translation of an HSP and its stress-associated functions.

The heat shock proteins perform protein folding through chaperone activity. The mechanism of chaperone activity is majorly driven by an adenosine triphosphate-adenosine diphosphate (ATP-

ADP)-dependent cycling of the nucleotide-binding domain and intercommunication of this domain with the substrate-binding domain of the chaperone (**Figure 1.8**). At first, a chaperone binds to the exposed hydrophobic region of the substrate followed by ATP hydrolysis that induces conformational changes in the substrate-binding region to release the substrate in a more folded state[118]. The chaperone activity is assisted by various co-chaperones like DnaJ and Hsp40 and certain cofactors. They aid the chaperones in substrate recognition, and delivery, and stimulate ATP hydrolysis[119]. Nucleotide exchange factors, like Bag1, contribute to the chaperone cycle by modulating the exchange of ADP for ATP[120].

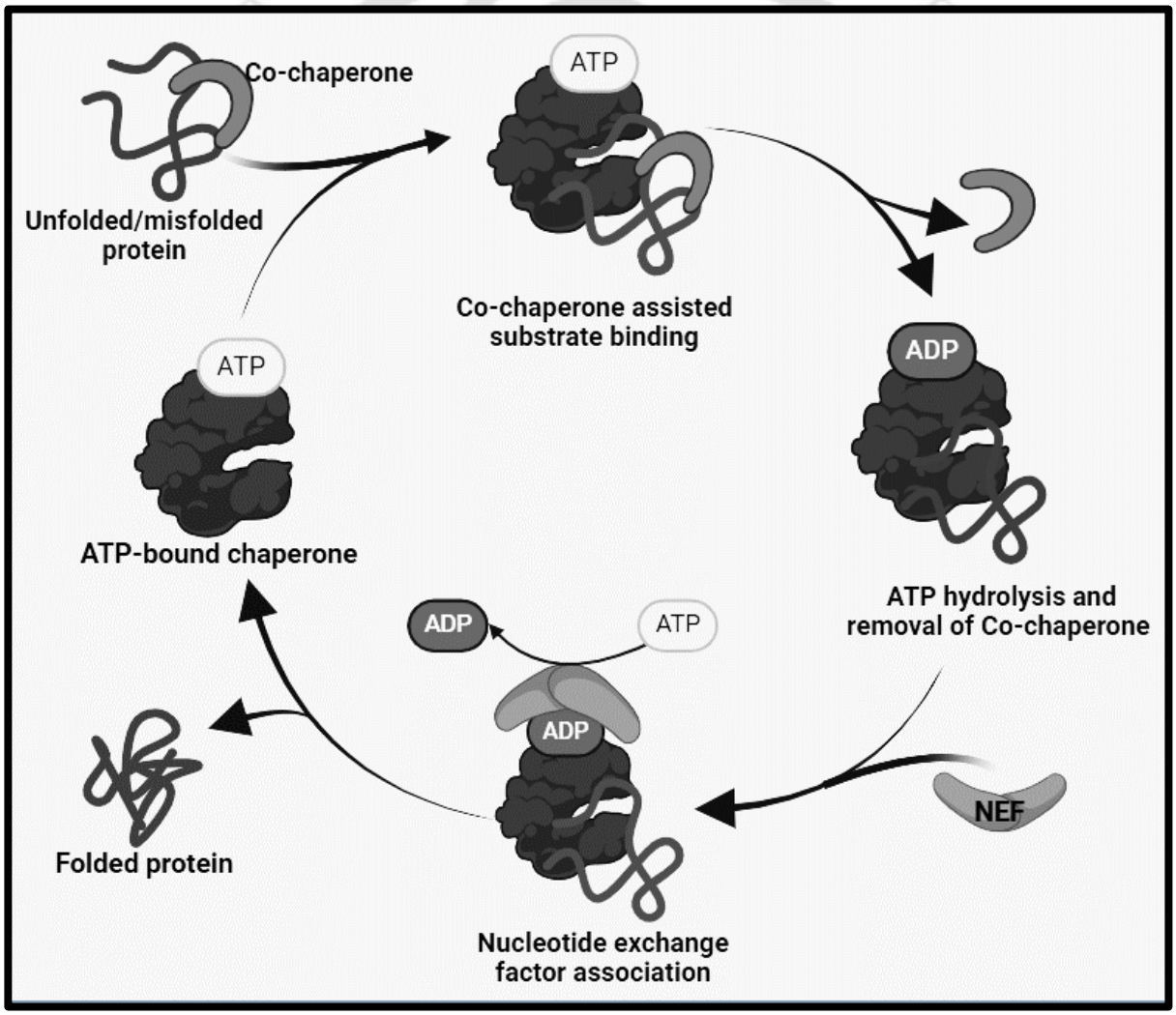

Figure 1.8: Protein folding by the chaperone cycle.

1.8.1 Heat Shock Protein Family A member 8 (HSPA8) – A highly active Stress-responsive protein

Heat shock protein family A member 8 (HSPA8), also known as heat shock cognate 70 (HSC70), is an important member of the heat shock protein 70 (Hsp70) family (**Figure 1.9A**). HSPA8 is composed of two distinct domains that intercommunicate to contribute to the chaperone cycle (**Figure 1.9C**). The N-terminus of HSPA8 consists of a 44kDa nucleotide bind domain (NBD) which binds to ATP and hydrolyzes it to ADP. The ATP binding induces conformational changes in HSPA8 to facilitate substrate binding and the ATP hydrolysis further facilitates the release of the substrate in a folded state. Adjacent to the NBD is the 29 kDa substrate-binding domain which consists of a highly flexible 10 kDa α-helix lid that opens and closes to facilitate the accessibility of a variety of substrate proteins. The conformational changes in this domain are linked to the nucleotide state of the NBD. This domain is also responsible for binding to the co-chaperones and other factors involved in the chaperone cycle[121, 122].

HSPA8 is highly conserved across species and is crucial for maintaining cellular homeostasis by assisting protein folding, transport, and degradation, particularly during stress conditions. The HSPA8 encoding gene is present on chromosome 11 in humans, and it is ubiquitously expressed in various tissues and cell types. The major function of HSPA8 is to facilitate proper protein folding and prevent the aggregation of denatured or misfolded proteins[121]. During normal conditions, it is involved in the proper folding of nascent polypeptides whereas, during stress conditions like heat shock and oxidative stress, it is upregulated to cope with the increased need for its chaperone activity. HSPA8 is also involved in the shuttling of proteins across cellular membranes. It is involved in the translocation of proteins across endoplasmic reticulum and mitochondrial membranes[123, 124]. HSPA8 is also involved in the cellular response to various stressors like oxidative stress, hypoxia, and toxins. It can activate stress-responsive signaling pathways and can modulate cell survival and apoptotic pathways, influencing the fate of stressed cells[125, 126].

HSPA8 is also involved in various human diseases (**Figure 1.9B**). Dysregulation of HSPA8 function is observed in neurodegenerative disorders[127], cancer[128], and cardiovascular

diseases[129]. HSPA8 is often upregulated in cancer and is associated with increased cell survival, drug resistance, and metastasis[130]. HSPA8 is involved in a myriad of cellular phenomena.

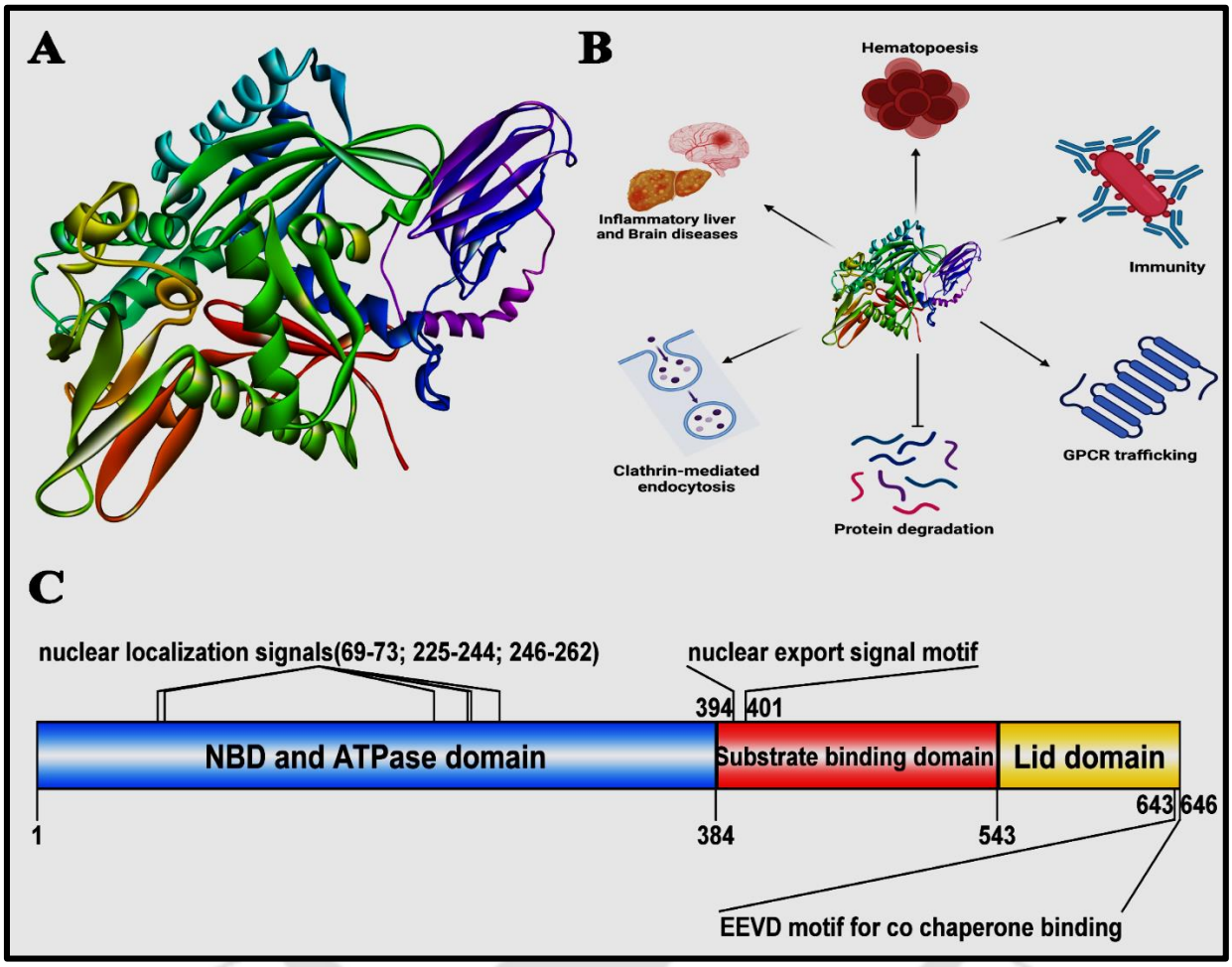

Figure1.9: Structure and Functions of HSPA8. A) Modelled structure of HSPA8 using Phyre2 software with 99 % sequence coverage and >90% confidence using multiple templates. The protein sequence is colour coded as VIBGYOR from C to N-terminus. **B)** Involvement of HSPA8 (center) in diverse cellular phenomenon. **C)** Domain diagram of HSPA8 with its structural motifs, developed using DOG 2.0 software.

1.9 Hypothesis of the study

Malaria is associated with a cyclic occurrence of coldness, chills, and high fever inflicting thermal stress to the body. Also during malaria and other hemolytic diseases, hemoglobin degradation and the release of pro-oxidant molecules induce very high oxidative stress to cells. Heat shock proteins are a major class of proteins highly active and involved in the cytoprotection process during both

heat and oxidative stress. In a previous study in our lab, it has been conclusively deduced that lipopolysaccharide (LPS) stimulation of macrophages leads to the secretion of a proteinaceous cytoprotective factor. This factor protects the macrophages from hemin toxicity by bringing about its polymerization in an H_2O_2-dependent manner. Later the cytoprotective factor was isolated and identified as the human heat shock protein family A member 8 (HSPA8). Based on these preliminary findings and the available literature describing the prominent roles of heat shock protein in the hemin-like environment, we explored the potential of HSPA8 in catalyzing heme polymerization. We also tried to look deeper into the mechanism of this polymerization process. Further, we also explored the impact of hemin on the catalytic ATPase activity of HSPA8 to understand any functional modulation occurring in HSPA8 due to the presence of hemin. Hemin is known to be highly toxic to various cells, tissues, and organs. Although a few studies have implications of hemin toxicity to the liver, much literature is not available describing the direct toxicological effects of hemin on liver cells. To better understand hemin-induced liver toxicity we explored various toxicological aspects that point towards liver damage and dysfunction. Further, we also explored the impact of HSPA8 on the hemin-induced liver toxicity. Based on our hypothesis we framed three major objectives for the study as listed in section 1.10.

1.10 Aims and Objectives of the Study

1. Understanding the in-depth mechanism of hemin detoxification by HSPA8.

- Exploring binding of hemin to HSPA8.
- Revealing the interactions and amino acid residues involved in the binding of hemin to HSPA8.
- Understanding the mechanism of conversion of hemin to heme polymer by HSPA8.

2. Study the modulation of catalytic ATPase activity of HSPA8 in a hemin-like environment.

- Effect of hemin on ATP affinity to HSPA8.
- Revealing the interactions of hemin to the ATPase activity modulation of HSPA8.
- Understanding the functional defect in HSPA8 in the presence of hemin.

3. Exploring the impact of HSPA8 in liver dysfunction and tissue damage caused by hemin accumulation.

- Exploring the role of hemin in liver dysfunction during malaria-like pathological conditions.
- Revealing the mechanism of liver dysfunction caused by hemin during malaria-like pathological conditions.
- Exploring the impact of HSPA8 in liver dysfunction caused by hemin accumulation.

1.11 References

1. Talapko, J., et al., Malaria: the past and the present. Microorganisms, 2019. **7**(6): p. 179.
2. Kokwaro, G., Ongoing challenges in the management of malaria. Malaria journal, 2009. **8**: p. 1-6.
3. Siciliano, G. and P. Alano, Enlightening the malaria parasite life cycle: bioluminescent Plasmodium in fundamental and applied research. Frontiers in microbiology, 2015. **6**: p. 134327.
4. Rother, R.P., et al., The clinical sequelae of intravascular hemolysis and extracellular plasma hemoglobin: a novel mechanism of human disease. Jama, 2005. **293**(13): p. 1653-1662.
5. Phillips, J. and A.C. Henderson, Hemolytic anemia: evaluation and differential diagnosis. American family physician, 2018. **98**(6): p. 354-361.
6. Schaer, D.J., et al., Hemolysis and free hemoglobin revisited: exploring hemoglobin and hemin scavengers as a novel class of therapeutic proteins. Blood, The Journal of the American Society of Hematology, 2013. **121**(8): p. 1276-1284.
7. Dhaliwal, G., P.A. Cornett, and L.M. Tierney Jr, Hemolytic anemia. American family physician, 2004. **69**(11): p. 2599-2607.
8. Robertson, J.J., E. Brem, and A. Koyfman, The acute hemolytic anemias: the importance of emergency diagnosis and management. The Journal of Emergency Medicine, 2017. **53**(2): p. 202-211.
9. Goldberg, D.E., et al., Hemoglobin degradation in the malaria parasite Plasmodium falciparum: an ordered process in a unique organelle. Proceedings of the National Academy of Sciences, 1990. **87**(8): p. 2931-2935.

10. Chan, C.-Y., et al., Erythrocyte degradation, metabolism, secretion, and communication with immune cells in the blood during sepsis: A review. Tzu-Chi Medical Journal, 2022. **34**(2): p. 125.
11. Goldberg, D., Hemoglobin degradation. Malaria: drugs, disease and post-genomic biology, 2005: p. 275-291.
12. Tenhunen, R., H.S. Marver, and R. Schmid, The enzymatic catabolism of hemoglobin: stimulation of microsomal heme oxygenase by hemin. The Journal of laboratory and clinical medicine, 1970. **75**(3): p. 410-421.
13. Rosenthal, P.J., Proteases and hemoglobin degradation. Molecular approaches to malaria, 2005: p. 311-326.
14. Coronado, L.M., C.T. Nadovich, and C. Spadafora, Malarial hemozoin: from target to tool. Biochimica et Biophysica Acta (BBA)-General Subjects, 2014. **1840**(6): p. 2032-2041.
15. Buehler, P.W. and F. D'Agnillo, Toxicological consequences of extracellular hemoglobin: biochemical and physiological perspectives. Antioxidants & redox signaling, 2010. **12**(2): p. 275-291.
16. Deshmukh, R. and V. Trivedi, Role of pro-oxidants from infected rbcs in disturbing homeostasis and pathogenesis during malaria. Austin Journal of Biotechnology & Bioengineering. Austin J Biotechnol Bioeng, 2014. **1**(7): p. 1-5.
17. Nagababu, E. and J.M. Rifkind, Reaction of hydrogen peroxide with ferrylhemoglobin: superoxide production and heme degradation. Biochemistry, 2000. **39**(40): p. 12503-12511.
18. Rodkey, F.L., A mechanism for the conversion of oxyhemoglobin to methemoglobin by nitrite. Clinical Chemistry, 1976. **22**(12): p. 1986-1990.
19. Davis, C.A., L.J. Crowley, and M.J. Barber, Cytochrome b5 reductase: the roles of the recessive congenital methemoglobinemia mutants P144L, L148P, and R159. Archives of biochemistry and biophysics, 2004. **431**(2): p. 233-244.
20. Behera, G., et al., Study of methaemoglobin in malaria patients. Indian Journal of Hematology and Blood Transfusion, 2016. **32**: p. 100-103.
21. Young, J., et al., Methaemoglobin production in normal adults inhaling low concentrations of nitric oxide. Intensive care medicine, 1994. **20**: p. 581-584.
22. D'sa, S., et al., Severe methemoglobinemia due to ingestion of toxicants. Clinical Toxicology, 2014. **52**(8): p. 897-900.
23. Gupta, V., et al., Mutation update: Variants of the CYB5R3 gene in recessive congenital methemoglobinemia. Human Mutation, 2020. **41**(4): p. 737-748.
24. Liu, X. and Z. Spolarics, Methemoglobin is a potent activator of endothelial cells by stimulating IL-6 and IL-8 production and E-selectin membrane expression. American Journal of Physiology-Cell Physiology, 2003. **285**(5): p. C1036-C1046.
25. Umbreit, J., Methemoglobin—it's not just blue: a concise review. American journal of hematology, 2007. **82**(2): p. 134-144.
26. Rifkind, J.M. and E. Nagababu, Hemoglobin redox reactions and red blood cell aging. Antioxidants & redox signaling, 2013. **18**(17): p. 2274-2283.
27. Fedorova, M., R.C. Bollineni, and R. Hoffmann, Protein carbonylation as a major hallmark of oxidative damage: update of analytical strategies. Mass spectrometry reviews, 2014. **33**(2): p. 79-97.

28. Balaji, S. and V. Trivedi, Extracellular methemoglobin mediated early ROS spike triggers osmotic fragility and RBC destruction: an insight into the enhanced hemolysis during malaria. Indian Journal of Clinical Biochemistry, 2012. **27**: p. 178-185.
29. Kanner, J. and S. Harel, Initiation of membranal lipid peroxidation by activated metmyoglobin and methemoglobin. Archives of Biochemistry and Biophysics, 1985. **237**(2): p. 314-321.
30. González-Sánchez, M.I., et al., Mechanism of acetaminophen oxidation by the peroxidase-like activity of methemoglobin. Chemical research in toxicology, 2009. **22**(11): p. 1841-1850.
31. González-Sánchez, M.I., et al., Catalase-like activity of human methemoglobin: A kinetic and mechanistic study. Archives of biochemistry and biophysics, 2011. **516**(1): p. 10-20.
32. Deshmukh, R. and V. Trivedi, Methemoglobin exposure produces toxicological effects in macrophages due to multiple ROS spike induced apoptosis. Toxicology in Vitro, 2013. **27**(1): p. 16-23.
33. Balla, J., et al., Endothelial-cell heme uptake from heme proteins: induction of sensitization and desensitization to oxidant damage. Proceedings of the National Academy of Sciences, 1993. **90**(20): p. 9285-9289.
34. Mumby, S., et al., Methemoglobin-induced signaling and chemokine responses in human alveolar epithelial cells. American Journal of Physiology-Lung Cellular and Molecular Physiology, 2014. **306**(1): p. L88-L100.
35. Wen, W.-N., Methemoglobin contributes to the growth of human tumor cells. Life sciences, 2002. **70**(8): p. 907-916.
36. Bastarache, J.A., J.L. Wynn, and L.B. Ware, Fanning the fire: can methemoglobin enhance neutrophil activation? EBioMedicine, 2015. **2**(3): p. 184-185.
37. Deshmukh, R. and V. Trivedi, Pro-stimulatory role of methemoglobin in inflammation through hemin oxidation and polymerization. Inflammation & Allergy-Drug Targets (Formerly Current Drug Targets-Inflammation & Allergy)(Discontinued), 2013. **12**(1): p. 68-78.
38. Geetha, A., et al., Level of oxidative stress in the red blood cells of patients with liver cirrhosis. Indian Journal of Medical Research, 2007. **126**(3): p. 204-210.
39. Saha, S.A., et al., Methemoglobinemia-induced cardio-respiratory failure secondary to topical anesthesia. American journal of therapeutics, 2006. **13**(6): p. 545-549.
40. Gram, M., et al., Hemoglobin induces inflammation after preterm intraventricular hemorrhage by methemoglobin formation. Journal of neuroinflammation, 2013. **10**(1): p. 1-13.
41. Lavezzi, A.M., et al., Brain iron accumulation in unexplained fetal and infant death victims with smoker mothers-the possible involvement of maternal methemoglobinemia. BMC pediatrics, 2011. **11**: p. 1-9.
42. Shumilova, T., et al., Oxygen regime in rat brain tissues under conditions of acute nitrite methemoglobinemia. Journal of Evolutionary Biochemistry and Physiology, 2006. **42**: p. 77-83.
43. Adhit, K.K., et al., Toxin-Induced Methemoglobinemia With Kidney Injury and Hypoxic Brain Injury in a Case of Pesticide Poisoning: A Case Report. Cureus, 2022. **14**(12).
44. Khan, F.A., et al., Headache and methemoglobinemia. Headache: The Journal of Head and Face Pain, 2020. **60**(1): p. 291-297.

45. Hirono, H., Lipids of myelin, white matter and gray matter in a case of generalized deficiency of cytochrome b5 reductase in congenital methemoglobinemia with mental retardation. Lipids, 1980. **15**(4): p. 272-275.
46. Qureshi, A.H., et al., Methemoglobinemia-induced acute kidney injury. The open urology & nephrology journal, 2013. **6**(1).
47. Ruiz-Guinazu, A., J. Coelho, and R. Paz, Methemoglobin-Induced Acute Renal Failure in the Rat: Invivo Observation Histology Micropuncture Measurements of Intratubular Postglomerular Vascular Pressures. Nephron, 1967. **4**(5): p. 257-275.
48. Lalich, J.J., The role of oxyhemoglobin and its derivatives in the pathogenesis of experimental hemoglobinuric nephrosis. The American Journal of Pathology, 1955. **31**(1): p. 153.
49. Fischer, H., On haemin and the relationships between haemin and chlorophyll. Nobel Lecture Dec, 1930. **11**.
50. Thirstrup, D. and G.S. Baird, Histochemical application of a peroxidase DNAzyme with a covalently attached hemin cofactor. Analytical chemistry, 2010. **82**(6): p. 2498-2504.
51. Kang, B., et al., Noncovalent minimal assembly of exogenous histamine with hemin cofactor as a peroxidase-mimicking cooperative catalyst. Iscience, 2022. **25**(10).
52. Suzuki, H., et al., Heme regulates gene expression by triggering Crm1-dependent nuclear export of Bach1. The EMBO journal, 2004. **23**(13): p. 2544-2553.
53. Georgiou-Siafis, S.K. and A.S. Tsiftsoglou, Activation of KEAP1/NRF2 stress signaling involved in the molecular basis of hemin-induced cytotoxicity in human pro-erythroid K562 cells. Biochemical pharmacology, 2020. **175**: p. 113900.
54. Lu, X., J. Chen-Roetling, and R.F. Regan, Systemic hemin therapy attenuates blood–brain barrier disruption after intracerebral hemorrhage. Neurobiology of disease, 2014. **70**: p. 245-251.
55. Anderson, K.E., et al., Recommendations for the diagnosis and treatment of the acute porphyrias. Annals of internal medicine, 2005. **142**(6): p. 439-450.
56. Sun, B., et al., Once-monthly hemin suppresses inflammatory and autoreactive CD4+ T cell responses to robustly ameliorate experimental rheumatoid arthritis. Iscience, 2021. **24**(10).
57. Pethő, D., et al., Heme cytotoxicity is the consequence of endoplasmic reticulum stress in atherosclerotic plaque progression. Scientific reports, 2021. **11**(1): p. 10435.
58. Grunwald, E.W. and M.P. Richards, Mechanisms of heme protein-mediated lipid oxidation using hemoglobin and myoglobin variants in raw and heated washed muscle. Journal of Agricultural and Food Chemistry, 2006. **54**(21): p. 8271-8280.
59. Vasconcellos, L.R., et al., Protein aggregation as a cellular response to oxidative stress induced by heme and iron. Proceedings of the National Academy of Sciences, 2016. **113**(47): p. E7474-E7482.
60. Gamage, S.M.K., et al., Hemin, a major heme molecule, induced cellular and genetic alterations in normal colonic and colon cancer cells. Pathology-Research and Practice, 2021. **224**: p. 153530.
61. Kumar, S. and U. Bandyopadhyay, Free heme toxicity and its detoxification systems in human. Toxicology letters, 2005. **157**(3): p. 175-188.
62. Kozlova, E., et al., Transformation of membrane nanosurface of red blood cells under hemin action. Scientific Reports, 2014. **4**(1): p. 6033.

63. Kirschner-Zilber, I., E. Rabizadeh, and N. Shaklai, The interaction of hemin and bilirubin with the human red cell membrane. Biochimica et Biophysica Acta (BBA)-Biomembranes, 1982. **690**(1): p. 20-30.
64. Nuchsongsin, F., et al., Effects of malaria heme products on red blood cell deformability. The American journal of tropical medicine and hygiene, 2007. **77**(4): p. 617-622.
65. Jarolim, P., et al., Effect of hemoglobin oxidation products on the stability of red cell membrane skeletons and the associations of skeletal proteins: correlation with a release of hemin. 1990.
66. Solar, I., J. Dulitzky, and N. Shaklai, Hemin-promoted peroxidation of red cell cytoskeletal proteins. Archives of biochemistry and biophysics, 1990. **283**(1): p. 81-89.
67. Schmitt, T.H., W. Frezzatti, and S. Schreier, Hemin-induced lipid membrane disorder and increased permeability: a molecular model for the mechanism of cell lysis. Archives of biochemistry and biophysics, 1993. **307**(1): p. 96-103.
68. Chiu, D.T., et al., Hemin-induced membrane sulfhydryl oxidation: possible involvement of thiyl radicils. Free radical research, 1997. **27**(1): p. 55-62.
69. Boas, F.E., L. Forman, and E. Beutler, Phosphatidylserine exposure and red cell viability in red cell aging and in hemolytic anemia. Proceedings of the National Academy of Sciences, 1998. **95**(6): p. 3077-3081.
70. Fader, C.M., et al., Hemin induces mitophagy in a leukemic erythroblast cell line. Biology of the Cell, 2016. **108**(4): p. 77-95.
71. Banesh, S., S. Layek, and V. Trivedi, Hemin acts as CD36 ligand to activate down-stream signalling to disturb immune responses and cytokine secretion from macrophages. Immunology Letters, 2022. **243**: p. 1-18.
72. Cambos, M. and T. Scorza, Robust erythrophagocytosis leads to macrophage apoptosis via a hemin-mediated redox imbalance: role in hemolytic disorders. Journal of leukocyte biology, 2011. **89**(1): p. 159-171.
73. Li, B., et al., Macrophage ferroptosis promotes MMP2/9 overexpression induced by hemin in hemorrhagic plaque. Thrombosis and Haemostasis, 2023.
74. Dang, T.N., et al., Uptake, metabolism and toxicity of hemin in cultured neurons. Neurochemistry international, 2011. **58**(7): p. 804-811.
75. Goldstein, L., et al., Hemin induces an iron-dependent, oxidative injury to human neuron-like cells. Journal of neuroscience research, 2003. **73**(1): p. 113-121.
76. Dang, T.N., et al., The metabolism and toxicity of hemin in astrocytes. Glia, 2011. **59**(10): p. 1540-1550.
77. Regan, R.F., et al., Activation of extracellular signal-regulated kinases potentiates hemin toxicity in astrocyte cultures. Journal of neurochemistry, 2001. **79**(3): p. 545-555.
78. Levy, Y.S., et al., Hemin-induced apoptosis in PC12 and neuroblastoma cells: implications for local neuronal death associated with intracerebral hemorrhage. Neurotoxicity research, 2002. **4**: p. 609-616.
79. Gemelli, C., et al., Cytotoxic effect of hemin in colonic epithelial cell line: Involvement of 18 kDa translocator protein (TSPO). Life Sciences, 2014. **107**(1-2): p. 14-20.
80. Wilson, S.J. and A.K. Keenan, Role of hemin in the modulation of H2O2-mediated endothelial cell injury. Vascular pharmacology, 2003. **40**(2): p. 109-118.
81. Higdon, A.N., et al., Hemin causes mitochondrial dysfunction in endothelial cells through promoting lipid peroxidation: the protective role of autophagy. American Journal of Physiology-Heart and Circulatory Physiology, 2012. **302**(7): p. H1394-H1409.

82. Robinson, S.R., et al., Hemin toxicity: a preventable source of brain damage following hemorrhagic stroke. Redox Report, 2009. **14**(6): p. 228-235.
83. Babu, R., et al., Thrombin and hemin as central factors in the mechanisms of intracerebral hemorrhage–induced secondary brain injury and as potential targets for intervention. Neurosurgical focus, 2012. **32**(4): p. E8.
84. Augustynek, B., et al., Hemin inhibits the large conductance potassium channel in brain mitochondria: a putative novel mechanism of neurodegeneration. Experimental neurology, 2014. **257**: p. 70-75.
85. Singla, S., et al., Hemin causes lung microvascular endothelial barrier dysfunction by necroptotic cell death. American journal of respiratory cell and molecular biology, 2017. **57**(3): p. 307-314.
86. Butt, O.I., P.W. Buehler, and F. D'Agnillo, Blood-brain barrier disruption and oxidative stress in guinea pig after systemic exposure to modified cell-free hemoglobin. The American journal of pathology, 2011. **178**(3): p. 1316-1328.
87. Dey, S., et al., Impact of intravascular hemolysis in malaria on liver dysfunction: involvement of hepatic free heme overload, NF-κB activation, and neutrophil infiltration. Journal of Biological Chemistry, 2012. **287**(32): p. 26630-26646.
88. Rossi, M., et al., Dual effect of hemin on renal ischemia-reperfusion injury. Biochemical and biophysical research communications, 2018. **503**(4): p. 2820-2825.
89. Tabibzadeh, N., et al., Plasma heme-induced renal toxicity is related to a capillary rarefaction. Scientific Reports, 2017. **7**(1): p. 40156.
90. Dalapati, T. and J.M. Moore, Hemozoin: A complex molecule with complex activities. Current clinical microbiology reports, 2021. **8**: p. 87-102.
91. Carney, C.K., et al., The basis of the immunomodulatory activity of malaria pigment (hemozoin). JBIC Journal of Biological Inorganic Chemistry, 2006. **11**: p. 917-929.
92. Sun, J., et al., Can hemozoin alone cause host anaemia? Parasitology research, 2016. **115**: p. 4611-4616.
93. Lamikanra, A.A., et al., Hemozoin (malarial pigment) directly promotes apoptosis of erythroid precursors. PloS one, 2009. **4**(12): p. e8446.
94. Skorokhod, O.A., et al., Inhibition of erythropoiesis in malaria anemia: role of hemozoin and hemozoin-generated 4-hydroxynonenal. Blood, The Journal of the American Society of Hematology, 2010. **116**(20): p. 4328-4337.
95. Coban, C., et al., Toll-like receptor 9 mediates innate immune activation by the malaria pigment hemozoin. The Journal of experimental medicine, 2005. **201**(1): p. 19-25.
96. Dostert, C., et al., Malarial hemozoin is a Nalp3 inflammasome activating danger signal. PloS one, 2009. **4**(8): p. e6510.
97. Schwarzer, E., et al., Malaria-parasitized erythrocytes and hemozoin nonenzymatically generate large amounts of hydroxy fatty acids that inhibit monocyte functions. Blood, The Journal of the American Society of Hematology, 2003. **101**(2): p. 722-728.
98. Schwarzer, E., et al., Increased levels of 4-hydroxynonenal in human monocytes fed with malarial pigment hemozoin A possible clue for hemozoin toxicity. FEBS letters, 1996. **388**(2-3): p. 119-122.
99. Prato, M., et al., Natural haemozoin modulates matrix metalloproteinases and induces morphological changes in human microvascular endothelium. Cellular Microbiology, 2011. **13**(8): p. 1275-1285.

100. Deroost, K., et al., Hemozoin induces lung inflammation and correlates with malaria-associated acute respiratory distress syndrome. American Journal of Respiratory cell and molecular biology, 2013. **48**(5): p. 589-600.
101. Eugenin, E.A., J.A. Martiney, and J.W. Berman, The malaria toxin hemozoin induces apoptosis in human neurons and astrocytes: potential role in the pathogenesis of cerebral malaria. Brain research, 2019. **1720**: p. 146317.
102. Pham, T.-T., et al., Hemozoin in malarial complications: more questions than answers. Trends in parasitology, 2021. **37**(3): p. 226-239.
103. Deroost, K., et al., Hemozoin induces hepatic inflammation in mice and is differentially associated with liver pathology depending on the Plasmodium strain. PloS one, 2014. **9**(11): p. e113519.
104. Levesque, M., A. Sullivan, and S. Meshnick, Splenic and hepatic hemozoin in mice after malaria parasite clearance. The Journal of parasitology, 1999: p. 570-573.
105. Arese, P. and E. Schwarzer, Malarial pigment (haemozoin): a very active 'inert'substance. Annals of Tropical Medicine & Parasitology, 1997. **91**(5): p. 501-516.
106. Lucchi, N.W., et al., Natural hemozoin stimulates syncytiotrophoblast to secrete chemokines and recruit peripheral blood mononuclear cells. Placenta, 2011. **32**(8): p. 579-585.
107. de Villiers, K.A. and T.J. Egan, Heme detoxification in the malaria parasite: A target for antimalarial drug development. Accounts of chemical research, 2021. **54**(11): p. 2649-2659.
108. Jani, D., et al., HDP—a novel heme detoxification protein from the malaria parasite. PLoS pathogens, 2008. **4**(4): p. e1000053.
109. Martin, R.E., The transportome of the malaria parasite. Biological Reviews, 2020. **95**(2): p. 305-332.
110. Chukwudi, I.N., C.A. Onyetugo, and I.N. Amarachi, Peroxidase, an example of enzymes with numerous applications. Asian Journal of Chemical Sciences, 2021. **10**(2): p. 11-22.
111. Trivedi, V., et al., Mechanism of horseradish peroxidase-catalyzed heme oxidation and polymerization (β-hematin formation). Biochimica et Biophysica Acta (BBA)-General Subjects, 2005. **1723**(1-3): p. 221-228.
112. Costa-Mattioli, M. and P. Walter, The integrated stress response: From mechanism to disease. Science, 2020. **368**(6489): p. eaat5314.
113. Pakos-Zebrucka, K., et al., The integrated stress response. EMBO reports, 2016. **17**(10): p. 1374-1395.
114. Hartl, F.U., A. Bracher, and M. Hayer-Hartl, Molecular chaperones in protein folding and proteostasis. Nature, 2011. **475**(7356): p. 324-332.
115. Meimaridou, E., S.B. Gooljar, and J.P. Chapple, From hatching to dispatching: the multiple cellular roles of the Hsp70 molecular chaperone machinery. Journal of molecular endocrinology, 2009. **42**(1): p. 1-9.
116. Voellmy, R. and F. Boellmann, Chaperone regulation of the heat shock protein response. Molecular aspects of the stress response: chaperones, membranes and networks, 2007: p. 89-99.
117. Kumsta, C. and U. Jakob, Redox-regulated chaperones. Biochemistry, 2009. **48**(22): p. 4666-4676.
118. Evstigneeva, Z., N. Solov'eva, and L. Sidel'nikova, Structures and functions of chaperones and chaperonins. Applied Biochemistry and Microbiology, 2001. **37**: p. 1-13.

119. Shiber, A. and T. Ravid, Chaperoning proteins for destruction: diverse roles of Hsp70 chaperones and their co-chaperones in targeting misfolded proteins to the proteasome. Biomolecules, 2014. **4**(3): p. 704-724.
120. Alberti, S., C. Esser, and J. Höhfeld, BAG-1—a nucleotide exchange factor of Hsc70 with multiple cellular functions. Cell stress & chaperones, 2003. **8**(3): p. 225.
121. Stricher, F., et al., HSPA8/HSC70 chaperone protein: structure, function, and chemical targeting. Autophagy, 2013. **9**(12): p. 1937-1954.
122. Silva, N.S.M., et al., Structural, thermodynamic and functional studies of human 71 kDa heat shock cognate protein (HSPA8/hHsc70). Biochimica et Biophysica Acta (BBA)-Proteins and Proteomics, 2021. **1869**(12): p. 140719.
123. Wang, F., et al., Blocking nuclear export of HSPA8 after heat shock stress severely alters cell survival. Scientific reports, 2018. **8**(1): p. 16820.
124. Kodiha, M., et al., Stress inhibits nucleocytoplasmic shuttling of heat shock protein hsc70. American Journal of Physiology-Cell Physiology, 2005. **289**(4): p. C1034-C1041.
125. Aggarwal, A., Effect of Thermal Stress on the Intracellular Localization of the Constitutively Expressed Heat Shock Protein HSPA8 (Hsc70) in Differentiated and Undifferentiated Cultured Human Neuronal Cells, 2019, University of Toronto (Canada).
126. Tian, H., et al., Effect of HSPA8 gene on the proliferation, apoptosis and immune function of HD11 cells. Developmental & Comparative Immunology, 2023. **142**: p. 104666.
127. Sirtori, R., et al., HSPA8 knock-down induces the accumulation of neurodegenerative disorder-associated proteins. Neuroscience letters, 2020. **736**: p. 135272.
128. Tian, Y., et al., Maslinic acid induces autophagy by down-regulating HSPA8 in pancreatic cancer cells. Phytotherapy Research, 2018. **32**(7): p. 1320-1331.
129. He, M., et al., Genetic variations in HSPA8 gene associated with coronary heart disease risk in a Chinese population. PLoS One, 2010. **5**(3): p. e9684.
130. Liu, Y.-y. and X.-b. He, High Expression of HSPA8 Is A Favorable Prognostic Factor in Colon Cancer. 2021.

Chapter II

Experimental Procedures

2.1 Introduction

The success of addressing a research problem and finding a logical and conclusive answer, to a great extent, relies on employing a foolproof scientific approach, proper experimental protocols, and the quality of the used resources. To ensure the reproducibility and comprehension of the findings of this research, this chapter emphasizes the details of the workflow undertaken to answer the addressed questions of the thesis (**Figure 2.1**), the procedures used to perform all the experiments, and the details of all the materials used in the experiments.

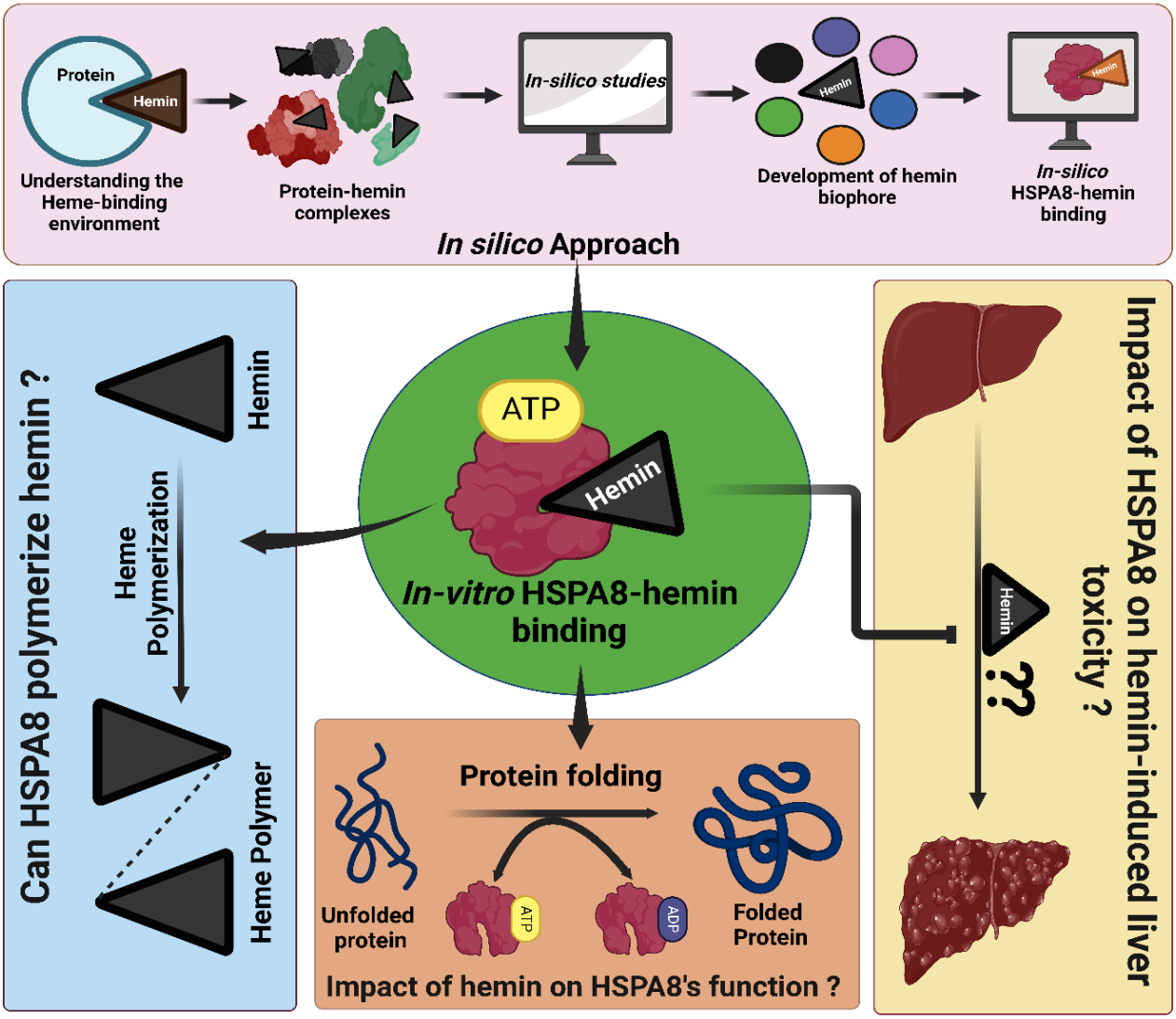

Figure 2.1: The hypothesis and experimental approach for the study presented in the thesis.

2.3 Materials

Human HSPA8 clone pcDNA5/FRT/TO HIS HSPA8 was gifted by Harm Kampinga (Addgene plasmid # 19541). DNA Ladder and Restriction enzymes BamHI (#R0136S) and XhoI (#R0146S) were from New England BioLabs, USA. EmeraldAmp GT PCR Master Mix (#RR310A) and Mighty TA cloning Kit (#6028) were purchased from Takara Bio INC, India. DNA Ligase was from genetics, India. DH5α and BL21-(DE3) bacterial strains and vectors (pET23a and pET28a) were purchased from Novagen, India. Sodium azide (#MB075) was purchased from Himedia, India. PBN (#B7263), and clotrimazole (#6019) were procured from Sigma-Aldrich, India. Guaiacol (#072826), potassium iodide (#1649167), and potassium chloride (#1649161) were ordered from SRL Diagnostics, India. Hemin (#H9039), dithiothreitol (#43819), and magnesium chloride (#M2670) were purchased from Sigma, India. Lysozyme (#MB098) from chicken egg white, ATP (#TC085), and Malachite green (#S020) were from Himedia, India. Ammonium molybdate (#014892) was from SRL, India, and the DH5α *E.coli* bacterial strain was obtained from Novagen, India. The chemicals and reagents used were of high quality and purity. Dulbecco's modified eagle's medium and 3-(4, 5-dimethylthiazol-2-yl)-2,5-diphenyltetrazolium bromide (MTT) from Sigma Aldrich (St. Louis, MO, USA). Acridine orange (AO), propidium iodide (PI), Ethidium bromide (Et-Br), DMSO (cell-culture grade), Proteinase K, RNase-A, ethylenediamine tetraacetic acid (EDTA), 100% ethanol, sodium chloride, Tris-base, NP-40 detergent and Triton-X 100 were purchased from Merck (Massachusetts, USA). DMEM: F12 media was purchased from GIBCO (USA). Foetal Bovine Serum (FBS), Penicillin-Streptomycin (100X) antibiotic solution, Phosphate Buffer Saline (PBS), Sodium Azide, tween-20, trypan blue, and trypsin were obtained from HiMedia (Mumbai, India). All the cell culture plates and dishes were purchased from Corning, Lowell, MA, USA. Death receptor antibody sampler kit (cat. # 29603), autophagy antibody sampler kit (cat. # 4445), apoptosis/necroptosis antibody sampler kit (cat. # 92570), and antibodies to cyclin A2 (cat. # 67955), GAPDH (cat. # 5174) were purchased from cell signaling technology, Inc (USA). Antibodies detecting β-actin (cat. # BB-AB0024), Bcl2 (cat. # BB-AB0230), and PARP-1 (cat. # BB-AB0280) were procured from Bio-Bharathi Life Science Private Ltd. (India).

2.4 *In-silico* Studies

2.4.1 Distance-based biophore fingerprinting

To predict the hemin biophore, heme-protein complexes from distantly related organisms exhibiting diverse functions were analyzed. A total of seven hemin-bound protein complexes from the protein data bank (PDB) database were downloaded. Heme or hemin similars bound to Rat Heme oxygenase (1DVE), sperm whale oxymyoglobin (1MBO), Human serum albumin (1O9X), Ferric cytochrome P450cam from *Pseudomonas puitida* (2Z97, 2ZAW), IsdG from *Staphylococcus aureus* (2ZDO), and Heme oxygenase from *Helicobacter pylori* (3GAS) were analyzed for the biophoric constituents. The immediate binding environment of hemin in the complexes was characterized using the ContPro web server[1]. We identified 10 recurring residues (occurrence >= 5) in the seven complexes with Phe, Leu, Val, Arg, and Ile as the most repeated (>8 repeats) residues. Atom-atom distance fingerprint of hemin and different proteins was constructed in the form of a distance matrix (104 X 45)) with color coding in the VIBGYOR scale.

2.4.2 Interaction-based biophore fingerprinting

An interaction matrix (27 X 16) was constructed by visualizing the type, bond length, and repetition of the interactions between hemin and protein atoms across all seven complexes using Biovia Discovery Studio[2]. Recurring residues were ranked for their significance based on the type of interaction (H-bond>Electrostatic>Hydrophobic) and the number of repeats of each interaction. Based on the analysis of the matrices, HSPA8 3D-structure was screened for the presence of any pocket having most of the identified residues, and hemin was docked in that pocket for validating its binding.

2.4.3 Molecular docking

A docking study using Autpdock tools-1.5.6[3] was performed to validate the determined hemin biophore. The crystal structure of HSC70/HSPA8 (1ATR) from *Bos Taurus*, having 100% sequence similarity to human HSPA8, was downloaded from PDB, and energy was minimized using the Swiss PDB viewer[4]. Hemin (ID: 401223) 3D-structure was downloaded from the

chemspider database and energy was minimized using chem3D ultra. Hemin was docked to HSPA8 at the site where biophoric interactions were high. A genetic algorithm run of 100, a cluster tolerance of 2 Å, and a torsional degree of freedom 8 were used as docking parameters. The docked conformations were ranked based on their respective binding energies.

2.4.4 Residue contribution analysis for Hemin binding

The contribution of residues in the binding and stability of the hemin-HSPA8 complex was analyzed through *in-silico* site-directed mutagenesis using an ABS scan web server[5]. The residues within 4.5 Å of the ligand in the docked complex with minimum binding energy were subjected to *in-silico* alanine mutation and the Gibbs free energy change upon each mutation was plotted. The residues were ranked for their relative prominence in hemin binding based on the observed Gibbs free energy change after each mutation.

2.4.5 Competitive docking of ATP and Hemin

To visualize the competition between ATP and hemin, docking of both the ligands was performed at the known ATP binding site of HSPA8 using Autodock 4.2. 3D structures of HSPA8 (PDB ID-1ATR), ATP, and hemin were downloaded from PDB. ATP and hemin were docked individually to compare their apparent binding affinities for the ATP binding site. For competitive docking, ATP was again docked to HSPA8 with hemin already present at the site to observe whether ATP can replace hemin from the pocket. Energy-minimized structures were used for docking and 100 GA runs were performed for each. The best-docked confirmations were analyzed, in Autodock to determine their binding energies and in Pymol 2.5.5 for residue-atom interactions. The Autodock results were further cross-verified based on the fitness score (total energy) obtained using iGEMDOCK version 2.1 docking software[6].

2.4.6 MD simulation studies of HSPA8-ATP complexes

Simulation studies using, GROMACS 2018.1[7], were performed to visualize the stability of the ATP-HSPA8 complexes in the absence and presence of hemin. CHARMM-GUI web server[8] was used for generating the topology files by employing the CHARMM36 force field. The system was energy minimized and the interactions were constrained using the Lincs algorithm. The system

temperature and pressure were 300 K and 1 atm pressure respectively and the solvation was done in a dodecahedron box with the complexes at a distance of 1 nm from the edges. Sodium (Na^+) and chloride (Cl^-) ions were used for charge neutralization. The run was performed for 100 ns with 2fs integration steps under NVT followed by NPT thermal equilibration conditions. The convergence of the 100 ns simulation run was confirmed by root mean square deviation and cluster population analysis. The results were analyzed for common simulation parameters to determine the stability and quality of the complexes using Pymol and images were generated in QtGrace 0.2.6 software.

2.5 Cloning of HSPA8 and its truncation products

The plasmid containing the HIS-tagged *hspa8* gene was isolated using the Nucleospin Plasmid isolation Kit (#749588.50) from Macherey-Nagel. Similar procedures were followed for the cloning of *hspa8* (1970 bps) in *pEt23a,* and *hspa8_nbd* (1158 bps) and *hspa8_ct* (780 bps) in the pET28a vectors with the isolated plasmid as a template. The genes were PCR amplified using a CG Palm cycler (#CG-9600-000) and the amplification was confirmed by agarose gel electrophoresis. The amplification parameters are listed in Table S1 in the supplementary information. The observed bands were gel-eluted using a Silica-kit (#MB503) from HiMedia, India, and the products were ligated to the corresponding vectors. The plasmids were isolated and subjected to double digestion. The cloning was finally confirmed by agarose gel electrophoresis.

2.6 Overexpression and purification of HSPA8 and its truncation products

The clones were transformed into BL21-(DE3) competent cells and the corresponding proteins were overexpressed by induction with 1mM IPTG for 4 hours in 5ml of LB media at 37ºC. The overexpression was confirmed through SDS-PAGE and western blot using anti-HIS antibodies. For purification, cells were harvested, from a 250ml culture, by centrifugation. The pellet was resuspended in 20 ml lysis buffer (50 mM Tris-HCl + 300 mM NaCl + 20 mM imidazole, pH 8.8) and subjected to sonication for 30 minutes in an ultrasonic processor (VC 505, Vibra-Cell). The lysate was then centrifuged at 13000 rpm, 30 minutes, 4ºC, and the supernatant was incubated with a pre-charged Ni-NTA manual column for 30 minutes at 4ºC. The proteins HSPA8, HSPA8_NBD,

and HSPA8_CT were eluted with lysis buffer containing 70 mM, 250 mM, and 250 mM imidazole, respectively. The purified protein bands were analyzed using SDS-PAGE. Imidazole in the eluted protein fractions was removed by dialysis and gel filtration before performing further experiments.

2.7 Heme polymerization activity of HSPA8

The heme polymerizing potential of HSPA8 and its domains was assayed using the Heme Polymerization assay as described earlier[9, 10]. Briefly, 0 to 100 µg/ml of HSPA8 or its domains were incubated with 100 µM hemin in 100 mM sodium acetate buffer (pH 5.2), and 5 mM H_2O_2 for 12 hours at 37°C. The reaction was stopped by centrifuging the mixture at 12000 rpm for 10 minutes. The pellet of heme polymer obtained was washed two times with 100 mM Tris_Hcl buffer (pH 7.8) containing 2.5% SDS and thrice with 100 mM bicarbonate buffer (pH 9.2). The pellet was then dissolved in 50 µl of 2N NaOH and heated at 60°C for complete dissolution. It was finally diluted to 1 ml with Milli-Q water and absorbance was recorded at 400 nm. The amount of polymer formed was calculated using an extinction coefficient of 91 $mM^{-1}cm^{-1}$. Inhi bition experiments were performed by adding the substrates or inhibitors before adding hemin and H_2O_2.

2.8 FT-IR spectroscopy of heme polymer formed by HSPA8

The FTIR spectrum was recorded by diffuse reflection method in a schimadzu FT-IR spectrophotometer (IRAffinity-1S, A221355). Lyophilized and dried powder (5 mg) of the heme polymer formed by HSPA8 was mixed with 50 mg of finely powdered KBr and kept in the sample container for the scan. 50 scans per sample were taken and KBr powder was used for taking the background spectrum. The obtained spectra were smoothened and the baseline was corrected. The FTIR spectrum of synthetic β-hematin powder and hemin powder was recorded for comparison with that of the heme polymer formed by HSPA8.

2.9 Optical difference spectroscopy for hemin binding

Optical difference spectroscopy was performed to determine the binding affinity of hemin for HSPA8 and its domains. Hemin stock (1 mM) was prepared by dissolving the required quantity in 50 µl of 2N NaOH and then diluting it to 1 ml with phosphate buffer, pH 7.2. 1 ml quartz cuvette in the sample cell was filled with 1 µM of protein dissolved in phosphate buffer pH 7. Hemin,

dissolved in the same buffer, was added in gradually increasing concentrations to the sample cuvette to observe a dipping peak around 400 nm, and parallelly an equal volume of the hemin was added to the reference cuvette containing only the buffer to nullify the effect of dilution. Absorbance difference was noted from the UV spectra recorded immediately after each addition and the K_d value was calculated using the following equation[11]

$$\mathbf{1/\Delta A = (K_d / \Delta A_\alpha)1/S + 1/\Delta A_\alpha}$$

Where ΔA denotes the absorbance difference, K_d is the dissociation constant, S is the ligand concentration, and ΔA_α is the absorption at saturating ligand concentration. The $1/\Delta A$ values were plotted against 1/[Hemin] values and the obtained plot was fitted as a straight line. The K_d values were calculated using the slope and intercept of the obtained linear equation.

2.10 Peroxidase activity assay of HSPA8-hemin complex

Guaiacol to tetraguaiacol conversion was monitored to determine the peroxidase activity of the complex as described[12]. Variable concentrations of guaiacol (0-100mM) were taken in a 300 µl reaction mixture containing 2 µM of complex, and 0.27 mM H_2O_2 in 100 mM acetate buffer pH 5.2. The amount of tetraguaiacol formed was quantified by recording the absorbance at 470 nm and using an extinction coefficient of 6.48 $mMcm^{-1}$. The reaction velocity versus substrate concentration was plotted to find out the enzymatic parameters like the turnover number, $V_{max,}$ and K_m using the Michaelis-Menten fit and Line Weaver-Burk plot.

2.11 Optical Spectroscopy to confirm single electron transfer

The HSPA8-hemin complex was prepared by incubating 1µM of HSPA8 with 10µM hemin for 30 minutes in sodium phosphate buffer pH 7.2 at room temperature with mild shaking and then dialyzing the mixture against the same buffer to remove unbound hemin. The absorption spectra before and immediately after the addition of H_2O_2 (3 µM) to 1 µM of the complex were recorded to observe any shift in the soret peak around 400 nm. Peroxidase substrate (20 mM) was added to observe the retention of the soret peak and formation of the product.

2.12 Measurement of ATPase activity of HSPA8

Effect of hemin on the known ATPase activity of HSPA8 was studied by measuring the activity in the absence and presence of hemin. The measurements of the ATPase activity were performed through a Malachite green assay[13].

2.12.1 Preparation of Malachite green Detection reagent

This reagent was prepared by first adding 60 ml of concentrated sulphuric acid slowly to 300 ml of milli-Q water and cooling it down to room temperature. To this 0.44g of malachite green was added and vortexed to dissolve completely. Two and a half ml of 7.5% ammonium molybdate was added to 10 ml of this solution just before adding it for detection.

2.12.2 Malachite green Assay

ATP stock (50 mM) was prepared in HNG buffer (20 mM Hepes + 13 mM NaCl + 5% glycerol, pH 8.5) and was mixed with an equal volume of 250 mM $MgCl_2$ to get a stock of 25 mM ATP and 125 mM $MgCl_2$. HSPA8 (0.2 µM) was incubated with different concentrations of ATP ranging from 0 to 12000 µM in HNG buffer for 45 minutes with or without hemin (0-50 µM). Following incubation, the reactions were stopped by keeping them at -80ºC for 30 minutes, and 50 µl of malachite green detection reagent was added to each reaction. Absorbance was taken at 650 nm using a Spinco spectrophotometer. The amount of free phosphate formed was calculated using the calibration curve of standard free phosphate concentrations. The processing of raw data was performed in origin-pro software[14] and the Michaelis-Menten fit was employed to calculate the kinetic parameters V_{max} and K_m using the equation:

$$\mathbf{v = V_{max}[S] / K_m + [S]}$$

where v is the velocity of enzymatic reaction, V_{max} denotes the maximum velocity, K_m is the Michaelis constant, and S denotes the substrate (ATP) concentration. A Lineweaver-Burk plot with 1/v on the y-axis and 1/[S] on the x-axis was plotted to further confirm the type of inhibition.

The inhibition constant (K_i) was calculated from the obtained V_{max} and K_m values by extrapolating the straight line obtained from the K_m/V_{max} Vs [S] graph. The point of intersection of the line on the x-axis corresponds to the K_i value. Controls for each ATP concentration were kept and subtracted from the test reaction to nullify the absorbance from the auto degradation of ATP.

2.13 Measurement of ATPase-dependent Chaperone activity of HSPA8

The effect of hemin on chaperone function was tested by examining the refolding of a model protein lysozyme by HSPA8 in the absence and presence of hemin. 100 μM Lysozyme stock was prepared in 10 mM sodium phosphate buffer, pH 7. Lysozyme was subjected to unfolding by heating at 42°C for 30 minutes in a water bath[15]. The unfolding of lysozyme leads to a decrease in its intrinsic fluorescence[16, 17]. First, the time and concentration of HSPA8 required for complete refolding of the heat-unfolded lysozyme was optimized and these parameters were used to examine the effect of hemin on its refolding activity.

2.13.1 Refolding of lysozyme by HSPA8

The refolding experiment was performed in refolding buffer containing 25 mM HEPES + 50 mM KCl + 2 mM ATP + 5 mM $MgCl_2$ + 10 mM DTT, pH 7.4. 20 μM of unfolded lysozyme was incubated with 25 μM HSPA8 and 0 to 100 μM hemin in the refolding buffer for 1 hour. Following incubation the refolding of lysozyme was analyzed by observing the change in the intrinsic fluorescence of lysozyme upon refolding. The competition between ATP and hemin was confirmed by testing the refolding of lysozyme at 25 μM HSPA8 plus 10 μM hemin and varying ATP concentrations (0-10mM). The refolding was further confirmed by analyzing the activity of native or unfolded or refolded lysozyme on DH5α *E.coli* cells[18].

2.13.2 Fluorescence Spectroscopy of Lysozyme

The intrinsic fluorescence by the native or unfolded or refolded lysozyme was measured at an excitation wavelength of 295 nm and emission at 350 nm using a Spincobiotech fluorescence spectrometer. The relative fluorescence unit values were converted to the percent of folded lysozyme considering the fluorescence of the native lysozyme as 100 percent. The background fluorescence due to HSPA8 or different hemin concentrations was subtracted to ensure specific fluorescence due to lysozyme only.

2.13.3 Lysozyme Activity Assay

The lysozyme activity assay was performed immediately after the refolding experiment. Overnight grown culture (OD_{600} = 0.6) of DH5α *E.coli* cells was pelleted down, washed thrice, and

resuspended in 20 mM Tris-HCl + 30 mM NaCl buffer pH 8.6. Equal volumes (200 µl) of uniformly resuspended bacteria were taken in different wells of a 96-well flat-bottom reaction plate. 50 µl of the reaction mixture from each reaction of the refolding experiment was added to different wells and optical density at 600 nm was taken after 30 minutes of incubation at 37°C using a Spincobiotech spectrophotometer. The observed OD values were converted to percent lysozyme activity using the OD of bacteria treated with native lysozyme as 100 percent. Only bacteria, the equivalent concentration of the native lysozyme, and completely unfolded lysozyme were kept as a control for comparison of activities in test samples. The effect of 25 µM HSPA8 on *E.coli* was tested to rule out the contribution of HSPA8 in the activity. The direct effect of hemin on *E.coli* and the lysozyme activity were also tested to eliminate the possibility of hemin contribution to the activity.

2.14 CD Spectroscopy of HSPA8

CD measurements were performed to determine HSPA8 (0.2 µM) structural integrity in the presence and absence of hemin (50 µM) using a Jasco-1500 spectropolarimeter (Japan Spectroscopic Company, Tokyo, Japan). Normally, 10–30 scans were recorded at ambient temperature (~27°C) between 190 and 260 nm, using a 1-mm optical path. Spectra were corrected for background scattering by subtracting a buffer only and buffer + hemin spectrum measured with an appropriate concentration of hemin in buffer without the protein. The data was baseline corrected and smoothened for clarity of peaks. The instrument software was used to find out the percentage of secondary structure elements like α-helix, β-sheets, and coiled loops present in the protein under both conditions. These values were used to calculate the percent changes in the secondary structure elements. Values of ellipticity (θ, mdeg)) were plotted on the y-axis against wavelength (nm) on the x-axis to observe any changes in the secondary structure elements of HSPA8 in the presence of hemin.

2.15 Gel filtration chromatography of HSPA8

The effect of hemin on HSPA8 integrity was further confirmed through gel filtration chromatography. The gel filtration column (Superdex 200 Increase 10/300 GL Cytiva) was washed with 4 column volumes of sterile Milli-Q and equilibrated with 2 CVs of the mobile phase

buffer (50 mM Tris + 300 mM Nacl buffer, pH 8.8). 500 µl of the sample containing only HSPA8 or HSPA8 preincubated with 50 µM hemin was injected into the column and was run at a flow rate of 1ml/min with the same buffer as the mobile phase. The corresponding peaks were analyzed where the retention volume, number of peaks, and peak sharpness were observed to confirm the structural integrity of the protein.

2.16 Isothermal calorimetry of HSPA8

To confirm the competition for binding to HSPA8 *in-vitro*, isothermal calorimetry of ATP with HSPA8 only and HSPA8 preincubated with hemin was performed using a Malvern Microcal-ITC instrument. The titrations were performed at an HSPA8 and ATP concentrations of 3 and 375 µM respectively and a hemin concentration of 10 µM. HSPA8, ATP, and hemin were dissolved in HNG buffer (pH 8.5) without the addition of $MgCl_2$ to prevent auto degradation of ATP. Protein was kept in the sample cell and the ligand was in the syringe. The reference power was set to 5 µW and 25 injections with 1.5 µl injection volume, 180-sec initial delay, and 150-sec time spacing were injected at a stirring speed of 500 rpm. The obtained isotherms were analyzed in the instrument software and the dissociation constants were determined. Control experiments including Protein –buffer and ligand buffer titrations were performed and subtracted. Isothermal calorimetry of hemin with HSPA8, its N-terminal domain (HSPA8_NBD), and C-terminal domain (HSPA8_CT) were also performed using similar procedures.

2.17 Cell culture and treatments

HepG2 is a human hepatoma cell line that has been widely used as a model for toxicological studies on human hepatocytes[19]. The cells were cultured in a Dulbecco's modified Eagle's medium containing fetal bovine serum (10%), and antibiotics penicillin (100 U/ml) and streptomycin (100 µg/ml). Cells were grown in a humidified 5% CO_2 incubator at 37°C.

2.18 Cell viability assay of hemin-treated HepG2 cells

Ten thousand cells per well were seeded in a 96-well plate overnight in complete media. After complete adherence, cells were washed with PBS and treated with varying hemin concentrations (0-120 µM) for 48 hours in serum-free media. After incubation, cells were washed once with PBS

and 50 µl of 0.5 mg/ml MTT dissolved in PBS was added to each well. After 4 hours, MTT was removed and cells were incubated with 100 µl of 100% DMSO for 20 minutes under mild shaking for complete dissolution of formazan formed. Absorbance was taken at 570 nm with reference absorbance at 630 nm. The absorbance from the untreated cells was considered to be coming from 100% viable cells and the percecntage viability of treated cells was calculated accordingly. To check the effect of HSPA8 on viability loss due to hemin, cells were treated with 20 µM of hemin and varying HSPA8 concentrations (0-100 µg/ml) for 48 hours under similar conditions.

2.19 Microscopic evaluation of hemin-treated HepG2 cells

HepG2 cells were treated with 20 µM of hemin for 48 hours as described in section 2.3. After treatment cells in each well were observed in a Nikon inverted microscope with 10X magnification. Images from six random fields were taken and analyzed for visible morphological changes upon treatment.

2.20 Wound healing assay of hemin-treated HepG2 cells

HepG2 cells (1 x 10^6) were seeded in a 6-well plate in complete media and allowed to grow until they formed a fully confluent monolayer. Cells were then washed with PBS thrice and a wound was formed by scratching the wells with a 200 µl tip while the cells were in PBS. Cells were again washed with PBS to remove the scratched-out cells. The cells were then kept untreated or treated with hemin (20 and 40 µM) in incomplete media. Wound healing in control and treated cells were monitored for 48 hours and images of the wound were taken using a Nikon inverted microscope with 4X objective.

2.21 Scanning electron microscopy of hemin-treated HepG2 cells

Cells (1 x 10^5) were seeded on poly-L-Lysine coated glass coverslips in complete media in a 6-well plate. After complete adherence, complete media was removed and the cells were washed 5X with PBS. Cells were kept either untreated or treated with hemin (20 µM) for 48 hours in a serum-free media. After incubation cells were washed 5X with PBS and fixed using 4% paraformaldehyde and 1% glutaraldehyde solution in sterile PBS for 20 minutes. After fixation, cells were washed with sterile MilliQ 5 times to remove salt deposition due to PBS. The coverslips containing fixed cells were kept overnight in a 37°C incubator for drying. Before imaging samples

were further dried with a hot air blower and coated with gold film coater. A total of six random fields were observed and images were taken with a scanning elctron microscope (Zeiss, Gemini-300) The instrument was set at 5 kV EHT, width 5 mm, and InLens signal.

2.22 Estimation of oxidative stress marker enzymes release

The release of three liver damage marker enzymes, serum glutamic pyruvic transaminase (SGPT), serum glutamic oxaloacetic transaminase (SGOT), and lactate dehydrogenase (LDH), into the cell culture media upon hemin treatment was tested. Cells (1×10^5) were seeded in a 96-well plate for 12 hours in complete media. After complete adherence, complete media was removed, cells were washed 3X with PBS, and treated with or without hemin concentrations (20 and 40 µM) for 48 hours. After treatment, the cell culture supernatant from each well was collected in different microcentrifuge tubes and centrifuged at 5000 rpm at RT to remove any debris. The quantity (Units/Liter) of each enzyme released in the supernatant was estimated as follows, and the relative percentage of the enzymes was calculated assuming the release from untreated cells as 0%.

SGPT: The quantity (U/L) of SGPT was estimated using an SGPT (ALT) detection kit (SGPT5x10-2306) from Diatek Healthcare Pvt. Ltd, India, according to the manufacturer's protocol. The two reagents (R1 & R2) supplied in the kit were mixed in the volume ratio of 4:1 to prepare the working reagent containing 0.18 mM NADH, 500 mM L-alanine, 15 mM α-ketoglutarate, 1200 U/L LDH, and 100 mM Tris buffer, pH 7.5. A 500 µl mixture of this reagent was added to 50 µl of the culture supernatant from each sample. Initial and final absorbance after 60 sec and 180 sec respectively were taken at 340 nm using a Spincobiotech spectrophotometer. The change in the absorbance per minute (ΔA/min), due to oxidation of NADH, was calculated and multiplied by a kinetic factor of 1746 to get the quantity (U/L) of the enzyme.

SGOT: The quantity (U/L) of SGOT was estimated using an SGOT (AST) detection kit (GOT 5x10-2306) from Diatek Healthcare Pvt. Ltd, India, according to the manufacturer's protocol. The same procedure was followed for the detection of SGOT as above with the working reagent containing 0.18 mM NADH, 240 mM L-aspartate, 12 mM α-ketoglutarate, >600 U/L MDH, and 800 mM tris buffer, pH 8.

LDH: The quantity of LDH was estimated by adding 500 µl of a reaction mixture containing 6.6 mM NADH, 30 mM sodium pyruvate, and 200 mM Tris-HCl, pH 7.3 to 50 µl of the culture

supernatant. Initial and final absorbance at 340 nm was taken after 60 sec and 180 sec respectively and change in the absorbance per minute was calculated. The quantity of LDH (U/L) in the supernatant was calculated from a standard curve drawn between ΔA/min and varying concentrations of pure LDH.

2.23 Cell cycle analysis of hemin-treated HepG2 cells

Cells (5×10^5) were seeded as earlier and kept untreated or treated with 20 and 40 µM of hemin for 48 hours in serum-free media. Post-treatment, media was removed and cells were scraped from the dishes using trypsin-EDTA and centrifuged at 1500 rpm for 2 minutes. The supernatant was discarded, cells were resuspended in 250 µl of PBS and kept on ice for a couple of minutes. One ml of 70% ice-cold ethanol was added from the walls of the tube under mild vortex conditions. The cells were kept at -20°C for 4 hours for complete fixation followed by centrifugation at 5000 rpm at 4°C for 10 minutes. Fixed cells were washed thrice and resuspended in 1 ml of ice-cold PBS followed by the addition of 50 µg/ml of RNase A and incubation at 37°C for 2 hours. Cells were then stained using 50 µg/ml of propidium iodide stain for 30 minutes before data acquisition. Thirty thousand events were acquired and cell cycle analysis was performed in a flow cytometer. The acquired data was analyzed for the distribution of various phases of the cell cycle in FCS express software.

2.24 DNA Fragmentation Analysis of hemin-treated HepG2 cells

Cells (1×10^6) were seeded in a 6-well plate overnight in 0.2ml complete media. After adhesion cells were washed with PBS and kept untreated or treated with 20 µM of hemin for 48 hours in incomplete media. After treatment cells were washed with PBS and lysed with buffer containing 200 mM Tris-HCl, pH 7.5, 200 mM EDTA, and 10% NP-40. The mixture was centrifuged at 3000 rpm for 5 minutes at 4°C and the lysate was collected. The cell lysate was then incubated with 50 µg/ml of RNase A for 2 hours at 56°C followed by incubation with 25 µg/ml of proteinase K for 2 hours at 37°C. Following incubation half the volume of 10 M ammonium acetate was added to the mixture and immediately 2.5 volume of ice-cold ethanol was added and mixed gently. The mixture was incubated at -80°C overnight and then centrifuged at 12000 rpm for 20 minutes. The pellet was washed with 200 µl of 80% ice-cold ethanol and air-dried for 10 minutes at RT. The pellet was dissolved in 50 µl of TE buffer and the samples were run in an agarose gel

electrophoresis system at 4°C for 4 hours. The fragments were visualized under UV light and images were captured in a BioRad Chemidoc system.

2.25 Determination of apoptotic and dead/necrotic cells

Cells (1 X 10^5) were seeded in complete media in a 6-well plate 12 hours before the treatment. Cells were either untreated or treated with 20 and 40 µM of hemin for 48 hours in serum-free media. Post-treatment cells were washed with PBS and scraped from the dishes using a cell scrapper. Cells were resuspended in PBS and stained with 25 µg/ml of acridine orange and 50 µg/ml of propidium iodide 30 minutes before flow cytometry. Thirty thousand events for each sample were recorded in a flow cytometer and healthy, early/late apoptotic, and necrotic/dead cells were analyzed using quadrant analysis in FCS express software.

2.26 Determination of apoptosis signaling pathway by Western blotting

Cells (1x 10^6) were seeded in 6-well plates overnight. Cells were washed with PBS and kept untreated or treated with 20 and 40 µM of hemin for 48 hours in serum-free media. Post-treatment, cells were harvested using a sterile cell scrapper, lysed using RIPA lysis buffer, and protein content in the lysate was determined using standard protein estimation protocols. The proteins were run on 10% SDS-PAGE and transferred to a nitrocellulose membrane (BioRad #162-0112) using Trans-Blot turbo (BioRad). Blocking was performed at RT for 1 hour 30 minutes with 5% BSA in TBST. The blots were then incubated with the corresponding anti-rabbit primary antibody overnight at 4°C. The blots were washed 3X in TBS and 3X in TBST followed by incubation with appropriate secondary antibody (HRP-conjugated) for 2 hours at RT. The bands were developed using Clarity™ western ECL substrate kit (BioRad) and visualized in the BioRad chemiDoc system for imaging.

2.27 Statistical analysis

All the experiments were performed in triplicates (N=3) and the values are expressed as mean ± standard deviation (SD). The IC_{50} calculation was done using a non-linear curve fit in OriginPro 2016 software. Statistical analysis was performed in applicable assays for significance of the data obtained.

2.28 References

1. Firoz, A., et al., ContPro: a web tool for calculating amino acid contact distances in protein from 3D-structures at different distance threshold. Bioinformation, 2010. 5(2): p. 55.
2. BIOVIA, D.S., Discovery studio modeling environment, release 2017, San Diego: DassaultSystèmes, 2016. Available from:(Accessed 1 September 2016), 2016.
3. Morris, G.M., et al., AutoDock4 and AutoDockTools4: Automated docking with selective receptor flexibility. Journal of computational chemistry, 2009. 30(16): p. 2785-2791.
4. Kaplan, W. and T.G. Littlejohn, Swiss-PDB viewer (deep view). Briefings in bioinformatics, 2001. 2(2): p. 195-197.
5. Anand, P., et al., ABS–Scan: In silico alanine scanning mutagenesis for binding site residues in protein–ligand complex. F1000Research, 2014. 3.
6. Hsu, K.-C., et al., iGEMDOCK: a graphical environment of enhancing GEMDOCK using pharmacological interactions and post-screening analysis. BMC bioinformatics, 2011. 12: p. 1-11.
7. Abraham, M.J., et al., GROMACS: High performance molecular simulations through multi-level parallelism from laptops to supercomputers. SoftwareX, 2015. 1: p. 19-25.
8. Jo, S., et al., CHARMM-GUI: a web-based graphical user interface for CHARMM. Journal of computational chemistry, 2008. 29(11): p. 1859-1865.
9. Trivedi, V., et al., Mechanism of horseradish peroxidase-catalyzed heme oxidation and polymerization (β-hematin formation). Biochimica et Biophysica Acta (BBA)-General Subjects, 2005. 1723(1-3): p. 221-228.
10. Pandey, A.V., et al., Assay of β-hematin formation by malaria parasite. Journal of pharmaceutical and biomedical analysis, 1999. 20(1-2): p. 203-207.
11. Schejter, A., A. Lanir, and N. Epstein, Binding of hydrogen donors to horseradish peroxidase: a spectroscopic study. Archives of biochemistry and biophysics, 1976. 174(1): p. 36-44.
12. Bandyopadhyay, U., et al., Irreversible inactivation of lactoperoxidase by mercaptomethylimidazole through generation of a thiyl radical: its use as a probe to study the active site. Biochemical Journal, 1995. 306(3): p. 751-757.
13. Rule, C.S., M. Patrick, and M. Sandkvist, Measuring in vitro ATPase activity for enzymatic characterization. JoVE (Journal of Visualized Experiments), 2016(114): p. e54305.

14. Pro, O., Origin Lab corporation [version Beta2 b9. 3.193]. Academic, Northampton, USA, 2016.
15. Esquembre, R., et al., Thermal unfolding and refolding of lysozyme in deep eutectic solvents and their aqueous dilutions. Physical Chemistry Chemical Physics, 2013. 15(27): p. 11248-11256.
16. Alkudaisi, N., et al., Detecting lysozyme unfolding via the fluorescence of lysozyme encapsulated gold nanoclusters. Journal of Materials Chemistry B, 2019. 7(7): p. 1167-1175.
17. Biswas, B., et al., Contrasting effects of guanidinium chloride and urea on the activity and unfolding of lysozyme. Acs Omega, 2018. 3(10): p. 14119-14126.
18. Sedov, S., et al., Lysis of Escherichia coli cells by lysozyme: discrimination between adsorption and enzyme action. Colloids and Surfaces B: Biointerfaces, 2011. 88(1): p. 131-133.
19. Arzumanian, V.A., O.I. Kiseleva, and E.V. Poverennaya, The curious case of the HepG2 cell line: 40 years of expertise. International journal of molecular sciences, 2021. 22(23): p. 13135.

Chapter III

Role Transformation of HSPA8 after Binding Hemin to Catalyze Heme Polymerization

Publication: " Pandey, A.K. and Trivedi V., 2023. Role Transformation of HSPA8 to Heme-peroxidase After Binding Hemin to Catalyze Heme Polymerization. The Protein Journal, pp-1-14."

3.1 Introduction

Hemin, a byproduct of hemoglobin breakdown, causes oxidative damage to cells[1-6]. As it accumulates, various proteins are recruited to detoxify heme, with heme oxygenase playing a pivotal role[7]. Heat shock proteins (HSPs) protect cells by preventing protein degradation and unfolding, and they also have other roles in similar stressful situations[8-11]. Proteins of the heat shock family have also evolutionarily diverged to adapt to challenges and confer diverse specialized functions[12]. HSPA8, a 73kDa HSP70 family member, serves diverse cellular functions under stress[13-16].

Increased production of HSPA8 and its protective role in stress conditions akin to those induced by free heme or hemin accumulation suggest its potential significance in pathologies involving hemin build-up. Given the existing literature on protein-mediated heme detoxification and polymerization[17], we investigated HSPA8's role in detoxifying free heme/hemin in the local environment during such pathologies. We proposed that hemin binds to HSPA8, forming a new HSPA8-hemin complex that could act as a heme-containing peroxidase. This complex might convert hemin into heme polymer through a mechanism involving single electron oxidation intermediate formation, akin to HRP. Our study indicates that the HSPA8-hemin complex possesses peroxidase activity, suggesting that HSPA8 may exhibit various peroxidase-like biological functions.

3.2 Experimental Procedures

3.2.1 Development of hemin biophore

Hemin biophore was developed *in-silico* by analyzing seven Protein-hemin complexes and constructing a distance-based (section 2.4.1) and an interaction-based matrix (section 2.4.2) as described in Chapter II.

3.2.2 Biophore validation

The developed biophore was validated *in-silico* through molecular docking (section 2.4.3) and residue contribution analysis (section 2.4.4) as described in Chapter II.

3.2.3 Cloning of the *hspa8* gene and its truncation products

The gene coding for HSPA8 was cloned in the *pET23a* and its domains HSPA8_NBD and HSPA8_CT were cloned in the *pET28a* vector using standard cloning protocols as described in

section 2.5 of Chapter II. The parameters used for PCR amplification of the three genes are listed in Table 3.1.

Table 3.1: Reaction parameters for PCR amplification of hspa8, hspa8_nbd, and hspa8_ct

S.Number	Clone Name	Primers (F-Forward, R-Reverse)	Reaction Parameters
1	*pET23a_hspa8*	F-5′-CGCGGATCCACCATGTCCAAG-3′ R-5′-TTTGCTCGAGCCCTTAATCAACCTCTTCA-3′	ID-95ºC, 3min D-95ºC, 30sec A-54ºC, 3sec E-72ºC, 1.5min FE-72ºC, 10min
2	*pET28a_hspa8_nbd*	F-5'-AGGATCCATGTCCAAGGGACCTGCAGTT-3' R-5′-AACTCGAGCTCAGACTTGTCTCCAGACAA-3′	ID-95ºC, 5min D-95ºC, 45sec A-50ºC, 45sec E-72ºC, 1.3min FE-72ºC, 10min
3	*pET28a_hspa8_ct*	F-5′-TCCATGGCAAATGTTCAAGATTTG-3’ R-5′-GCTCGAGATCAACCTCTTCAAT-3′	ID-95ºC, 4min D-95ºC, 45sec A-57ºC, 45sec E-72ºC, 50sec FE-72ºC, 10min

(ID- Initial Denaturation, D- Denaturation, A- Annealing, E- extension, and FE- Final extension)

3.2.4 Overexpression and purification of HSPA8, and its truncation products. The full-length HSPA8 and its domains HSPA8_NBD and HSPA8_CT were overexpressed in bacterial expression systems and were purified using Ni-NTA affinity chromatography as described in section 2.6 of Chapter II

3.2.5 Optical Difference Spectroscopy of HSPA8

The binding of hemin to HSPA8 and its domains was tested through optical difference spectroscopy as described in section 2.9 of Chapter II.

3.2.6 Peroxidase activity assay of HSPA8-hemin complex

The capability of the HSPA8-hemin complex to exhibit peroxidase activity was tested through a peroxidase activity assay using guaiacol as substrate as described in section 2.10 of Chapter II.

3.2.7 Heme polymerization activity

The heme polymerizing potential of the HSPA8 and its domains were tested through a heme polymerization activity assay as described in section 2.7 of Chapter II.

3.2.8 FT-IR Spectroscopy of heme polymer formed by HSPA8

The heme polymer formed by HSPA8 was characterized through FT-IR spectroscopy as described in section 2.8 of Chapter II.

3.2.9 Optical spectroscopy to confirm single electron transfer

The formation of a single electron transfer intermediate and reversal of the complex to its native state was examined through optical spectroscopy as described in section 2.11 of Chapter II.

3.3 Results

3.3.1 Cloning, Overexpression, and Purification of HSPA8 full length and its domains

HSPA8 consists of a 44kDa N-terminal ATPase domain and a 29kDa C-terminal substrate binding domain**.** The HSPA8 full-length clone was successfully sub-cloned in a pET23a vector (**Fig. 3.1**).

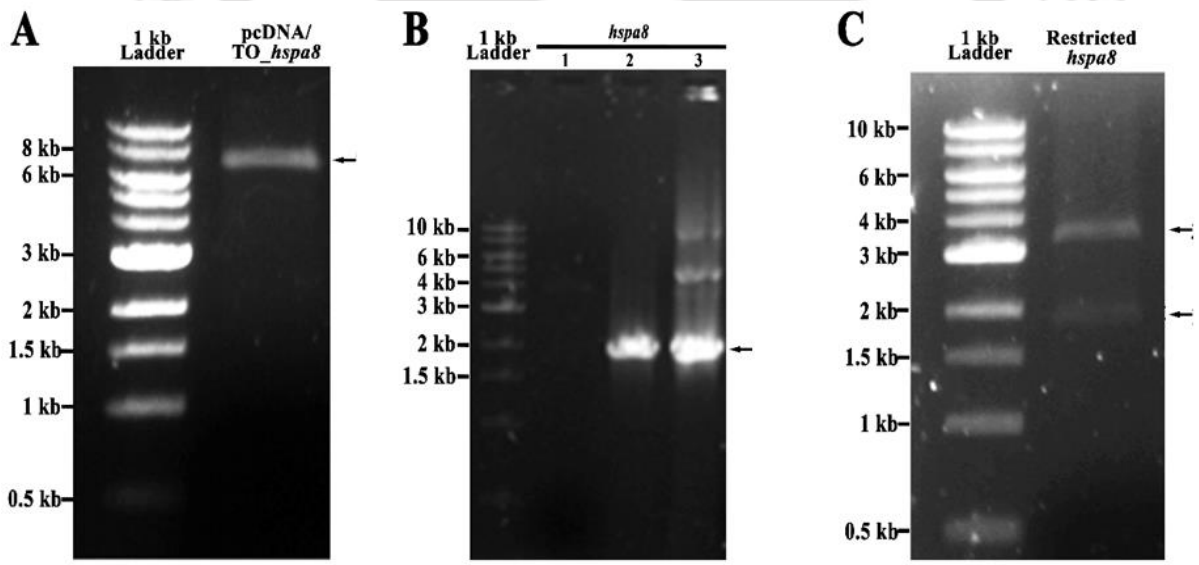

Figure 3.1: **Cloning of the *hspa8* gene in a pET23a expression vector. A)** Agarose gel (1%) electrophoresis of pcDNA5/TO_hspa8 (7056 bps) plasmid isolated from the purchased clone (pcDNA5/TO HIS HSPA8). **B)** PCR amplification of the hspa8 gene at 52°C (lane1), 54°C (lane2), and 56°C (lane3) annealing temperatures using pcDNA5/TO_hspa8 as a template. The PCR product from lane 2 was gel eluted and ligated to the *pET23a* vector using T4 DNA ligase. 10µl of ligation mixture was transformed into DH5α E.coli cells for plasmid isolation. The isolated plasmid was subjected to restriction digestion using BamHI and XhoI restriction enzymes. **C)** Restricted bands of *pET23a* (3666 bps) and *hspa8* (1970 bps) after the restriction digestion.

The protein was over-expressing well in the BL21 *E. coli* bacterial expression system (**Figure 3.2A**) and was observed in the soluble fraction. The overexpression was confirmed by western blotting using an anti-His antibody (**Figure 3.2B**) and the protein was purified to homogeneity using Ni-NTA affinity chromatography (**Figure 3.2C**). Imidazole was removed from the eluted fractions before performing the experiments.

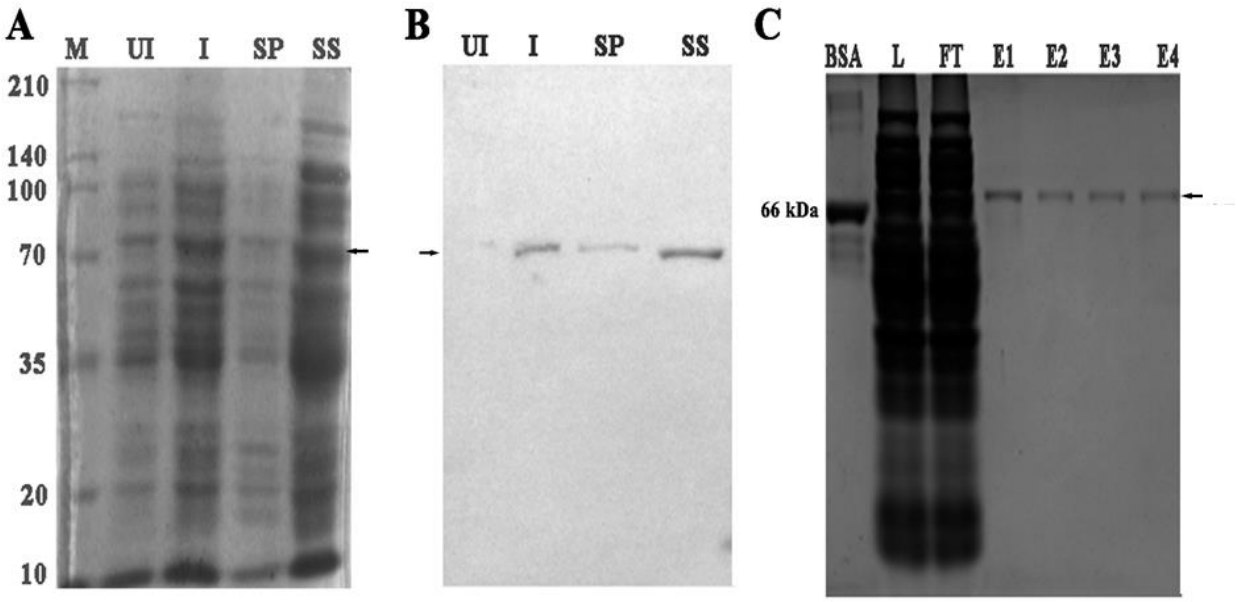

Figure 3.2: Overexpression and purification of the HSPA8 (73 kDa) full protein. A) 10 % SDS-PAGE gel showing protein marker (M), uninduced (UI), induced (I), pellet after sonication (SP), and supernatant after sonication (SS) fractions to confirm the overexpression. HSPA8 was overexpressed in the soluble fraction (SS). **B)** Western blot (developed using DAB) of the corresponding overexpression fractions, uninduced (UI), induced (I), pellet after sonication (SP), and supernatant after sonication (SS), using an Anti-HIS antibody to confirm the HIS-tagged HSPA8 full protein. C) 12 % SDS-PAGE gel showing purification of HSPA8 by Ni-NTA affinity chromatography. A single band was observed in all elution fractions. (BSA as a marker, Load (L), flow-through (FT), and elutions with 70 mM imidazole (E1, E2, E3, and E4).

Subsequently, the N-terminal ATPase domain (*hspa8_nbd*) was successfully cloned in the *pET28a* vector (**Figure 3.3**). The full-length HSPA8 containing plasmid was used as a template to PCR amplify *hspa8_nbd* (**Figure 3.3A**). The amplified product was gel eluted and ligated to the T-vector using T4 DNA ligase. The ligated product was transformed into DH5α cells and positive clones were confirmed through colony PCR (**Figure 3.3B**) and restriction digestion (**Figure 3.3C**). The restricted *hspa8_nbd* insert was further subcloned in the *pET28a* vector and the clone was

confirmed through restriction digestion (**Figure 3.3D)** and PCR using the clone as a template (**Figure 3.3E**).

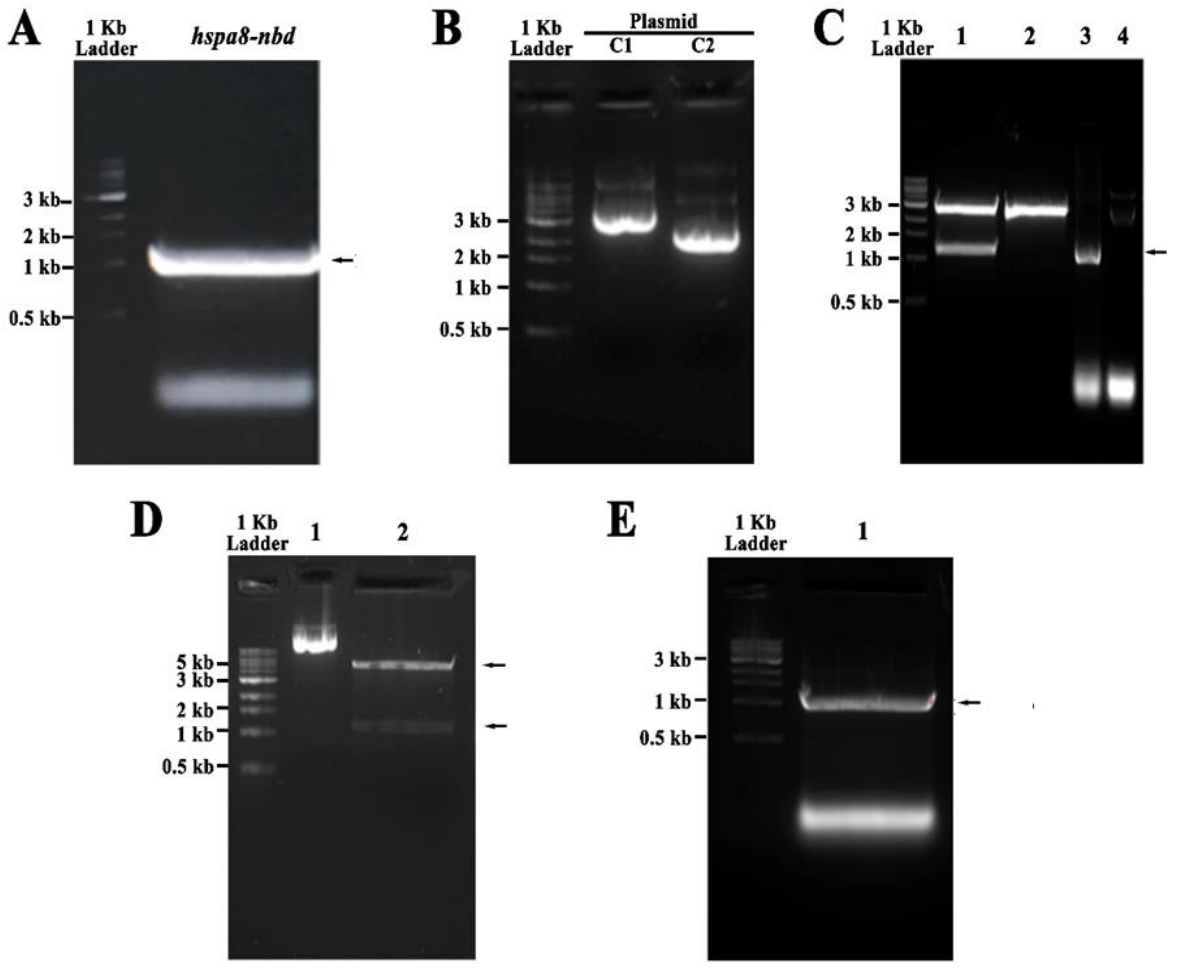

Figure 3.3: Cloning of the N-terminal of HSPA8 (hspa8_nbd). A) Agarose gel (1%) showing PCR amplification of hspa8_nbd (1158 bps, lane 1) using pET23a_hspa8 as a template. The PCR product was gel eluted and ligated to pMD20 T-vector using T4 DNA ligase. The ligated product was transformed into DH5α E.coli cells for plasmid isolation. **B)** Plasmid isolated from two different colonies (C1 and C2) following ligation and transformation. The isolated plasmids were subjected to double digestion using BamHI and XhoI restriction enzymes. **C)** Restriction digestion of plasmids isolated from C1 (lane 1) and C2 (lane 2), and PCR amplification using isolated plasmids from C1 (lane 3) and C2 (lane 4) as templates. Lane 1 shows restricted bands of both the T-vector pMD20 (2736 bps) and the insert hspa8_nbd (1158 bps), and lane 3 shows the pcr product of the desired size (1158 bps). Insert from lane 1 was gel eluted and ligated to the pET28a vector using T4 DNA ligase. The ligated product was again transformed into DH5α E.coli cells for plasmid isolation. The clone was confirmed by, double digestion of the isolated plasmid using BamHI and XhoI restriction enzymes and pcr amplification using the plasmid as a template. **D)** Lane1, Undigested pET28a_hspa8_nbd clone (6527 bps), and lane 2 digested bands of pET28a (5369 bps) and hspa8_nbd (1158 bps). **E)** lane1, PCR amplification of hspa8_nbd using pET28a_hspa8_nbd as a template.

Following cloning, the protein HSPA8_NBD was overexpressed in a bacterial expression system. The protein expressed well in BL21(DE3) cells and was observed in the soluble fraction (**Figure 3.4 A**). The overexpression was confirmed by western blotting using an anti-His antibody (**Figure 3.4B**). The protein was then purified to homogeneity using HIS-tagged Ni-NTA beads. A single band was observed in all the elution fractions (**Figure 3.4C**). Imidazole from the eluted fractions was removed either by gel filtration or dialysis before performing the experiments.

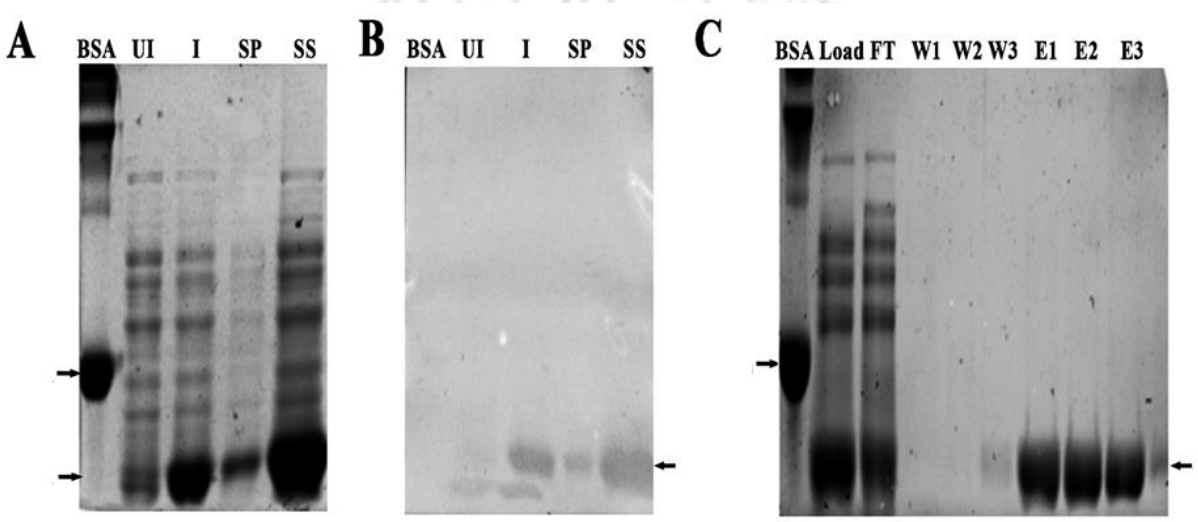

Figure 3.4: Overexpression and purification of the N-terminal of HSPA8 (HSPA8_NBD). A) 10% SDS_PAGE gel showing BSA (as a marker), uninduced (UI), induced (I), pellet after sonication (SP), and supernatant after sonication (SS) fractions to confirm the overexpression. HSPA8_NBD (44 kDa) was overexpressed in the soluble fraction (SS). **B)** Western blot (developed using DAB) of the corresponding overexpression fractions, BSA (as a marker), uninduced (UI), induced (I), pellet after sonication (SP), and supernatant after sonication (SS), using an Anti-HIS antibody to confirm the HIS-tagged HSPA8_NBD. **C)** 10 % SDS-PAGE gel showing purification of HSPA8_NBD by Ni-NTA affinity chromatography. A single band was observed in all elution fractions. (BSA as a marker, Load (L), flow-through (FT), lysis buffer wash (W1), 20 mM imidazole wash (W2), 50 mM imidazole wash (W3), and elutions with 250 mM imidazole (E1, E2, and E3).

Subsequently, the C-terminal ATPase domain (*hspa8_ct*) was also successfully cloned in the *pET28a* vector (**Figure 3.5**). The full-length HSPA8 containing plasmid was used as a template to PCR amplify *hspa8_ct* (**Figure 3.5A**). The amplified product was gel eluted and ligated to the T-vector using T4 DNA ligase. The ligated product was transformed into DH5α cells and positive clones were confirmed through colony PCR (**Figure 3.5B**) and restriction digestion (**Figure 3.5C**).

The restricted *hspa8-ct* insert was further subcloned in the *pET28a* vector and the clone was confirmed through restriction digestion (**Figure 3.5D)** and PCR using the clone as a template (**Figure 3.5E**).

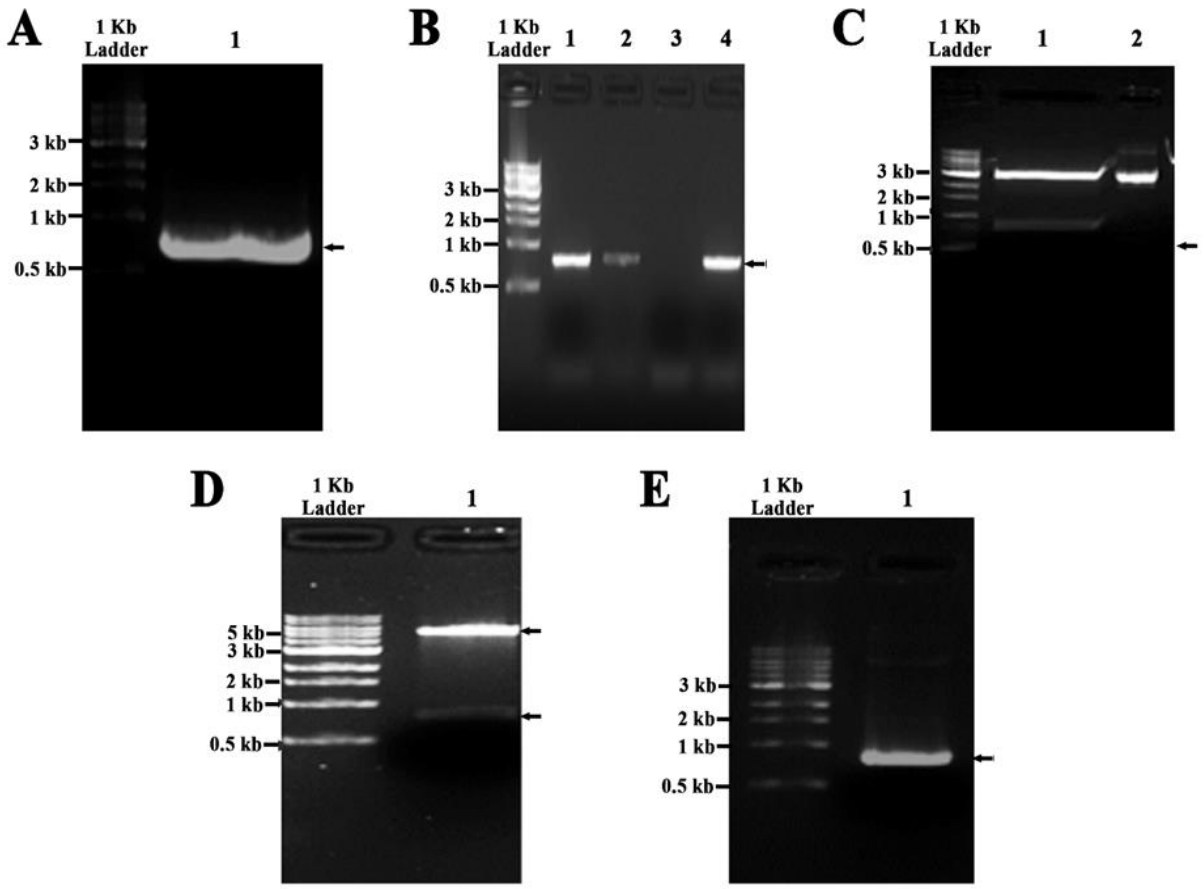

Figure 3.5: Cloning of the C-terminal of HSPA8 (hspa8_ct). A) Agarose gel (1%) showing PCR amplification of *hspa8_ct* (780 bps, lane 1) using *pET23a_hspa8* as a template. The PCR product was gel eluted and ligated to *pMD20* T-vector using T4 DNA ligase. The ligated product was transformed into DH5α E.coli cells. **B)** Colony PCR using four different colonies (1, 2, 3, and 4) following ligation and transformation. Colonies 1, 2, and 4 showed positive bands of *hspa8_ct* (780 bps). The plasmid isolated from colony 4 was subjected to double digestion using BamHI and XhoI restriction enzymes. **C)** Restriction digestion of plasmid isolated from colony 4 (lane1, digested bands of both the T-vector *pMD20* (2736 bps) and the insert *hspa8_ct* (780 bps) and lane2, undigested *pMD20_hspa8_ct* plasmid (3516 bps). The insert from lane 1 was gel-eluted and ligated to the *pET28a* vector using T4 DNA ligase. The ligation mixture was transformed into DH5α E.coli cells for plasmid isolation. The clone was confirmed by, double digestion of the isolated plasmid using BamHI and XhoI restriction enzymes and pcr amplification using the plasmid as a template. **D)** Lane1, digested bands of *pET28a* (5369 bps) and *hspa8_ct* (780 bps). **E)** lane1, PCR amplification of *hspa8_ct* using pET28a_ct as a template.

Following cloning, the protein was overexpressed in a bacterial expression system. The protein expressed well in BL21(DE3) cells and was observed in the soluble fraction (**Figure 3.6 A**). The protein was then purified to homogeneity using HIS-tagged Ni-NTA beads. A single band was observed in all the elution fractions (**Figure 3.6B**). Imidazole from the eluted fractions was removed either by gel filtration or dialysis before performing the experiments.

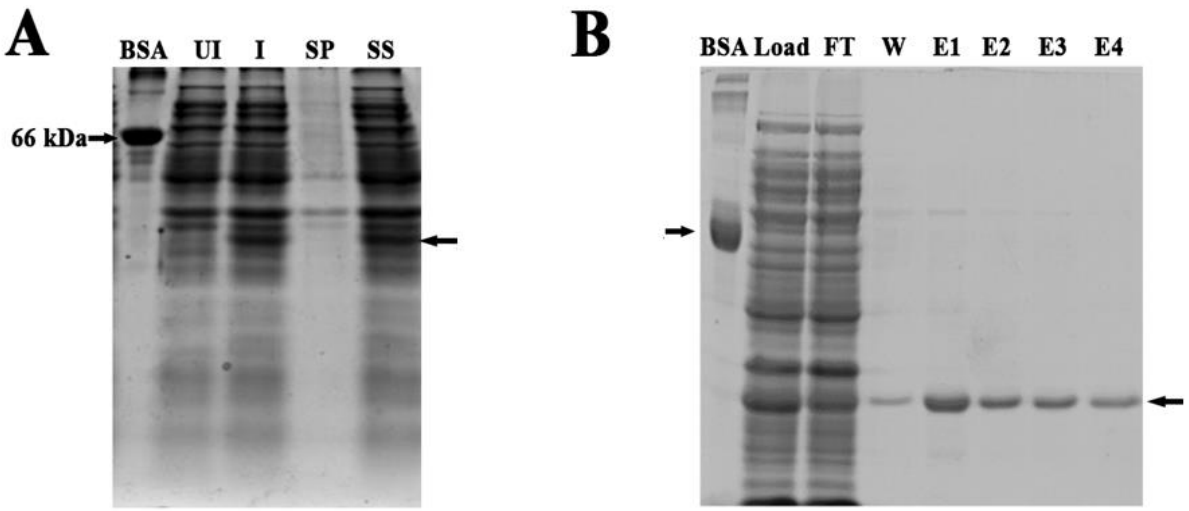

Figure 3.6: Overexpression and purification of the C-terminal of HSPA8 (HSPA8_CT). A) 15% SDS_PAGE gel showing BSA (as a marker), uninduced (UI), induced (I), pellet after sonication (SP), and supernatant after sonication (SS) fractions to confirm the overexpression. HSPA8_CT (29 kDa) was overexpressed in the soluble fraction (SS). **B)** 12 % SDS-PAGE gel showing purification of HSPA8_CT by Ni-NTA affinity chromatography. A single band was observed in all elution fractions. (BSA as a marker, Load (L), flow-through (FT), 50 mM imidazole wash (W), and elutions with 250 mM imidazole (E1, E2, E3, and E4).

3.3.2 Hemin biophore is a well-defined region consisting of Phe, Arg, Ile, Lys, and Val.

Hemin is the major pro-oxidant molecule present in the micro-environment during malaria, arthritis, etc[18]. Under such cellular stress, HSPA8 is secreted from cells to participate in cell-survival strategies[19] by binding to several substrates. To assess the possibility of HSPA8 hemoprotein formation and locate the probable hemin binding region in HSPA8 we carefully compared the structure of hemin binding proteins with HSPA8 and it is evident that the HSPA8 has hemin neutralizing capability. In our previous study, we employed a similar approach to locate the hemin biophore in CD36 protein, after considering the structure of several hemin-binding proteins[20]. Analysis of the binding pockets of seven hemin-protein complexes showed that

residues Phe, Leu, Val, Arg, and Ile are the most recurring amino acids (>8 times) involved in interaction with hemin (**Table 3.2**).

Alanine was also found to be recurring 10 times but was excluded because of its low size and small side chain. Its recurrence could be due to less steric hindrance. The small side chain offers very little possibility of interaction with hemin. Moreover, there is no literature supporting the importance of alanine in the binding of heme to proteins.

Table 3.2: Recurring (>8 times) amino acids in the seven hemin-protein complexes downloaded from the Protein data bank.

PDB/AA	A	F	G	H	I	K	L	R	V	Y
1DVE	1	2	0	0	0	3	2	1	0	2
1MBO	1	2	0	3	2	1	4	1	1	1
1O9X	1	3	0	0	1	0	3	1	0	2
2Z97	2	3	4	1	0	0	4	1	3	0
2ZAW	2	3	4	0	0	0	4	1	3	0
2ZDO	2	3	0	1	4	0	2	2	2	0
3GAS	1	3	0	0	2	1	0	3	2	1
Total	**10**	**19**	**8**	**5**	**9**	**5**	**19**	**10**	**11**	**6**

The distance matrix analysis revealed that these residues are easily accommodated within a distance of 6 Å from hemin atoms exposing features to facilitate hemin binding (**Figure 3.7**). Arg and Lys residues were majorly found to be in the vicinity of the hemin carboxylate group forming a hydrophilic-environment facilitating binding. Phe, Ile, and Val were found closer to the porphyrin ring of hemin ensuring hydrophobic interactions.

The interaction matrix (**Figure 3.8**) analysis showed that N, NE, and NH1 atoms of Arg recurringly form an H-bond with an O1D atom of hemin. NH2 of Arg forms an H-bond with O1A of hemin. Also, CD and NE of Arg form an H-bond with O2D of hemin. Similarly, CE and NZ of Lys form an H-bond with O2A and O1D of hemin respectively. Ile forms an H-bond with O2D of hemin. Recurring electrostatic interactions were observed between NH1 and NH2 of Arg with O2A and

O2D of hemin. NZ of Lys shows electrostatic interaction with O2A and O2D of hemin. The pi-orbitals of Phe, Leu, Val, and Ile atoms were found to be involved in several hydrophobic interactions with the porphyrin ring of hemin. A picture showing an atomic definition of hemin is shown in **Figure 3.9** to understand the interactions better.

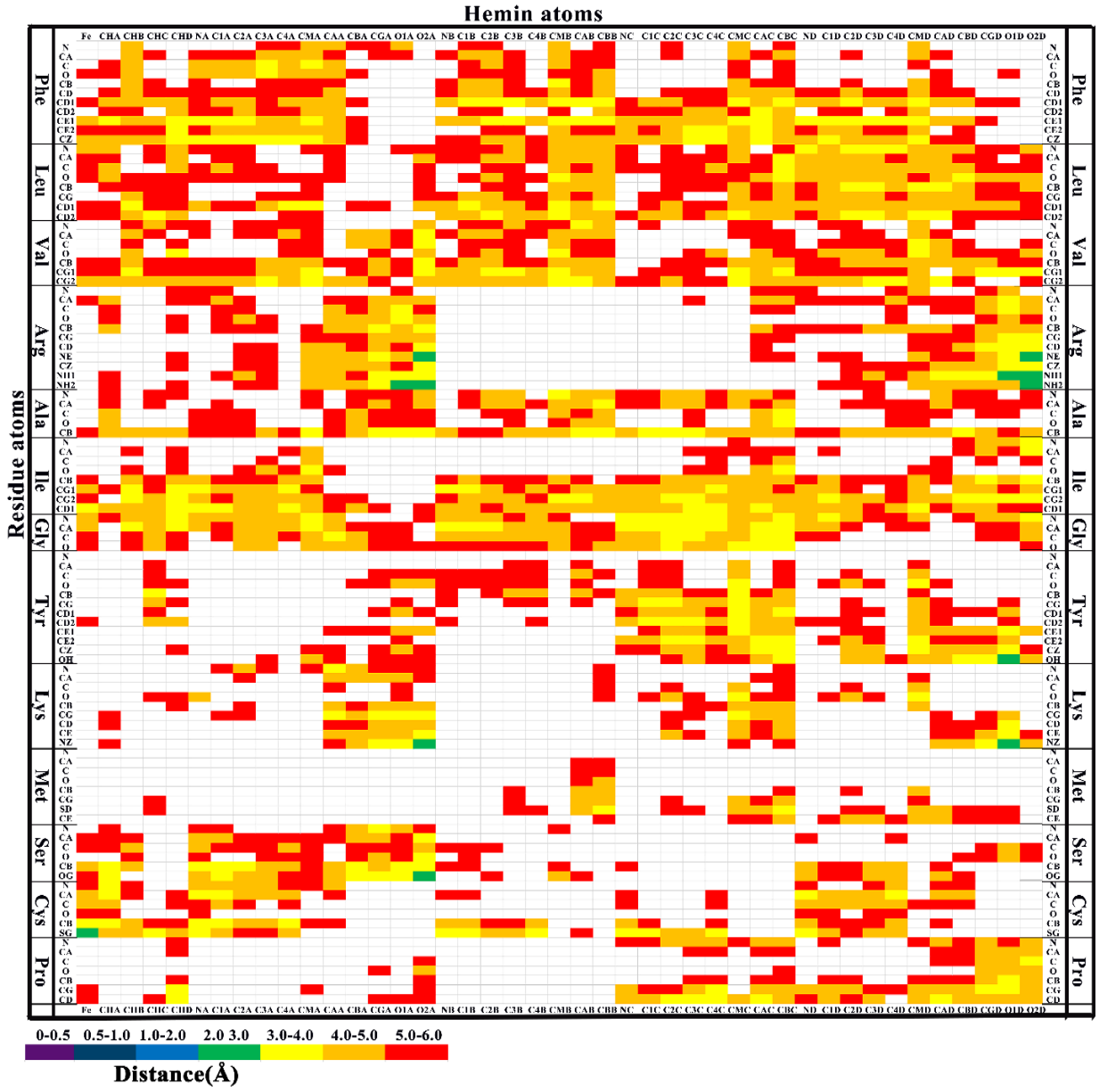

Figure 3.7: Distance-based Protein-hemin biophore heat map. To discover the presence of a pocket for hemin binding in HSPA8 the atom-atom distance between the backbone and side chain atoms of biophoric residues and the hemin atoms of the seven complexes were mapped. The distances (1 to 6Å) are represented on a VIBGYOR scale with violet as the smallest and red as the largest distance.

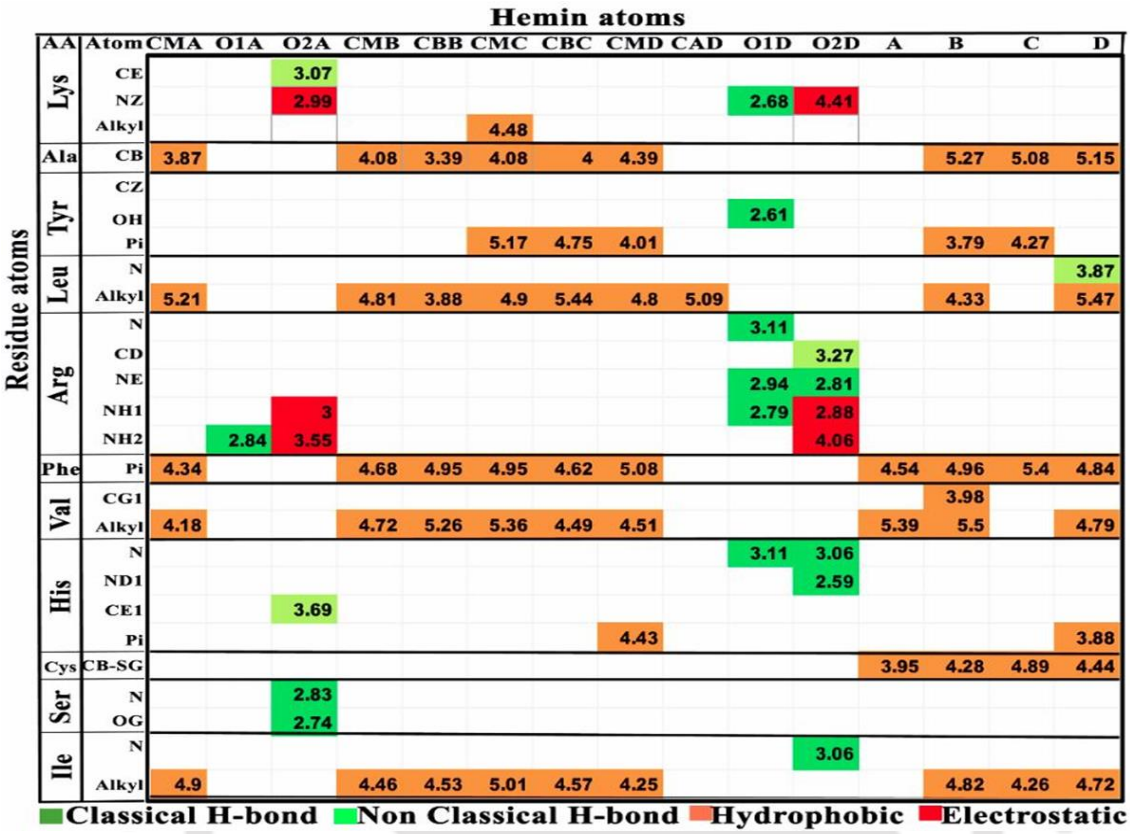

Figure 3.8: Interaction-based Protein-hemin biophore heat map. Hemin interactions, emphasizing the bond type and distance, of the seven hemin-protein complexes analyzed. The matrix reveals the requirement of electrostatic (red), hydrophobic (orange) and hydrogen bonding (green) features for hemin binding.

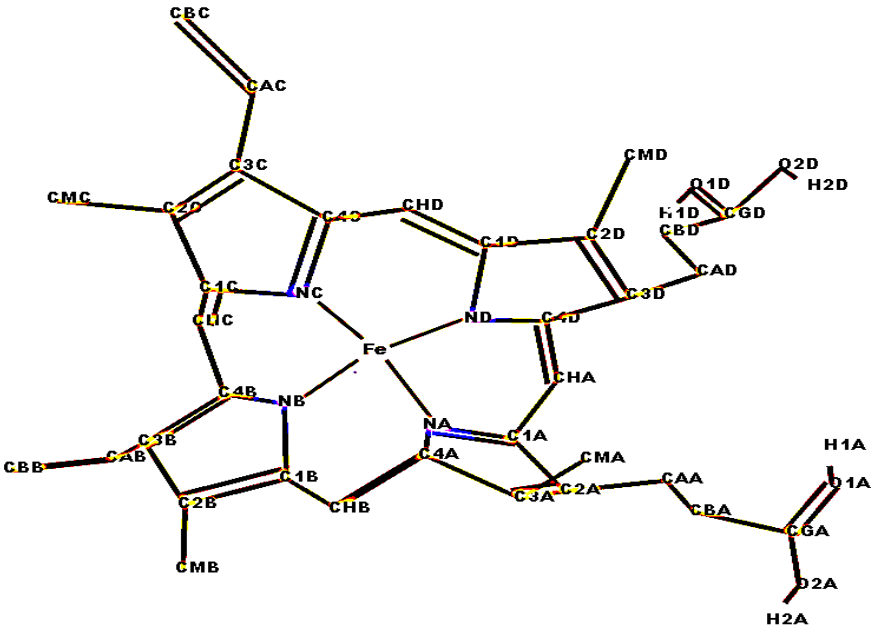

Figure 3.9: Atomic definition of Hemin.

Based on the distance and interaction-based fingerprint studies it was inferred that Phe, Arg, Leu, Ile, Lys, and Val are critical for hemin binding, and a region with residues forming a pocket can facilitate hemin binding in HSPA8 (**Figure 3.10**). Charged residues, Arginine and Lysine can exhibit hydrogen binding and electrostatic interactions whereas non-polar residues, Phe, Leu, Val, and Ile can provide several hydrophobic features.

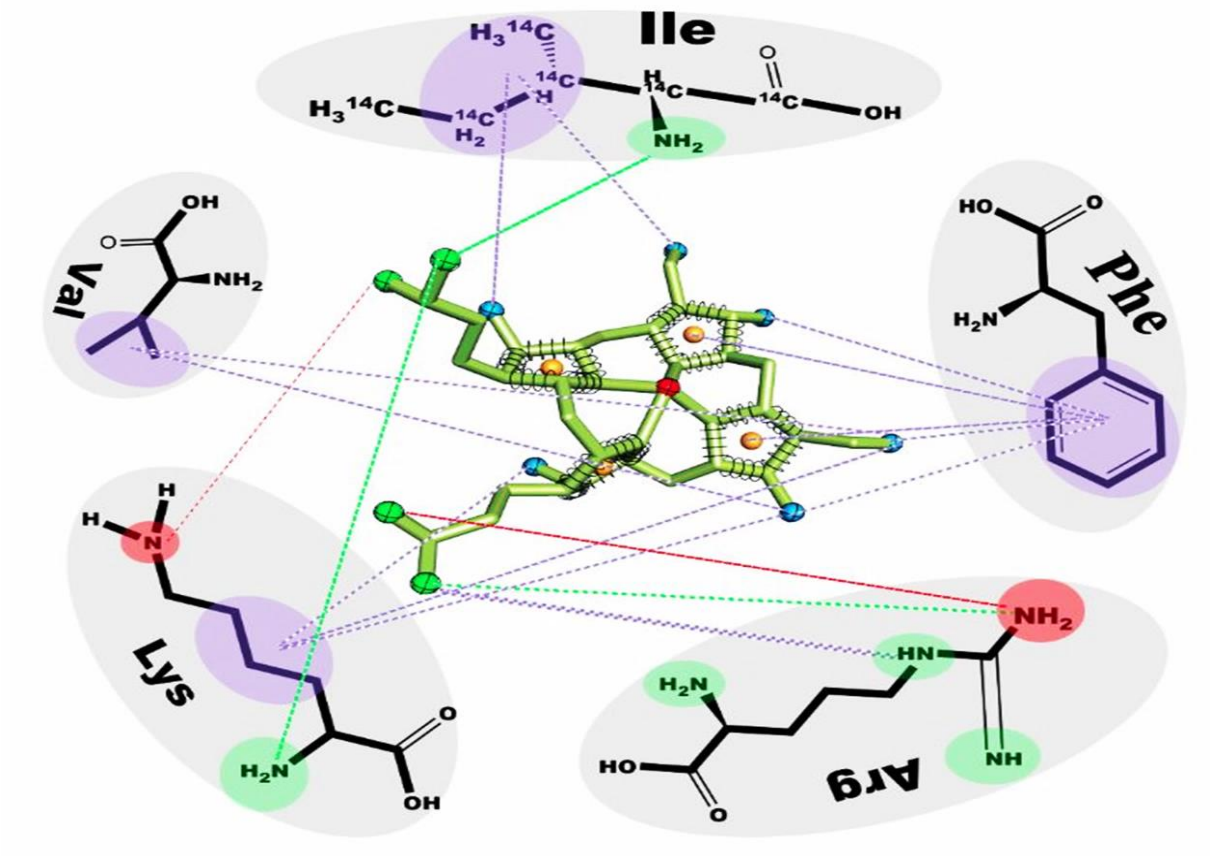

Figure 3.10: Hemin biophore developed by analyzing both the atom-atom distance and interaction-based matrices. It indicates that a region having Ile, Phe, Arg, Val, and Lys residues in a binding pocket arrangement can serve as a well-defined site for hemin binding to a protein. The phenyl ring of Phe, the CB-CG1-CG2 atom groups of Ile and Val, and the CB-CG-CD group of lysine provide hydrophobic features (purple) for hemin interaction. The terminal N atom of Lys and Arg side chains serve as point features (red) for electrostatic interactions. The N atoms of the amino group in Arg, Ile, and Lys serve as H-bond acceptor point features (green) for hemin binding.

We screened the complete HSPA8 3D structure and were able to locate a probable biophore in the N-terminal domain around the residue range from 150 to 175. It showed significant binding in

molecular docking studies with a binding energy of -9.97 kcal/mol. Hemin showed various interactions with the biophoric residues (**Figure 3.11**), Phe 150, Asp 152, Arg155, Lys159, Val169, Arg171, Asn174, I172, and I173 which is in good agreement with the requirements for hemin binding discussed previously.

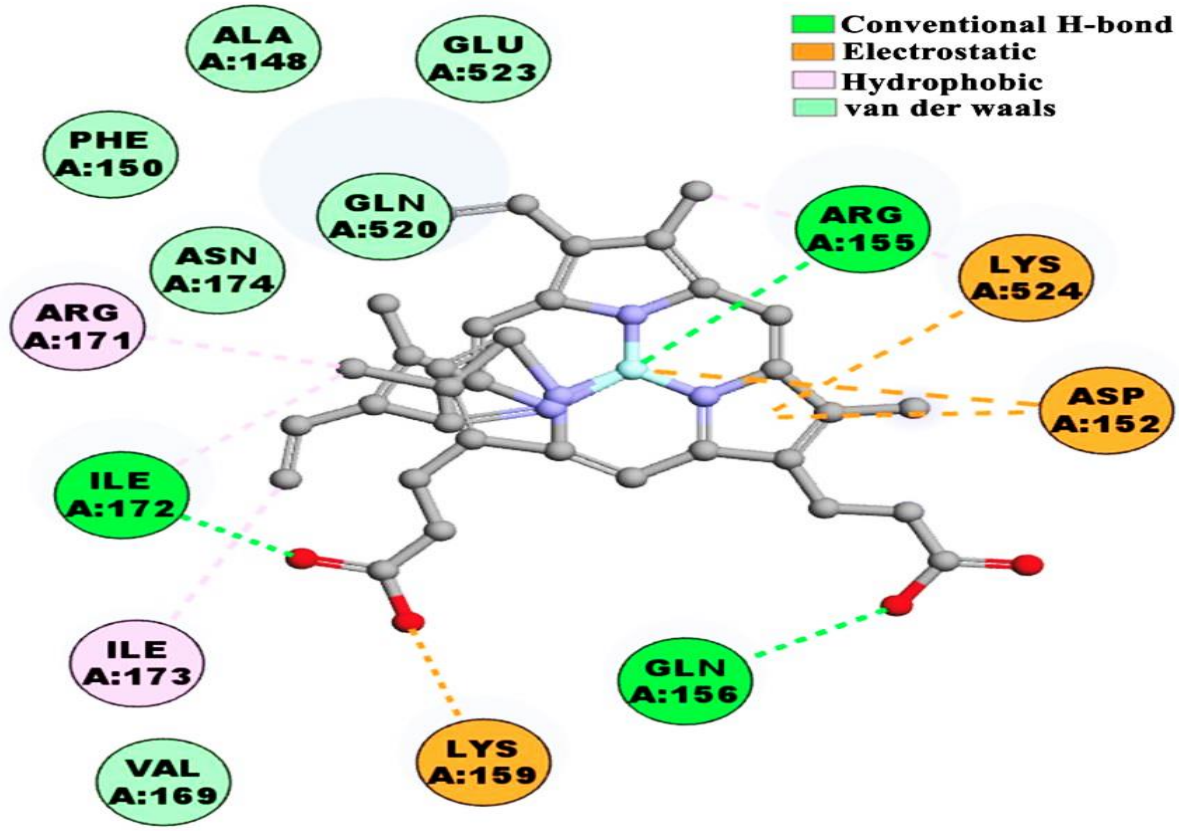

Figure 3.11: Docking of hemin to HSPA8 at the biophoric site. The docking results are in good agreement with the predicted biophore. Arg155 and Ile172 form H-bond, Lys159 show electrostatic interactions, Ile173 show hydrophobic interactions, and Phe150 and Val 169 show van der Waals interaction with hemin atoms.

The findings give an insight that HSPA8 can accommodate hemin in its N-terminal domain (1-383). Further, we investigated the contribution of these residues to the stability of the HSPA8-hemin complex. The relative contribution of each pocket residue was examined through *in-silico* alanine mutations and then the change in the total Gibb's free energy of the complex. The mutations R155A, I172A, R171A, K159A, and V219A showed relatively high positive values of the changes in Gibbs free energy (ΔΔG) indicating destabilization of the complex (**Figure 3.12**).

The mutation of Arg 155 was found to be most destabilizing suggesting its higher contribution to the binding and stability of the complex as compared to other biophoric residues.

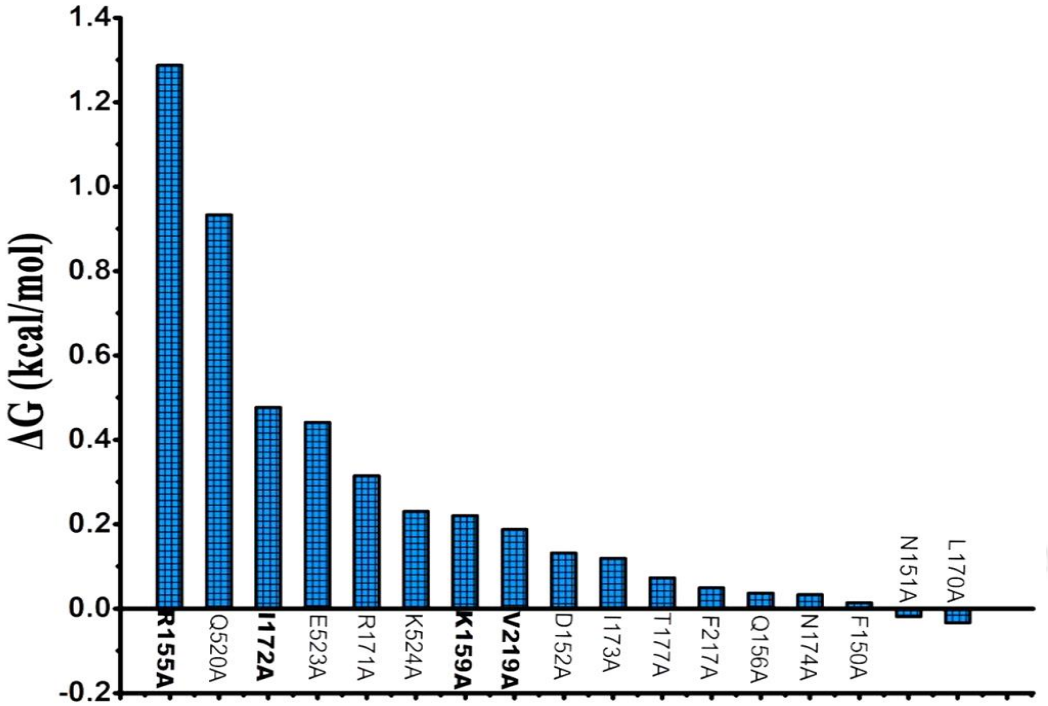

Figure 3.12: *In-silico* alanine mutations of critical residues to determine the relative contribution of each residue in HSPA8-hemin complex overall stability. The free energy difference upon mutation was used as a criterion to determine the residue contribution. R155A, I172A, R171A, K159A, and V219A mutations show significant free energy change upon alanine mutation and thus were figured as principal components for hemin binding to HSPA8.

3.3.3 HSPA8 forms a complex with hemin through its N-terminal domain

HSPA8 possesses a critical region within its protein core that plays a pivotal role in facilitating the binding of hemin. To validate the formation of this complex *in-vitro*, optical difference spectroscopy was conducted. The outcomes of these experiments indicate that hemin interacts with HSPA8 in a dose-dependent manner, with a calculated dissociation constant (K_d) value of 5.9 ± 0.04 µM (**Figure 3.13A**). Hemin, characterized by its hydrophobic nature, has been observed to bind to various proteins, including BSA[21]. To investigate the specificity of hemin's interaction with HSPA8, we generated truncation mutants to express distinct fragments of the

protein. Specifically, we expressed the N-terminal (NBD) and C-terminal (CT) fragments. Our experiments revealed that the NBD fragment binds to hemin in a manner that depends on the hemin concentration, with a calculated K_d value of 2.05 ± 0.01 µM (**Figure 3.13B**).

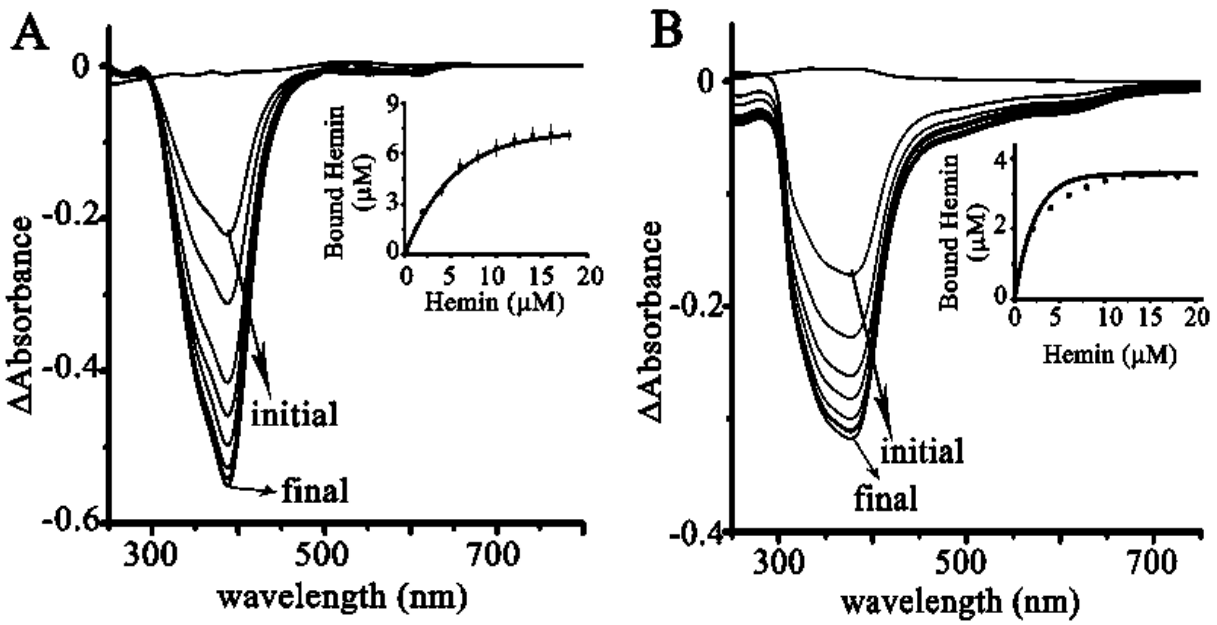

Figure 3.13: Optical difference spectroscopy to establish the *in-vitro* binding of hemin to HSPA8. The results show, **A)** a saturating dip in the soret peak due to differential absorbance of hemin resulting from its binding to HSPA8. The calculated K_d value from the observed absorbance difference of hemin binding to HSPA8 was **5.9 ± 0.04** µM, **B)** similar dip in the soret peak due to differential absorbance of hemin after binding to the N-terminal domain. The calculated K_d value of hemin binding to the N-terminal was **2.04 ± 0.003** µM, which supports the heme polymer formation by HSPA8_NBD independently. Insets in A and B show the respective binding isotherms for hemin binding. An Extinction coefficient of 91mMcm^{-1} was used to calculate the concentration of bound hemin.

Interestingly, the C-terminal domain of HSPA8 did not exhibit any significant shift or dips in peaks around 400 nm, indicating a lack of saturation with increasing hemin concentrations (**Figure 3.14**). This observation suggests either insignificant or no binding of hemin to the C-terminal domain. It is worth noting that the HIS-tag present in proteins has been reported to facilitate hemin binding[22]. However, since the C-terminal domain of HSPA8, which includes the HIS-tag, did not exhibit any binding, we excluded the possibility of non-specific binding mediated by the HIS-tag in the case of HSPA8 and its N-terminal domain as well.

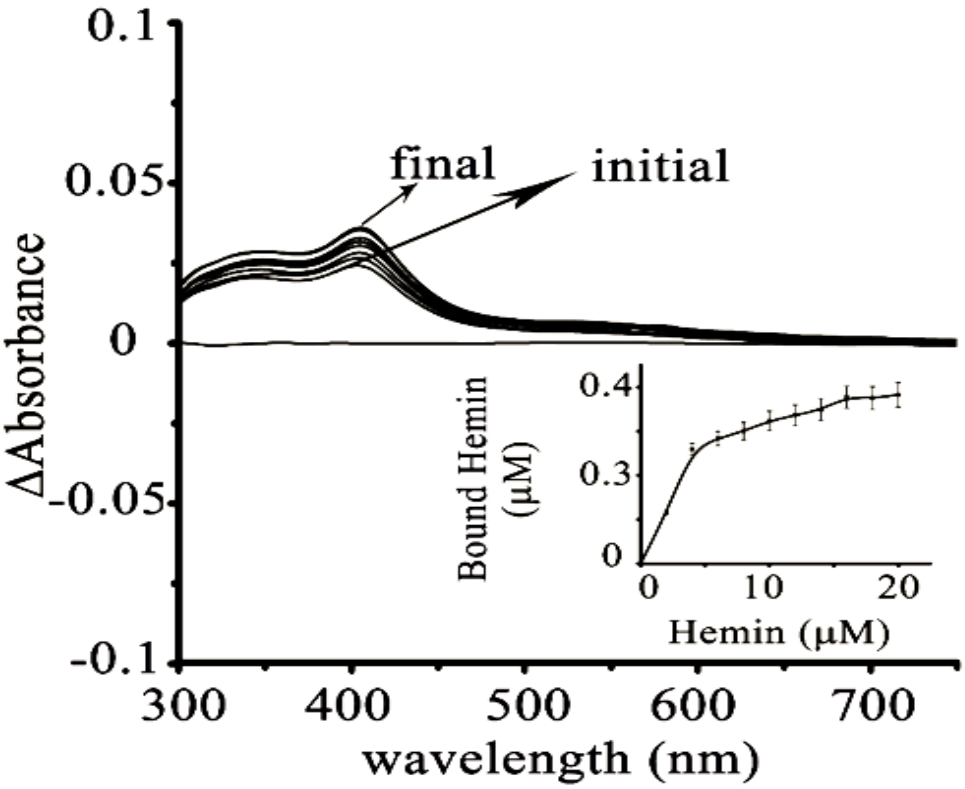

Figure 3.14 Optical difference spectroscopy to examine the binding of hemin to the C-terminal domain of HSPA8. The C-terminal domain does not show any dip after the titrations suggesting no binding. Instead positive peaks of very small magnitude were observed after each titration. Such small magnitudes do not support any binding. The peaks also do not seem to be saturated up to the tested concentrations of hemin.

The data from the optical spectroscopy indicate a specific but moderate interaction between hemin and HSPA8, primarily through the N-terminal region of the protein. When hemin binds to proteins, forming hemoproteins, it can impart various functional properties to the protein[23]. For instance, hemoproteins can exhibit peroxidase activity in the presence of hydrogen peroxide (H_2O_2)[24]. The binding studies of the HSPA8-hemin complex with H_2O_2 demonstrated that the complex reacts with H_2O_2 in a dose-dependent manner. Interestingly the dip observed in the spectra did not reach saturation (**Figure 3.15**), suggesting the formation of a less stable product, possibly the intermediate compounds formed in a classical peroxidase cycle. This observation prompted us to investigate whether this complex exhibits peroxidase activity, as professional heme-peroxidases show a similar phenotype of intermediate formation in the presence of H_2O_2.

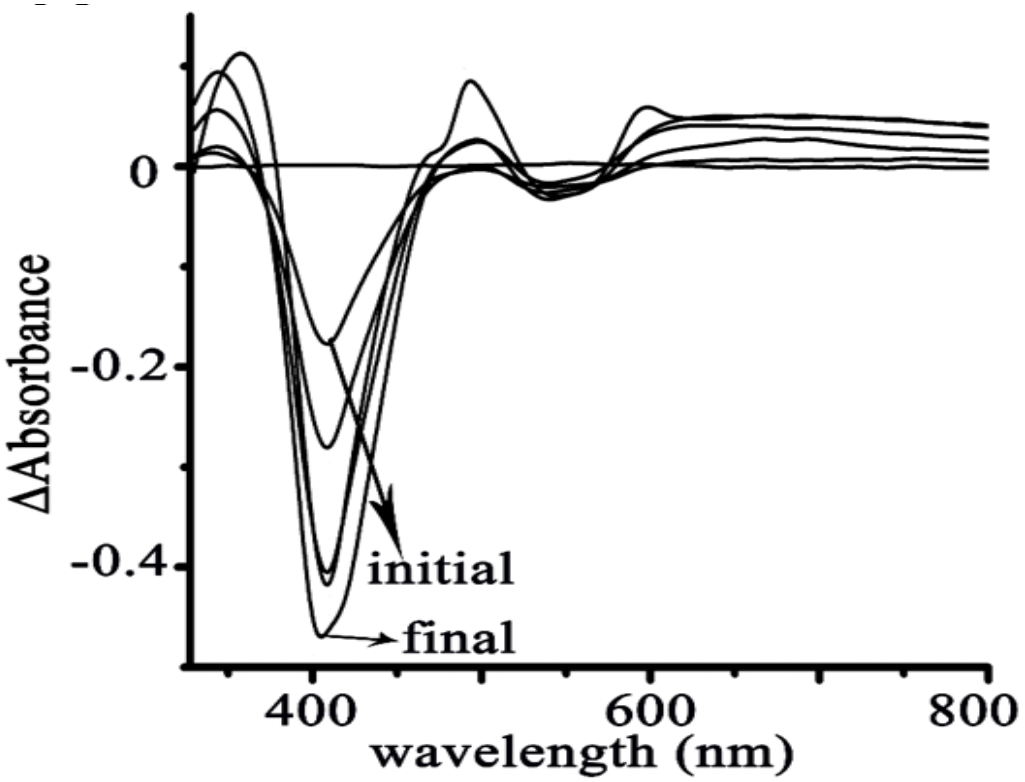

Figure 3.15: Optical difference spectroscopy of H_2O_2 (0-25 µM) binding to HSPA8-hemin complex. The spectra were recorded immediately after the addition of H_2O_2 to the complex. The data shows a difference and slight red shift in the absorbance of the complex upon the addition of H_2O_2 suggesting its reaction to the complex. The dips do not seem to be saturating suggesting that although H_2O_2 reacts with the complex, it does not form a stable complex with it. The unstable complex formed can be the intermediate compound I of the peroxidase cycle. This finding forms the basis for hypothesizing the involvement of the peroxidase-H_2O_2 system in the polymerization process.

Indeed we found that the HSPA8-hemin complex is capable of oxidizing the aromatic substrate guaiacol in the presence of H_2O_2 to form tetraguaiacol. To confirm the specificity of the activity by the HSPA8-hemin complex, we performed the assay under different conditions. The results show that the complex specifically exhibits peroxidase activity because the non-specific conversion was minimal in the absence of H_2O_2 and with the protein or hemin alone (**Table 3.3**). At a concentration of 2 µM, the complex showed significant peroxidase activity, with a V_{max} and K_m value of 56.2 ± 7 µmol/min and 3.3 ± 1.8 mM, respectively (**Figure 3.16**).

Table 3.3: Polymerization of guaiacol by HSPA8-hemin complex.

S. Number.	Reaction	Tetraguaiacol formed (µmol/min), M ± S.D.
1	Buffer + HSPA8-hemin complex + Guaiacol + H_2O_2	70.5 ± 9.5
2	Buffer + Hemin + Guaiacol + H_2O_2	11.2 ± 4.3
3	Buffer + HSPA8-hemin complex + Guaiacol	10.6 ± 2.7
4	Buffer + HSPA8-hemin complex + H_2O_2	0.00
5	Buffer + HSPA8-hemin complex	0.00
6	Buffer + Guaiacol	2.3 ± 2.2
7	Buffer	0.00

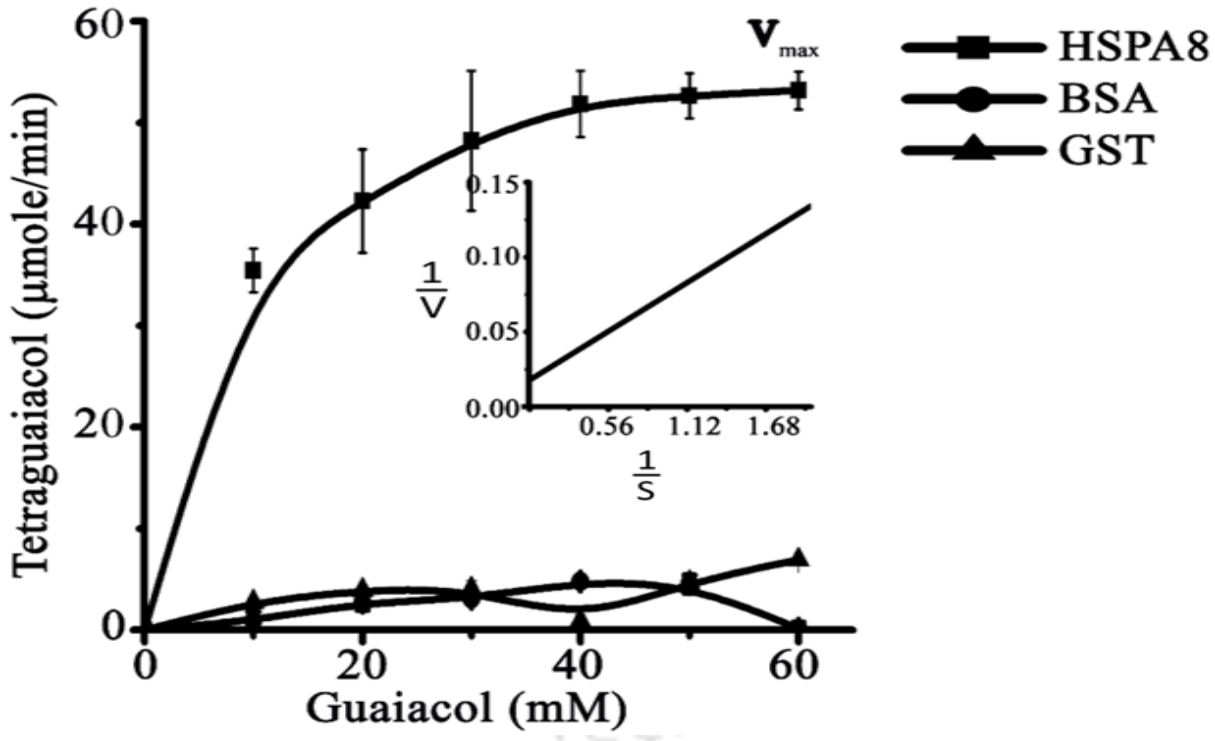

Figure 3.16: Peroxidase activity assay: The involvement of the peroxidase –H_2O_2 system was tested by a substrate-dependent peroxidase activity assay of the HSPA8-hemin complex as described (section 2.8) using Guaiacol as substrate. The data were plotted in the form of a Michaelis-Menten curve and Lineweaver Burk plot (inset) The complex (2 µM) showed significant peroxidase activity with a V_{max} and K_m values of 56.08 ± 7.02 µmol/min and 3.26 ± 1.77 mM respectively. The graph shows individual data points as scattered with standard deviations and the fitting curve as a line. Control experiments with equal concentrations of two other heme-binding proteins, BSA and GST, showed minimal activity as compared to the complex.

The turnover number of the complex for the guaiacol substrate was calculated to be 0.2 ± 0.02 min^{-1}. This suggests that the HSPA8-hemin complex may act as a peroxidase under heme stress conditions, potentially enabling the protein to exhibit various biological functions. Notably, the peroxidase activity was specific to the HSPA8-hemin complex, as control proteins such as HSPA8 (not bound to hemin) and two other heme-binding proteins, BSA (Bovine Serum Albumin) and GST (Glutathione-S-Transferase), did not show significant activity at the same concentration as the complex. Additionally, we also investigated the difference in the binding affinity of HSPA8 to hemin as compared to two other heme-binding proteins BSA and GST (**Figure 3.17**).

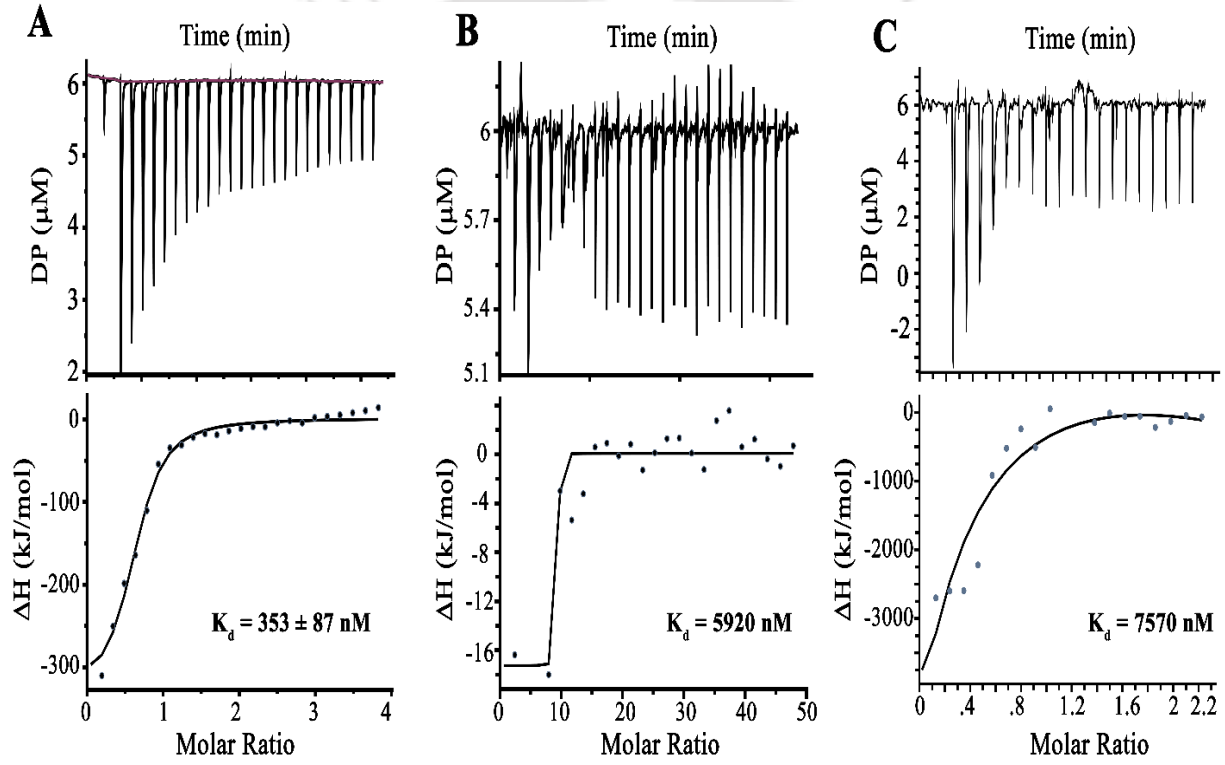

Figure 3.17: Isothermal calorimetry of HSPA8, BSA, and GST with hemin. A) Hemin (100 µM) to HSPA8 (5 µM) titrations showed a clear saturating curve for the differential power (DP) Vs. time graph. The integrated heat plot (below) was fitted to a one-site model and the apparent K_d value was obtained to be 353 ± 87 nM. **B)** Hemin to BSA titration curves were not seen to be saturated due to a large heat of dilutions for BSA. After subtracting the control (buffer Vs. BSA) data from the data obtained upon titration of hemin to BSA, the integrated heat plot showed a better fitting line (using simplex fit). The apparent K_d value was determined to be 5920 nM. **C)** Hemin to GST titrations were found to be saturated and the integrated heat plot was fitted using simplex fit. The apparent K_d value for hemin binding to GST was found to be 7570 nM. The data shows that hemin has a very strong affinity for binding to HSPA8 (K_d in nanomolar range) as compared to the control proteins BSA and GST (K_d in micromolar range).

The binding of hemin to HSPA8, BSA, and GST was confirmed through isothermal calorimetry experiments under similar experimental conditions. HSPA8 exhibited strong binding to hemin, with a dissociation constant (K_d) value of 353 ± 87 nM. In contrast, BSA and GST showed much weaker binding to hemin, with apparent K_d values of 5920 and 7570 nM, respectively.

3.3.4 HSPA8 hemoprotein oxidizes hemin to form heme polymer utilizing the N-terminal domain

Peroxidases exhibit a wide range of functions due to their ability to interact with various aromatic substrates. In a prior investigation, we observed the professional heme-peroxidase HRP utilizes its peroxidase activity to oxidize heme into heme polymer[24]. Given that the HSPA8 hemoprotein can oxidize the aromatic substrate guaiacol to produce tetraguaiacol, we were intrigued to explore whether it could oxidize heme into a heme polymer similar to HRP. Therefore we conducted assays using HSPA8 hemoprotein, as well as its truncation products (NBD and CT), and two control heme-binding proteins BSA and GST. Surprisingly, we found that both HSPA8 and its N-terminal domain (NBD) catalyzed heme polymer formation independently, while the C-terminal domain (CT) did not show any such activity (**Figure 3.18A**). This polymerization was specific to HSPA8 or NBD as neither BSA nor GST exhibited any heme polymerization activity within the tested concentration range. Furthermore, we observed that HSPA8 catalyzed heme polymerization in a dose-dependent manner, reaching saturation at approximately 0.9 µM of HSPA8 with 100 µM of hemin. The maximum amount of heme polymer formed was approximately 18-20 µM, with a turnover number (K_{cat}) of 0.42 ± 0.07 $hour^{-1}$ for HSPA8. Consistent with our binding studies, NBD was also capable of independently polymerizing hemin. We also performed a time-dependent heme polymerization assay of HSPA8 to better understand the nature of the process. The results show no polymerization up to 2 hours of incubation, after which the amount of polymer formed gradually increased with time and reached saturation after 9 hours. It took around 9 hours for HSPA8 to form the maximum amount of heme polymer from 100 µM of hemin (**Figure 3.18B).** Heme polymerization is known to be a slow process in an *in-vitro* system due to the presence of the microenvironment and other biological factors inside infected red blood cells[17].

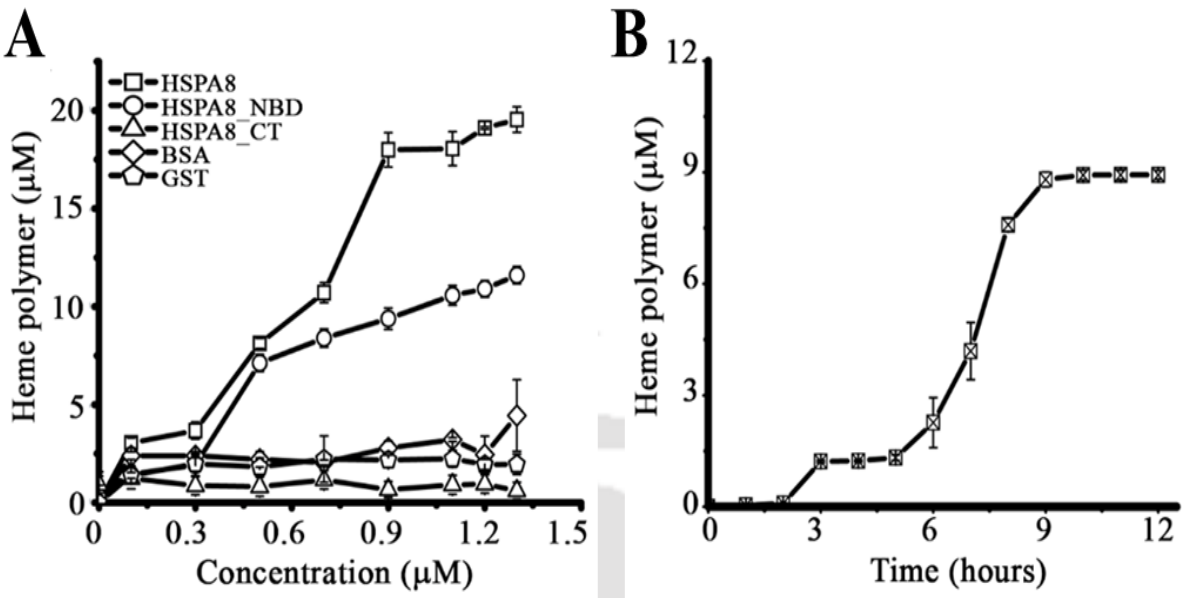

Figure 3.18: A) HSPA8 converts hemin into heme polymer through its N-terminal domain. Oxidation of hemin (as aromatic substrate) by HSPA8, its domains, and control proteins BSA and GST were tested through dose-dependent heme polymerization assay. A concentration of 0-1.3 μM of each protein was tested for their ability to form heme polymer from 100 μM hemin in the presence of 5 mM H_2O_2. The curves show that HSPA8 and its N-terminal (HSPA8_NBD) independently form heme polymer with a maximum of 18 μM and 12 μM heme polymer concentration respectively. The C-terminal (HSPA8_CT), BSA, and GST do not show any heme polymerization activity in the tested concentration range. **B) A Time-dependent heme polymerization assay** was performed to confirm the nature of the polymerization process. HSPA8 (1 μM) was assayed for its activity. The curve shows saturation at around 9 μM heme polymer concentration after 9 hours of incubation which supports the slow nature of the heme polymerization process.

To ensure the specificity of the polymerization process, we performed the assay under various control conditions, and the results are summarized in **Table 3.4.** HSPA8 showed a significant amount of polymerization with 19.5 ± 0.7 μM of heme polymer formed. The non-specific polymerization under control conditions like the absence of H_2O_2, hemin, or HSPA8 showed a minimal amount of polymerization confirming the specificity of the complex. The polymerization by HSPA8 was reduced significantly in the presence of classical peroxidase substrates like guaiacol and potassium chloride and a spin trap agent PBN. The presence of peroxidase inhibitors like sodium azide and clotrimazole completely inhibited the polymerization process giving an insight into the involvement of peroxidase-like mechanism in the process.

Table 3.4: Heme Polymerization by HSPA8.

S. Number	Reaction	Heme polymer formed (μM), M ± S.D.
1	Buffer + HSPA8 +Hemin + H_2O_2	19.5 ± 0.7
2	Buffer + HSPA8 + Hemin	0.1 ± 0.004
3	Buffer + HSPA8 + H_2O_2	0.6 ± 0.008
4	Buffer + Hemin + H_2O_2	0.02 ± 0.002
5	Buffer + HSPA8	0.00
6	Buffer + Hemin	0.00
7	Buffer	0.00
8	Buffer + HSPA8 +Hemin + H_2O_2 + PBN (200 μM)	2.5 ± 0.1
9	Buffer + HSPA8 +Hemin + H_2O_2 + Guaiacol (50 mM)	0.2 ± 0.1
10	Buffer + HSPA8 +Hemin + H_2O_2 + KI (50 mM)	1.6 ± 0.1
11	Buffer + HSPA8 +Hemin + H_2O_2 + KCl (50 mM)	4.1 ± 0.1
12	Buffer + HSPA8 +Hemin + H_2O_2 + Clotrimazole (50 mM)	0.00
13	Buffer + HSPA8 +Hemin + H_2O_2 + Sodium Azide (50 mM)	0.00

A comparison of the infrared (IR) spectra of the heme polymer formed by HSPA8 with synthetic β-hematin revealed structural similarities, particularly in the peaks at 1525 cm^{-1} and 1718 cm^{-1}., corresponding to the iron-carboxylate bond (**Figure 3.19)**.

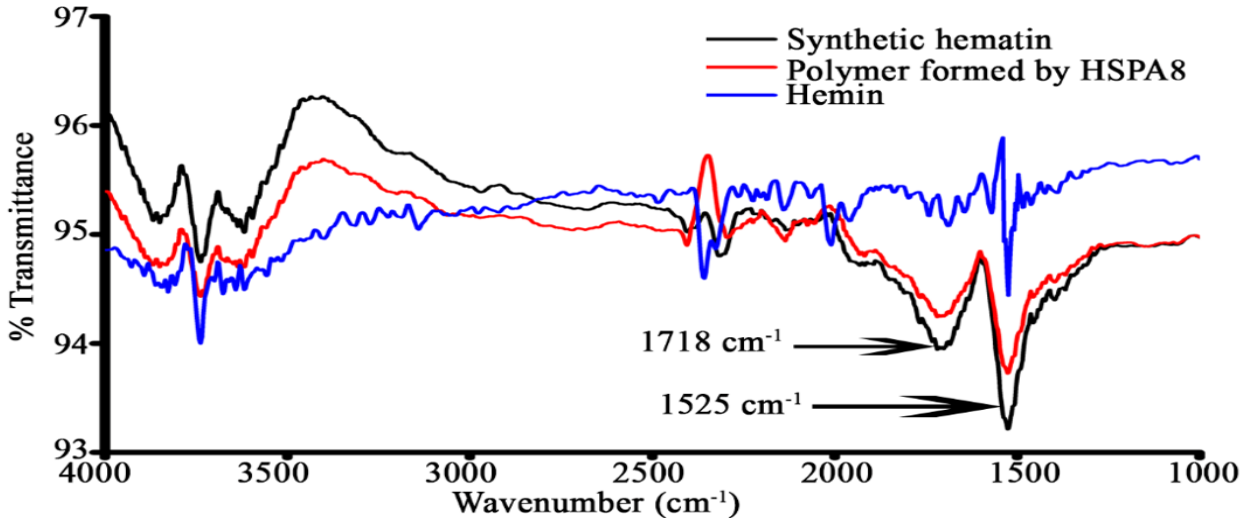

Figure 3.19: Characterization of heme polymer formed by HSPA8. The heme polymer formed by HSPA8 was characterized through FTIR spectroscopy with synthetic β-hematin as standard.

Both polymers showed significantly similar spectra with common peaks at 1525 and 1718 cm^{-1} suggesting significant structural similarity of the heme polymer with synthetic β-hematin. β-hematin is a heme dimer formed by the mutual covalent interaction between the carboxylic group and iron atom of two hemin molecules. The presence of the iron-carboxylate peak suggests the covalent nature of the heme polymer produced by HSPA8.

3.3.5 HSPA8-hemin complex polymerizes hemin involving hemin free radical mechanism

The process of heme polymerization, demonstrated using a model peroxidase (HRP), is initiated by the oxidation of ferric (Fe-III) heme within the peroxidase by H_2O_2, resulting in the formation of a single-electron transfer ferryl (Fe-IV=O) intermediate. This intermediate is subsequently reduced to its native HRP (Fe-III) in the presence of the substrate, heme, leading to the formation of a heme-free radical. The heme polymer is then formed through radical-radical interaction between the generated radicals[24].

The confirmation of the formation of a single-electron transfer intermediate was achieved through optical spectroscopy (**Figure 3.20A**). Interestingly, the HSPA8 hemoprotein exhibited an absorbance peak at 400 nm (peak "a"), indicating heme iron coordination with certain HSPA8 residues**,** possibly Arg155, as suggested by docking studies. Upon the addition of H_2O_2, the soret peak shifted to 407 nm (peak "b"). However, upon further addition of 20 mM of Guaiacol or hemin, the peak returned to 400 nm (peak "c" and "e"), confirming substrate oxidation and the reduction of the intermediate to the native complex. Additionally, the appearance of a tetraguaiacol peak at 470 nm (peak "d") confirmed the polymerization of guaiacol.

The heme polymerization by HRP involves the generation of substrate-free radicals. To confirm free radicals in the HSPA8-hemin complex catalyzed heme polymerization, a heme polymerization assay was performed in the presence of varying concentrations (0-1000 µM) of a spin trap, phenyl N-t-butyl nitrone (PBN). The results show that the polymerization was completely inhibited at 200 µM and above concentrations of PBN (**Figure 3.20B**) indicating the involvement of a heme-free radical in the polymerization process. The calculated IC_{50} value for the inhibition by PBN was found to be 65.03 µM.

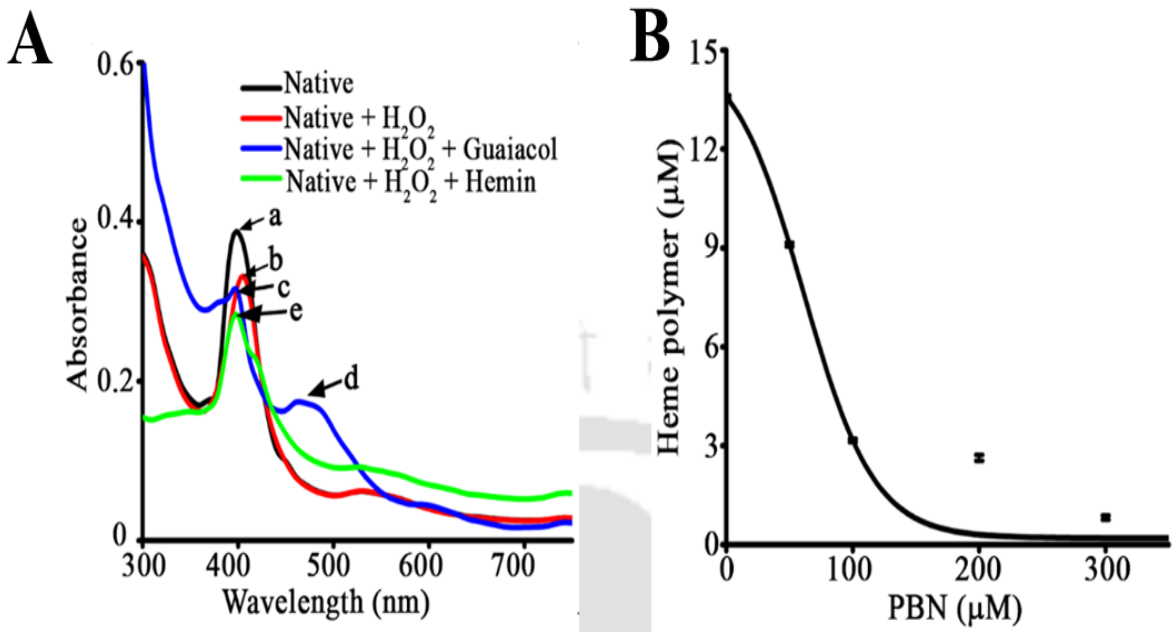

Figure 3.20: A) UV Spectroscopy to confirm the formation of a single-electron transfer intermediate by HSPA8-hemin complex with 3 µM H_2O_2. The complex gives a soret peak (peak a) at 400 nm which showed a slight red shift (peak b) to 407 nm upon the addition of H_2O_2 suggesting an intermediate formation. It was further confirmed by the addition of 20 mM of the aromatic substrates guaiacol and hemin. Upon titration with guaiacol, the peak shifted back to 400 nm (peak c) and a peak appeared at 470 nm (peak d) which is characteristic of the oxidation product tetraguaiacol, thus confirming the polymerization of Guaiacol. Similarly, after the addition of hemin, the peak shifted back to 400 nm (peak e), confirming the retention of the native complex. **B) Heme polymerization assay in the presence of a spin-trap agent.** The involvement of a free radical in the process was tested by performing the heme polymerization activity in the presence of increasing concentration (0-1000 µM) of a spin-trap agent PBN. Complete inhibition was observed after a concentration of 400 µM confirming the free radical involvement.

To validate the role of peroxidase activity in heme polymerization, the effects of peroxidase inhibitors and competition with aromatic/halide substrates were examined. Peroxidase inhibitors, sodium azide, and clotrimazole exhibited complete inhibition of heme polymerization activity above 30 mM, while the activity was reduced in the presence of substrates such as the halide substrate potassium chloride (>50%), potassium chloride (>80%), and the aromatic substrate guaiacol (>95%) at their highest concentrations (**Figure 3.21**). These findings collectively suggest the involvement of a single electron transfer intermediate and a free radical in the polymerization of hemin to heme polymer through a peroxidase-H_2O_2 system**.**

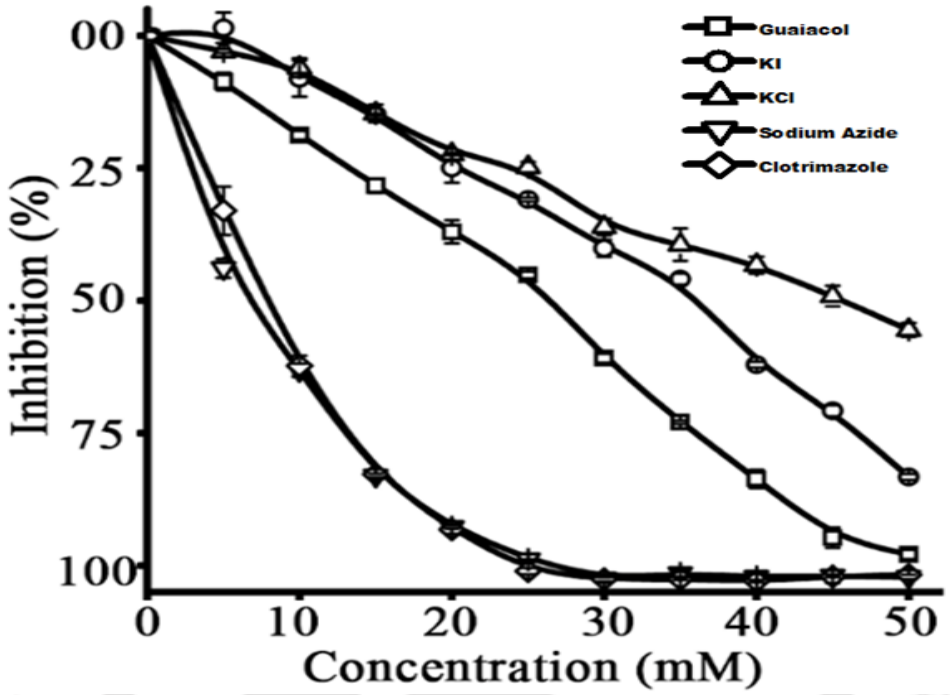

Figure 3.21: Heme polymerization assay in the presence of substrates and inhibitors. The involvement of the peroxidase mechanism in the process was further confirmed by performing a heme polymerization assay in the presence of peroxidase substrates, Guaiacol (aromatic), Potassium iodide, and Potassium chloride (halides), and classical peroxidase inhibitors (sodium azide and clotrimazole). The activity was significantly reduced in the presence of substrates guaiacol (square, >95%), potassium iodide (circle, >80%), and potassium chloride (triangle, >50%) suggesting a competition between hemin and the tested substrates. Complete inhibition of the activity was found with peroxidase inhibitors sodium azide (rhombus) and clotrimazole (reverse triangle) confirming the involvement of the peroxidase mechanism in the polymerization process.

3.4 Discussion

HSPA8, a protein known for its chaperone function, contains a region that binds hemin with remarkable affinity, especially at elevated physiological heme levels (up to 20 µM)seen during conditions like severe hemolysis and hemoglobin degradation[25]. Its constitutive expression allows HSPA8 to counteract hemin toxicity, in almost all cell types, by converting it into a less harmful heme polymer. This conversion is not unique to humans but is also found in various organisms, such as the malarial *Parasite falciparum*, the blood-feeding insect *Rhodnius prolixus*, the blood fluke *Schistosoma mansoni*, and the protozoan *Haemoproteus columbae*[26-29].

Different proteins are involved in heme detoxification across different organisms, including heme oxygenase in humans and specific plasmodium proteins in the parasite[30, 31].

In situations of heme stress, HSPA8 undergoes a transformation into a heme-peroxidase, facilitating the polymerization of hemin. This represents an additional role of HSPA8 during heme stress, highlighting its versatility. A similar type of functional shift, from a peroxidase to a chaperone, has been observed in two cytosolic yeast peroxiredoxins (cPrxI and cPrxII) and *Oryza sativa* ascorbate peroxidase[32, 33].

This study marks the first observation of a chaperone transitioning into a peroxidase, expanding our understanding of the adaptive capabilities of proteins under stress conditions. Despite its primary chaperone role under stress, HSPA8's ability to function as a peroxidase to alleviate heme stress is noteworthy. This dual functionality underscores the protein's importance in responding to cellular homeostasis under challenging conditions. The dose- and time-dependent heme polymerization activity of HSPA8 further supports this notion, suggesting a controlled and gradual process rather than a spontaneous one[17, 34]. The ability of HSPA8 to neutralize hemin by its polymerization is crucial for cell survival, particularly in situations of elevated heme levels. This process not only protects cells from damage but also contributes to the overall detoxification processes in the body. The evolutionary conservation of this mechanism across various organisms suggests its fundamental importance in cellular physiology and adaptation to sudden challenges.

Histidine, Arginine, and Phenylalanine are essential for substrate binding in the formation of intermediate compounds in the peroxidase cycle of HRP[35, 36]. While no Histidine residues were found near the hemin binding region in the HSPA8 hemoprotein, Arginine and Phenylalanine residues could potentially aid in hemin binding and its polymerization. In contrast, in HRP, the Histidine residue plays a crucial role in electron transfer. The specific HSPA8 residue involved in forming electron transfer intermediates remains unknown. Detailed insights into the interaction between hemin and HSPA8, including atom-atom and aton-residue interactions, and the type of hemin free radical formed, could provide, a better understanding of the complex formation and its peroxidase-like mechanism.

Structural changes necessary for HSPA8 to transition from a chaperone to peroxidase and a similar kind of functional switch can be well explored with other stress-responsive HSPs. Exploiting the intraction between hemin and HSPA8 could be valuable in drug discovery and modulating disease pathologies involving free heme generation. Heme binding to various heme-responsive sensors

can alter their function[23]. Given that HSPA8 transforms into a peroxidase upon heme binding, it is plausible that HSPA8 also acts as a heme sensor protein.

3.5 Conclusions:

In our study, we tried to discover the role of chaperones in heme detoxification during its accumulation.

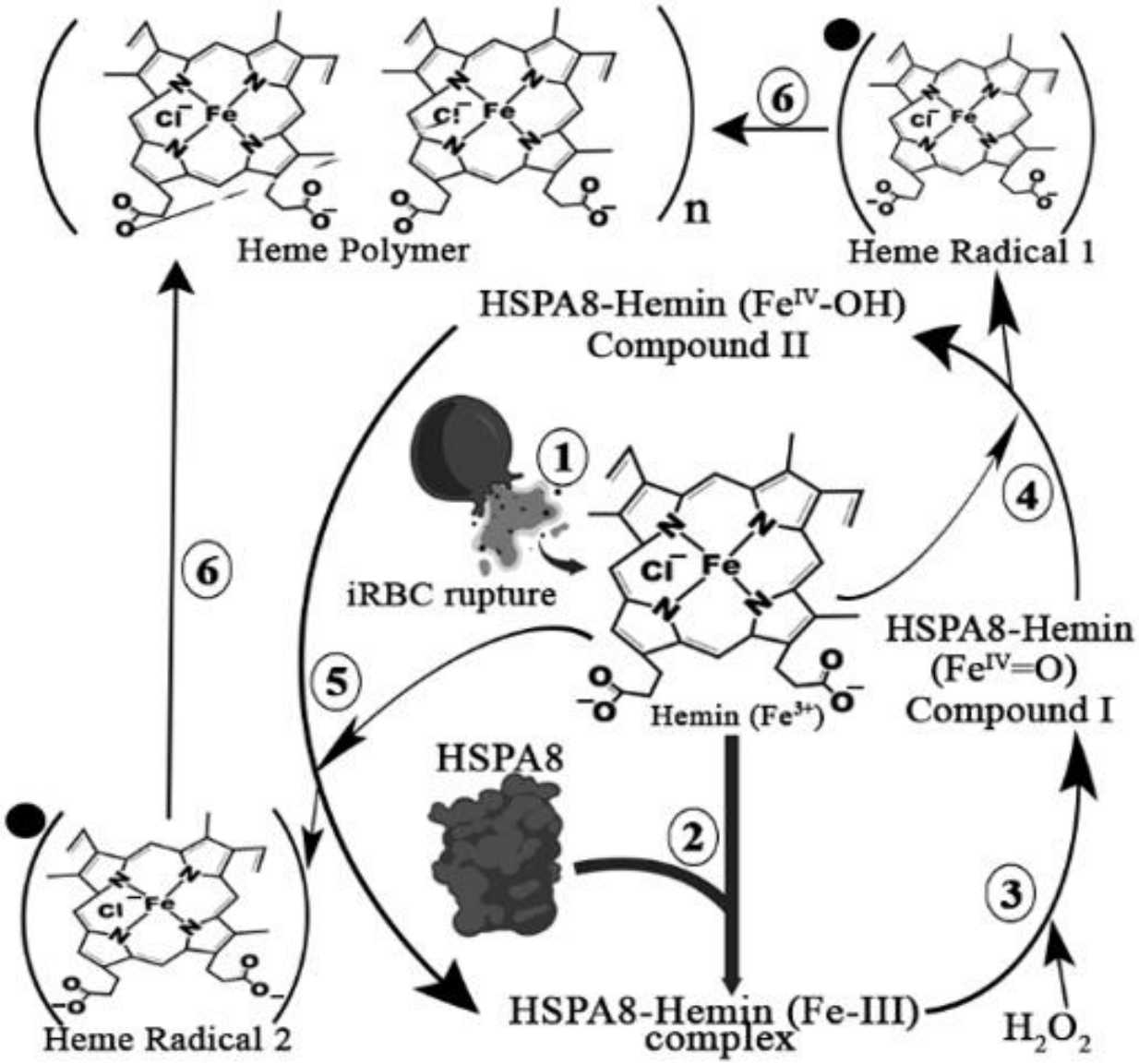

Figure 3.22: A hypothetical model illustrating the complete process of polymerization of hemin into heme polymer by the protein HSPA8.

The chaperone HSPA8 binds hemin and transforms into a hemoprotein. The hemoprotein exhibits peroxidase activity utilizing which it converts aromatic hemin into less toxic heme polymer. The hemoprotein binds H_2O_2 to form a ferryl intermediate (FeIV=0) which reverts to its native state (Fe-III) on the addition of a substrate. The polymerization of hemin is completely inhibited in the presence of a spin trap agent suggesting free radical formation in the process. The polymerization is also diminished in the presence of classical peroxidase substrates and completely vanishes with peroxidase inhibitors further suggesting an involvement of a peroxidase-like mechanism in the process. Our findings suggest the polymerization of hemin by the HSPA8-hemoprotein in the presence of H_2O_2 in a fashion similar to HRP. In this process, a single electron gets transferred to hemin forming free radicals which further interact to form heme polymer. Together, the data allow us to propose a suggestive model to explain the role of HSPA8 during malaria-like environments with high hemin (**Figure 3.23**).

3.7 References

1. Kumar, S. and U. Bandyopadhyay, Free heme toxicity and its detoxification systems in human. Toxicology letters, 2005. **157**(3): p. 175-188.
2. Grunwald, E.W. and M.P. Richards, Mechanisms of heme protein-mediated lipid oxidation using hemoglobin and myoglobin variants in raw and heated washed muscle. Journal of Agricultural and Food Chemistry, 2006. **54**(21): p. 8271-8280.
3. Gamage, S.M.K., et al., Hemin, a major heme molecule, induced cellular and genetic alterations in normal colonic and colon cancer cells. Pathology-Research and Practice, 2021. **224**: p. 153530.
4. Vasconcellos, L.R., et al., Protein aggregation as a cellular response to oxidative stress induced by heme and iron. Proceedings of the National Academy of Sciences, 2016. **113**(47): p. E7474-E7482.
5. Butt, O.I., P.W. Buehler, and F. D'Agnillo, Blood-brain barrier disruption and oxidative stress in guinea pig after systemic exposure to modified cell-free hemoglobin. The American journal of pathology, 2011. **178**(3): p. 1316-1328.
6. Balla, G., et al., Exposure of endothelial cells to free heme potentiates damage mediated by granulocytes and toxic oxygen species. Laboratory investigation; a journal of technical methods and pathology, 1991. **64**(5): p. 648-655.
7. Maines, M.D., Heme oxygenase: function, multiplicity, regulatory mechanisms, and clinical applications. The FASEB journal, 1988. **2**(10): p. 2557-2568.
8. Straus, D., W. Walter, and C.A. Gross, DnaK, DnaJ, and GrpE heat shock proteins negatively regulate heat shock gene expression by controlling the synthesis and stability of sigma 32. Genes & Development, 1990. **4**(12a): p. 2202-2209.

9. Szyller, J. and I. Bil-Lula, Heat shock proteins in oxidative stress and ischemia/reperfusion injury and benefits from physical exercises: A review to the current knowledge. Oxidative Medicine and Cellular Longevity, 2021. **2021**.
10. Brocchieri, L., E. Conway de Macario, and A.J. Macario, hsp70 genes in the human genome: Conservation and differentiation patterns predict a wide array of overlapping and specialized functions. BMC evolutionary biology, 2008. **8**(1): p. 1-20.
11. Multhoff, G., Heat shock proteins in immunity. Molecular Chaperones in Health and Disease, 2006: p. 279-304.
12. McCallister, C., et al., Functional diversification and specialization of cytosolic 70-kDa heat shock proteins. Scientific reports, 2015. **5**(1): p. 1-11.
13. Ferrarini, M., et al., Unusual expression and localization of heat-shock proteins in human tumor cells. International Journal of Cancer, 1992. **51**(4): p. 613-619.
14. TSUBOI, N., et al., Monoclonal antibody specifically reacting against 73-kilodalton heat shock cognate protein: possible expression on mammalian cell surface. Hybridoma, 1994. **13**(5): p. 373-381.
15. Page, N., et al., HSC70 blockade by the therapeutic peptide P140 affects autophagic processes and endogenous MHCII presentation in murine lupus. Annals of the rheumatic diseases, 2011. **70**(5): p. 837-843.
16. Yun, H.R., et al., Roles of autophagy in oxidative stress. International journal of molecular sciences, 2020. **21**(9): p. 3289.
17. Sullivan Jr, D.J., I.Y. Gluzman, and D.E. Goldberg, Plasmodium hemozoin formation mediated by histidine-rich proteins. Science, 1996. **271**(5246): p. 219-222.
18. Deshmukh, R. and V. Trivedi, Pro-stimulatory role of methemoglobin in inflammation through hemin oxidation and polymerization. Inflammation & Allergy-Drug Targets (Formerly Current Drug Targets-Inflammation & Allergy)(Discontinued), 2013. **12**(1): p. 68-78.
19. Santos, T.G., V.R. Martins, and G.N.M. Hajj, Unconventional secretion of heat shock proteins in cancer. International journal of molecular sciences, 2017. **18**(5): p. 946.
20. Banesh, S., S. Layek, and V. Trivedi, Hemin acts as CD36 ligand to activate down-stream signalling to disturb immune responses and cytokine secretion from macrophages. Immunology Letters, 2022. **243**: p. 1-18.
21. Makarska-Bialokoz, M., Interactions of hemin with bovine serum albumin and human hemoglobin: A fluorescence quenching study. Spectrochimica Acta Part A: Molecular and Biomolecular Spectroscopy, 2018. **193**: p. 23-32.
22. Owens, C.P., et al., Characterization of heme ligation properties of Rv0203, a secreted heme binding protein involved in Mycobacterium tuberculosis heme uptake. Biochemistry, 2012. **51**(7): p. 1518-1531.
23. Shimizu, T., et al., Heme: emergent roles of heme in signal transduction, functional regulation and as catalytic centres. Chemical Society Reviews, 2019. **48**(24): p. 5624-5657.
24. Trivedi, V., et al., Mechanism of horseradish peroxidase-catalyzed heme oxidation and polymerization (β-hematin formation). Biochimica et Biophysica Acta (BBA)-General Subjects, 2005. **1723**(1-3): p. 221-228.
25. Pethő, D., et al., Heme cytotoxicity is the consequence of endoplasmic reticulum stress in atherosclerotic plaque progression. Scientific reports, 2021. **11**(1): p. 1-23.

26. de Villiers, K.A. and T.J. Egan, Heme detoxification in the malaria parasite: a target for antimalarial drug development. Accounts of Chemical Research, 2021. **54**(11): p. 2649-2659.
27. Oliveira, M.F., et al., Haemozoin formation in the midgut of the blood-sucking insect Rhodnius prolixus. Febs Letters, 2000. **477**(1-2): p. 95-98.
28. Oliveira, M.F., et al., Haemozoin in Schistosoma mansoni. Molecular and biochemical parasitology, 2000. **111**(1): p. 217-221.
29. Chen, M.M., L. Shi, and D.J. Sullivan Jr, Haemoproteus and Schistosoma synthesize heme polymers similar to Plasmodium hemozoin and β-hematin. Molecular and biochemical parasitology, 2001. **113**(1): p. 1-8.
30. Gozzelino, R., V. Jeney, and M.P. Soares, Mechanisms of cell protection by heme oxygenase-1. Annual review of pharmacology and toxicology, 2010. **50**(1): p. 323-354.
31. Jani, D., et al., HDP—a novel heme detoxification protein from the malaria parasite. PLoS pathogens, 2008. **4**(4): p. e1000053.
32. Jang, H.H., et al., Two enzymes in one: two yeast peroxiredoxins display oxidative stress-dependent switching from a peroxidase to a molecular chaperone function. Cell, 2004. **117**(5): p. 625-635.
33. Hong, S.H., et al., Functional switching of ascorbate peroxidase 2 of rice (OsAPX2) between peroxidase and molecular chaperone. Scientific reports, 2018. **8**(1): p. 1-9.
34. Pandey, A.V. and B.L. Tekwani, Formation of haemozoin/β-haematin under physiological conditions is not spontaneous. FEBS letters, 1996. **393**(2-3): p. 189-192.
35. Rodriguez-Lopez, J.N., A.T. Smith, and R.N. Thorneley, Role of Arginine 38 in Horseradish Peroxidase: A CRITICAL RESIDUE FOR SUBSTRATE BINDING AND CATALYSIS (∗). Journal of Biological Chemistry, 1996. **271**(8): p. 4023-4030.
36. Bandyopadhyay, U., S. Adak, and R.K. Banerjee, Role of active site residues in peroxidase catalysis: studies on horseradish peroxidase. Proceedings of the Indian National Science Academy-Part B: Biological Sciences, 1999. **65**(5): p. 315-330.

Chapter IV

Hemin Competitively Inhibits HSPA8 ATPase Activity Mitigating its Foldase Function

Publication: " Pandey, A.K. and Trivedi, V., 2024. Hemin competitively inhibits HSPA8 ATPase activity mitigating its foldase function. Archives of Biochemistry and Biophysics, 752, p.109889."

4.1 Introduction

Hemolysis, the rupture of red blood cells, leads to the release of hemoglobin, which is eventually degraded into hemin[1]. Elevated hemin levels in the systemic circulation are detrimental to cells and tissues, playing a significant role in the pathogenesis of diseases such as severe malaria[2, 3]. To attenuate such situations cells employ several proteins that bind to hemin and facilitate its degradation and removal from the system[4]. Hemin's chemical properties and structure make it hydrophobic, allowing it to bind to several proteins[5]. It comprises pharmacophoric features that capacitate it to bind to many proteins. Hemin, structurally a planar metalloporphyrin with a ferric ion (Fe^{3+}), differs from heme, which contains a ferrous ion (Fe^{2+}). Although hemin binding is predominantly driven by hydrophobic interactions through its porphyrin ring, the iron of hemin helps in anchoring it through electrostatic interactions[6, 7]. In addition to binding with its detoxifying proteins hemin is known to bind to many other proteins[8]. This binding can modify the function of these proteins, impacting various cellular processes. Hemin is a potent inhibitor of proteins like cytoplasmic DNA polymerase[9] and ribonuclease[10] of the red blood cells, hindering their primary functions. Additionally, it can impede ATP-dependent protein degradation and the aggregation of proteins like β-amyloid[11]. It is recognized as a robust inhibitor of protein misfolding and has been suggested to compete with ATP for binding to the chaperone HSP90, thereby inhibiting HIF-1α induction[12].

Heat shock proteins(HSPs), a class of highly conserved proteins in eukaryotes, play a critical role in regulating the misfolding, and degradation of proteins. They contribute to cytoprotection in various diseases and stress conditions[13, 14]. Hemin, with its pro-oxidant and hydrophobic nature, can induce abnormal oxidative stress in cells by penetrating their membrane[15, 16]. During such stress, HSPs activate chaperone-mediated autophagy[17], maintain the redox state[18, 19], and ensure proteome health[20]. These proteins primarily function through an ATP-dependent cycling between ATP and ADP-bound states, making inhibitors of their ATPase activity impactful on cellular function, primarily in oxidative stress[21].

HSPA8, a heat shock protein weighing 73 KDa and belonging to the HSP70 family, is known to have significant implications in various diseases and stressful states, including Alzheimer's disease[22, 23] and cancer[24-26]. It also plays a protective role in oxidative stress by aiding in the refolding of unfolded proteins. However, its role during heme-induced stress is not well

understood. Considering that HSPs are evolutionarily conserved and some of them are known to bind hemin, we analyzed the structure of HSPA8 to understand its requirements for binding to hemin. Our analysis revealed that HSPA8 can accommodate hemin in its N-terminal. We hypothesized that hemin after binding to the N-terminal ATPase domain of HSPA8 may modulate its activity and functions. The findings of our study indicate that hemin competitively competes with ATP for binding to HSPA8, thereby preventing its major function of protein folding. This loss of HSPA8's cytoprotective function due to hemin binding may represent a novel pathway contributing to the overall cellular damage during pathological conditions characterized by high hemin levels, such as malaria. Understanding the mechanism by which hemin affects these proteins is crucial for developing targeted therapies for diseases associated with hemin-induced stress.

4.2 Experimental Procedures

4.2.1 Cloning, overexpression, and purification of recombinant HSPA8

The full-length HSPA8 and its N-terminal domain were cloned, overexpressed, and purified to homogeneity as described in **sections 2.5 and 2.6** of Chapter II.

4.2.2 Measurement of ATPase activity of HSPA8

The effect of hemin on the ATP hydrolysis by HSPA8 was examined in the absence and presence of hemin by a Malachite green ATPase activity assay as described in **section 2.12** of Chapter II.

4.2.3 Measurement of ATPase-dependent Chaperone activity of HSPA8

The chaperone activity of HSPA8 in the presence and absence of hemin was tested by examining the modulation in its foldase function using a model enzyme lysozyme as described in **section 2.13** of Chapter II.

4.2.4 CD Spectroscopy

The impact of hemin on the secondary structure elements of HSPA8 was tested through CD spectroscopy of HSPA8 in the absence and presence of hemin as described in **section 2.14** of Chapter II.

4.2.5 Gel filtration chromatography

The impact of hemin on the oligomeric status of HSPA8 was tested through Gel Filtration chromatography of HSPA8 in the absence and presence of hemin as described in **section 2.15** of Chapter II.

4.2.6 Competitive docking of ATP and Hemin

The competition of hemin with ATP for the ATP-binding site of HSPA8 was tested through docking studies as described in **section 2.4.5** of Chapter II.

4.2.7 MD simulation studies of HSPA8-ATP complexes

The stability of HSPA8-ATP complexes formed in the competitive docking was tested through MD simulation studies as described in **section 2.4.6** of Chapter II.

4.2.8 Isothermal calorimetry

The impact of hemin on the *in-vitro* binding affinity of ATP towards HSPA8 was tested through ITC of ATP with HSPA8 in the absence and presence of hemin as described in **section 2.16** of Chapter III.

4.3 Results

4.3.1 Purification of full-length HSPA8 and its Nucleotide-binding domain truncation mutant

The full-length HSPA8 and its nucleotide-binding domain were successfully subcloned in pET23a(+) and pET28(a+) vectors respectively. Both the proteins were substantially overexpressed in BL21(DE3) *E.coli* cells and purified to homogeneity using Ni-NTA affinity chromatography (**Figures 3.1, 3.2, 3.3, and 3.4** of Chapter III).

4.3.2 Hemin competitively inhibits HSPA8 ATPase activity

Hemin competes with ATP for binding to certain chaperones[12]. Our previous study suggested that HSPA8 has the necessary microenvironment to bind hemin in its N-terminal domain. This led us to think that hemin might influence the ATPase activity of HSPA8 and its ATP-dependent function, a hypothesis we tested as described in the Experimental section**.** To investigate this, we first subjected the raw data obtained from the ATPase activity assay to a Michaelis-Menten fitting

(**Figure 4.1A)** using OriginPro software[27]. Subsequently, we constructed a Lineweaver-Burk plot to understand the nature of inhibition of the activity (**Figure 4.1B**).

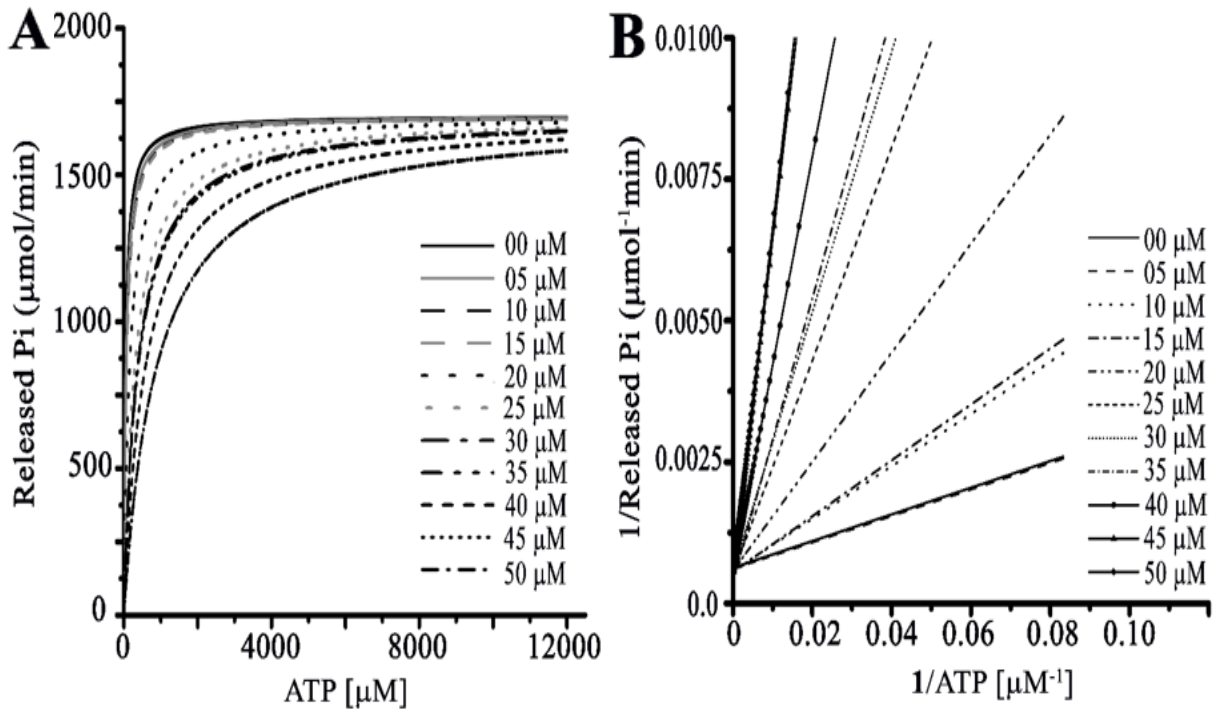

Figure 4.1: Hemin competitively inhibits HSPA8 ATPase activity. A) Hemin shows a competitive type of inhibition for HSPA8 ATPase activity. The Michaelis-Menten fits show a constant maximum value for the rate of free phosphate released (V_{max}) and gradually increasing values of K_m for ATP with increasing inhibitor concentration. The legends denote the micromolar concentrations of hemin as an inhibitor. Because of a very high number of data points, only the fitted data points are shown for the clarity of the figure. **B)** The Line-weaver burk plot of the processed raw data again confirms the competitive inhibition showing straight line curves getting steeper with increasing inhibitor concentration, with a constant y-axis intercept. The plot was used to determine the reported values of V_{max} and K_m at each tested concentration of hemin

The processed data revealed that as hemin concentration increased (from 0 to 50 µM), the maximum velocity (V_{max}) for the enzymatic reaction remained constant at 1701.25 µmole/min. However, the Michaelis constant (K_m) for the ATP substrate showed a drastic increase, rising approximately 19-fold from 47.7 ± 12.6 µM at zero hemin concentration to 899.67 ± 67.4 µM at 50 µM hemin concentration (**Table 4.1**).

Table 4.1: V_{max} and K_m for HSPA8's ATPase activity in the presence of varying hemin concentration.

S. Number	Hemin (μM)	Maximum reaction rate (V_{max}) (μmole/min)	Michaelis constant (K_m) (μM), mean ± S.D.
1	00	1701.25	47.7 ± 12.6
2	05	1701.25	60.8 ± 8.8
3	10	1701.25	69.9 ± 10.8
4	15	1701.25	72.2 ± 14.3
5	20	1701.25	158 ± 20
6	25	1701.25	298 ± 26.3
7	30	1701.25	373.4 ± 23.6
8	35	1701.25	392.2 ± 26.4
9	40	1701.25	590.6 ± 67.8
10	45	1701.25	895.2 ± 148
11	50	1701.25	899 ± 67.4

The Lineweaver_Burk plot displayed straight lines with increasing slope and a constant intercept on the y-axis for each hemin concentration, indicating a competitive type of inhibition. Using the equation for the straight-line curves (y=mx + c), we determined V_{max} and K_m values. The reciprocal of the intercept (1/c) on the y-axis equated to V_{max}, while the slope equated to K_m/V_{max}. These values allowed us to calculate the inhibition constant (K_i) for hemin (section), which was found to be 5.75 ± 0.15 μM for the inhibition of ATPase activity of HSPA8 by hemin.

4.3.4 Hemin prevents HSPA8 ATP-dependent chaperone function

HSPA8 and other chaperones rely on ATP hydrolysis for their protein folding function[28]. Inhibiting their ATPase activity is expected to hinder this function. To confirm this, we tested HSPA8's ability to refold a model protein Lysozyme in the absence and presence of hemin. The results showed that while HSPA8 (25 μM) alone completely refolded 20 μM of lysozyme, it failed to do so in the presence of 10 μM hemin. The percentage of folded lysozyme dropped to 0% upon

heat unfolding, increased to nearly 100% upon HSPA8-mediated refolding, and decreased back to almost 0% in the presence of hemin (**Figure 4.2A**).

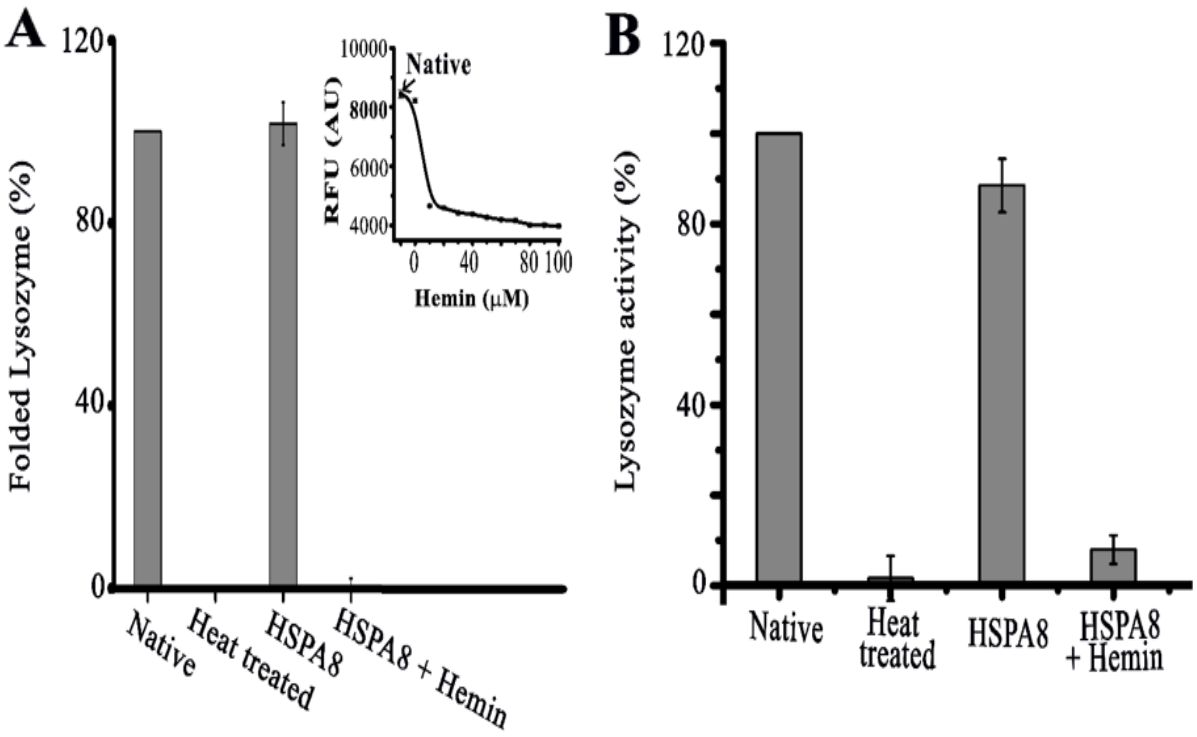

Figure 4.2: Hemin prevents HSPA8's foldase function. A) Extent of folding in lysozyme with native lysozyme (Native) as 100 percent folded. The heat-unfolded lysozyme (Heat-treated) shows zero percent folding. The lysozyme refolded by HSPA8 (HSPA8) shows almost 100 % folding in the tested conditions whereas the refolding by HSPA8 completely vanished in the presence of hemin (HSPA8 + Hemin). The inset shows the loss of lysozyme intrinsic fluorescence (y-axis) due to the prevention of the refolding function of HSPA8 by increasing hemin concentration (x-axis). The value reaches close to the intrinsic fluorescence of completely unfolded lysozyme at 10 μM hemin and so on. **B)** The percent activity of lysozyme on *E.coli* in different refolding conditions with the activity of native lysozyme (Native) as 100 %. The heat-unfolded lysozyme (Heat-treated) shows no activity. The lysozyme refolded by HSPA8 (HSPA8) shows nearly 90% activity in the tested conditions whereas less than 10% activity was observed by the lysozyme refolded by HSPA8 in the presence of hemin (HSPA8 +Hemin). All the experiments were performed in triplicates and presented as mean ± standard deviation.

The refolding was further confirmed by lysozyme activity experiments. The results show approximately 90% activity regain in the HSPA8-refolded lysozyme, comparable to native

lysozyme activity. However, the activity dropped to below 10% in the presence of hemin. HSPA8 alone did not contribute to the activity (**Figure 4.2B**). Additionally, we tested hemin's direct effect on lysozyme activity and its ability to lyse *E.coli* cells. Hemin showed no direct effect on these factors in the tested experimental conditions (**Figure 4.3 A & 4.3B)**.

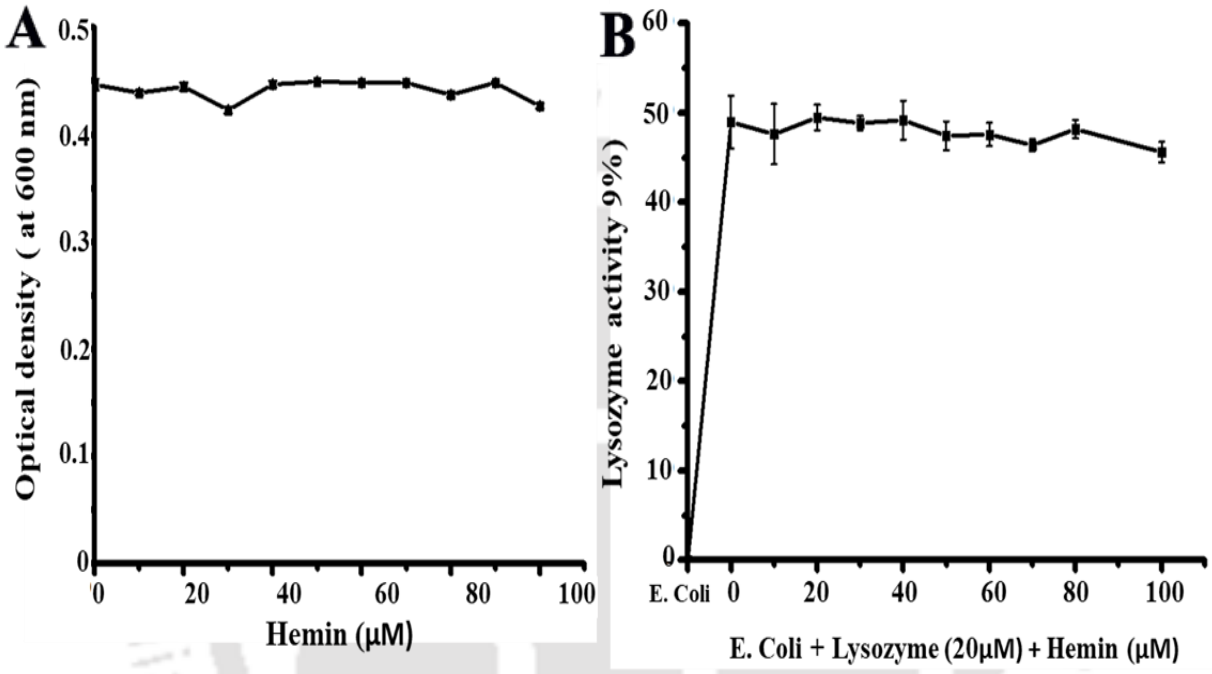

Figure 4.3: Direct effect of hemin on *E. coli* and lysozyme activity. **A)** Equal number of bacterial cells (OD_{600}= 0.5) were treated with varying hemin concentrations (0-100 μM) to test bacterial killing by hemin. OD_{600} due to hemin only was subtracted for each hemin concentration. Hemin does not cause any change in the optical density in the tested conditions suggesting no killing of E.coli cells by hemin in the tested range. **B)** Lysozyme activity with 20 μM lysozyme in the presence of varying hemin concentrations (0-100 μM) was tested and % lysozyme activity was calculated considering the activity in untreated *E.coli* cells as 0%. 50% activity was found in the absence of hemin and approximately the same activity was also seen in the presence of increasing hemin concentration. The data suggests that hemin does not show any hindrance in the activity of lysozyme in the tested conditions.

The impediment to lysozyme refolding by HSPA8 may be attributed to various factors, including the modulation of HSPA8's global 3D structure by hemin, a direct interaction of hemin with ATP, and the competitive binding between hemin and ATP. To explore these possibilities, a hypothetical model illustrating these factors was constructed (**Figure 4.4**). Subsequently, both *in-*

silico and *in-vitro* methods were employed to provide a conclusive explanation for the competition between ATP and hemin as the likely cause for the loss of HSPA8 function.

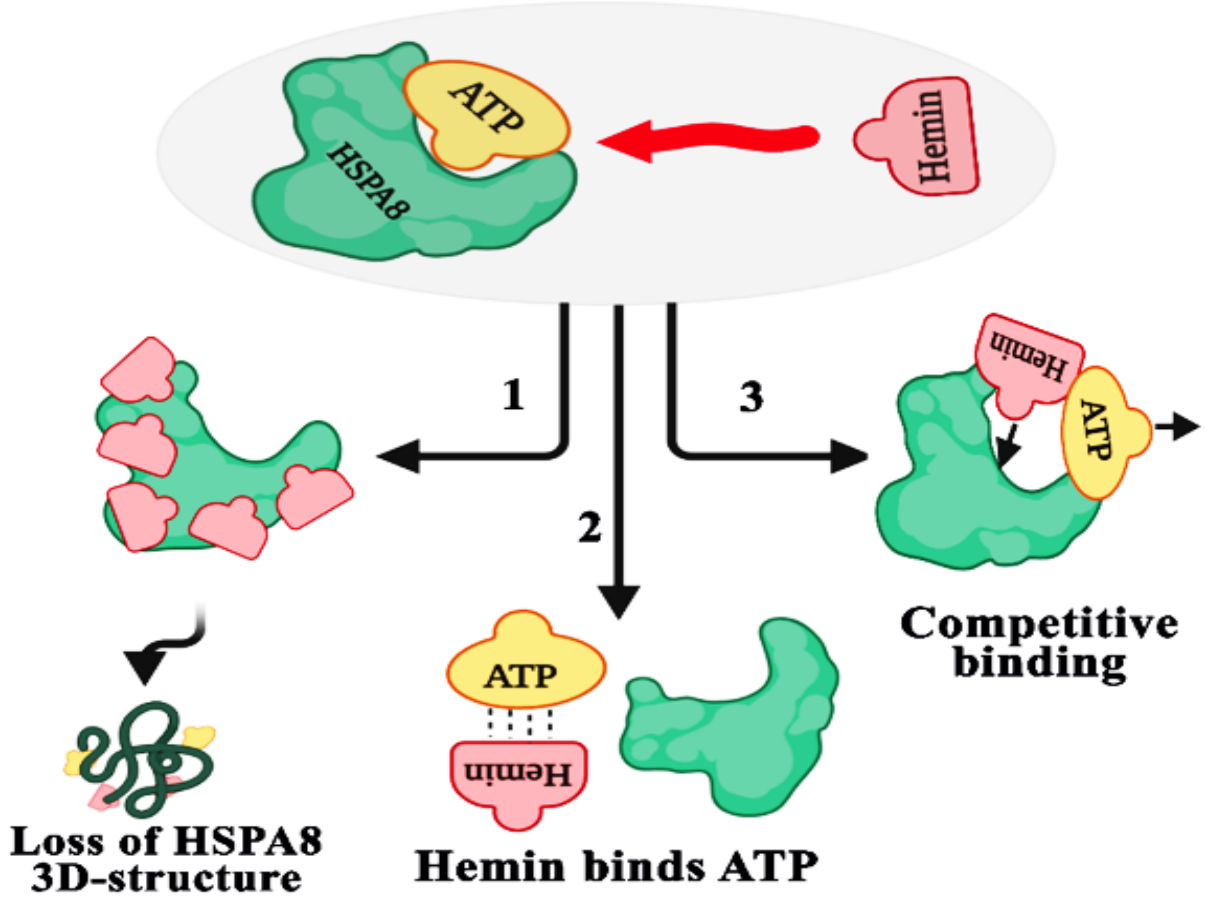

Figure 4.4: A hypothetical model illustrating the possible factors leading to the loss of HSPA8 foldase function in the presence of hemin. The possibility of the involvement of these factors was checked by performing concluding experiments.

4.3.5 The inhibition is not through modulation in HSPA8's structural integrity: Hemin, a highly reactive molecule, can induce structural changes in proteins[29], and thus can potentially affect their function. To assess whether such changes alter the HSPA8 ATPase activity, CD spectroscopy, and gel filtration chromatography were conducted on HSPA8 in the absence and presence of 50 μM of hemin. The CD data revealed minimal alterations in HSPA8 secondary structure elements, with α-helix content increasing slightly from 35.9% to 38%, β-sheets increasing from 30% to 30.5%, turns decreasing from 13% to 10.8%, and random coils decreasing from 21.2% to 20.7% (**Figure 4.5A).** These changes, while indicative of local structural alterations

due to the binding of hemin, did not significantly compromise the protein's overall structural integrity.

The gel filtration chromatography results supported these findings, showing no changes in HSPA8's chromatogram or retention volume with hemin (**Figure 4.5B**). The single peak obtained in both the tested conditions suggests no hemin-induced degradation of aggregation of HSPA8. These results collectively indicate that while hemin may cause minor local structural changes in HSPA8, its global structural integrity remains unaffected.

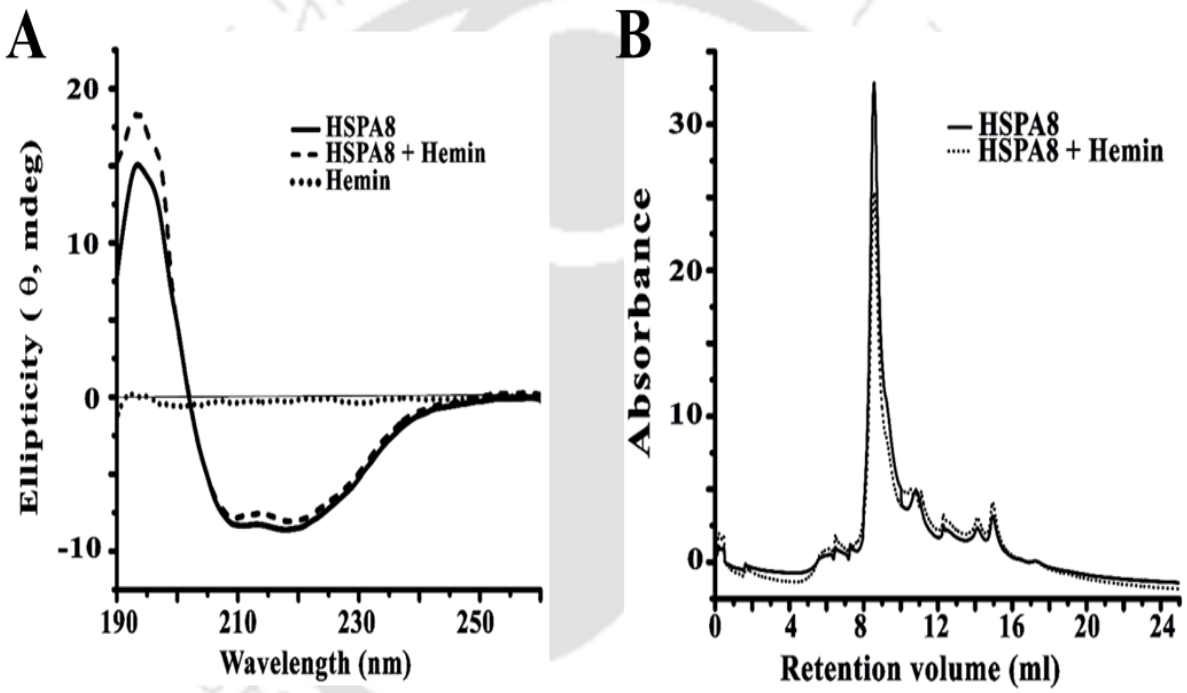

Figure 4.5: A) CD spectroscopy of HSPA8 in the absence and presence of hemin. There is no considerable change in the percent of overall secondary structure elements of HSPA8 in the absence and presence of hemin as the CD spectral curves appeared to be similar in both conditions. This suggests that HSPA8 maintains its structural integrity in the presence of hemin. **B) Gel Filtration chromatography of HSPA8 in the absence and presence of hemin.** Gel filtration chromatography results in a similar chromatogram profile, retention volume, and a single sharp peak of HSPA8 observed in both conditions. These suggest that HSPA8 oligomeric status is not altered by hemin and hemin does not cause any degradation of the protein.

4.3.6 Hemin does not interact with ATP: Hemin's impact on HSPA8 ATPase activity could involve sequestering ATP, thereby hindering its availability for binding to HSPA8. To investigate

this, isothermal calorimetry was used to examine the interaction between hemin and ATP. Titrations were performed using a 1:40 ATP to hemin concentration ratio. The results revealed no interaction between hemin and ATP, as evidenced by a flat isotherm and minimal heat change following the titrations (**Figure 4.6**). This observation excludes the possibility of loss in HSPA8 function due to hemin's direct interaction with ATP.

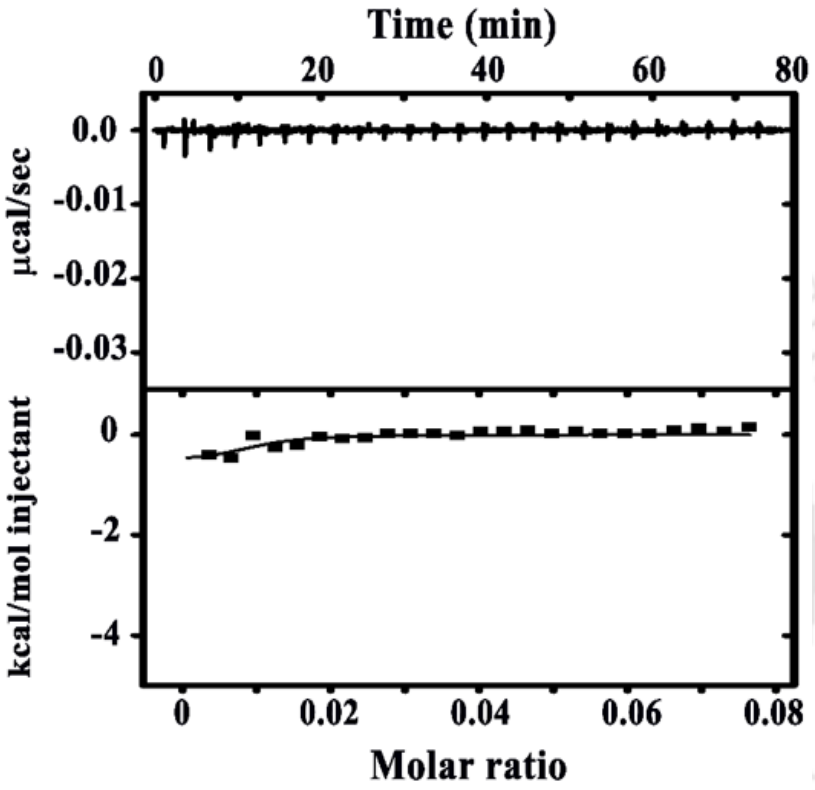

Figure 4.6: Isothermal calorimetry of ATP with hemin: The loss in the activity is not due to the direct interaction of hemin with ATP as the obtained isotherm was almost flat and there were no observable heat changes found in the isothermal calorimetric titrations between ATP and hemin.

.

4.3.7 Competitive docking of ATP and hemin at ATP-binding site of HSPA8: Competitive inhibitors vie with the substrate of an enzyme for the same binding site[30]. To examine the site-directed competition between ATP and Hemin, both individual and competitive docking of ATP and hemin with HSPA8 was conducted. ATP (**Figure 4.7A**) and hemin (**Figure 4.7B**) both effectively docked at the ATP-binding site of HSPA8 with binding energies of -9.39 kcal/mol and -10.57 kcal/mol, respectively. The interaction analysis revealed that most of the interacting amino

acids were common for both ligands, with residues R342, K56, D366, T37, E231, K271, and S340 forming H-bonds with ATP, and residues R342, K56, and Y15 forming H-bonds with hemin. The majority of hemin interactions were hydrophobically driven, as expected, and were the principal contributors to the total binding energy.

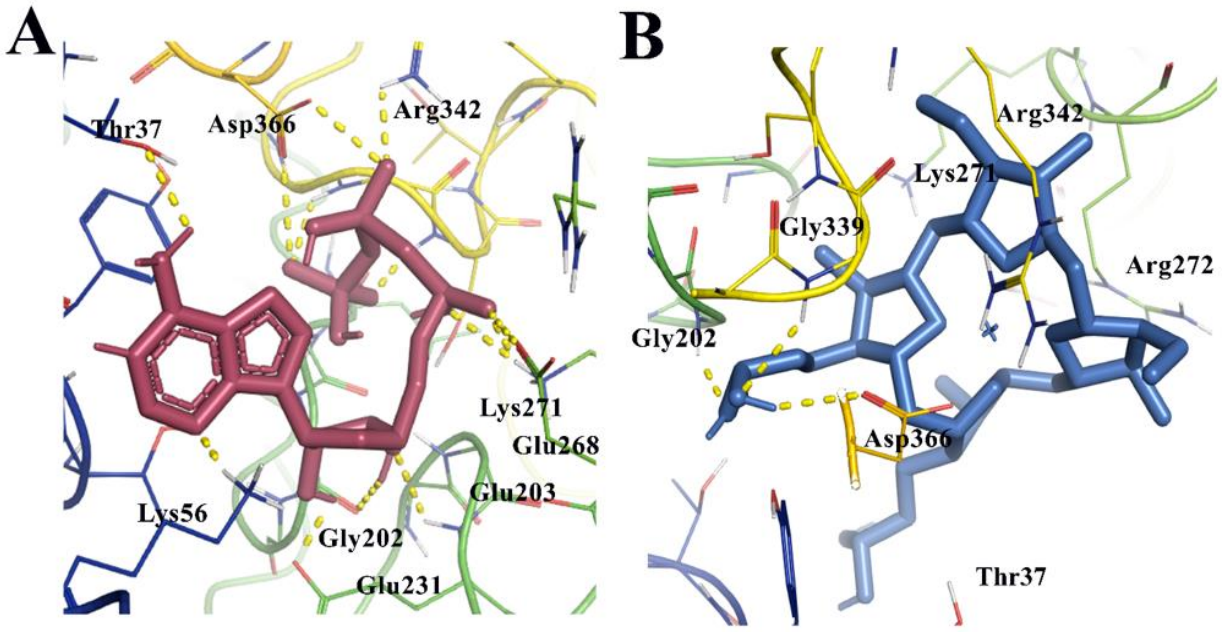

Figure 4.7: Docking of ATP and hemin at the ATP-binding site of HSPA8. A) ATP docks well at its known binding site of the HSPA8 protein and shows interactions with almost all residues known to be involved in binding. **B)** Hemin also docks well at the same site with a better binding energy suggesting a higher affinity as compared to ATP. Hemin interacts with almost all the residues critical for ATP binding along with a few additional interactions driven through hydrophobic features, plausibly contributing to the higher binding energy.

The competitive docking of ATP in the presence of hemin indicated that ATP was unable to displace hemin from the binding site in a 100 GA run. While a common interaction with K56 was observed for both ligands, ATP failed to interact with any other residues of its typical pocket (**Figure 4.8**). Instead, ATP occupied a non-specific site, exhibiting a predicted binding energy of -8.78 kcal/mol, which is lower than ATP binding alone to its typical site. A detailed comparison of the amino acid interacting with ATP in the best-docked poses, both in the presence and absence of hemin, revealed that ATP interacts with most of the typical pocket residues when it is alone. However, in the presence of hemin, it loses almost all interactions with both ligands, retaining only LYS56 and GLU268 as common interacting residues (**Table 4.2**).

Table 4.2: Details of atom-atom interactions of hemin docked at the ATP binding site of HSPA8 and ATP docked at its known site in the absence and presence of hemin.

S. Number	ATP pocket residues	ATP interaction with pocket residues		Hemin interactions
		ATP only	**ATP with hemin**	
1	**THR13**	No interaction	No interaction	No interaction
2	**THR14**	THR14:O-ATP: C (3.2 Å)	No interaction	HEM:H1D-THR14:O (1.9 Å) HEM:H2D-THR14:O (2.9 Å)
3	**TYR15**	TYR15:CB-ATP: Pi orbitals (3.72 Å)	No interaction	HEM:H2D-TYR15:OH (2.2 Å)
4	**LYS56**	LYS56:HZ2-ATP:N (2.07 Å) LYS56:HZ1-ATP:O (2.79 Å)	LYS56:HZ1-ATP:N (2.08 Å)	LYS56:NZ-Hem:O2A (31. Å)
5	**GLY202**	ATP: H-GLY202:O (2.56 Å)	No interaction	GLY202:CA-HEM:O2D (3.2 Å)
6	**GLY230**	GLY230:CA-ATP:O (2.85 Å)	No interaction	No interaction
7	**GLU268**	ATP:P-GLU268:OE1 (3.9 Å)	ATP:P-GLU268:OE2 (3.2 Å)	No interaction
8	**LYS271**	LYS271:HZ1-ATP:O (1.9 Å) LYS271:HZ2-ATP:O (3.08 Å)	No interaction	LYS271:NZ-HEM:O2A (4.5 Å) HEM:CBC-LYS271 (4.8 Å)
9	**ARG272**	ATP: Pi orbitals-ARG272: Alkyl (5.37 Å, 5.04 Å)	No interaction	HEM:CMB-ARG272 (4.7 Å) HEM:CBB-ARG272 (3.9 Å)
10	**SER275**	No interaction	No interaction	No interaction
11	**GLY338**	No interaction	No interaction	GLY338:CA-HEM:O2D (3.3 Å)
12	**GLY339**	GLY330: HN-ATP:O (2.23 Å) GLY339:CA- ATP:O (2.84 Å)	No interaction	GLY339:CA-HEM:O2D (4.3 Å)
13	**SER340**	SER340:HN-ATP:O (2.51 Å) SER340:CA-ATP:N (3.2 Å)	No interaction	No interaction
14	**Arg342**	ARG342:HH11-ATP:O (2.18 Å) ARG342:HH12-ATP:N (2.63 Å) ATP: Pi orbitals-ARG342:Alkyl (5 Å)	No interaction	AGR342:HH11-HEM:Fe (2.7 AGR342:NH1-HEM:Fe (2.7

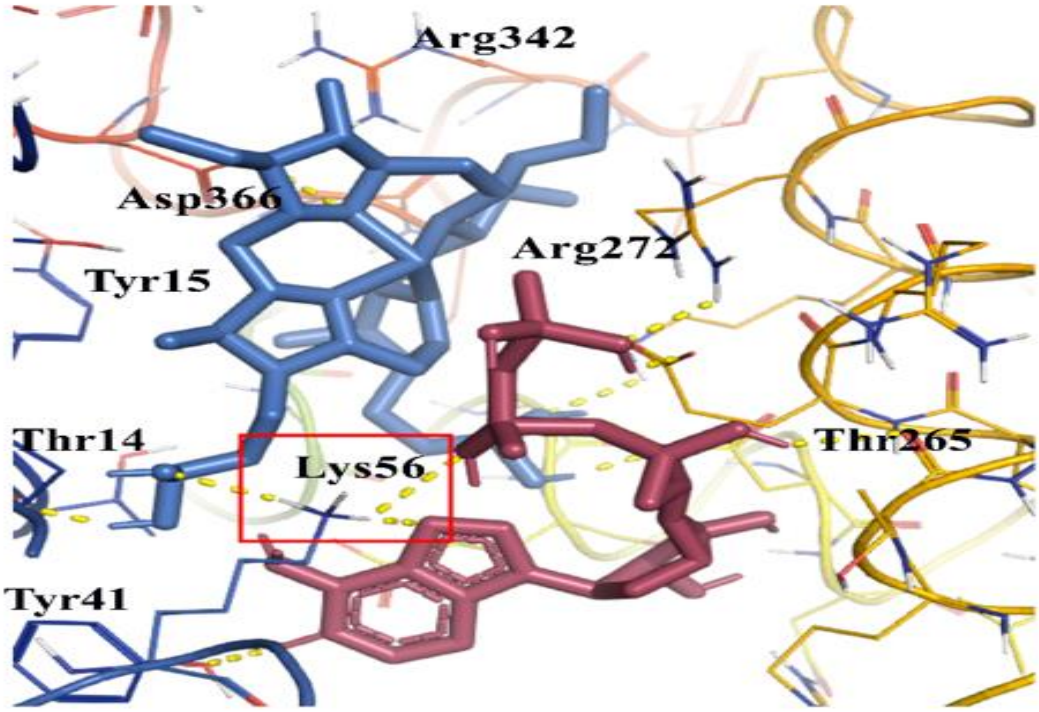

Figure 4.8: Competitive docking of ATP and hemin. ATP, when docked competitively with hemin, was not able to replace hemin and establish its site-specific interactions with the pocket. ATP majorly showed non-specific interactions with only two of the known interactions found in common between the two ligands. The docking results suggest that hemin has a higher affinity for HSPA8 than ATP and it prevents the re-establishment of known ATP interactions The stability of the non-specific complex was examined through MD simulation runs.

The cross-verification using iGEMDOCK exhibited a consistent trend in the total energy of binding compared to Autodock energies, albeit with differing absolute values. The total energy of binding of ATP in the absence and presence of hemin were -93.9959 kJ/mol and -80.1425 kJ/mol respectively. Hemin's total energy of binding to HSPA8 was -109. 084 kJ/mol. These cumulative docking outcomes were predictive, indicating that hemin has a superior affinity for binding to the ATP-binding site of HSPA8 compared to ATP, especially evident in competition scenarios.

4.3.8 The presence of hemin results in an unstable and non-specific ATP-HSPA8 complex *in-silico*: To validate the docking outcomes, a molecular dynamics (MD) simulation was conducted on ATP complexes both in the presence and absence of hemin. The results indicated that the non-specific complex in the presence of hemin was unstable over a 100 ns simulation run, unlike ATP

alone, which remained stable at its recognized binding pocket throughout the simulation (**Figure 4.9**).

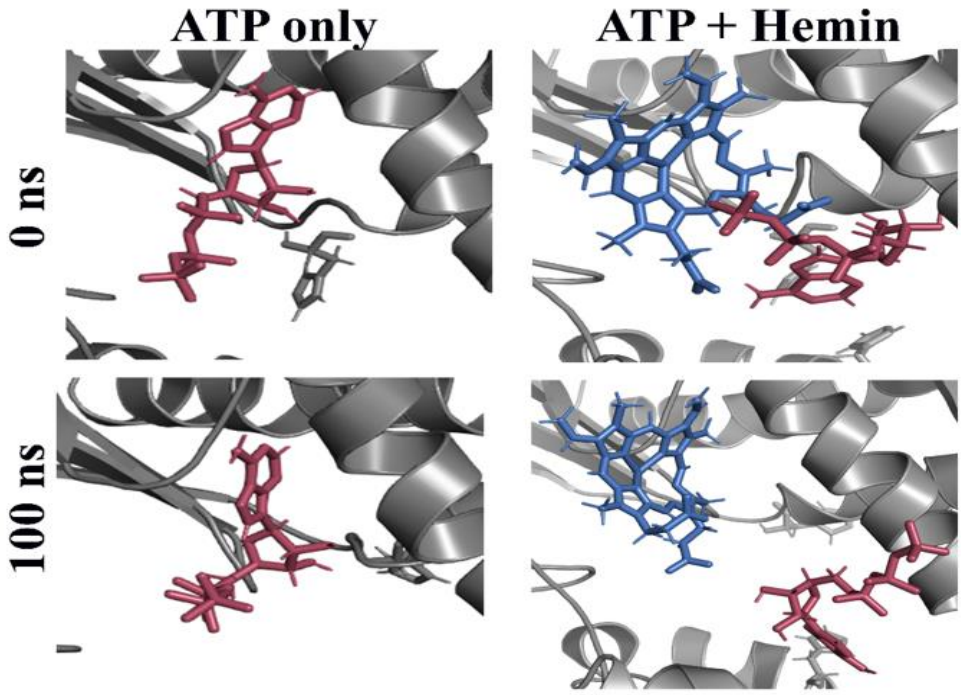

Figure 4.9: MD simulation of HSPA8-ATP complexes. Poses from the MD simulation run of ATP complexes in the absence (left) and presence (right) of hemin at 0 and 100 ns of the simulation run. ATP completely moves out of its pocket and remains at the protein surface till 100 ns.

In the former complex, ATP began to exit the pocket at around 2 ns and completely vacated it by approximately 20 ns into the run. Following its departure from the pocket ATP migrated towards the protein surface, where it remained until the end of the simulation.

The binding energies calculated from the entire 100 ns run exhibited different absolute values but mirrored the same trend observed in the docking studies. HSPA8 complexed with ATP in the absence of hemin displayed a binding energy of -59.060 kJ/mol, which decreased to -44.097 kJ/mol in the presence of hemin, indicating a reduced affinity of ATP. Hemin alone demonstrated a binding energy of -65.00 kJ/mol, supporting the notion that hemin exhibits a higher affinity towards HSPA8 compared to ATP. Further analysis of the complexes included the global root mean square deviation (RMSD) (**Figure 4.10),** revealing that ATP alone formed a more stable complex with HSPA8, exhibiting an RMSD of 0.1935 compared to the protein alone, which had an RMSD of

0.2025. Conversely, in the presence of hemin, the complex displayed an RMSD of 0.2120, indicating a higher instability compared to the protein alone.

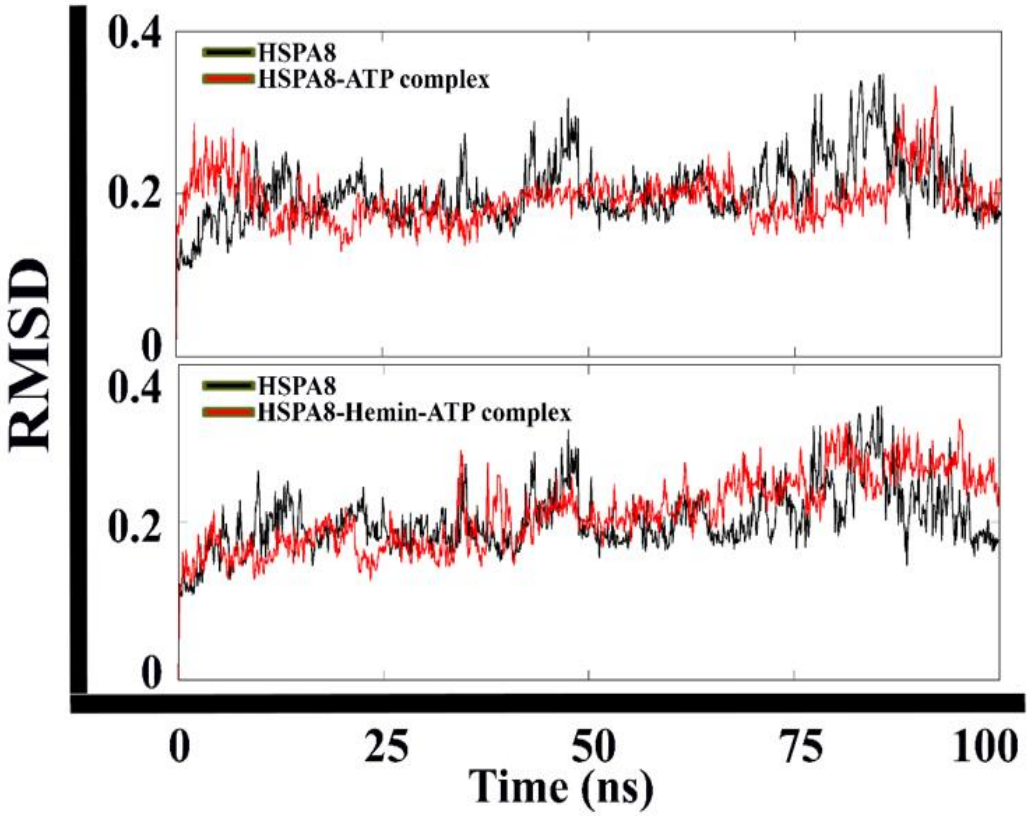

Figure 4.10: The RMSD plot of the HSPA8-ATP complexes shows that ATP at its specific site provides stability to the overall complex whereas the non-specific complex formed in the presence of hemin was less stable as compared to HSPA8 only.

Additional stability parameters such as root mean square fluctuation (RMSF), the average number of H-bonds, and the RMSD and residual fluctuation of the binding pocket, were derived from the simulation experiment and analyzed. The results were consistent with the RMSD calculation (**Figure 4.11**).

In summary, the presence of hemin appears to prevent ATP from binding to its known pocket, instead forcing ATP to form a complex at a non-specific site. While this non-specific complex exhibited comparatively lower but still considerable binding energy in docking studies., it proved to be unstable during the MD simulation run as ATP was not able to stay in its known pocket for more than 2 seconds of the 100 ns simulation run.

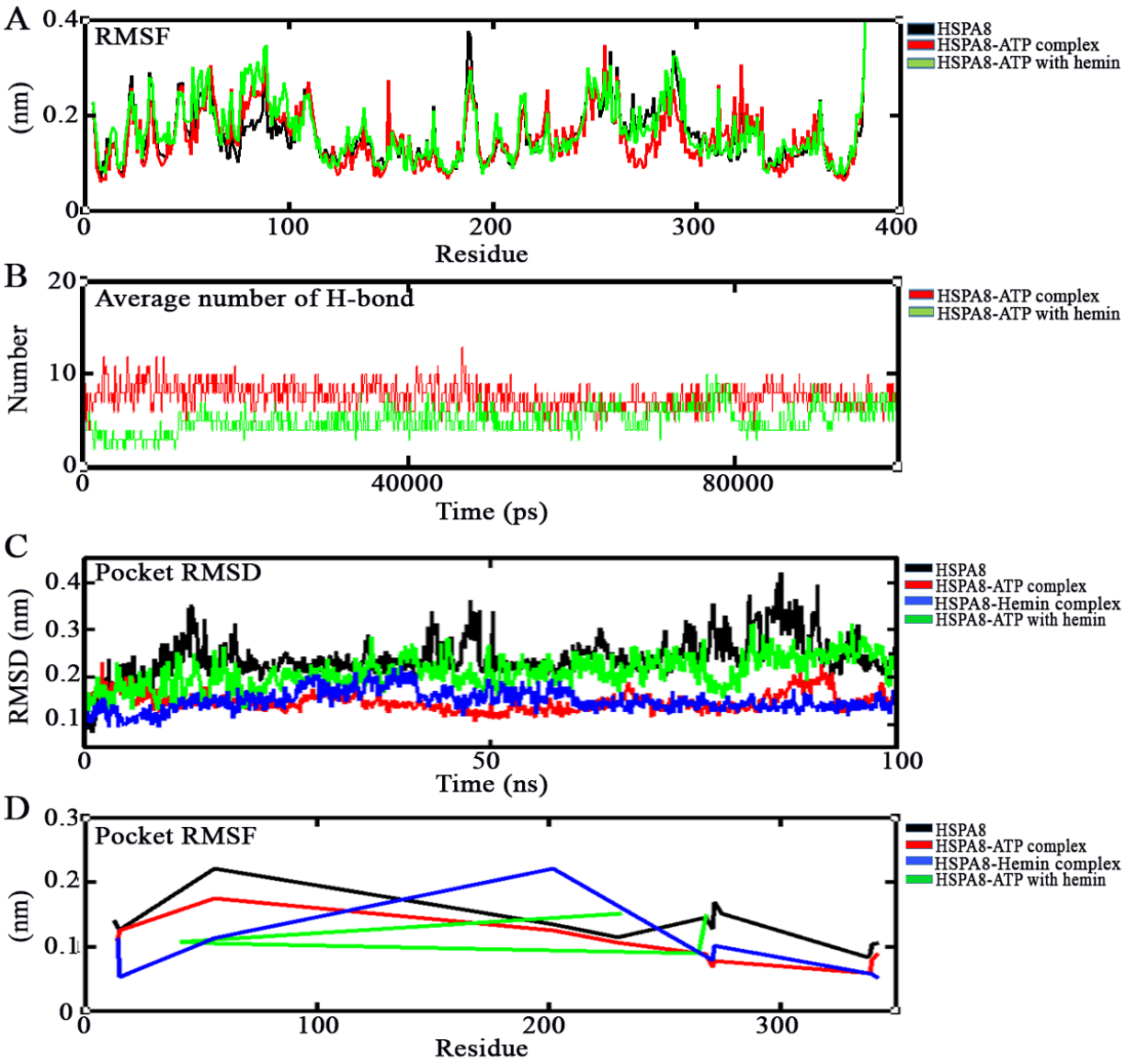

Figure 4.11: Stability parameters for simulation run of the complexes obtained from competitive docking. A) Root mean square fluctuations of the full complexes. The fluctuations in the HSPA8-ATP complex formed in the presence of hemin (green) are more as compared to that in the absence of hemin (red) suggesting a lesser stability of the prior complex. **B)** The average number of H-bonds formed in the HSPA8-ATP complex in the presence of hemin (green) was lesser than that formed in the absence of hemin (red) suggesting lesser stability of the prior complex. **C)** The RMSD of the binding pocket was increased throughout the run for the HSPA8-ATP complex formed in the presence of hemin (green) as compared to that formed in the absence of hemin (red) suggesting a less stable binding pocket. The pocket RMSD for the HSPA8-hemin complex was comparable to the HSPA8-ATP complex and was less than that of HSPA8 only. **D) The pocket residual fluctuations were higher** for the HSPA8-ATP complex formed in the presence of hemin (green) as compared to that formed in the absence of hemin (red) suggesting a less stable binding pocket. The pocket fluctuations for the HSPA8-hemin complex were comparable to the HSPA8-ATP complex.

4.3.9 Hemin competes with ATP and reduces its affinity for binding to HSPA8 *in-vitro*: Substrates and inhibitors of an enzyme activity both exhibit affinities towards the same target. ATP serves as a known substrate for HSPA8 activity. The binding of hemin was investigated using isothermal calorimetry at a micromolar concentration ratio of 1:60. Hemin demonstrated strong binding in the nanomolar range, with a K_d value of 377 ± 79.8 nM for full-length HSPA8 (**Figure 4.12A**).

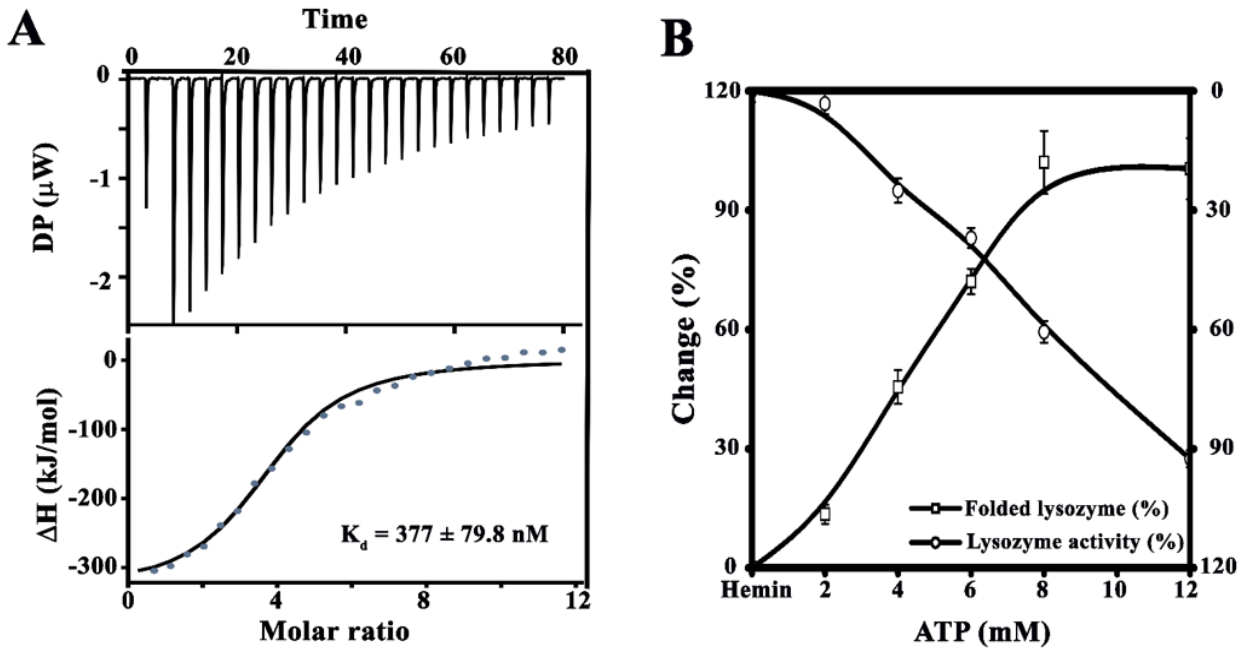

Figure 4.12: Hemin –binding and its competition with ATP. A) Isothermal calorimetry of hemin binding to HSPA8. A sigmoidal isotherm was obtained and is completely saturated at the last few injections of the ligand suggesting binding of hemin to HSPA8. Hemin strongly binds to HSPA8 in the nanomolar range with a K_d value of 377 ± 79.8 nM. **B)** The inhibition of HSPA8 foldase function was due to competition between ATP and hemin. The loss in the **f**unction due to hemin, as tested on lysozyme, was regained by increasing the ATP substrate concentration (x-axis) in a dose-dependent manner with around 8 mM ATP causing the complete regain in the function. At 8 mM and above ATP concentrations both the extent of lysozyme folding (square, right y-axis) and consequently its activity (circle, left y-axis)) on *E. coli* cells were found to be close to 100%. The experiments were performed in triplicates and presented as mean ± standard deviation.

The loss of HSPA8 function was attributed to hemin's competition with ATP, as refolding and activity of lysozyme were restored by gradually increasing the concentration of ATP, with 8 mM ATP causing complete functional restoration (**Figure 4.12B**).

To validate the *in-silico* findings, *in-vitro* isothermal calorimetry of ATP as a ligand and HSPA8 as the target was conducted in the absence and presence of hemin. The results aligned with the *in-silico* predictions, as the ATP binding isotherm did not reach saturation in the presence of hemin under the same ATP to HSPA8 concentration ratio and other titration conditions as observed with ATP alone. In the absence of hemin, ATP showed a saturating isotherm with a calculated dissociation constant (K_d) value of 90.25 ± 12.6 µM (**Figure 4.13A**). However, in the presence of hemin, the K_d value increased approximately 22-fold to 1980 ± 0.4 µM (**Figure 4.13B**), indicating a significant reduction in ATP's affinity for binding to HSPA8. This substantial decrease is attributed to hemin's considerably higher *in-vitro* affinity for HSPA8 compared to ATP.

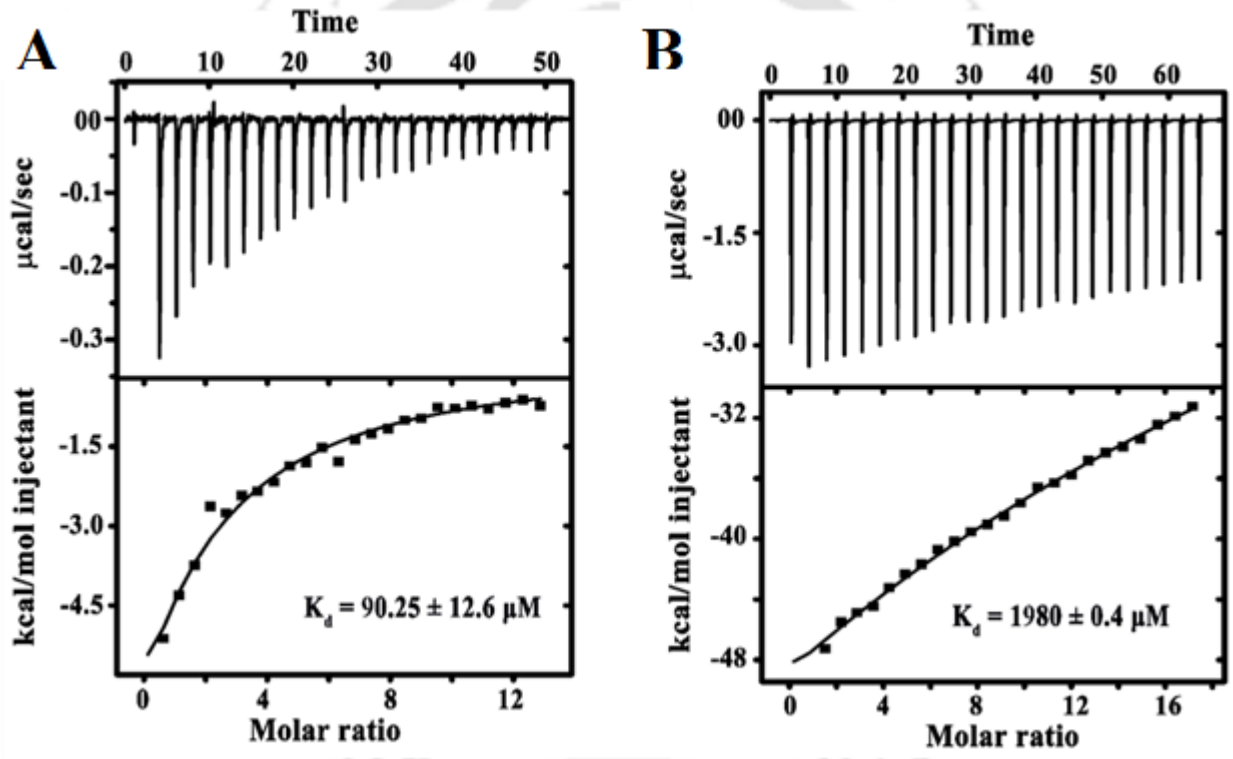

Figure 4.13: ITC of ATP with HSPA8 in the absence and presence of hemin. A) ATP in the absence of hemin showed a completely saturated sigmoidal isotherm with a weak binding of ATP to HSPA8 as is reported in the literature. The binding isotherm in the presence of hemin was found to be not saturated after titrating with the same ATP concentration and the dissociation constant was drastically increased (around 22 times) suggesting a huge reduction in the affinity of ATP for HSPA8 in the presence of hemin.

The binding of hemin to the N-terminal and C-terminal domains of HSPA8 was also tested through ITC. Hemin, as expected, demonstrated a strong binding to the N-terminal domain (K_d = 223 ±

31.5 nM) (**Figure 4.14A**). Notably, hemin did not exhibit any binding to the C-terminal domain of HSPA8 (**Figure 4.14B).**

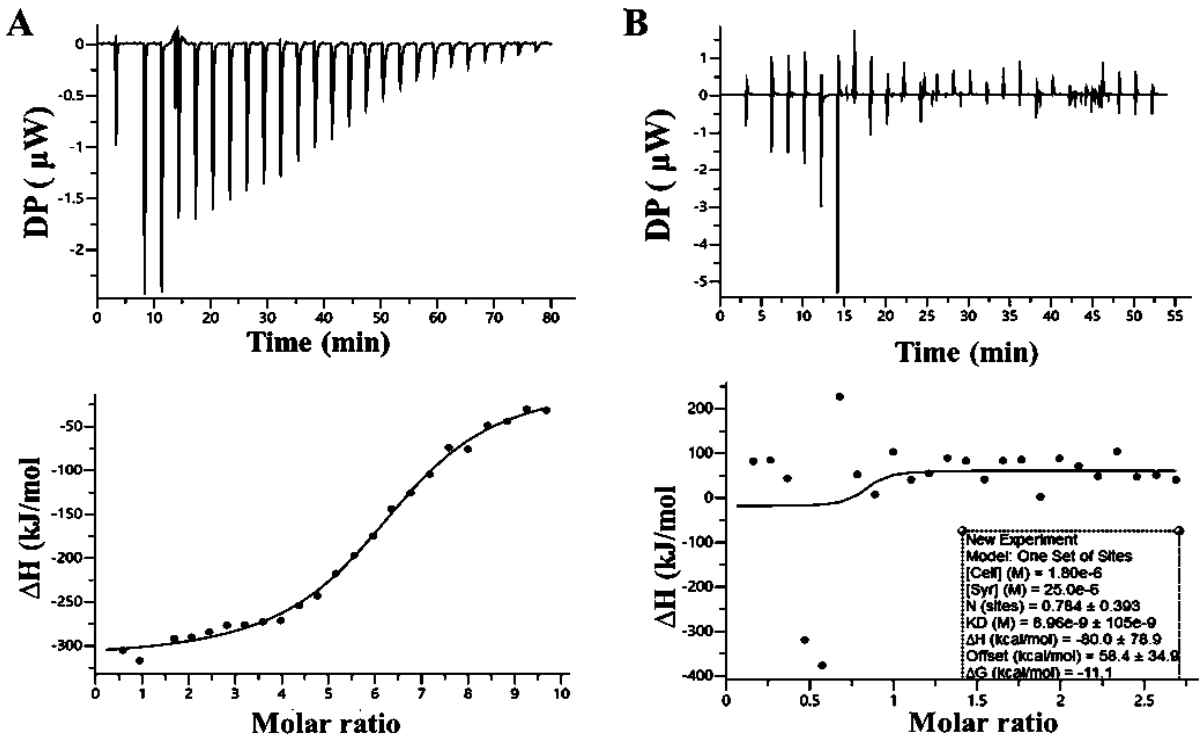

Figure 4.14: Isothermal calorimetry of hemin with HSPA8 domains. A) Hemin showed strong binding to the N-terminal domain with a K_d value of 223 ± 31.5 nM which is close to that of full-length HSPA8. The experiment was performed to confirm the binding of hemin in the nucleotide-binding domain (ATP-binding domain) of HSPA8. The titrations were performed at an HSPA8 to hemin concentration ratio of 1:50. A very high affinity of hemin for the N-terminal domain of HSPA8 is responsible for reduced ATP affinity in the presence of hemin. **B)** Hemin does not show any binding to the C-terminal domain of HSPA8. The titrations were performed at an HSPA8 to hemin concentration ratio of 1:50.

4.4 Discussion

Various pathological conditions, such as severe malaria, sepsis, sickle cell anemia, and hemorrhage, contribute to cell and tissue damage through distinct physiological mechanisms. One common is the accumulation of hemoglobin and its byproducts in different cells and tissues[31, 32]. Elevated levels of hemin, reaching approximately 20 µM, can be found in both intra- and extra-cellular compartments in diseases like malaria, hemorrhage, and sickle cell disease, leading to significant damage to vital tissues and organs[33]. Hemin, a product of hemoglobin breakdown, induces

oxidative stress in cells[4], at high physiological levels, can cause liver damage[34], and disrupt the Blood-brain barrier[35].

During conditions of high free heme levels, cytoprotective proteins play a crucial role. While some proteins aid in the degradation, or sequestration of heme[4], others mitigate the adverse effects of heme accumulation[36, 37]. Heat shock proteins (HSPs), such as HSPA8, belong to a class of cell-protective proteins that respond to such stress conditions by assisting in the refolding and degradation of misfolded proteins, thereby preventing their aggregation[21]. Therefore, functional changes in HSPs can significantly impact cellular health[38, 39], particularly in situations of high heme load.

This study highlights that hemin, aside from its direct toxicity to cells, can also deteriorate cellular health by impeding the cell-protective machinery, particularly through functional alterations in HSPs like HSPA8. Inhibitors of HSPA8, such as rifampicin, have been shown to affect various cellular processes, including autophagy and synaptic vesicle cycling defects during amyotrophic lateral sclerosis[40, 41].

Our findings identify hemin as a novel inhibitor of HSPA8, competing with ATP and preventing the chaperone from performing its ATP-dependent functions. This interaction between hemin and HSPA8 presents a new avenue for research in the field of chaperones and hemin toxicity. Further exploration of this interaction could provide insights into its impact on various cellular processes where HSPA8 or other HSPs play an ATP-dependent role. One critical ATP-dependent function of HSPA8 is its cytoplasm-to-nucleus shuttling for the import of various proteins into the nucleus. Blocking this shuttling during stress conditions has been shown to drastically affect cell survival[42]. Investigating the effect of hemin on inhibiting this ATP-dependent shuttling could provide insights into other functional modulations in HSPA8 due to hemin during stress conditions. Furthermore. The interaction between hemin and HSPA8 could be leveraged to mitigate cell damage in diseases like severe malaria and hemorrhage.

4.5 Conclusions

Based on the data presented, we have concluded that hemin competitively inhibits the ATPase activity of the chaperone HSPA8. This inference stems from ATPase activity assays of the enzyme conducted both in the absence and presence of hemin. The loss in the activity cannot be attributed to non-specific factors such as structural damage to the enzyme by hemin, as indicated by CD

spectroscopy and gel filtration chromatography results, or direct interaction of hemin with ATP. This inhibition results in the functional modulation of the ATP-dependent foldase function of the protein, as evidenced by a significant decrease in the refolding function of the chaperone when tested on the model protein lysozyme. Importantly, the loss of foldase function caused by hemin is reversible, as HSPA8 restores the refolding of lysozyme upon a gradual increase in ATP concentration in the presence of an inhibitory concentration of hemin. The competitive nature of this inhibition, involving the same binding, was collectively inferred from *in-silico* and *in-vitro* binding results obtained through molecular docking, molecular dynamic simulation, and isothermal calorimetry experiments.

4.6 References

1. Schaer, D.J., et al., Hemolysis and free hemoglobin revisited: exploring hemoglobin and hemin scavengers as a novel class of therapeutic proteins. Blood, The Journal of the American Society of Hematology, 2013. 121(8): p. 1276-1284.
2. Owen, J.E., G.M. Bishop, and S.R. Robinson, Uptake and toxicity of hemin and iron in cultured mouse astrocytes. Neurochemical Research, 2016. 41: p. 298-306.
3. Rifkind, J.M., J.G. Mohanty, and E. Nagababu, The pathophysiology of extracellular hemoglobin associated with enhanced oxidative reactions. Frontiers in physiology, 2015. 5: p. 500.
4. Kumar, S. and U. Bandyopadhyay, Free heme toxicity and its detoxification systems in human. Toxicology letters, 2005. 157(3): p. 175-188.
5. Aft, R.L. and G. Mueller, Hemin-mediated oxidative degradation of proteins. Journal of Biological Chemistry, 1984. 259(1): p. 301-305.
6. Li, T., H.L. Bonkovsky, and J.-t. Guo, Structural analysis of heme proteins: implications for design and prediction. BMC structural biology, 2011. 11(1): p. 1-13.
7. Schneider, S., et al., Diversity and conservation of interactions for binding heme in b-type heme proteins. Natural product reports, 2007. 24(3): p. 621-630.
8. Piazza, M., et al., Hemin and a metabolic derivative coprohemin modulate the TLR4 pathway differently through different molecular targets. Innate immunity, 2011. 17(3): p. 293-301.
9. Byrnes, J.J., et al., Mechanism of hemin inhibition of erythroid cytoplasmic DNA polymerase. Biochemistry, 1975. 14(4): p. 796-799.
10. Burka, E.R., Hemin: an inhibitor of erythroid cell ribonuclease. Science, 1968. 162(3859): p. 1287-1287.
11. Haas, A.L. and I.A. Rose, Hemin inhibits ATP-dependent ubiquitin-dependent proteolysis: role of hemin in regulating ubiquitin conjugate degradation. Proceedings of the National Academy of Sciences, 1981. 78(11): p. 6845-6848.

12. Lee, J.M., et al., Hemin, an iron-binding porphyrin, inhibits HIF-1α induction through its binding with heat shock protein 90. International journal of cancer, 2012. 130(3): p. 716-727.
13. Macario, A. and E. Conway de Macario, Stress and molecular chaperones in disease. International Journal of Clinical and Laboratory Research, 2000. 30: p. 49-66.
14. Broadley, S.A. and F.U. Hartl, The role of molecular chaperones in human misfolding diseases. FEBS letters, 2009. 583(16): p. 2647-2653.
15. Solar, I., et al., Long-term intercalation of residual hemin in erythrocyte membranes distorts the cell. Biochimica et Biophysica Acta (BBA)-Biomembranes, 1991. 1062(1): p. 51-58.
16. Giri, R., et al., Continuous uptake or saturation—Investigation of concentration and surface-packing-specific hemin interaction with lipid membranes. The Journal of Physical Chemistry B, 2018. 122(30): p. 7547-7554.
17. Kiffin, R., et al., Activation of chaperone-mediated autophagy during oxidative stress. Molecular biology of the cell, 2004. 15(11): p. 4829-4840.
18. Kumsta, C. and U. Jakob, Redox-regulated chaperones. Biochemistry, 2009. 48(22): p. 4666-4676.
19. Wang, L., X. Wang, and C.-c. Wang, Protein disulfide–isomerase, a folding catalyst and a redox-regulated chaperone. Free Radical Biology and Medicine, 2015. 83: p. 305-313.
20. Reichmann, D., W. Voth, and U. Jakob, Maintaining a healthy proteome during oxidative stress. Molecular cell, 2018. 69(2): p. 203-213.
21. Stricher, F., et al., HSPA8/HSC70 chaperone protein: structure, function, and chemical targeting. Autophagy, 2013. 9(12): p. 1937-1954.
22. Silva, P.N., et al., Analysis of HSPA8 and HSPA9 mRNA expression and promoter methylation in the brain and blood of Alzheimer's disease patients. Journal of Alzheimer's disease, 2014. 38(1): p. 165-170.
23. !!! INVALID CITATION !!!
24. Tian, Y., et al., Maslinic acid induces autophagy by down-regulating HSPA8 in pancreatic cancer cells. Phytotherapy Research, 2018. 32(7): p. 1320-1331.
25. Zagouri, F., et al., HSP90, HSPA8, HIF-1 alpha and HSP70-2 polymorphisms in breast cancer: a case–control study. Molecular biology reports, 2012. 39: p. 10873-10879.
26. Shan, N., et al., Identification of HSPA8 as a candidate biomarker for endometrial carcinoma by using iTRAQ-based proteomic analysis. OncoTargets and therapy, 2016: p. 2169-2179.
27. Pro, O., Origin Lab corporation [version Beta2 b9. 3.193]. Academic, Northampton, USA, 2016.
28. Mayer, M. and B. Bukau, Hsp70 chaperones: cellular functions and molecular mechanism. Cellular and molecular life sciences, 2005. 62: p. 670-684.
29. Zhang, J., et al., Influence of hemin on structure and emulsifying properties of soybean protein isolate. Food Chemistry, 2023. 421: p. 136183.
30. Alberca, L.N., et al., In silico guided drug repurposing: discovery of new competitive and non-competitive inhibitors of falcipain-2. Frontiers in chemistry, 2019. 7: p. 534.
31. Rother, R.P., et al., The clinical sequelae of intravascular hemolysis and extracellular plasma hemoglobin: a novel mechanism of human disease. Jama, 2005. 293(13): p. 1653-1662.

32. Alperin, J.B., P.A. Dow, and M.B. Petteway, Hemoglobin A2 levels in health and various hematologic disorders. American Journal of Clinical Pathology, 1977. 67(3): p. 219-226.
33. Pethő, D., et al., Heme cytotoxicity is the consequence of endoplasmic reticulum stress in atherosclerotic plaque progression. Scientific reports, 2021. 11(1): p. 10435.
34. Dey, S., et al., Impact of intravascular hemolysis in malaria on liver dysfunction: involvement of hepatic free heme overload, NF-κB activation, and neutrophil infiltration. Journal of Biological Chemistry, 2012. 287(32): p. 26630-26646.
35. Butt, O.I., P.W. Buehler, and F. D'Agnillo, Blood-brain barrier disruption and oxidative stress in guinea pig after systemic exposure to modified cell-free hemoglobin. The American journal of pathology, 2011. 178(3): p. 1316-1328.
36. Abdelmohsen, K., et al., Posttranscriptional gene regulation by RNA-binding proteins during oxidative stress: implications for cellular senescence. 2008.
37. Gopalakrishna, B. and B.S. Varashree, Oxidative stress and proteolytic activity in erythrocytes of diabetic patients. 2010.
38. Altinok, S., et al., With or without you: co-chaperones mediate health and disease by modifying chaperone function and protein triage. Cells, 2021. 10(11): p. 3121.
39. Hubert, V., et al., Modulating chaperone-mediated autophagy and its clinical applications in cancer. Cells, 2022. 11(16): p. 2562.
40. Zhou, J., et al., Inhibition of HSPA8 by rifampicin contributes to ferroptosis via enhancing autophagy. Liver International, 2022. 42(12): p. 2889-2899.
41. Coyne, A.N., et al., Post-transcriptional inhibition of Hsc70-4/HSPA8 expression leads to synaptic vesicle cycling defects in multiple models of ALS. Cell reports, 2017. 21(1): p. 110-125.
42. Wang, F., et al., Blocking nuclear export of HSPA8 after heat shock stress severely alters cell survival. Scientific reports, 2018. 8(1): p. 16820.

Chapter V

HSPA8 impedes Hemin-induced Cellular Toxicity in the Liver

5.1 Introduction

Hemolytic diseases, such as malaria, are characterized by the release of hemoglobin (Hb) from red blood cells, a process that leads to the excessive breakdown of RBCs and abnormal accumulation of free Hb outside the cells and in tissues surrounding blood vessels[1]. The oxidation of free Hb produces various heme moieties, including methemoglobin (Hb-Fe^{3+}), free heme (Fe^{3+}), hemin (Fe^{3+}-Cl), hematin (Fe^{3+}-OH), and the heme ferryl intermediate (Fe^{4+}), all of which exhibit high toxicity to a range of cells and tissues[2]. During malaria and other hemolytic disorders, the degradation of ferric hemoglobin (Hb- Fe^{3+}) results in the build-up of hemin, further contributing to the pathophysiology of these conditions[3].

Hemin, an iron-containing porphyrin, exhibits pro-oxidant properties due to its free iron content. Its hydrophobic nature enables it to easily penetrate cell membranes, causing the release of oxidants and leading to cell death[4]. Pathological conditions such as hemorrhage and malaria can result in abnormally high hemin levels, reaching up to 20 μM, through excessive hemolysis[5, 6]. Despite cellular anti-oxidant defenses and heme detoxification systems, these levels often overwhelm the body's ability to neutralize hemin, leading to its detrimental effects.

Hemin has been implicated in causing acute hemolysis, inducing the peroxidation of cellular lipids through the generation of ROS, and promoting protein aggregation and degradation, as well as damage to DNA[7-12]. Additionally, hemin exposure is associated with cell injury and inflammation[13, 14]. The excessive presence of hemin is harmful to various tissues and organs, contributing to the disruption of the Blood-Brain Barrier and dysfunction through oxidative stress caused by cell-free hemoglobin or its degradation products[15, 16]. Furthermore, hemin iron exacerbates endothelial damage caused by granulocytes and ROS, and abnormal hemin levels have been shown to prompt acute lung injury in a sickle cell disease mouse model[17, 18]. In the heart, free hemin can lead to arrhythmic beating and loss of contractility in the myocardium, highlighting its catastrophic effects on cardiac functions[19].

The liver is an essential organ with diverse physiological functions, including nutrient metabolism, metabolic detoxification, toxin and drug inactivation, and storage of minerals and vitamins. Additionally, it plays a crucial role in endocrine and immunoregulatory functions [20]. The role of the liver is crucial in many diseased states[21-24]. The liver possesses a unique innate immune

system that detects and initiates immune responses against pathogenic and non-pathogenic antigens. This localized immune response is particularly important in establishing tolerance to blood-stage malaria[25, 26].

Hemolysis, a significant pathological outcome in malaria, is well-documented for its impact on the liver, particularly concerning hemoglobin degradation products. Studies reveal that *Plasmodium yoelli* can induce oxidative stress, leading to apoptosis in the liver[27]. The progression of hemolytic anemia can culminate in liver failure[28, 29], and its connection with alcoholic fatty liver and cirrhosis is noted[30]. Additionally, alloimmune hemolytic anemia in newborns is associated with iron overload and subsequent cholestasis[31]. The accumulation of heme during persistent intravascular hemolysis in malaria contributes to liver damage through mechanisms such as NF-κB activation, neutrophil infiltration, and TNFα release[32]

Extensive research has focused on the cytotoxicity of hemoglobin (Hb) derived products in various cell lines. For instance, methemoglobin has been shown to reduce cellular viability and integrity of J774A.1 macrophage cell lines through the induction of reactive oxygen species (ROS) and subsequent apoptosis[33]. Similarly, hemin has demonstrated toxicity to Caco-2 epithelial cells in a concentration- and time-dependent manner, involving the translocator protein TSPO[34]. This compound has also been implicated in DNA damage in HT29 human colon cancer cells and primary colonocytes[35]. Furthermore, hemin exhibits cytotoxic effects on neurons and glial cells in the brain and spinal cord[36, 37].

Despite the well-known hepatotoxicity of hemin, there is a lack of reports regarding its direct toxicological effects on liver cells and the underlying mechanisms. To address this gap, we conducted studies to assess the impact of hemin on the viability, morphology, and release of liver damage marker enzymes in HepG2 liver cells. Additionally, in our research, we have investigated the mechanism and cell signaling pathway responsible for hemin's toxic response towards hepatocytes. Our previous study has suggested that the heat shock protein HSPA8 can convert hemin into a less toxic heme polymer[38]. Building on this finding, through our investigations, we have explored the impact of HSPA8 on hemin toxicity in liver cells.

5.2 Experimental procedures

5.2.1 Cell culture and treatments

HepG2 liver cells, a model for human hepatocytes, were used for the study and cultured in DMEM as described in **section 2.17** of Chapter II.

5.2.2 Cell viability assay

The effect of hemin and HSPA8 on the viability of HepG2 cells was tested using 3-(4, 5-dimethylthiazol-2-yl)-2,5-diphenyltetrazolium bromide (MTT) dye-based assay as described in the **section 2.18** of Chapter II.

5.2.3 Microscopic evaluation

The hemin-treated HepG2 cells were microscopically observed using a Cytell cell imaging system as described in **section 2.19** of Chapter II.

5.2.4 Wound healing assay

The impact of hemin on the wound healing potential of HepG2 cells was tested through a scratch assay as described in **section 2.20** of Chapter II.

5.2.5 Scanning Electron Microscopy

The morphological changes in HepG2 cells upon hemin treatment were tested through SEM evaluation as described in **section 2.21** of Chapter II.

5.2.6 Estimation of oxidative stress marker enzymes

The effect of hemin on the release of liver damage marker enzymes was tested through analysis of the enzymes SGPT, SGOT, and LDH released in the cell culture supernatant as described in **section 2.22** of Chapter II.

5.2.7 Cell Cycle analysis

The perturbation in the cell division process of HepG2 cells upon hemin treatment was tested through FACS as described in **section 2.23** of Chapter II.

5.2.8 DNA Fragmentation analysis

To confirm the hemin-induced apoptosis in HepG2 cells upon hemin treatment, ladder DNA formation was tested as described in **section 2.24** of Chapter II.

5.2.9 Determination of apoptotic and dead/necrotic cells

Hemin-induced apoptosis in HepG2 cells was by FACS analysis using preferred dyes as described in **section 2.25** of Chapter II.

5.2.10 Determination of apoptosis signaling pathway by Western blotting

The cell signaling pathway involved in the hemin-induced apoptosis of HepG2 cells was revealed through western blotting experiments as described in **section 2.26** of Chapter II.

5.3 Results

5.3.1 Hemin exhibits toxicological effects in hepatocytes

During hemolysis-associated pathophysiologies like malaria and sickle cell disease, hemin level reaches abnormal states[5, 6]. In our study, we tested the effect of such hemin concentrations on the viability of HepG2 liver cells. Cells treated with increasing hemin concentrations (0-120 µM) for 48 hours showed a dose-dependent reduction in their viability as compared to the untreated cells (**Figure 5.1A**). At 100 µM or above complete loss of cellular viability was seen and the IC_{50} of hemin for HepG2 cells was calculated to be 18.81 ± 1.82 µM. Hemin was also found to time-dependently reduce the viability of HepG2 cells. Cells treated with IC_{50} concentration of hemin showed a decrease in viability with time and reached around 40% in 48 hours whereas the untreated cells showed comparatively better viability with above 80% viable cells after 48 hours. (**Figure 5.1B)**.

The microscopic observation of hemin-treated cells with a 40X objective showed visible changes in their cell count and surface morphology. The hemin-treated cells demonstrated less cell count and shrunk cells with compromised membrane integrity. In contrast, the untreated cells looked healthy, more in number, and expanded with intact cell membranes (**Figure 5.1C**).

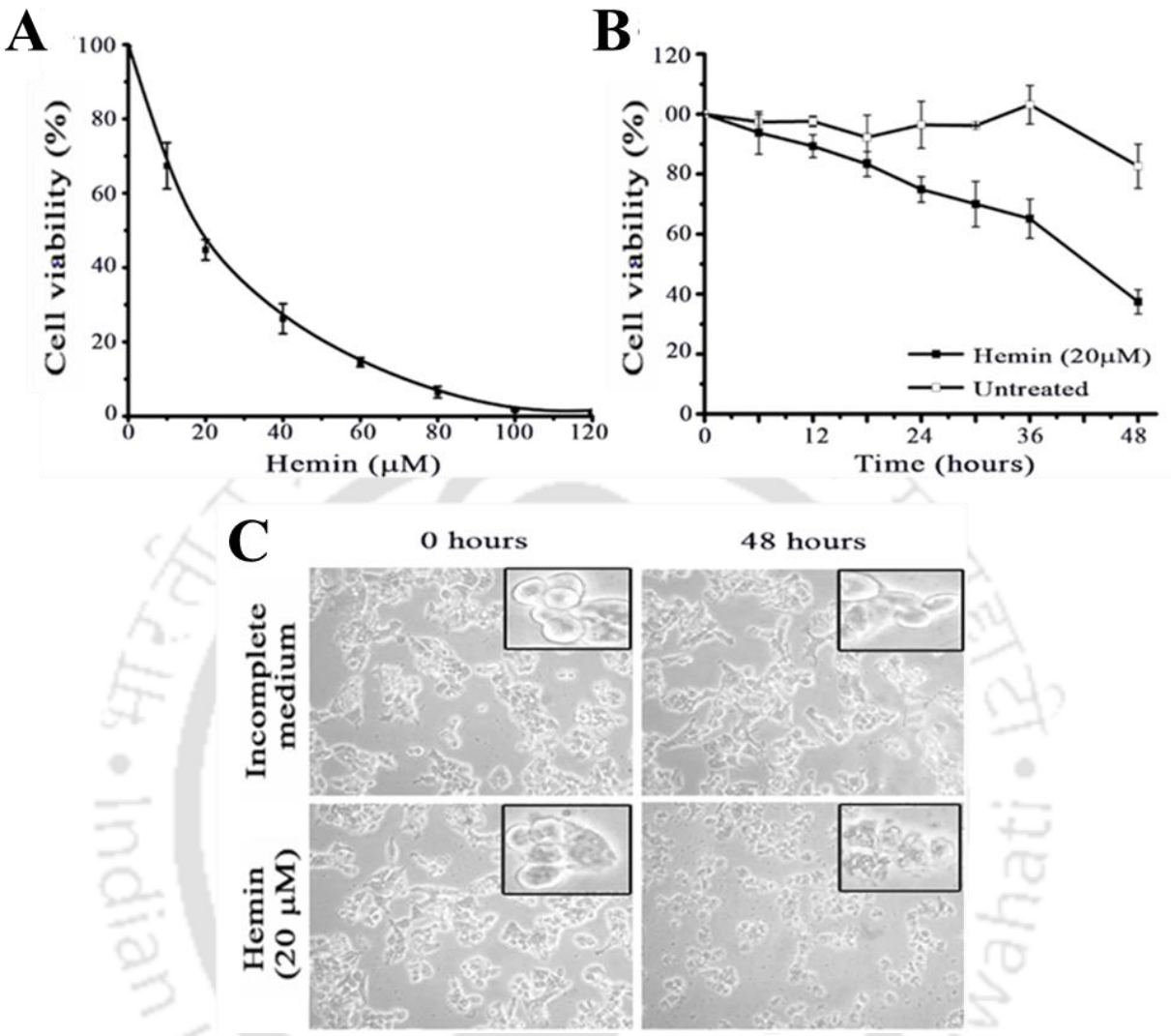

Figure 5.1: Cell viability assay of HepG2 cells in the presence of hemin. A) A Dose-dependent cell viability assay of hemin-treated HepG2 cells. The cells showed a reduction in viability which reaches 0% at around 100 μM of hemin. **B)** A time-dependent cell viability assay of hemin-treated HepG2 cells. The cells were treated for 48 hours with the IC_{50} concentration of hemin obtained from the dose-dependent experiment. **C)** Microscopic images of hemin-treated HepG2 cells taken using a Nikon inverted microscope. The data is presented as the Mean ± standard deviation of three independent experiments.

A more critical morphological investigation by scanning electron microscopy at 20X magnification, again showed a loss of membrane integrity and shrunken cells with perforations on the surface of the hemin-treated cells (**Figure 5.2**) which is indicative of apoptotic cells[39]. The untreated cells however were observed to be healthy, intact, and in their normal surface morphology.

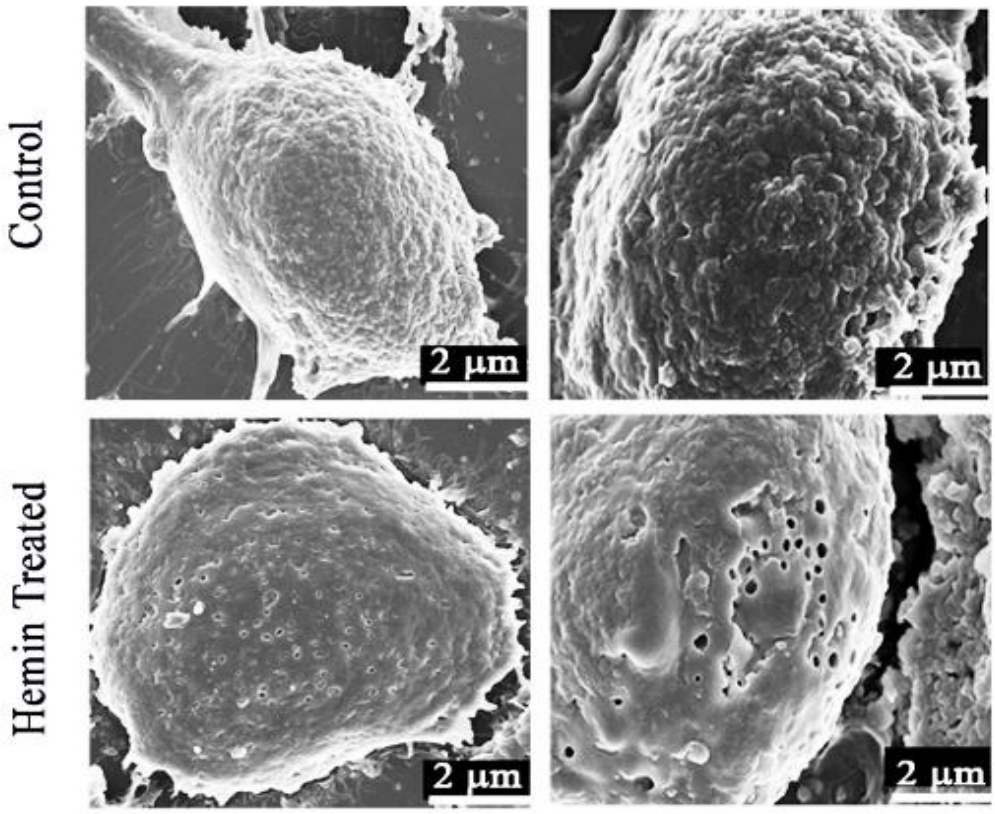

Figure 5.2: SEM analysis of hemin-treated and untreated HepG2 cells using a Zeiss, Gemini-300 scanning electron microscope. The hemin-treated cells showed shrinking of the cells, and compromised membrane integrity with perforations on the cell surface indicative of apoptosis. However, the control cells were observed to be healthy with intact membranes and normal morphology. The images were taken at 20X magnification.

The perforation in HepG2 cells can lead to the extracellular release of various cytoplasmic factors. Hemin is a highly reactive pro-oxidant molecule capable of causing oxidative damage to cells[4]. Oxidative damage to the liver results in liver dysfunction and the release of certain liver damage hallmark enzymes into the plasma[40, 41]. To investigate whether hemin can cause liver dysfunction, we investigated the release of three such enzymes, SGPT (Serum glutamic pyruvic transaminase), that catalyzes the reversible transfer of amino groups between an amino acid and α-Keto acids, SGOT (Serum glutamic-oxaloacetic transaminase), that catalyzes the interconversion of aspartate and α-Ketoglutarate to oxaloacetate and glutamate, and LDH (Lactate dehydrogenase), that catalyzes the conversion of pyruvate to lactate and back, from hemin-treated

HepG2 cells in the cell culture medium (**Figure 5.3**). The results suggest that hemin can cause oxidative damage to the liver resulting in the release of these enzymes into the systemic circulation and thus affecting the liver function.

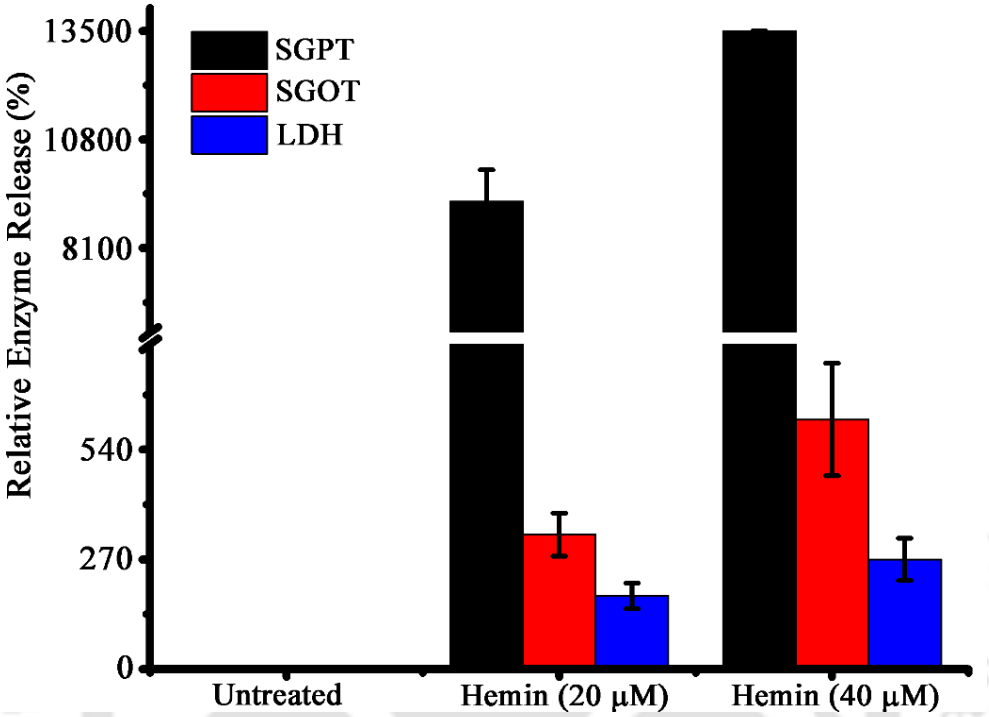

Figure 5.3: Estimation of liver enzymes released from HepG2 cells upon hemin treatment. The untreated cells show a basal level of the released enzymes in the cell culture supernatant which was assumed to be 0%. The hemin-treated cells show a significant increase in the levels of SGPT, SGOT, and LDH in the cell culture supernatant. The data is presented as mean ± standard deviation of three independent experiments.

The untreated cells showed a basal level release of the enzymes which was assumed to be 0% and the relative percentage of release from treated cells was calculated. The treated cells showed a drastic increase of 9000% and 13500 % in the release of SGPT with 20 and 40 µM of hemin respectively. The amount of SGOT released was increased to 331 % and 614%, and that of LDH increased to 180% and 270% with 20 and 40 µM of hemin respectively. This result suggests that hemin inflicts damage to the liver and abides by the available literature stating that hemin has a role in liver dysfunction during malaria[32].

Further, we also tested the hemin toxicity to HepG2 cells by examining its impact on the wound healing capacity of the cells. Although complete healing was not observed after 48 hours in the untreated cells, they showed around 60% healing of the wound. The hemin-treated cells, however, were not able to migrate at all at both the treated concentrations resulting in almost 0% wound healing up to 48 hours (**Figure 5.4**).

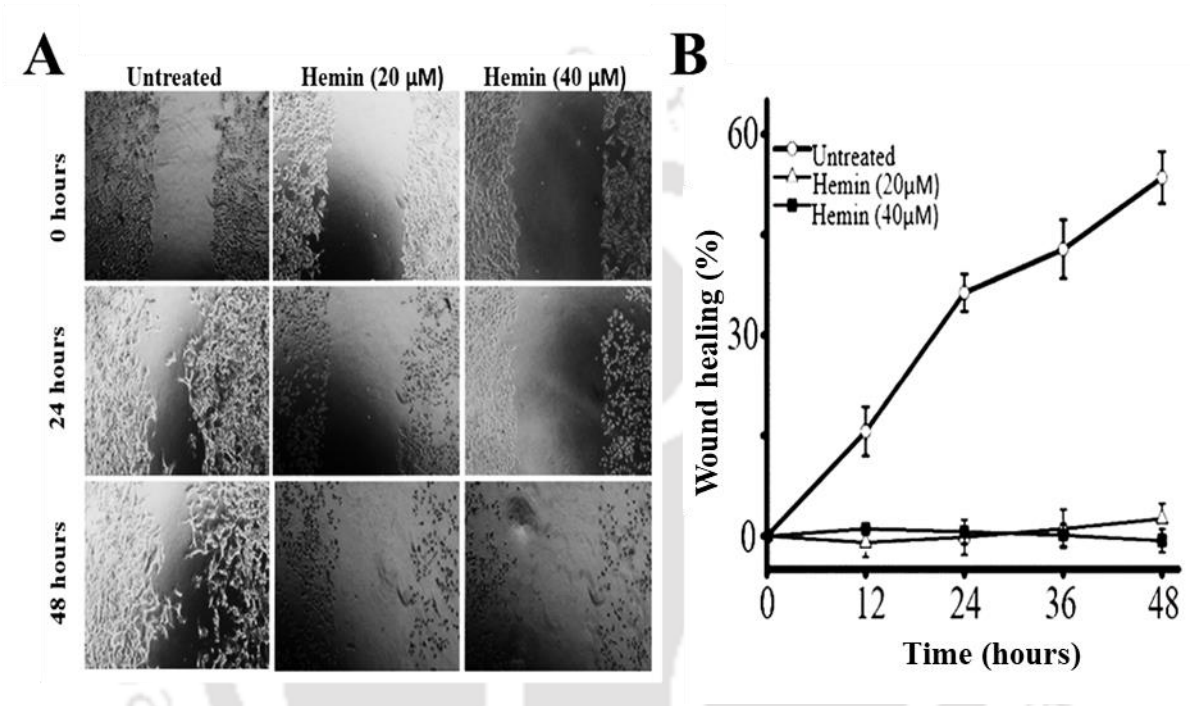

Figure 5.4: Impact of hemin on the wound healing capacity of HepG2 cells. A) The untreated cells show a considerable migration of the cells along the wound after 48 hours. In contrast, the hemin-treated cells were not able to heal the wound at all even after 48 hours of incubation. B) Graph showing the healed area of the wound in both untreated and hemin-treated cells after 48 hours of incubation.

5.3.2 Hemin causes perturbation in the cell cycle progression of HepG2 cells.

The experiments to test hemin toxicity give a clear insight into hemin exposure-related stress to HepG2 cells. During such stress, cells employ pro-survival strategies for energy conservation, leading to disturbances in the fundamental cellular processes like the cell cycle progression[42]. It is well-known that mammalian cells divide through four different stages of the cell cycle viz. G1, S, G2, and M phase[43]. Owing to the high cellular toxicity of hemin, we tested its effect on the

cell cycle progression of HepG2 cells through FACS using propidium iodide stain. The percent population of cells in different phases of the cell cycle was obtained using FCS express software. The control cells show a population distribution of 67 ± 4.6%, 26.54 ± 3.3%, and 6.46 ± 1.3% in the G1, S, and G2 phases respectively. The hemin-treated cells, however, showed an increase in the population of cells in the S phase and a decrease in the G1 and G2 phases at both the tested hemin concentrations, indicating an arrest in the S phase of the cell cycle (**Figure 5.5**). The S phase population in cells treated with 20 µM and 40 µM of hemin was increased to 33.45 ± 3.6% and 37.88 ± 4.2% respectively. The increase in the S phase population of treated cells indicates that hemin causes an arrest in the S phase of the cell cycle.

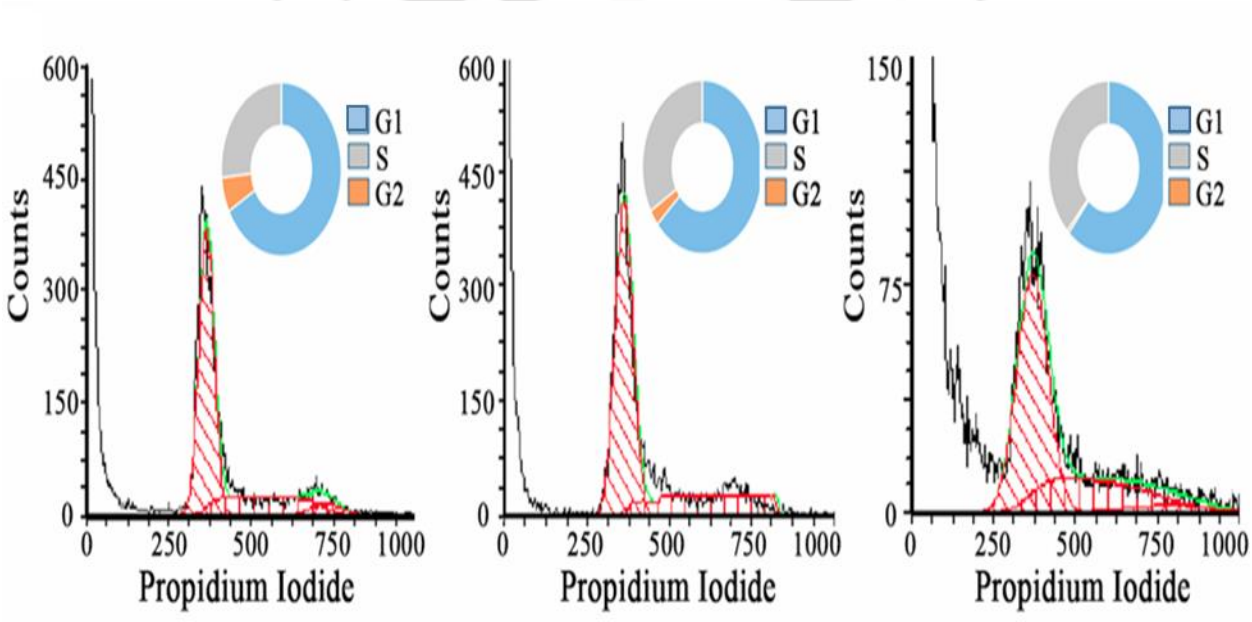

Figure 5.5: Cell cycle analysis of hemin-treated HepG2 cells. The population distribution of HepG2 cells in tested conditions is represented. The treated cells show an increase in the population of S Phase cells with increasing hemin concentrations (middle and right) as compared to the untreated cells (left) indicating an arrest in the S Phase of the cell cycle.

5.3.3 Hemin induces apoptosis in HepG2 liver cells.

The high hemin toxicity, especially the perforations on the cell surface of HepG2 cells after hemin treatment is indicative of apoptosis. Also, such stress conditions trigger cell death through programmed physiological processes like autophagy, apoptosis, necrosis, and necroptosis[44]. To confirm the hemin-induced apoptosis we carried out a DNA fragmentation analysis and apoptosis/necrosis detection of Annexin V-FITC and propidium iodide-stained cells. The results

show that hemin causes fragmentation of HepG2 genomic DNA which is evident from the smear and ladder-like DNA fragments visible in the agarose gel electrophoresis of genomic DNA isolated from hemin-treated cells. However, the DNA isolated from untreated cells was fully intact and no fragmentation was observed (**Figure 5.6**).

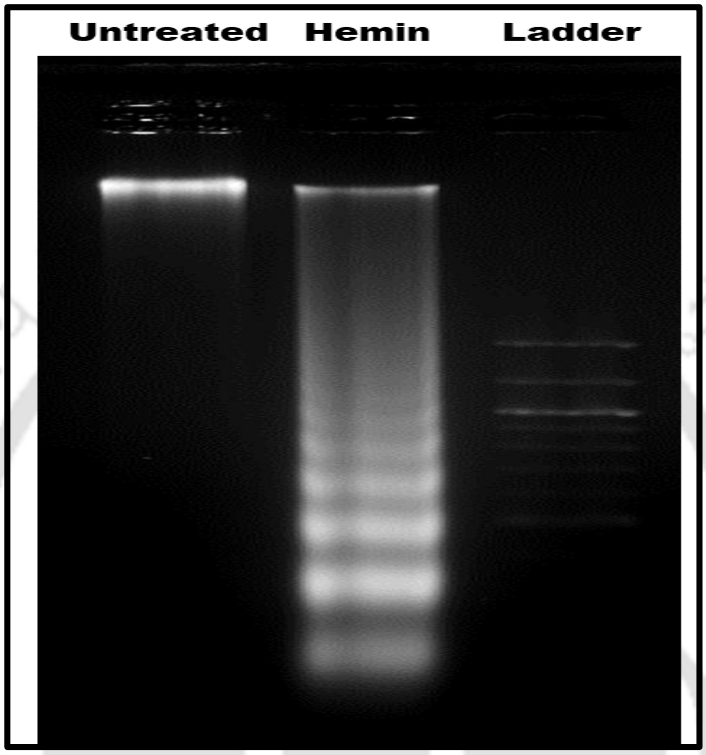

Figure 5.6: DNA Fragmentation Analysis of hemin-treated HepG2 cells: The genomic DNA isolated from hemin-treated cells showed a clear ladder formation (middle lane) with fragments of around 180-200 bps indicative of fragmentation. The untreated cells showed no fragmentation of DNA (left lane). The right lane shows a 100 bps DNA ladder.

The validation of induced apoptosis through FACS showed that hemin exposure with 20 and 40 μM increases the population of early and late apoptotic cells. The untreated cells showed a population with most of the cells (≈ 99%) in the first quadrant of the dot plot indicating live and normal cells. However, the hemin-treated cells showed a significant decrease in the population of live cells with 32.49% and 33.96% cells observed with 20 and 40 μM hemin respectively. The gross population of early (second quadrant) and late apoptotic (third quadrant) cells increased to 64.84 % and 61.88% with 20 and 40 μM hemin respectively (**Figure 5.7)**. The percentage of

necrotic cells also increased from zero percent in untreated cells to 2.67 % and 4.16% in cells treated with 20 and 40 μM of hemin. The DNA fragmentation analysis and FACS analysis collectively confirmed the hemin-induced apoptosis of the HepG2 cells.

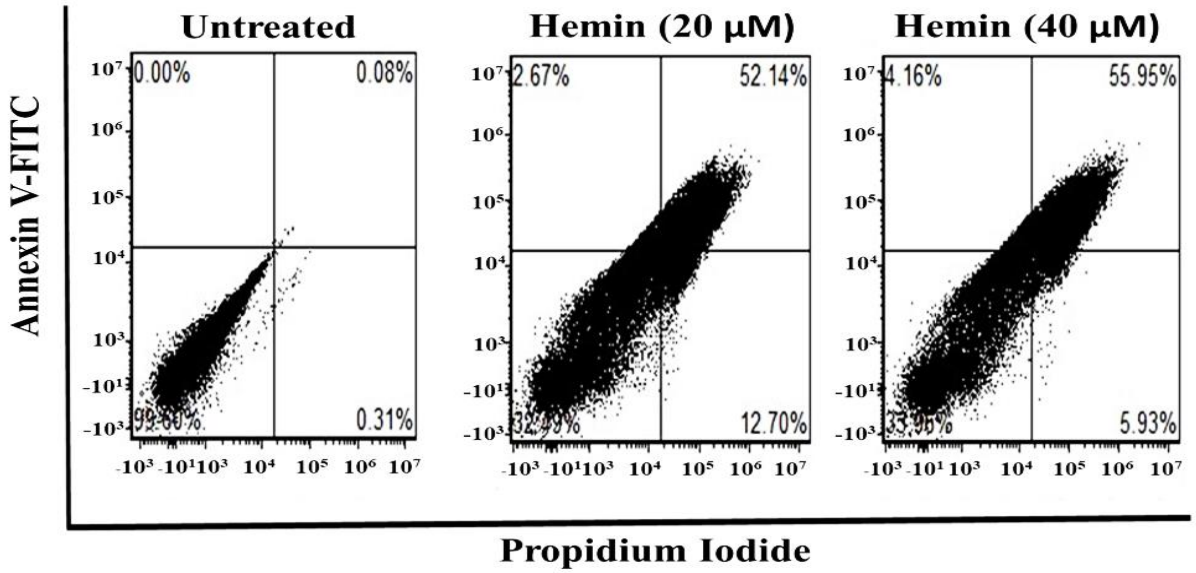

Figure 5.7: Hemin induces apoptosis in HepG2 cells. Hemin-treated and untreated cells were dual-stained with annexin V-FITC and PI and were analyzed using FACS. In the untreated sample, almost all the cell population was observed in the first quadrant indicating live cells. However, the population of live cells in hemin-treated samples was drastically reduced and the total early and late apoptotic cell population was drastically increased indicating hemin-induced apoptosis.

5.3.4 Hemin triggers both the intrinsic and extrinsic pathways of apoptosis in HepG2 liver cells.

Apoptosis is a tightly regulated phenomenon crucial to maintaining homeostasis and removing impaired cells. It can be initiated either through an intrinsic (mitochondrial) pathway or an extrinsic (death receptor) pathway[45]. Oxidative stress can trigger both the intrinsic and extrinsic pathways of apoptosis[46, 47].To reveal the pathway involved in hemin-induced toxicity we performed western blot analysis to determine the expression levels of apoptotis-related proteins of hemin-treated and untreated cells using protein-specific antibodies. The results show that hemin is globally toxic to HepG2 cells triggering both the apoptotic pathways. The expression levels of the

intrinsic pathway markers like caspase 3, cleaved caspase 3, PARP1, cleaved PARP1, and caspase 9 in treated cells were increased as compared to that in untreated cells. Additionally, the extrinsic pathway markers like DR3, DR4, TNFR1, TNFR2, cleaved caspase 8, ATP, and p-RIP were also found to be upregulated due to hemin treatment. The anti-apoptotic protein BCl2 was found to be downregulated by hemin confirming the apoptosis caused by hemin (**Figure 5.8**).

The overall immunoblotting results suggest the involvement of both the intrinsic and extrinsic pathways in the apoptosis of HepG2 cells induced by hemin.

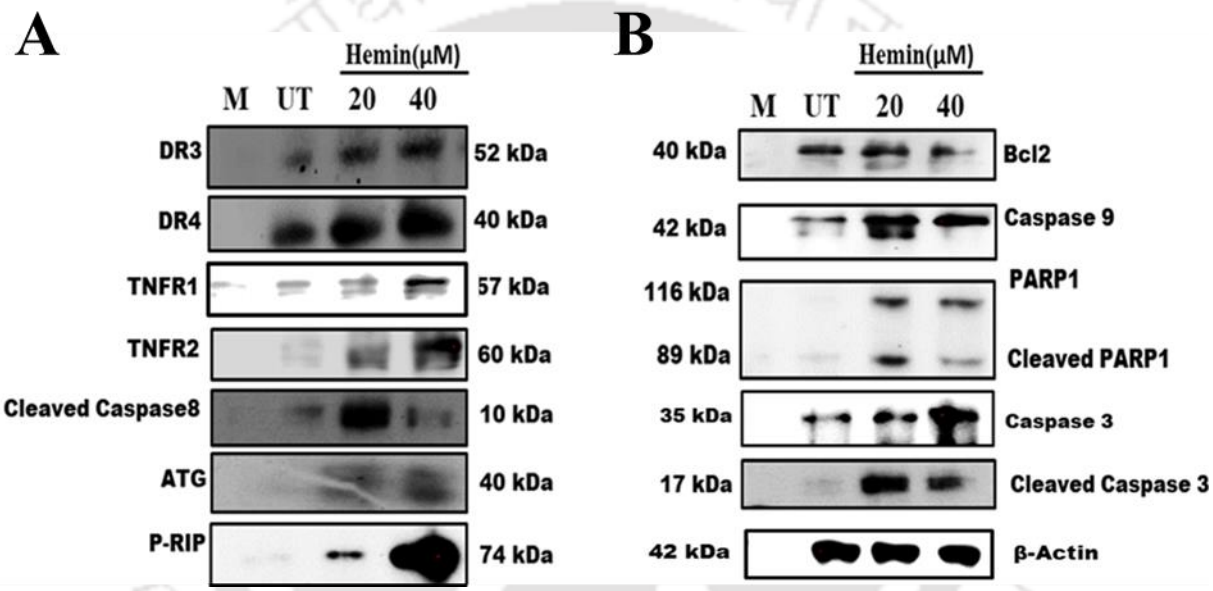

Figure 5.8: Western blot analysis of apoptosis marker proteins. The untreated and hemin-treated cells were analyzed to check the expression levels of various pathway-specific apoptotic proteins. **A)** Hemin upregulates all the tested member proteins of the extrinsic pathway of apoptosis, like DR3, DR4, TNFR1, TNFR2, cleaved caspase 8, ATG, and p-RIP. **B)** Hemin increases the expression and causes the cleavage of caspase 3 into cleaved caspase 3. The expression level of PARP1 and cleaved PARP also increased indicating intrinsic apoptosis pathway. Other intrinsic pathway marker like caspase 9 was also upregulated. Hemin also downregulates the anti-apoptotic protein BCl2 confirming the apoptosis.

5.3.5 HSPA8 impedes the toxic effects of hemin on HepG2 cells

Heat shock proteins play a crucial role in maintaining cellular health by attenuating the adverse outcomes of miscellaneous stressors[48, 49]. They are majorly known to be involved in proteostasis management in conditions leading to abnormal protein folding[50]. In our study, we

have discovered a secondary role of the heat shock protein HSPA8 specifically during heme stress. The hemoprotein formed by hemin binding to HSPA8 polymerizes hemin into less toxic heme polymer[38]. Hence, we were intrigued to find out the impact of HSPA8 on the hemin-generated toxicity towards HepG2 liver cells. The modulation in various toxic effects of hemin observed previously was tested in the absence and presence of HSPA8 as well. The cumulative results indicating that HSPA8 is cytoprotective to HepG2 cells against hemin-toxicity are discussed below.

HepG2 cells treated with the IC_{50} concentration of hemin along with an increasing concentration of purified HSPA8 show that HSPA8 prevents the loss in the cellular viability of these cells caused by hemin (**Figure 5.9**).

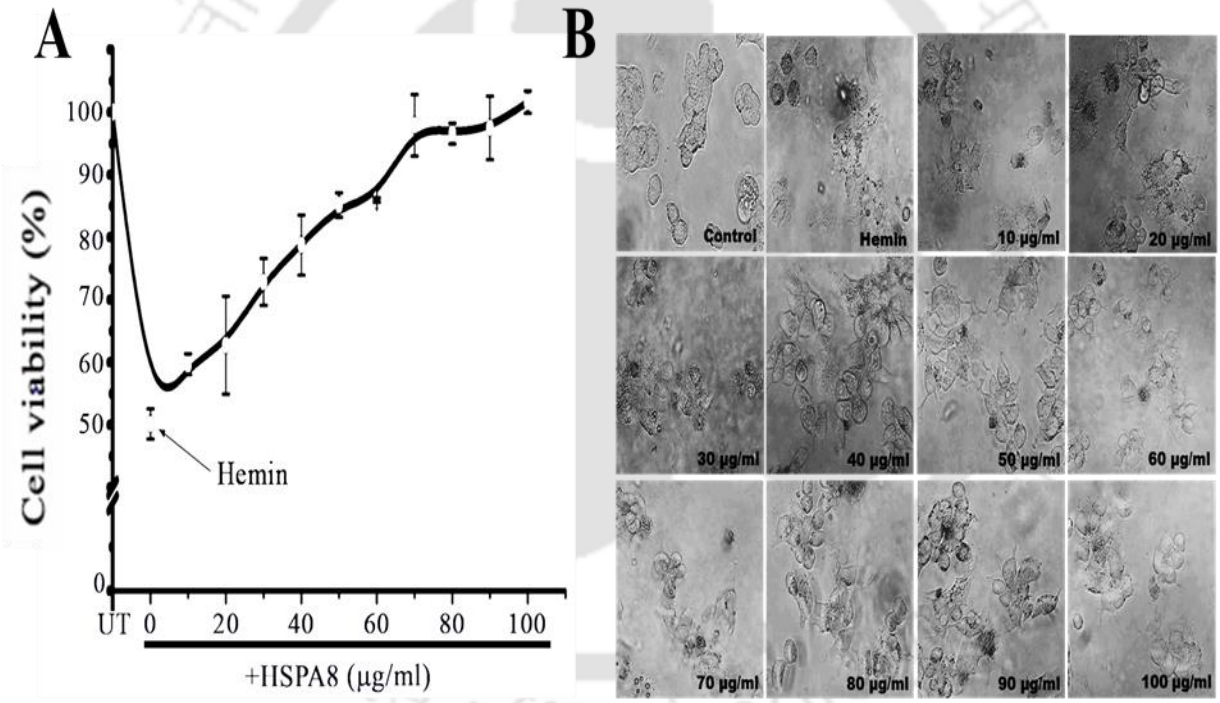

Figure 5.9: HSPA8 prevents the loss in viability of HepG2 cells caused by hemin. A) Graph showing a gradual increase in the viability of HepG2 cells upon simultaneous treatment of hemin with HSPA8.The HSPA8 concentrations above 80 µg/ml caused an almost complete regain in viability. **B)** Images of HepG2 cells after a 48-hour treatment with hemin as well as hemin in the presence of varying HSPA8 concentrations. The images were taken using a Cytell cell imaging system.

Hemin alone leads to the reduction in the percentage of viable cells to below 60%. However, a gradual increase in the percentage of viable cells, as compared to hemin only, was observed with increasing concentrations (0-100 µg/ml) of HSPA8. Almost a complete regain in viability was seen at 80 µg/ml of HSPA8 and above.

Hemin exposure causes the release of liver damage marker enzymes into the cell culture supernatant as observed previously. Simultaneous treatment of HSPA8 with hemin shows that the presence of HSPA8 reduces the amount of enzyme released caused due to hemin exposure (**Figure 5.10**).

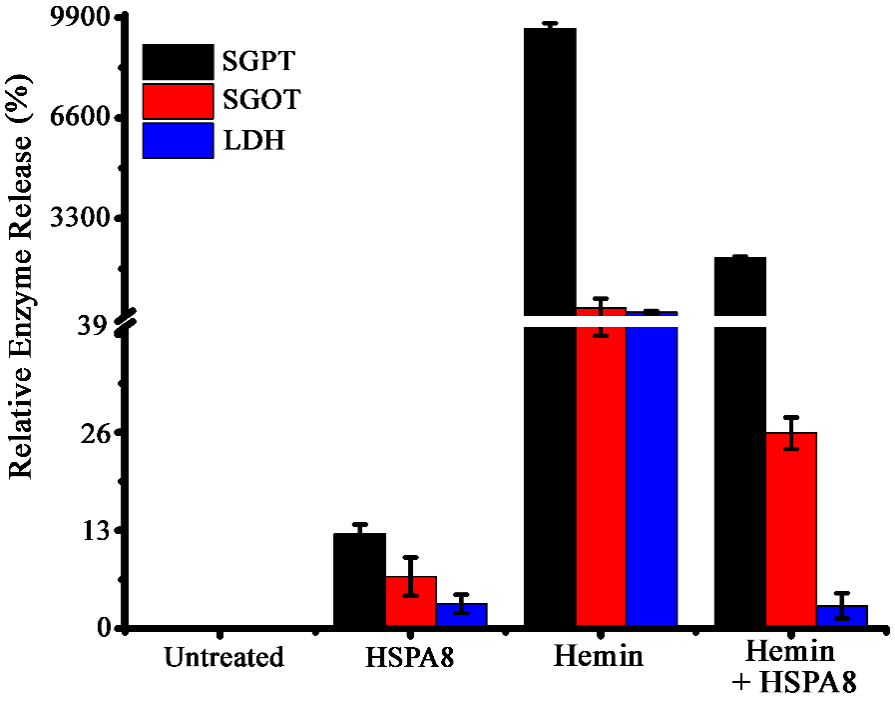

Figure 5.10: HSPA8 reduces liver damage caused by hemin. Cells treated with hemin show a drastic increase in the amount of released enzymes with 20 µM concentrations. However, when the cells were treated with the same hemin concentrations along with 0.5 µM HSPA8, the amount of all three enzymes was significantly reduced. Treatment with HSPA8 alone does not show any significant change in the released enzymes.

Hemin (20 µM) exposure resulted in an increase of approximately 9500%, 353%, and 221% of SGPT, SGOT, and LDH respectively. When the cells were treated with 20 µM hemin and 0.5 µM HSPA8 simultaneously, the amount of SGPT, SGOT, and LDH reduced to 2000%, 26%, and 3%

respectively. HSPA8-only treatment, however, does not significantly modulate the release of these enzymes indicating no considerable effect of HSPA8 in modulating the levels of these enzymes. The release of these enzymes out of the cell is a hallmark of liver damage[40]. The above results indicate that HSPA8 along with its known function of maintaining proteome health also has a protective role in hemin-induced liver damage and modulation in the release of certain liver enzymes.

Hemin was found to reduce the wound healing capability of HepG2 cells in previous experiments. The simultaneous treatment of hemin toxic concentrations along with HSPA8 resulted in the regain of the wound healing potential of the cells. HSPA8 treatment was found to reduce the hemin-induced loss in wound healing by HepG2 cells (**Figure 5.11**).

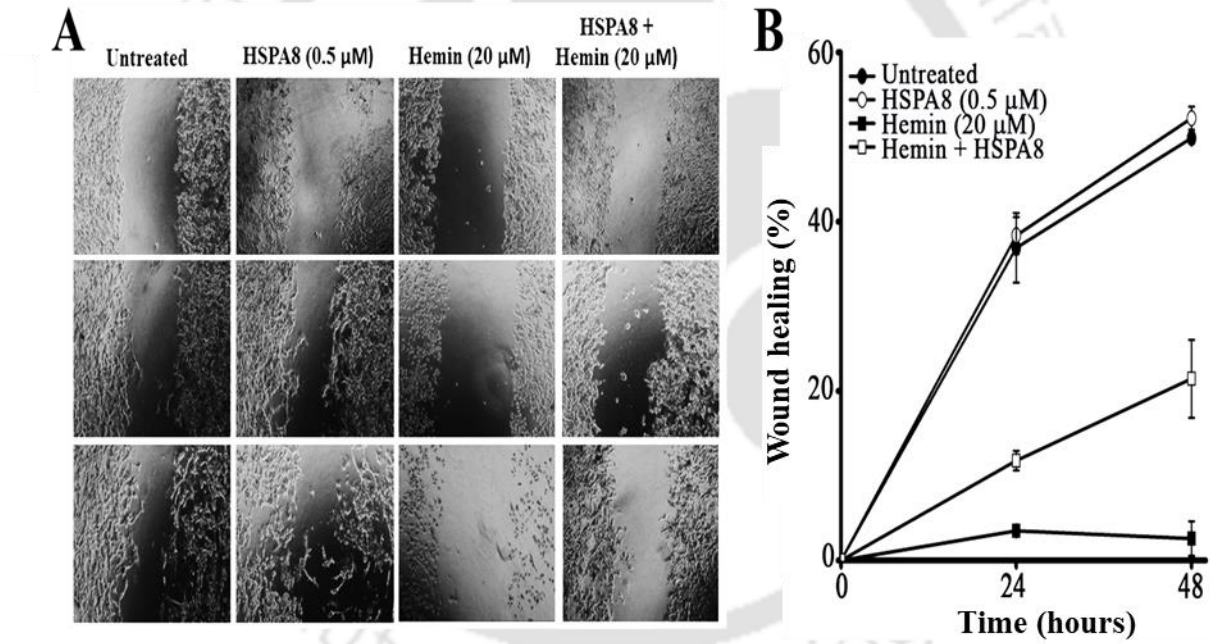

Figure 5.11: HSPA8 prevents loss in wound healing of HepG2 cells caused by hemin. A) Images showing the healed area of the wound after 24 and 48 hours of incubation. The untreated and HSPA8-only treated cells show considerable healing of the wound. The hemin-only treated cells show almost no wound healing whereas the cells treated with hemin plus HSPA8 showed a significant increase in the healed area of the wound. **B)** A graph showing a time-dependent area of wound healing in different treatment conditions. The graph was plotted after calculating the healed area of the wound through image analysis using ImageJ software.

After 48 hours of incubation, the untreated cells showed a wound healing of 49.88%. In the cells treated with 20 μM of hemin, the wound healing was found to be drastically reduced to 2.59%. However, the cells treated with both 20 μM of hemin and 0.5 μM of HSPA8 simultaneously showed a regain in wound healing to 21.45% indicating HSPA8's role in preventing the loss in the wound healing potential of HepG2 cells due to hemin. The cells treated with HSPA8 alone showed wound healing of 52.22% indicating no direct impact of HSPA8 on the wound healing potential of HepG2 cells.

5.3.6 HSPA8 reverses the cell cycle arrest by hemin in HepG2 cells.

Hemin treatment was found to cause an arrest in the S Phase of the cell cycle in HepG2 cells. To check whether HSPA8 can reverse this impact, we performed FACS analysis of propidium iodide stained cells in untreated, hemin-treated, and HSPA8 plus hemin-treated conditions. The results show that as compared to hemin-treated cells, the S phase population in the HSPA8 plus hemin-treated cells was significantly reduced indicating a reversal in the arrest caused by hemin alone (**Figure 5.12)**.

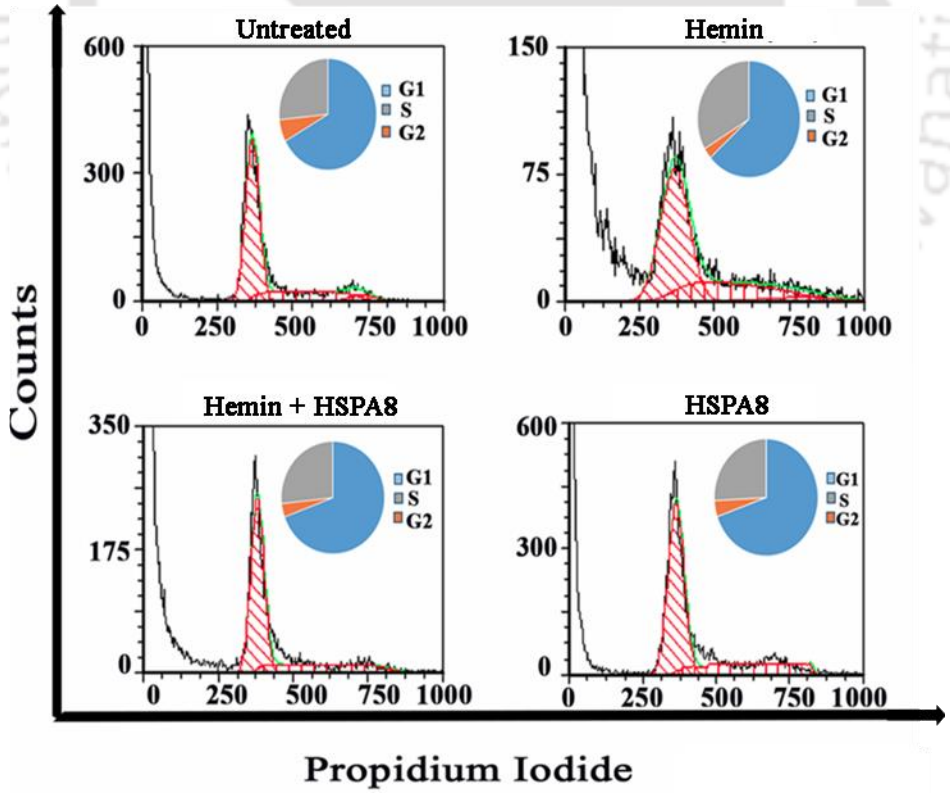

Figure 5.12: HSPA8 reverses cell cycle arrest by hemin. The results show an increase in the S Phase population of the hemin-treated cells, compared to the untreated cells suggesting an

arrest in S Phase. However, simultaneous treatment of HSPA8 with hemin reverses this effect of hemin and the population distribution was found to be similar to that of control cells. HSPA8-only cells do not show any change in the population distribution indicating no direct effect of HSPA8 on the cell cycle progression.

The hemin-treated (20 μM) cells show a cell population of 33.45% in the S phase of the cell cycle. However, with the simultaneous treatment of HSPA8 (0.5 μM) with 20 μM hemin the S phase population reduced to 26.7%. The G1 and G2-phase population in 20 μM hemin-only treated cells was 63.52% and 3.03% respectively. HSPA8 treatment along with the same hemin concentrations showed a population distribution of 69.42% and 3.89% respectively in G1 and G2 phases. The untreated and HSPA8-only treated cells showed almost similar patterns of population distribution in G1, G2, and S phase indicating no direct effect of HSPA8 on the cell cycle progression by HepG2 cells. The G1, G2, and S phase population in untreated cells was 67%, 26.54%, and 6.46% respectively and in HSPA8-only treated cells were 69.7%, 25.85%, and 4.45% respectively.

5.3.7 HSPA8 protects HepG2 cells from hemin-induced apoptosis.

Other than the primary function of maintaining proteome health, heat shock proteins are also known to act as anti-apoptotic proteins during oxidative stress[48]. In our previous experiments, we found that hemin treatment leads to the fragmentation of genomic DNA and induces apoptosis in HepG2 cells. HSPA8, being cytoprotective to HepG2 cells against hemin is expected to protect these cells from hemin-induced apoptosis. We performed DNA fragmentation analysis and FACS analysis, using Annexin V-FITC and propidium iodide staining, of untreated, hemin-treated, and hemin plus HSPA8 treated cells to confirm if HSPA8 protects these cells from apoptosis caused by hemin. While the untreated cells show no sign of apoptosis with approximately 99% of the cells observed in the first quadrant of the dot plot (**Figure 5.13**), the hemin-treated cells show 12.70% early and 52.14 % late apoptotic cells with 20 μM hemin treatment. However, when the cells were simultaneously treated with HSPA8 (0.5 μM) and hemin (20 μM), the percentage of late apoptotic cells reduced to 23.63% and that of early apoptotic cells increased to 32.27%. The reduction in the population of late apoptotic cells and the increase in early apoptotic cells indicate that the presence of HSPA8 prevented a significant population of cells from moving to the late apoptotic stage from the early apoptotic stage but was not able to completely protect the cells from being subjected to apoptosis. In the hemin-only treated cells, a considerably large percentage of cells were found to

move up to the late apoptotic stage and the population in the early apoptotic stage was comparatively very low.

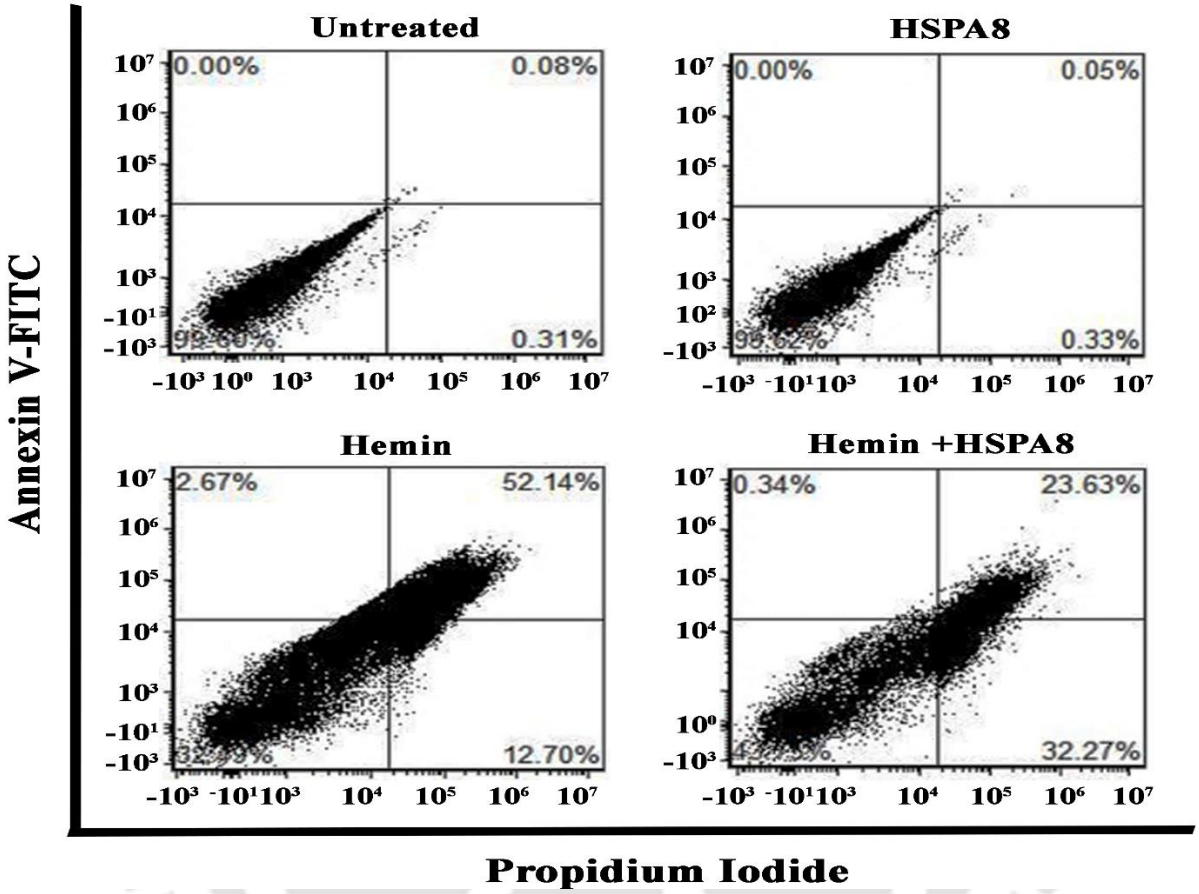

Figure 5.13: HSPA8 reverses the apoptotic effect of hemin on HepG2 cells: The population of apoptotic cells increased in the hemin-treated cells as compared to the untreated cells. However, in the presence of HSPA8 and hemin, the apoptotic cell population reduced significantly. The HSPA8-only treated cells show a population distribution similar to that of untreated cells indicating no direct effect of HSPA8 in inducing apoptosis.

Thus it can be fairly concluded that HSPA8 impedes the extent of hemin-induced apoptosis in HepG2 cells and prevents them from moving to the late apoptotic stage, in contrast to what was observed in the hemin-only treated cells.

Additionally, the DNA fragmentation analysis of the cells treated under similar conditions as above also indicated the prevention of hemin-induced apoptosis in HepG2 cells. The concentration of HSPA8 (1 μM) exhibiting complete protection in the cell viability assay was chosen for this

experiment expecting complete protection of the HepG2 genomic DNA from fragmentation because even a partial fragmentation may not be confirmatory to interpret the protection by HSPA8. While the genomic DNA isolated from untreated and HSPA8-only treated cells show intact DNA with no fragmentation, the hemin-treated samples show a clear ladder formation (**Figure 5.14**). However, when the cells were treated with hemin along with HSPA8, again there was no fragmentation of DNA observed indicating that HSPA8 protects the DNA fragmentation caused by hemin. The DNA fragmentation and FACS analysis collectively indicate that HSPA8 minimizes the hemin toxicity to HepG2 cells and prevents them from apoptosis.

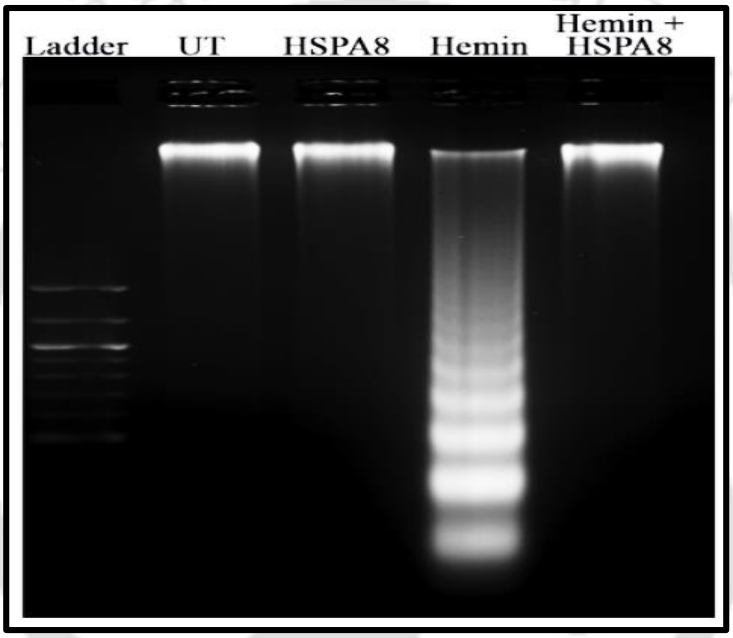

Figure 5.14: HSPA8 prevents HepG2 cells from DNA fragmentation caused by hemin. The untreated and HSPA8-only treated samples do not show any sign of DNA fragmentation. The hemin-treated cells show a clear ladder formation indicating fragmented DNA. However, treatment with HSPA8 and hemin both, again show intact DNA with no fragmentation indicating protection by HSPA8 against DNA fragmentation caused by hemin.

5.3.8 The protection from hemin toxicity appears to be through its polymerization

We have discovered that when HSPA8 is provided externally with hemin, it is protecting HepG2 cells from the hemin toxicity. It is well-known that HSPA8 is a constitutive protein[51] and is

secreted out in the microenvironment during stress conditions[52]. HSPA8's protective role in the outside environment during heme stress gives an insight that hemin treatment might lead to the secretion of HSPA8 in the extracellular environment of HepG2 cells. Since HSPA8 can polymerize hemin into heme polymer, its secretion is expected to impart a heme polymerizing potential to the cell culture media of hemin-treated cells. We tested the dose and time-dependent heme polymerizing potential of the culture supernatant of HepG2 cells treated with increasing hemin concentration. The results were in agreement with our hypothesis as hemin treatment increased the heme polymerizing potential of the cell culture supernatant in a dose-dependent as well as time-dependent manner (**Figure 5.15**). Culture media from cells treated with 0 to 100 µM hemin exhibit heme polymerization activity leading to the increase in the formation of heme polymer in a dose-dependent manner with approximately 8-10 µM of polymer formed at 100 µM. The time-dependent experiment with 100 µM hemin treatment also showed a gradual increase in the heme polymerizing potential of the cell culture media with approximately 9 µM of heme polymer formed by the media from cells treated for 48 hours.

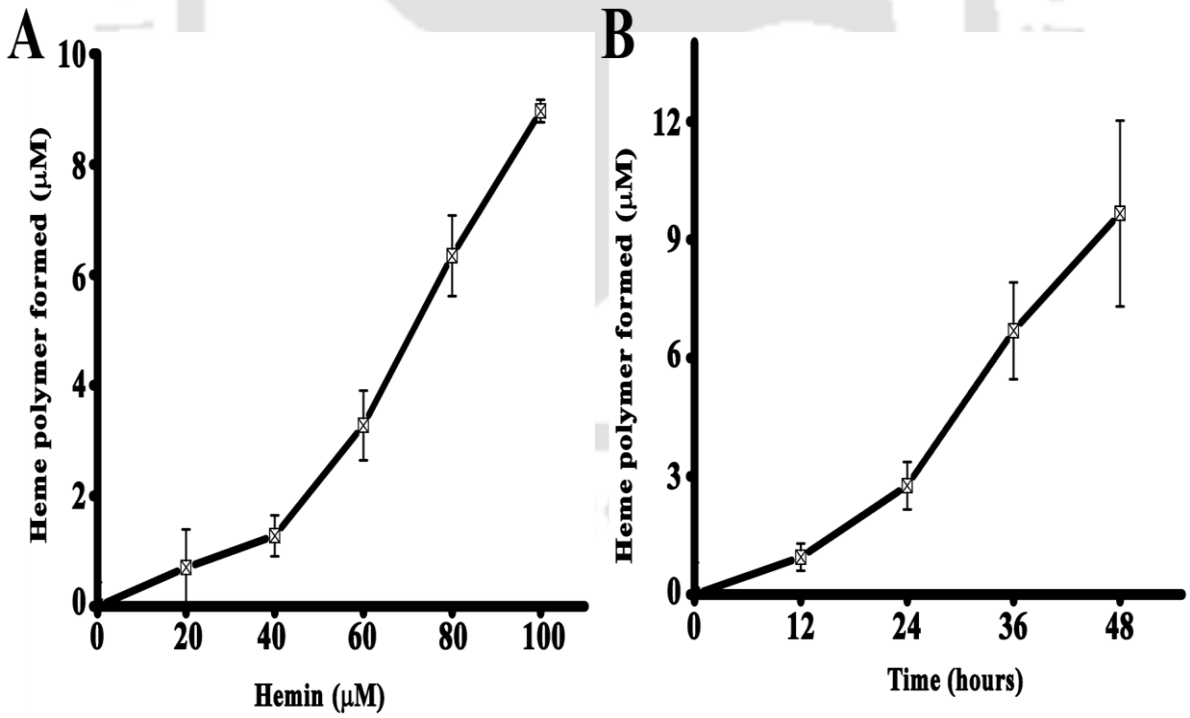

Figure 5.15 Heme polymerization by cell culture media from hemin-treated HepG2 cells. **A)** Dose-dependent heme polymerization by the cell culture media from HepG2 cells treated

with 0 to 100 µM hemin. **B)** A 48-hour time-dependent heme polymerization by cell culture media from HepG2 cells treated with 100 µM of hemin.

5.4 Discussions

The liver is one of the most important organs and its proper functioning is crucial for human health and survival. Impairment in liver function can lead to digestive problems, nutrient deficiencies, and abnormalities in various detoxification processes[20]. Severe liver damage can even be fatal. Hemin/heme accumulation in the liver can be a consequence of several diseases or pathological conditions like severe malaria, where there is prominent hemolysis and hemoglobin degradation[53, 54]. The accumulation of hemin can cause several abnormalities in the liver[55]. It can lead to liver dysfunction[32], liver injury[56], oxidative damage to DNA[57], proteins[10], and lipids[8], etc. Heme is known to undermine microcirculation in the liver leading to hepatic injury[58]. A very high level of hemin can even lead to complete hepatic failure. In our study, we have further elaborated the heme toxicity towards the liver by exploring the harmful impacts of hemin on the HepG2 cell line. Our findings support the idea that hemin/heme is highly toxic to the liver and can bring about several phenotypic changes that are indicative of damage to the liver.

Detoxification of xenobiotics including chemicals and drugs is one of the major functions of the liver[59]. It executes several pathways of detoxification to metabolize and excrete these harmful agents out of the body[60]. During heme stress, a constitutive enzyme heme oxygenase-1 (HO-1), is the major player protecting the liver from the harmful effects of heme[61, 62]. While the detoxification by HO-1 involves the breaking down of heme into smaller and less toxic molecules, a few other proteins like haptoglobin and hemopexin sequester the free heme or heme iron forming respective complexes.

Other than the oxidative stress by hemin, HO-1 (aka heat shock protein 32) is also induced during heat stress in the liver[63]. Several other heat shock proteins (HSPs) are also known to be responsive to oxidative stress in the liver[64]. It has been shown that oxidative stress can lead to the induction of HSPs like cytosolic HSP25, HSP40, HSP70, HSP105, and microsomal HSP32 (HO-1) in TAMH, a murine hepatocyte cell line[65]. Heat shock proteins, especially HSP70s are actively involved in protecting the liver from oxidative damage occurring during hemorrhage[66]. In our study, we have also discovered the protective role of an HSP70 member protein HSPA8

against oxidative damage caused by hemin. HSPA8 can reverse the tested hemin-related toxic outcomes in HepG2 cells. HSPA8 is known to have a protective role in the liver and various other diseases. It is involved in clathrin-mediated autophagy[67] and the protection of liver cells from rifampicin-induced ferroptosis[68]. Attenuation of HSPA8 expression induces apoptosis in prostate cancer cells[69]. It is associated with Nonalcoholic Fatty Liver disease-associated atherosclerosis of the carotid artery[70]. It is also upregulated in hepatocellular carcinoma patients with depression[71]. Although many HSPs are involved in the protection of the liver, there are no such reports of an HSP involved in liver protection against hemin-toxicity. Here we are reporting HSPA8 as a novel cytoprotective HSP during heme/hemin stress to the liver. Externally provided HSPA8 protects HepG2 cells from the overall hemin-induced toxicity.

The integrated cellular response during such stress conditions leads to the selective activation of the heat shock factor triggering the transcription of heat shock proteins[72, 73]. These proteins are then translocated to various cellular compartments depending on their functional requirement. Heat shock proteins are actively found in the cytoplasm, at the cell surface, can be translocated to the nucleus, and are also secreted out of the cell depending upon their targeted localization[74-77]. In our study, we found that externally supplied HSPA8 protects the liver cells from the toxic effects of hemin. Owing to this it can be fairly assumed that hemin-treatment may lead to secretion of HSPA8 out of the cells for its protective action. HSPA8 can polymerize hemin *in-vitro* [38]. Although the determination of specific HSPA8 levels in the supernatant is important to reach any conclusion, the fact that the cell culture supernatant of the hemin-treated cells showed a heme polymerizing potential supports the insight that HSPA8 is secreted out after hemin treatment. The secretion of proteins out of the cell is governed by specific cellular processes [78]. Other than the classical secretory pathways, HSPs can also be secreted out through unconventional processes during stress conditions[52, 79]. The secretory pathway responsible for the secretion of HSPA8 due to hemin exposure to cells remains unclear. The revelation of the pathway involved can provide a better understanding of the cellular response to hemin treatment and can be exploited well for unveiling any therapeutic potential of HSPA8 during diseases involving heme accumulation.

5.5 Conclusions

Hemin reduces cell viability and wound healing potential of HepG2 cells and brings about morphological changes like cell shrinkage, loss of membrane integrity, and perforations indicative of apoptosis. Hemin also causes liver damage resulting in the release of stress-marker enzymes like SGPT, SGOT, and LDH in the extracellular environment. Hemin hinders the proliferation of HepG2 cells by arresting them in the S phase of their cell cycle progression. It also leads to the fragmentation of genomic DNA and induces apoptosis in HepG2 cells by triggering both the extrinsic and intrinsic pathways of apoptosis. Hemin treatment leads to the modulation in the expression level of many pathway-specific apoptosis marker proteins. It leads to the upregulation and cleavage of caspase 3, further leading to the cleavage of PARP1 indicating the involvement of the intrinsic pathway of apoptosis. It also upregulates caspase 9 and downregulates the anti-apoptotic protein BCl2. Hemin also upregulates many proteins of the extrinsic (death receptor) pathway like DR3, DR4, TNRF1, TNRF2, cleaved caspase 8, ATG, and p-RIP. Conclusively, it can be interpreted that hemin is globally toxic to HepG2 cells triggering various apoptotic pathways.

However, the hemin treatment at its toxic concentrations along with HSPA8 shows a reversal in the hemin-induced toxicity to HepG2 cells. In the presence of HSPA8, the cells show improved viability, a reduction in the release of stress-indicative liver enzymes, improved cell cycle progression, and prevention from DNA fragmentation and apoptosis. HSPA8 reverses the modulation caused by hemin in the expression levels of various apoptotic proteins of both extrinsic and intrinsic apoptotic pathways. The outcomes of this study allow us to conclude that hemin inflicts very high toxicity to HepG2 cells which can be attenuated by the heat shock protein HSPA8.

5.6 References

1. Rother, R.P., et al., The clinical sequelae of intravascular hemolysis and extracellular plasma hemoglobin: a novel mechanism of human disease. Jama, 2005. **293**(13): p. 1653-1662.

2. Rifkind, J.M., J.G. Mohanty, and E. Nagababu, The pathophysiology of extracellular hemoglobin associated with enhanced oxidative reactions. Frontiers in physiology, 2015. **5**: p. 500.
3. Schaer, D.J., et al., Hemolysis and free hemoglobin revisited: exploring hemoglobin and hemin scavengers as a novel class of therapeutic proteins. Blood, The Journal of the American Society of Hematology, 2013. **121**(8): p. 1276-1284.
4. Kumar, S. and U. Bandyopadhyay, Free heme toxicity and its detoxification systems in human. Toxicology letters, 2005. **157**(3): p. 175-188.
5. Arruda, M.A., et al., Heme inhibits human neutrophil apoptosis: involvement of phosphoinositide 3-kinase, MAPK, and NF-κB. The Journal of Immunology, 2004. **173**(3): p. 2023-2030.
6. Pethő, D., et al., Heme cytotoxicity is the consequence of endoplasmic reticulum stress in atherosclerotic plaque progression. Scientific reports, 2021. **11**(1): p. 10435.
7. Li, S.-D., et al., Hemin-mediated hemolysis in erythrocytes: effects of ascorbic acid and glutathione. Acta Biochimica et Biophysica Sinica, 2006. **38**(1): p. 63-69.
8. Higdon, A.N., et al., Hemin causes mitochondrial dysfunction in endothelial cells through promoting lipid peroxidation: the protective role of autophagy. American Journal of Physiology-Heart and Circulatory Physiology, 2012. **302**(7): p. H1394-H1409.
9. Aft, R.L. and G. Mueller, Hemin-mediated oxidative degradation of proteins. Journal of Biological Chemistry, 1984. **259**(1): p. 301-305.
10. Vasconcellos, L.R., et al., Protein aggregation as a cellular response to oxidative stress induced by heme and iron. Proceedings of the National Academy of Sciences, 2016. **113**(47): p. E7474-E7482.
11. Ishikawa, S.i., et al., Heme induces DNA damage and hyperproliferation of colonic epithelial cells via hydrogen peroxide produced by heme oxygenase: A possible mechanism of heme-induced colon cancer. Molecular nutrition & food research, 2010. **54**(8): p. 1182-1191.
12. Gamage, S.M.K., et al., Hemin, a major heme molecule, induced cellular and genetic alterations in normal colonic and colon cancer cells. Pathology-Research and Practice, 2021. **224**: p. 153530.
13. Goldstein, L., et al., Hemin induces an iron-dependent, oxidative injury to human neuron-like cells. Journal of neuroscience research, 2003. **73**(1): p. 113-121.
14. Wilson, S.J. and A.K. Keenan, Role of hemin in the modulation of H2O2-mediated endothelial cell injury. Vascular pharmacology, 2003. **40**(2): p. 109-118.
15. Imai, T., et al., Intracellular Fe2+ accumulation in endothelial cells and pericytes induces blood-brain barrier dysfunction in secondary brain injury after brain hemorrhage. Scientific reports, 2019. **9**(1): p. 6228.
16. Butt, O.I., P.W. Buehler, and F. D'Agnillo, Blood-brain barrier disruption and oxidative stress in guinea pig after systemic exposure to modified cell-free hemoglobin. The American journal of pathology, 2011. **178**(3): p. 1316-1328.
17. Balla, G., et al., Exposure of endothelial cells to free heme potentiates damage mediated by granulocytes and toxic oxygen species. Laboratory investigation; a journal of technical methods and pathology, 1991. **64**(5): p. 648-655.
18. Ghosh, S., et al., Extracellular hemin crisis triggers acute chest syndrome in sickle mice. The Journal of clinical investigation, 2013. **123**(11): p. 4809-4820.

19. Bhoite-Solomon, V., G. Kessler-Icekson, and N. Shaklai, Myocyte injury by hemin. In Vitro Cellular & Developmental Biology-Animal, 1993. **29**: p. 636-642.
20. Ozougwu, J.C., Physiology of the liver. International Journal of Research in Pharmacy and Biosciences, 2017. **4**(8): p. 13-24.
21. Gracia-Sancho, J., et al., Role of liver sinusoidal endothelial cells in liver diseases. Nature Reviews Gastroenterology & Hepatology, 2021. **18**(6): p. 411-431.
22. Wang, Y. and C. Zhang, The roles of liver-resident lymphocytes in liver diseases. Frontiers in immunology, 2019. **10**: p. 1582.
23. Zhan, Y.-T. and W. An, Roles of liver innate immune cells in nonalcoholic fatty liver disease. World journal of gastroenterology: WJG, 2010. **16**(37): p. 4652.
24. Gao, B., S. Radaeva, and O. Park, Liver natural killer and natural killer T cells: immunobiology and emerging roles in liver diseases. Journal of leukocyte biology, 2009. **86**(3): p. 513-528.
25. Wunderlich, F., S. Al-Quraishy, and M.A. Dkhil, Liver-inherent immune system: its role in blood-stage malaria. Frontiers in Microbiology, 2014. **5**: p. 559.
26. Holz, L.E., D. Fernandez-Ruiz, and W.R. Heath, Protective immunity to liver-stage malaria. Clinical & translational immunology, 2016. **5**(10): p. e105.
27. Guha, M., et al., Apoptosis in liver during malaria: role of oxidative stress and implication of mitochondrial pathway. The FASEB Journal, 2006. **20**(8): p. 1224-1226.
28. Key, N.S., et al., Hemolytic anemia in protoporphyria: possible precipitating role of liver failure and photic stress. American journal of hematology, 1992. **39**(3): p. 202-207.
29. Pop, T.L., et al., Acute liver failure with hemolytic anemia in children with Wilson's disease: Genotype-phenotype correlations? World Journal of Hepatology, 2021. **13**(10): p. 1428.
30. ZIEVE, L., Jaundice, hyperlipemia and hemolytic anemia: a heretofore unrecognized syndrome associated with alcoholic fatty liver and cirrhosis. Annals of internal medicine, 1958. **48**(3): p. 471-496.
31. Smits-Wintjens, V.E., et al., Cholestasis in neonates with red cell alloimmune hemolytic disease: incidence, risk factors and outcome. Neonatology, 2012. **101**(4): p. 306-310.
32. Dey, S., et al., Impact of intravascular hemolysis in malaria on liver dysfunction: involvement of hepatic free heme overload, NF-κB activation, and neutrophil infiltration. Journal of Biological Chemistry, 2012. **287**(32): p. 26630-26646.
33. Deshmukh, R. and V. Trivedi, Methemoglobin exposure produces toxicological effects in macrophages due to multiple ROS spike induced apoptosis. Toxicology in Vitro, 2013. **27**(1): p. 16-23.
34. Gemelli, C., et al., Cytotoxic effect of hemin in colonic epithelial cell line: Involvement of 18 kDa translocator protein (TSPO). Life Sciences, 2014. **107**(1-2): p. 14-20.
35. Glei, M., et al., Hemoglobin and hemin induce DNA damage in human colon tumor cells HT29 clone 19A and in primary human colonocytes. Mutation Research/Fundamental and Molecular Mechanisms of Mutagenesis, 2006. **594**(1-2): p. 162-171.
36. Dang, T.N., et al., The metabolism and toxicity of hemin in astrocytes. Glia, 2011. **59**(10): p. 1540-1550.
37. Dang, T.N., et al., Uptake, metabolism and toxicity of hemin in cultured neurons. Neurochemistry international, 2011. **58**(7): p. 804-811.
38. Pandey, A.K. and V. Trivedi, Role Transformation of HSPA8 to Heme-peroxidase After Binding Hemin to Catalyze Heme Polymerization. The Protein Journal, 2023: p. 1-14.

39. Neuman, M.G., Apoptosis in diseases of the liver. Critical reviews in clinical laboratory sciences, 2001. **38**(2): p. 109-166.
40. Dufour, D.R., et al., Diagnosis and monitoring of hepatic injury. I. Performance characteristics of laboratory tests. Clinical chemistry, 2000. **46**(12): p. 2027-2049.
41. Raja, S., et al., Antioxidant effect of Cytisus scoparius against carbon tetrachloride treated liver injury in rats. Journal of ethnopharmacology, 2007. **109**(1): p. 41-47.
42. Fulda, S., et al., Cellular stress responses: cell survival and cell death. International journal of cell biology, 2010. **2010**.
43. Vermeulen, K., D.R. Van Bockstaele, and Z.N. Berneman, The cell cycle: a review of regulation, deregulation and therapeutic targets in cancer. Cell proliferation, 2003. **36**(3): p. 131-149.
44. Conradt, B. and D. Xue, Programmed cell death. WormBook: The Online Review of C. elegans Biology [Internet], 2005.
45. Elmore, S., Apoptosis: a review of programmed cell death. Toxicologic pathology, 2007. **35**(4): p. 495-516.
46. Yuan, J., et al., Involvement of cytochrome c release and caspase-3 activation in the oxidative stress-induced apoptosis in human tendon fibroblasts. Biochimica et Biophysica Acta (BBA)-Molecular Cell Research, 2003. **1641**(1): p. 35-41.
47. Annunziato, L., et al., Apoptosis induced in neuronal cells by oxidative stress: role played by caspases and intracellular calcium ions. Toxicology letters, 2003. **139**(2-3): p. 125-133.
48. Kalmar, B. and L. Greensmith, Induction of heat shock proteins for protection against oxidative stress. Advanced drug delivery reviews, 2009. **61**(4): p. 310-318.
49. Kim, H.P., D. Morse, and A.M. Choi, Heat-shock proteins: new keys to the development of cytoprotective therapies. Expert opinion on therapeutic targets, 2006. **10**(5): p. 759-769.
50. Lang, B.J., et al., The functions and regulation of heat shock proteins; key orchestrators of proteostasis and the heat shock response. Archives of toxicology, 2021. **95**(6): p. 1943-1970.
51. Stricher, F., et al., HSPA8/HSC70 chaperone protein: structure, function, and chemical targeting. Autophagy, 2013. **9**(12): p. 1937-1954.
52. Santos, T.G., V.R. Martins, and G.N.M. Hajj, Unconventional secretion of heat shock proteins in cancer. International journal of molecular sciences, 2017. **18**(5): p. 946.
53. Morse, E.E., Mechanisms of hemolysis in liver disease. Annals of Clinical & Laboratory Science, 1990. **20**(3): p. 169-174.
54. Drozdowska-Szymczak, A., et al., Liver Dysfunction with Severe Cholestasis and Coagulation Disorders in the Course of Hemolytic Disease of the Newborn Requiring Chelation Therapy—A Case Report and Review of the Literature. Journal of Clinical Medicine, 2023. **12**(24): p. 7645.
55. Seidel, R.A., et al., Impact of higher-order heme degradation products on hepatic function and hemodynamics. Journal of Hepatology, 2017. **67**(2): p. 272-281.
56. Zhao, Y., et al., Effects of flavonoids extracted from Scutellaria baicalensis Georgi on hemin–nitrite–H2O2 induced liver injury. European journal of pharmacology, 2006. **536**(1-2): p. 192-199.
57. Suliman, H.B., et al., Rapid mtDNA deletion by oxidants in rat liver mitochondria after hemin exposure. Free Radical Biology and Medicine, 2002. **32**(3): p. 246-256.
58. Englert, F.A., et al., Labile heme impairs hepatic microcirculation and promotes hepatic injury. Archives of biochemistry and biophysics, 2019. **672**: p. 108075.

59. Apte, U. and P. Krishnamurthy, Detoxification functions of the liver. Molecular pathology of liver diseases, 2011: p. 147-163.
60. Grant, D., Detoxification pathways in the liver. Journal of inherited metabolic disease, 1991. **14**: p. 421-430.
61. Origassa, C.S.T. and N.O.S. Câmara, Cytoprotective role of heme oxygenase-1 and heme degradation derived end products in liver injury. World journal of hepatology, 2013. **5**(10): p. 541.
62. Sass, G., R. Barikbin, and G. Tiegs, The multiple functions of heme oxygenase-1 in the liver. Zeitschrift für Gastroenterologie, 2012. **50**(01): p. 34-40.
63. Bauer, I., et al., Expression pattern and regulation of heme oxygenase-1/heat shock protein 32 in human liver cells. Shock, 2003. **20**(2): p. 116-122.
64. Schiaffonati, L. and L. Tiberio, Gene expression in liver after toxic injury: analysis of heat shock response and oxidative stress-inducible genes. Liver, 1997. **17**(4): p. 183-191.
65. Ho, H.K., et al., Cytosolic heat shock proteins and heme oxygenase-1 are preferentially induced in response to specific and localized intramitochondrial damage by tetrafluoroethylcysteine. Biochemical pharmacology, 2006. **72**(1): p. 80-90.
66. Mizushima, Y., et al., Preinduction of heat shock proteins protects cardiac and hepatic functions following trauma and hemorrhage. American Journal of Physiology-Regulatory, Integrative and Comparative Physiology, 2000. **278**(2): p. R352-R359.
67. Bonam, S.R., M. Ruff, and S. Muller, HSPA8/HSC70 in immune disorders: a molecular rheostat that adjusts chaperone-mediated autophagy substrates. Cells, 2019. **8**(8): p. 849.
68. Zhou, J., et al., Inhibition of HSPA8 by rifampicin contributes to ferroptosis via enhancing autophagy. Liver International, 2022. **42**(12): p. 2889-2899.
69. Tao, Y., et al., Raltitrexed induces apoptosis through activating ROS-mediated ER stress by impeding HSPA8 expression in prostate cancer cells. Biochimica et Biophysica Acta (BBA)-Molecular Cell Research, 2024. **1871**(3): p. 119684.
70. Zhao, W., et al., HSPA8 Single-Nucleotide Polymorphism Is Associated with Serum HSC70 Concentration and Carotid Artery Atherosclerosis in Nonalcoholic Fatty Liver Disease. Genes, 2022. **13**(7): p. 1265.
71. Xiang, X., X.-M. You, and L.-Q. Li, Expression of HSP90AA1/HSPA8 in hepatocellular carcinoma patients with depression. OncoTargets and therapy, 2018: p. 3013-3023.
72. Costa-Mattioli, M. and P. Walter, The integrated stress response: From mechanism to disease. Science, 2020. **368**(6489): p. eaat5314.
73. Pakos-Zebrucka, K., et al., The integrated stress response. EMBO reports, 2016. **17**(10): p. 1374-1395.
74. Velazques, J.M., B.J. DiDomenico, and S. Lindquist, Intracellular localization of heat shock proteins in Drosophila. Cell, 1980. **20**(3): p. 679-689.
75. Knowlton, A. and M. Salfity, Nuclear localization and the heat shock proteins. Journal of Biosciences, 1996. **21**: p. 123-132.
76. Multhoff, G., Heat shock protein 70 (Hsp70): membrane location, export and immunological relevance. Methods, 2007. **43**(3): p. 229-237.
77. De Maio, A. and D. Vazquez, Extracellular heat shock proteins: a new location, a new function. Shock, 2013. **40**(4): p. 239-246.
78. Barlowe, C.K. and E.A. Miller, Secretory protein biogenesis and traffic in the early secretory pathway. Genetics, 2013. **193**(2): p. 383-410.

79. Rabouille, C., Pathways of unconventional protein secretion. Trends in cell biology, 2017. **27**(3): p. 230-240.

List of Publications

1. **Pandey, A.K.** and Trivedi V., 2023. Role Transformation of HSPA8 to Heme-peroxidase After Binding Hemin to Catalyze Heme Polymerization. The Protein Journal, pp-1-14. **(https://doi.org/10.1007/s10930-023-10167-9)**.
2. **Pandey, A.K.** and Trivedi, V., 2024. Hemin competitively inhibits HSPA8 ATPase activity mitigating its foldase function. Archives of Biochemistry and Biophysics, 752, p.109889. **(https://doi.org/10.1016/j.abb.2024.10988)**.
3. **Pandey, A.K.** and Trivedi, V., Heat Shock Protein HSPA8 impedes the hemin-induced cellular toxicity in the Liver. (**In writing**)
4. Deshmukh, R., Mishra, A., **Pandey, A.K.** and Trivedi, V., Oxidative stress-dependent secretion of HSc70 in LPS stimulated macrophages protect cells from hemin toxicity. International Journal of Biological Macromolecules **(In communication**)

Conference

1. Poster Presentation in " Research and Industrial Conclave 2022-An Amalgamation of Academia, Industry and Startups", Indian Institute of Technology, 20-23 January 2022.

The Protein Journal
https://doi.org/10.1007/s10930-023-10167-9

Role Transformation of HSPA8 to Heme-peroxidase After Binding Hemin to Catalyze Heme Polymerization

Alok Kumar Pandey[1] · **Vishal Trivedi**[1]

Accepted: 27 October 2023

Abstract
Hemin, a byproduct of hemoglobin degradation, inflicts oxidative insult to cells. Following its accumulation, several proteins are recruited for heme detoxification with heme oxygenase playing the key role. Chaperones play a protective role primarily by preventing protein degradation and unfolding. They also are known to have miscellaneous secondary roles during similar situations. To discover a secondary role of chaperones during heme stress we studied the role of the chaperone HSPA8 in the detoxification of hemin. In-silico studies indicated that HSPA8 has a well-defined biophoric environment to bind hemin. Through optical difference spectroscopy, we found that HSPA8 binds hemin through its N-terminal domain with a K_d value of 5.9 ± 0.04 µM and transforms into a hemoprotein. The hemoprotein was tested for exhibiting peroxidase activity using guaiacol as substrate. The complex formed reacts with H_2O_2 and exhibits classical peroxidase activity with an ability to oxidize aromatic and halide substrates. HSPA8 is dose-dependently catalyzing heme polymerization through its N-terminal domain. The IR results reveal that the polymer formed exhibits structural similarities to β-hematin suggesting its covalent nature. The polymerization mechanism was tested through optical spectroscopy, spin-trap, and activity inhibition experiments. The results suggest that the polymerization occurs through a peroxidase-H_2O_2 system involving a one-electron transfer mechanism, and the formation of free radical and radical-radical interaction. It highlights a possible role of the HSPA8-hemin complex in exhibiting cytoprotective function during pathological conditions like malaria, sickle cell disease, etc.

Keywords Heme polymer · Hemin · HSPA8 · Malaria · Peroxidase · Peroxidase-H_2O_2 System

1 Introduction

Heme, a protoporphyrin IX-iron complex, is essential for all aerobic organisms. The iron of heme exists in ferrous (Fe^{2+}), as in free heme (ferroprotoporphyrin IX), or is autoxidized to ferric (Fe^{3+}), as in hemin (ferric protoporphyrin IX) state [1].

Heme-containing proteins serve many crucial biological functions like oxygen transport and storage and, electron transport, etc. [2, 3]. A few hemoproteins may also function as peroxidases in the presence of H_2O_2 and exhibit various functions like gastric acid secretion and ulceration, thyroxine formation [4], as an antimicrobial system [5], and, heme polymerization [6], etc.

✉ Vishal Trivedi
vtrivedi@iitg.ernet.in; Vishalash_1999@yahoo.com

[1] Malaria Research Group, Department of Bioscience and Bioengineering, Indian Institute of Technology-Guwahati, Guwahati, Assam 781039, India

Besides its role in several cellular functions, the accumulation of high levels of heme poses a severe threat to various cells and tissues [7]. It may lead to inflammation, cellular injury, ROS-inducing lipid peroxidation [3], DNA impairment [8], and protein aggregation [9]. It can cause BBB (Blood Brain barrier) disruption and oxidative insult [10]. Heme, being hydrophobic, can easily penetrate through cell membranes and make them susceptible to killing via the release of oxidants [2, 11].

Excessive heme triggers several heme detoxification factors in humans and other organisms. Heme oxygenase (HO), a pervasive microsomal enzyme, majorly superintend the breaking down of heme into equivalent amounts of free iron (Fe^{2+}), carbon monoxide, and biliverdin [12]. Two types of HO (HO-1, and HO-2) with differential expressions between cell type and tissue constitute the HO system in mammalian cells [13, 14]. Several systems in addition to HO systems in mammals, including hemopexin, albumin, alpha-1 microglobulin, reduced glutathione(GSH), HBP23 (Heme binding protein 23), ferritin, etc., also contribute towards

Published online: 08 December 2023

Archives of Biochemistry and Biophysics 752 (2024) 109889

Contents lists available at ScienceDirect

Archives of Biochemistry and Biophysics

journal homepage: www.elsevier.com/locate/yabbi

Hemin competitively inhibits HSPA8 ATPase activity mitigating its foldase function

Alok Kumar Pandey, Vishal Trivedi *

Malaria Research Group, Department of Bioscience and Bioengineering, Indian Institute of Technology-Guwahati, Guwahati, 781039, Assam, India

ARTICLE INFO

Keywords:
Competitive-inhibition
Foldase
Hemin
HSPA8
Malaria
Oxidative stress

ABSTRACT

Hemolysis in red blood cells followed by hemoglobin degradation results in high hemin levels in the systemic circulation. Such a level of hemin is disastrous for cells and tissues and is considerably responsible for the pathologies of diseases like severe malaria. Hemin's hydrophobic chemical nature and structure allow it to bind several proteins leading to their functional modification. Such modifications in physiologically relevant proteins can have a high impact on various cellular processes. HSPA8 is a chaperone that has a protective role in oxidative stress by aiding protein refolding. Through ATPase activity assays we found that hemin can competitively inhibit ATP hydrolysis by the chaperone HSPA8. Hemin as such does not affect the structural integrity of the protein which is inferred from CD spectroscopy and Gel filtration but it hinders the ATP-dependent foldase function of the chaperone. HSPA8 was not able to cause the refolding of the model protein lysozyme in the presence of hemin. The loss in HSPA8 function was due to competition between hemin and ATP as the chaperone was able to regain the foldase function when the concentration of ATP was gradually increased with hemin present at the inhibitory concentration. *In-silico* studies to establish the competition for the specific binding site revealed that ATP was unable to replace hemin from the ATP binding pocket of HSPA8 and was forced to form a non-specific and unstable complex. *In-vitro* isothermal calorimetry revealed that the affinity of ATP for binding to HSPA8 was reduced 22 folds in the presence of hemin. The prevention of HSPA8's cytoprotective function by hemin can be a major factor contributing to the overall cellular damage during hemin accumulation in the case of severe malaria and other hemolytic diseases.

1. Introduction

Hemin (protoporphyrin IX-iron) is released through ferric hemoglobin (Hb-Fe^{3+}) degradation during conditions of abnormal extracellular or extravascular Hb accumulation e.g. malaria [1]. Hemin crystals, also mentioned as "Teichmann crystals" were first crystallized by Ludwik Karol Teichmann in 1853 from blood. Later in 1930, it was chemically synthesized by Hans Fischer [2]. It can be assembled endogenously from heme group containing entities, for example, during the turnover of aged RBCs and can be accumulated in the body during hemolysis and vascular injuries. Elevated In conditions of high levels of released hemin, cells' anti-oxidant arsenal fails to combat the induced cytotoxicity resulting in oxidative damage to macromolecules and cell death [3,4]. To attenuate such situations cells employ several proteins that bind to hemin and facilitate its degradation and removal from the system [5].

Structurally hemin consists of a planar metalloporphyrin ring containing iron in its ferric(Fe^{3+}) state, unlike heme where the iron is in ferrous (Fe^{2+}). In hemin, the coordinating ion with iron is a chloride (Cl^-) ion which makes it different from its related compound hematin where the coordinating ion is a hydroxide (OH^-) ion [6]. It comprises pharmacophoric features that capacitate it to bind to many proteins. Although hemin binding is predominantly driven by hydrophobic interactions through its porphyrin ring, the iron of hemin helps in anchoring it through electrostatic interactions [7,8]. In addition to binding with its detoxifying proteins hemin is known to bind to many other proteins and alter their function [9,10].

Hemin is proven to be a potent inhibitor of the primary functions of proteins like cytoplasmic DNA polymerase of red blood cells [11] and erythrocytic ribonuclease [12]. It can prevent ATP-dependent protein degradation by ubiquitin [13] and the aggregation of proteins like β-amyloid [14]. It has been described as a common and robust inhibitor

* Corresponding author. Malaria Research Group, Department of Biosciences and Bioengineering, Indian Institute of Technology-Guwahati, Guwahati, 781039, Assam, India.
E-mail addresses: vtrivedi@iitg.ernet.in, Vishalash_1999@yahoo.com (V. Trivedi).

https://doi.org/10.1016/j.abb.2024.109889
Received 17 October 2023; Received in revised form 19 December 2023; Accepted 9 January 2024
Available online 10 January 2024